



Etude de la voie de biosynthèse des phlorotannins chez les algues brunes, de la caractérisation biochimique d'enzymes recombinantes à l'étude des réponses écophysiolologiques

Emeline Creis

► To cite this version:

Emeline Creis. Etude de la voie de biosynthèse des phlorotannins chez les algues brunes, de la caractérisation biochimique d'enzymes recombinantes à l'étude des réponses écophysiolologiques. Biologie végétale. Université Pierre et Marie Curie - Paris VI, 2015. Français. NNT: 2015PA066095 . tel-01284701

HAL Id: tel-01284701

<https://theses.hal.science/tel-01284701>

Submitted on 8 Mar 2016

HAL is a multi-disciplinary open access archive for the deposit and dissemination of scientific research documents, whether they are published or not. The documents may come from teaching and research institutions in France or abroad, or from public or private research centers.

L'archive ouverte pluridisciplinaire **HAL**, est destinée au dépôt et à la diffusion de documents scientifiques de niveau recherche, publiés ou non, émanant des établissements d'enseignement et de recherche français ou étrangers, des laboratoires publics ou privés.

Université Pierre et Marie Curie**Ecole Doctorale Complexité du Vivant ED515****Laboratoire de Biologie Intégrative des Modèles Marins****Equipe Signalisation et défense chimique chez les macroalgues****Spécialité****Biologie Marine**

Etude de la voie de biosynthèse des phlorotannins chez les algues brunes, de la caractérisation biochimique d'enzymes recombinantes à l'étude des réponses écophysiologiques.

Présentée par**Emeline Creis****Thèse de doctorat de Biologie****Présentée et soutenue publiquement le 6 mars 2015****Devant le jury composé de :**

M. Alain Bouchereau	Professeur IGEPP INRA (Rennes 1)	Rapporteur
M. Joël Boustie	Professeur Faculté des Sciences (Rennes 1)	Rapporteur
Mme Geneviève Chiapusio	Maître de Conférence Université de Franche-Comté (Montbéliard)	Examinaterice
M. Weinberger Florian	Chercheur GEOMAR (Kiel)	Examinateur
M. Destombe Christophe	Professeur Station Biologique CNRS (Roscoff)	Examinateur
M. Philippe Potin	Directeur de recherche Station Biologique CNRS (Roscoff)	Directeur de thèse
M. Erwan Ar Gall	Maître de Conférence LEMAR IUEM UBO(Brest)	Co-Directeur de thèse

*Je dédie cette thèse à ma famille
qui a toujours su me soutenir à tous moments,
et en particulier à mon Grand-Père qui m'aura communiqué
cette envie de découvrir la Nature et qui m'aura inculqué
l'importance de toujours aller jusqu'au bout des choses entreprises.*

Remerciements

Je tiens tout d'abord à remercier la Station Biologique de Roscoff, son directeur Bernard Kloareg de m'avoir permis de réaliser cette thèse dans d'aussi bonnes conditions.

Je tiens également à remercier la Région Bretagne pour le financement de cette thèse, le projet Phlorotan'ING soutenu par le GIS Europôle Mer ainsi que le projet Idealg. Merci également à l'UBO d'avoir financé la prolongation de cette thèse.

Merci aux rapporteurs et examinateurs d'avoir accordé de leur temps pour juger ce travail et pour leur participation à ce jury.

Merci au Gdr Biochimar, au Gdr Médiatec et à l'association des Jeunes Chercheurs en Ecologie Chimique de m'avoir fait découvrir une communauté de scientifiques aussi passionnés les uns que les autres.

Merci à Catherine Boyen et Mirjam Czjzek directrices de l'unité 8227 pour votre travail et votre soutien qui nous permettent de travailler dans de très bonnes conditions.

Un grand merci également à tous les membres de l'Equipe Signalisation et Défense Chimique chez les Macroalgues, Gaëlle, Céline, Léa, JB, merci Catherine pour ton soutien et ton dynamisme, merci Ludo mon pti chef sans toi cette thèse ne serait pas ce qu'elle est aujourd'hui, merci pour tout ce que tu as pu m'enseigner depuis maintenant plus de 4 ans, de ta disponibilité et de ton écoute. L'un n'allant pas sans l'autre, merci également à toi Laurence pour toute ton aide apportée pendant le master et le début de cette thèse ainsi qu'après ton départ.

Philippe, comment te remercier à ta juste valeur, merci de m'avoir offert cette opportunité d'effectuer cette thèse avec toi, j'ai beaucoup de respect pour le scientifique passionné que tu es mais également pour l'homme qui sais rester juste, ouvert et à l'écoute des autres. Tu m'as permis de rencontrer Florian mais aussi Raj, des gens qui comme toi partagent ces mêmes valeurs morales et scientifiques.

Erwan, notre histoire à commencé il y a un bout de temps maintenant (7 ans), c'est toi qui m'aura donné le virus « Algue » et je t'en remercie ! Merci pour ton écoute et ton soutien tout au long de cette thèse.

Merci à toutes les personnes ayant séjournées plus ou moins longtemps au bureau 351, les actuelles Maria et Amandine, merci pour votre soutien lors des derniers moments de l'écriture.

Plus largement et pour n'oublier personne, merci à tous les membres de l'UMR 8227 pour ces 4 années et ces bons moments passés en votre compagnie.

Mon petit scarabé et oui je t'avais promis une place dans ces remerciements, alors merci pour ta bonne humeur ton accent brezhoneg qui en fait palir plus d'un, tu fais partie de ces rares personnes qui ont toujours la patate quel est donc ton secret ? Reste comme tu es, unique en ton genre !

Alexandra et Sophie, merci à toutes les deux pour tout ce que vous m'apportez pour votre bienveillance, vos conseils, j'ai rencontré ici bien plus que des collègues merci pour tout !

Monique, un grand merci pour ta présence réconfortante toujours de bon conseil, calme, rationnelle (enfin ça dépend ;)) merci d'être là.

Comment vous dissocier tous les 4, Rémy, Kévin, Héloïse et Camille, les inséparables merci à tous les quatres, je pense que vous savez que les bretons ne donnent leur amitié qu'une seule fois, ça c'est fait, j'espère que l'avenir nous permettra de nous voir encore et encore dans les quatre coins du monde !

Ma petite Alexia, c'est ton tour, merci poulette pour tous ces bons moments passés avec toi j'ai hâte d'entendre le récit de tes aventures de l'autre côté de l'Atlantique !

Merci Adrien, Anaïs, Aurélie, Vanessa, Julien, Charlotte, Benoît, Perrine, Alice pour votre amitié.

Je souhaite particulièrement remercier toute ma famille qui m'a toujours soutenue et qui est présente en toute circonstance, merci pour tous ces bonheurs que vous m'apportez. Le meilleur pour la fin, Steve, « merci » n'est pas un mot assez fort pour te remercier, tu auras réussi à me donner l'énergie nécessaire pour écrire cette thèse, ton enthousiasme, ton envie de toujours faire au mieux, me donnent chaque jour l'envie d'aller toujours plus loin

Une thèse, bien plus qu'un diplôme c'est le temps privilégié pour passer de la vie d'étudiant à la vie d'adulte, dans un cadre comme Roscoff en passant par Kiel puis Truro, cette aventure aura certainement été pour moi la plus enrichissante autant professionnellement que personnellement,

Merci à toutes et à tous !

<i>Introduction Générale</i>	1
I. De l'endosymbiose primaire, à l'émergence des macroalgues brunes	1
Phylogénie et classification des algues.....	1
Les algues marines pluricellulaires:	3
Les macroalgues brunes dans l'Evolution:.....	5
II. Les macroalgues brunes : une richesse de composés originaux	6
Des métabolismes originaux:.....	6
Les polysaccharides :.....	6
Le mannitol	6
Le métabolisme halogéné :.....	7
Les phlorotannins : composés phénoliques des macroalgues brunes	7
• Structures chimiques.....	7
• Localisation cellulaire	9
• Fonctions.....	11
III. Connaissances acquises sur la synthèse des composés phénoliques:.....	17
Chez les plantes terrestres : Les flavonoïdes.....	19
Chez les angiospermes et algues vertes : Les tannins hydrolysables	25
Chez les algues brunes : Les phlorotannins	26
IV. Contexte et objectifs du projet de thèse.....	27
<i>Partie I : Etude de la voie de biosynthèse des phlorotannins</i>	28
<i>Chapitre 1: Caractérisation de la Polyketide Synthase de type III d'Ectocarpus.....</i>	29
<i>Chapitre 2: Caractérisation biochimique et fonctionnelle de Chalcone Isomérasés-like d'Ectocarpus.</i>	46
Abstract	48
Introduction.....	49
Materials and Methods:	51
Results and discussion	60
Conclusion and prospects.....	70
References :	71
<i>Chapitre 3: Etude préliminaire des aryl-sulfotransférases d'Ectocarpus: Surexpression des enzymes recombinantes.....</i>	73
Introduction.....	74
Matériel et Méthodes.....	78
Résultats	81
Discussion et Perspectives.....	83
<i>Synthèse de la Partie I</i>	84

<u>Partie II: Ecophysiologie : étude de l'implication des phlorotannins dans la réponse aux stress biotiques et abiotiques chez <i>Fucus vesiculosus</i></u>	86
Contexte général :	87
Chapitre 4 : Implication des phlorotannins dans la réponse à une irradiation chronique aux UV-B.	89
Constitutive or inducible protective mechanisms against UV-B radiation in the brown alga <i>Fucus vesiculosus</i> ? A study of gene expression and phlorotannin content responses.	90
Abstract	91
Introduction.....	92
Material and methods:	94
Results	99
Discussion	105
Supporting information	109
References	116
Chapitre 5 : Effet du stress biotique du brouteur <i>Littorina littorea</i> sur la synthèse de phlorotannins chez <i>Fucus vesiculosus</i>	119
Short-term variations in the metabolism of phlorotannins in response to the herbivore <i>Littorina littorea</i> in the brown alga <i>Fucus vesiculosus</i>	120
Introduction:.....	121
Material and methods:	123
Results:	128
Discussion:	131
References	133
Chapitre 6: Essai biologique : test de molécules d'intérêt sur le comportement et l'attachement au substrat des Littorines	137
Chemical cues of algal origin determine creeping behavior, escape and retraction in the herbivorous periwinkle <i>Littorina littorea</i>	138
Introduction	139
Material and methods	142
Results	146
Discussion	156
Conclusion.....	159
Literature	159
Synthèse de la Partie 2.	162
Conclusions et Perspectives	165
Références bibliographiques	175

Table des illustrations

Figure 1: Schéma de l'origine et de l'évolution des plastes acquis par endosymbiose primaire, puis secondaire.....	2
Figure 2: Diversité morphologique chez les algues multicellulaires	3
Figure 3: Répartitions verticales des espèces de macroalgues sur un estran rocheux.....	4
Figure 4: Arbre phylogénétique présentant l'évolution des Eucaryotes	5
Figure 5: Structure chimique du phloroglucinol.....	8
Figure 6: Illustration de la diversité structurale des phlorotannins.....	8
Figure 7: localisation sub-cellulaire de la biosynthèse des phlorotannins.....	10
Figure 8: Localisation des physodes.	10
Figure 9: Modèle présentant la complexation des phlorotannins à l'acide alginique	11
Figure 10: Illustration des différentes étapes du stress photo-oxydant	14
Figure 11: Noyau phénol représentant la structure commune aux polyphénols	17
Figure 12: Schéma représentant les principales voies de biosynthèse connues des composés phénoliques chez les végétaux.....	18
Figure 13: A. Flavanone B. Nodulation sur le système racinaire d'une légumineuse	20
Figure 14: Arbre phylogénétique des PKS III dans l'arbre du vivant.	21
Figure 15: Classification des quatre types de chalcones isomérasées	22
Figure 16: Schéma représentant la synthèse de flavanone.	22
Figure 17: Phylogénie simplifiée des CHI.	23
Figure 18: Réaction enzymatique d'une sulfotransférase (ST) utilisant le PAPS.....	24
Figure 19: Conversion enzymatique de l'acide shikimique en acide gallique.....	25
Figure 20: Répartition géographique de l'algue brune <i>Fucus vesiculosus</i>	88
Figure 21 : <i>Fucus vesiculosus</i> L.	88
Figure 22: Modélisation schématique de la cavité de liaison des acides gras comparée entre AtFAP1 et AtFAP3.....	168
Figure 23 : Localisation subcellulaire de la polyketide synthase de type III EsiPKS1	174
Figure 2.1: Comparison of the EFP protein with its relatives.....	50
Figure 2.2: Scheme of the principle of the BP Clonase II Gateway strategy	55
Figure 2.3: Scheme representing the following steps in the LR Clonase II Gateway strategy	57
Figure 2.4: Phylogenetic tree of FAP, CHI and CHIL proteins.	58

Table des illustrations

Figure 2.5: Model of the superposition of AtFAP3 and EsiCHIL1.....	62
Figure 2.6: A.B.C Purification of EsiCHIL1.....	63
Figure 2.6: D.E. Purification of EsiCHIL2.....	64
Figure 2.7: Analysis of ligands associated with purified recombinant Esi-CHIL proteins.....	65
Figure 2.8: Relative gene expression in T-DNA insertion line of <i>Arabidopsis thaliana</i> CHIL1.....	66
Figure 2.9: Subcellular localisation of EsiCHIL1 in tobacco cells.	67
Figure 2.10: Relative gene expression in transgenic lines of <i>Arabidopsis thaliana</i> for Esi-CHIL1 and Esi-CHIL2 genes.....	68
Figure 3.1: Structures chimiques de phlorotannins sulfatés.....	74
Figure 3.2: Régions conservées entre les sulfotransférases PAPS dépendantes	75
Figure 3.3: Arbre phylogénétique représentatif de la diversité des sulfotransférases (STs).....	77
Figure 3.4 : Schéma présentant les caractéristiques du plasmide pQE80L (Qiagen).....	79
Figure 3.5: Représentation des domaines conservés Région I et IV, dépendantes du PAPS.....	81
Figure 3.6: Expressions des AST.	82
Figure 4.1: Photosynthesis efficiency of <i>Fucus vesiculosus</i>	101
Figure 4.2: Relative gene expression in <i>Fucus vesiculosus</i> exposed to UV-B.....	103
Figure 4.3: Quantification of total soluble phenol contents	104
Figure 4.4: Quantification of soluble phenol contents in semi-purified fractions.	105
Figure 4.5: Ultra-HPLC-ESI-MS analysis	106
Figure 5.1: Relative gene expression in <i>Fucus vesiculosus</i>	130
Figure 5.2: Quantification of total soluble phenol contents	131
Figure 6.1: Crawling velocity of <i>L. littorea</i> on specimens of <i>F. vesiculosus</i>	148
Figure 6.2: Relationships between FC phenols in <i>F. vesiculosus</i> individuals.....	150
Figure 6.3: Crawling velocity (A), frequency of escapes (B) and odds variation for attachment (C) of <i>Littorina littorea</i> on agar substrate.....	152
Figure 6.4: Odds for attachment of <i>Littorina littorea</i> on agar substrate	154
Figure 6.5: Crawling velocity (A), frequency of escapes (B) and odds for attachment (C) of <i>Littorina littorea</i> on agar substrate containing phloroglucin at various concentrations.	156

Liste des tableaux

Table 2.1: Results of microscale thermophoresis EsiCHIL1	65
Table 2.2: Fatty Acid Methyl Esterified (FAME) Standard C8 to C24	69
Table 2.3: Fatty acids in wild type leaf	Table 2.4: Fatty acids in AtCHIL1 mutant leaf....
Table 3.1: Séquences nucléotidiques des amorces utilisées pour le clonage des AST	78
Table 4.1: Primers used for the qRT-PCR analysis on control and UV-B conditions.....	97
Table 5.1: Primers used for the qRT-PCR analysis on control and grazing conditions.	126
Table 6.1: Analysis of non-linear regression between FC phenols and creeping velocity of <i>L. littorea</i>	148
Table 6.2: Stepwise regression of FC phenols, RDA phenols and mannitol in extracts.....	154

Liste des abréviations

ADN : acide désoxyribonucléique	PCR : réaction de polymérisation en chaîne
ADNc : ADN complémentaire	PKS : polycétide synthase
ANOVA : analyse de la variance	RT : transcription inverse
ARN : acide ribonucléique	RT-qPCR : PCR quantitative couplée à la transcription inverse
AST : aryl-sulfotransférases	ROS : espèces réatives de l'oxygène
C4H : cinnamate-4-hydroxylase	Tris : trishydroxyméthylaminométhane
CHI : chalcone isomérase	TUA : tubuline α
CHIL : chalcone isomérase-like	UDP-Glc : uridine diphosphate glucose
CHS : chalcone synthase	UV : lumière ultraviolette
Cyp450 : cytochrome P450	v-BPO : bromopéroxidase dépendante du vanadium
DP : degré de polymérisation	4CL : 4-coumaryl-CoA-ligase
DNase : désoxyribonucléase	
DSDG : déhydroshikimate déhydrogenase	
EF1 α : facteur d'elongation α	
EST: marqueurs de séquence exprimée	
FAP : <i>Fatty acid protein</i>	
HSP70 : <i>Heat shock protein 70</i>	
IPTG: isopropyl β -D-A-thiogalactopyranoside	
NADPH : nicotinamide adenine dinucleotide phosphate	
PAPS : 3'-phosphate-5'-phosphosulfate	
PAL : phénylalanine ammonia-lyase	
PAR : radiation photosynthétiquement active	

Introduction Générale

I.	De l'endosymbiose primaire, à l'émergence des macroalgues brunes	1
	Phylogénie et classification des algues.....	1
	Les algues marines pluricellulaires:	3
	Les macroalgues brunes dans l'Evolution:.....	5
II.	Les macroalgues brunes : une richesse de composés originaux	6
	Des métabolismes originaux:.....	6
	Les polysaccharides :.....	6
	Le mannitol	6
	Le métabolisme halogéné :.....	7
	Les phlorotannins : composés phénoliques des macroalgues brunes	7
	• Structures chimiques.....	7
	• Localisation cellulaire	9
	• Fonctions	11
III.	Connaissances acquises sur la synthèse des composés phénoliques:.....	17
	Chez les plantes terrestres : Les flavonoïdes.....	19
	Chez les angiospermes et algues vertes : Les tannins hydrolysables	25
	Chez les algues brunes : Les phlorotannins	26
IV.	Contexte et objectifs du projet de thèse.....	27

I. De l'endosymbiose primaire, à l'émergence des macroalgues brunes

Phylogénie et classification des algues

Les algues sont des organismes photosynthétiques, unicellulaires ou pluricellulaires, généralement aquatiques. Ces organismes sont considérés comme primitifs dans le sens où ils ont émergé il y a plus d'un milliard d'années en lignées évolutives indépendantes, bien avant l'apparition des végétaux verts terrestres. Fruits de différents évènements endosymbiotiques (Figure 1), les lignées rouges et vertes ont toutes pour point commun l'origine de la photosynthèse oxygénique chez les eucaryotes. Cette caractéristique a été acquise à partir d'une endosymbiose primaire entre une cellule eucaryote non photosynthétique et des bactéries (les cyanobactéries autrefois dénommées algues bleues). C'est à l'issue de cette endosymbiose primaire que vont émerger les algues rouges, les glaucophytes et les algues vertes (dont les ancêtres des plantes vertes terrestres) appartenant aux lignées d'eucaryotes du phylum des Archaeplastida (Figure 4).

En revanche, les autres lignées d'algues représentées notamment par les cryptophytes, les haptophytes, les algues brun-doré et les dinophytes, sont des eucaryotes sans lien de parenté direct avec les plantes terrestres ([Archibald and Keeling 2002](#)). Ces lignées sont issues d'une endosymbiose secondaire entre un eucaryote primitif non photosynthétique et une algue unicellulaire rouge pour les lignées RAS (Rhizaria, Alvéolés, Stramenopiles) ou Chromealvéolés, ou avec une algue unicellulaire verte pour les euglénophycées et les chlorarachniophycées. Des endosymbioses multiples semblent aussi être très importantes dans l'évolution des dinophytes. Beaucoup de ces lignées sont représentées essentiellement par des organismes unicellulaires, mais la multicellularité est apparue par convergence évolutive dans les trois lignées vertes, rouges et brunes ([Cock et al., 2013](#)).

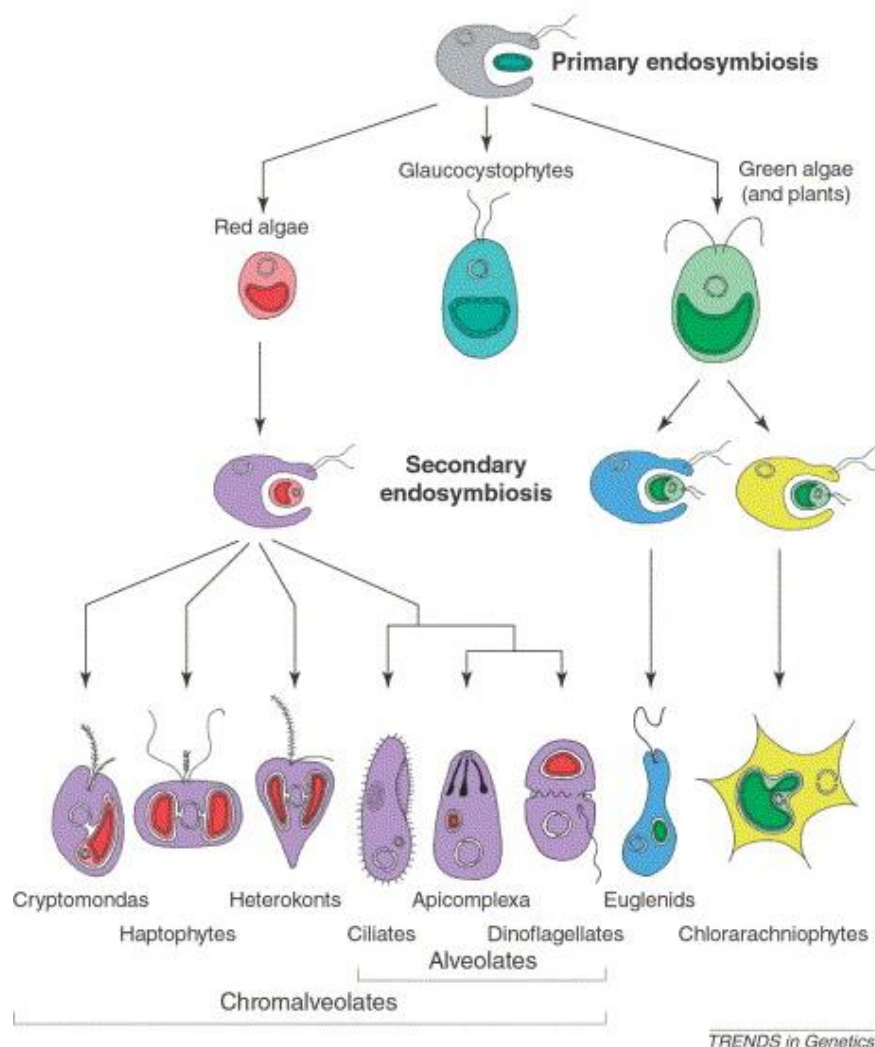


Figure 1: Schéma de l'origine et de l'évolution des plastes acquis par endosymbiose primaire, puis secondaire. Une endosymbiose primaire unique entre un eucaryote primitif hétérotrophe (gris) et une cyanobactérie a conduit aux trois lignées possédant des plastes primaires (en haut). Deux endosymbioses secondaires impliquant deux algues vertes et des hôtes non apparentés ont conduits aux Euglènes (bleu) et au chlorarachniophytes (jaune). Une endosymbiose unique entre une algue rouge et un hôte hétérotrophe a permis l'émergence de toutes les autres lignées restantes d'eucaryotes. La perte du plaste a été répandue dans plusieurs lignées, et chez les ciliés, la lignée entière est non photosynthétique. (Recycled plastids: a 'green movement' in eukaryotic evolution Trends in genetics 18, 577–584 Archibald and Keeling 2002)

Les algues marines pluricellulaires:

Les trois grandes lignées d’algues pluricellulaires, brunes, rouges et vertes, sont majoritairement présentes en milieu marin, mais certaines familles ont aussi conquis les eaux douces (De Reviers, 2001, 2013). Elles possèdent des chlorophylles ainsi que des pigments additionnels jaunes, rouges ou bleu, qui ont permis de les classer depuis des temps anciens en trois groupes différents: les **macroalgues vertes** (Chlorobiontes) qui possèdent des chlorophylles de type a et b, les **macroalgues rouges** (Rhodophycées) présentant de la chlorophylle a et des phycobilines rouges (phycoérythrine) et bleues (phycocyanine) et enfin les **macroalgues brunes** (Phéophycées) possédant de la chlorophylle c en plus de la chlorophylle a et de fortes teneurs en caroténoïdes (De Reviers, 2001, 2013).

Il existe une très grande diversité de morphologies chez toutes ces macroalgues allant du filament unisériel simple (*Ectocarpus sp.*, Fig 2a), aux lanières des haricots de mer (*Himanthalia elongata*, Fig 2b), en passant par les thalles complexes des Laminaires (Fig 2c), ou encore par les tubes creux (*Enteromorpha sp.*, Fig 2d) et les thalles incrustés sur les roches (*Lithophyllum incrassans*, Fig 2e).

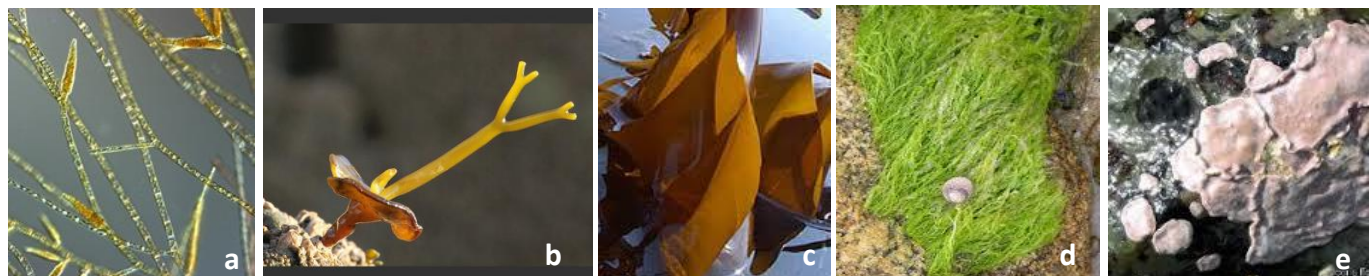
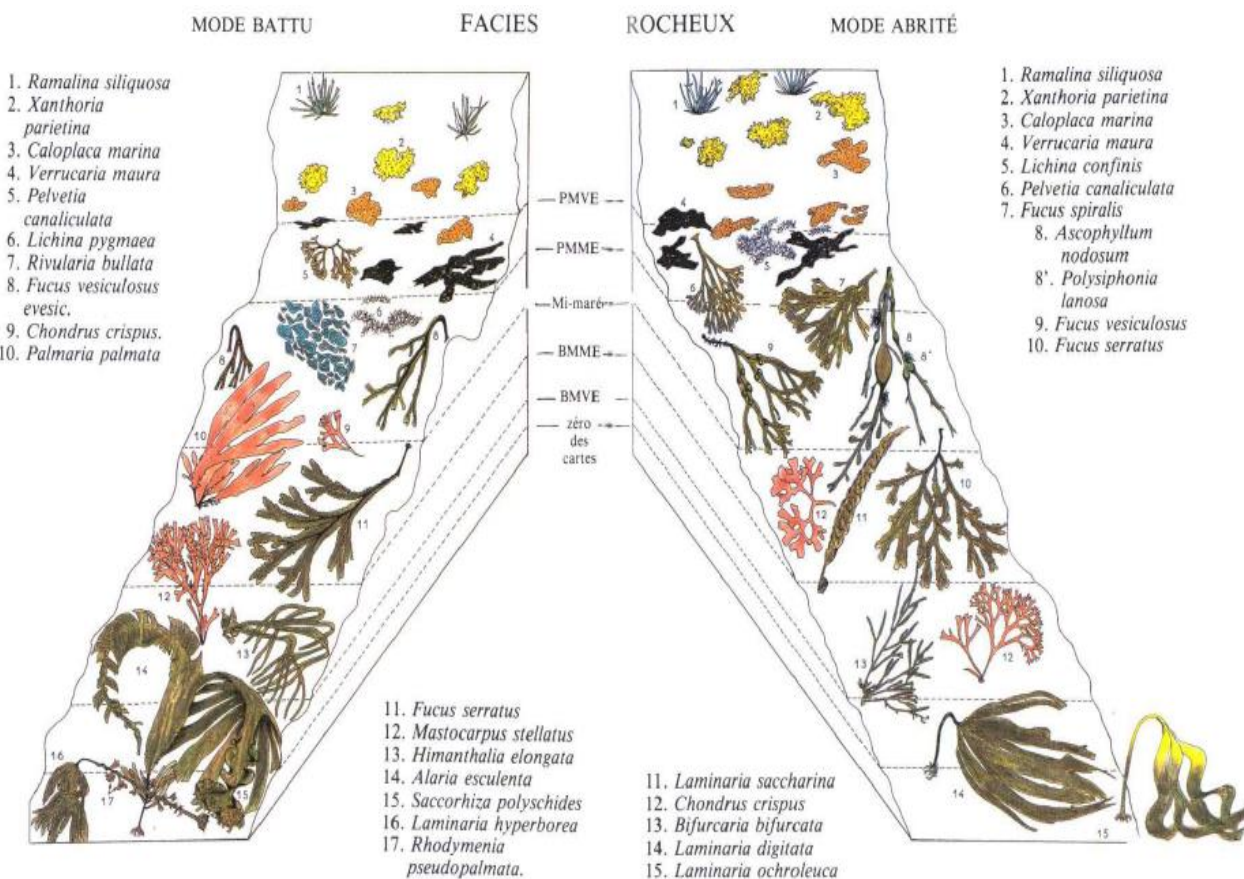


Figure 2 : Photos montrant la diversité morphologique chez les algues multicellulaires a. *Ectocarpus sp.*, b. *Himanthalia elongata*, c. *Laminaria digitata*, d. *Enteromorpha sp.*, e. *Lithophyllum incrassans*.

Les thalles sont pour la plupart fixés au substrat par des rhizoïdes, un disque basal ou encore un crampon, afin de résister aux contraintes hydrodynamiques du milieu.

Les espèces de macroalgues se répartissent sur l'estran en fonction de gradients de conditions environnementales (Figure 3), notamment la durée moyenne d'émersion qui se traduit par des variations plus ou moins importantes d'intensité lumineuse, de salinité ou de température. Chacune des espèces va ainsi vivre dans un milieu auquel elle est adaptée en fonction de ses propres paramètres physiologiques, de ses capacités de résistance aux changements d'état du milieu notamment lors des marées basses, ou encore de son aptitude à se défendre face aux agressions biotiques comme la prédation ou à la compétition pour le substrat. Ces échanges avec l'environnement vont ainsi être au cœur des recherches en écologie chimique, afin de comprendre les mécanismes mis en jeu par les espèces pour survivre dans des environnements changeants, tels que les milieux côtiers, voire extrêmes comme les hauts d'estran.



Les macroalgues brunes dans l'Evolution:

Les macroalgues brunes (Phéophycées), tout comme les oomycètes et les diatomées appartiennent au phylum des Stramenopiles (Figure 4). L'émergence du groupe des Eucaryotes Stramenopiles est datée de plus d'un milliard d'années et est la résultante d'une endosymbiose secondaire d'une algue rouge unicellulaire avec un protiste ancestral (Reyes-Prieto et al. 2007). Les algues brunes se sont ensuite développées il y a environ 200 millions d'années et se présentent comme la seule lignée de ce phylum ayant acquis la multicellularité complexe (Cock, et al. 2011). Elles ont évolué indépendamment des végétaux terrestres, et plus largement du phylum des Archaeplastida qui regroupe aussi les algues vertes et rouges. Ainsi, les algues brunes sont sur le plan phylogénétique aussi distantes des animaux que des algues vertes et rouges (Baldauf 2003). La position phylogénétique de ces algues brunes en fait des modèles d'étude particulièrement intéressants, notamment par la présence de métabolismes originaux tel que celui des polysaccharides anioniques, celui du mannitol, de l'iode, ou encore celui des phlorotannins (Cock et al. 2011).

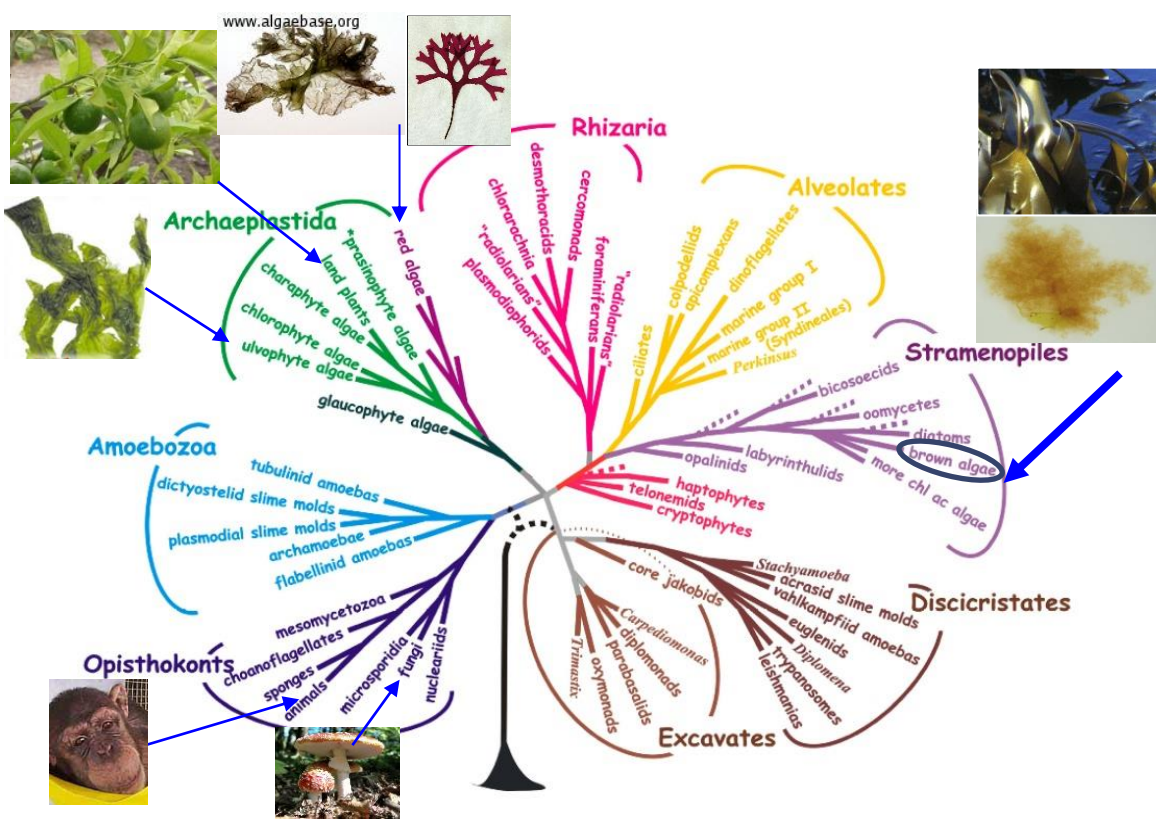


Figure 4 : Arbre phylogénétique présentant l'évolution des Eucaryotes selon Baldauf (2003)

II. Les macroalgues brunes : une richesse de composés originaux

Les algues brunes ont depuis très longtemps été exploitées à des fins agricoles pour l'amendement des sols, dans l'industrie du verre au 17^{ème} siècle par la fabrication de pains de soude (carbonates) issue du brûlage des laminaires, elles ont également permis la découverte de l'iode à la fin du 18^{ème} siècle qui sera très utilisé en tant que désinfectant ([Arzel, 1987](#)). Aujourd'hui, ces algues brunes sont toujours exploitées mais pour l'extraction de produits dit de haute valeur ajoutée.

Des métabolismes originaux:

Les polysaccharides :

La paroi des algues brunes est principalement composée d'une partie cristalline, essentiellement de la cellulose et de polysaccharides anioniques : acide alginique, alginat (polysaccharides carboxylés, sels d'alginate) et fucanes, fucoïdanes (polysaccharides sulfatés) qui constituent plus de 40% du poids sec du thalle ([Mabeau and Kloareg 1987](#)). Les alginates sont utilisés dans l'industrie des hydrocolloïdes en tant que texturants retrouvés sous la dénomination E400 à E405. Etant dépourvues de propriétés rhéologiques, certains polysaccharides notamment les fucoïdanes, possédant un ou plusieurs groupements sulfates présentent des activités anti-oxydantes, anticoagulantes, antivirales, voire anti-tumorales ([Nishino, & al, 1994 ; Senthilkumar & Kim, 2014](#)).

Le mannitol

Le métabolisme du mannitol présente également un grand intérêt. Il est avec la laminarine la principale réserve carbonée chez les algues brunes ([Michel et al., 2010](#)). La synthèse du mannitol est effectuée à partir de fructose-6-phosphate directement issu de la photosynthèse. Ce photosynthétat a été montré comme pouvant être impliqué dans l'osmorégulation ([Davison](#)

& Reed, 1985 ; Reed, et al. 1985) et permettant ainsi une tolérance importante des algues brunes aux variations de salinité.

Le métabolisme halogéné :

Un autre métabolisme important chez les algues brunes, est le métabolisme halogéné. Ce métabolisme est principalement retrouvé en milieu marin au vu des concentrations en halogènes plus importantes que celles retrouvées en milieu terrestre (Butler and Walker 1993). L'halogénéation des composés organiques peut se faire de manière spontanée ou par l'intermédiaire d'haloperoxidases. Chez les algues brunes, ces enzymes sont dépendantes du vanadium qui est utilisé comme co-facteur d'où leur dénomination de vanadium-halopéroxydases (La Barre et al. 2010). Ces enzymes participent à la détoxification des espèces réactives de l'oxygène par l'utilisation du peroxyde d'hydrogène (H_2O_2) afin d'oxyder les halogénures conduisant à la formation des composés organiques halogénés. L'halogénéation de composés participe à l'augmentation de l'activité biologique de certains métabolites secondaires (La Barre et al. 2010). Les bromoperoxidases sont les enzymes les mieux caractérisées chez les algues brunes, ces enzymes agissent notamment sur les composés phénoliques pouvant former des bromophénols très actifs dans la défense face aux herbivores (Shibata et al. 2014) mais ces enzymes seraient aussi impliquées dans la construction des parois par la complexation des composés phénoliques aux alginates (Salgado et al. 2009a)

Les phlorotannins : composés phénoliques des macroalgues brunes

Structures chimiques

Comme nous l'avons vu précédemment, les macroalgues brunes sont sur le plan phylogénétique des organismes très distants de la lignée verte (Figure 4). Elles possèdent ainsi des composés phénoliques qui leurs sont spécifiques : les phlorotannins (Ragan and Glombitza 1986). Ceux-ci

sont constitués d'oligomères et de polymères du phloroglucinol (1,3,5-trihydroxybenzene) (Figure 5).

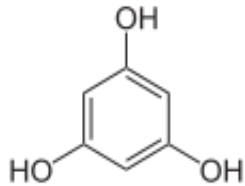


Figure 5: Structure chimique du phloroglucinol

Les phlorotannins sont subdivisés en six groupes en fonction de leur structure et du type de liaison entre les unités phloroglucinol (Ragan and Glombitza 1986) (Figure 6) : fucols, phlorehols, fucophlorehols, fuhalols, isofuhalols et eckols. Ainsi, les fucols sont formés par des liaisons aryl-aryl entre les monomères de phloroglucinol, les phlorehols par des liaisons aryl-ether, tandis que les fuhalols sont construits par la liaison para et ortho entre les monomères avec addition d'un groupement -OH tous les trois cycles. A cette diversité structurale de base peut s'ajouter des substitutions d'halogènes tels que le brome (Br) ou d'ester sulfates, par l'intervention d'enzymes de type haloperoxidase à vanadium ou sulfotransférase.

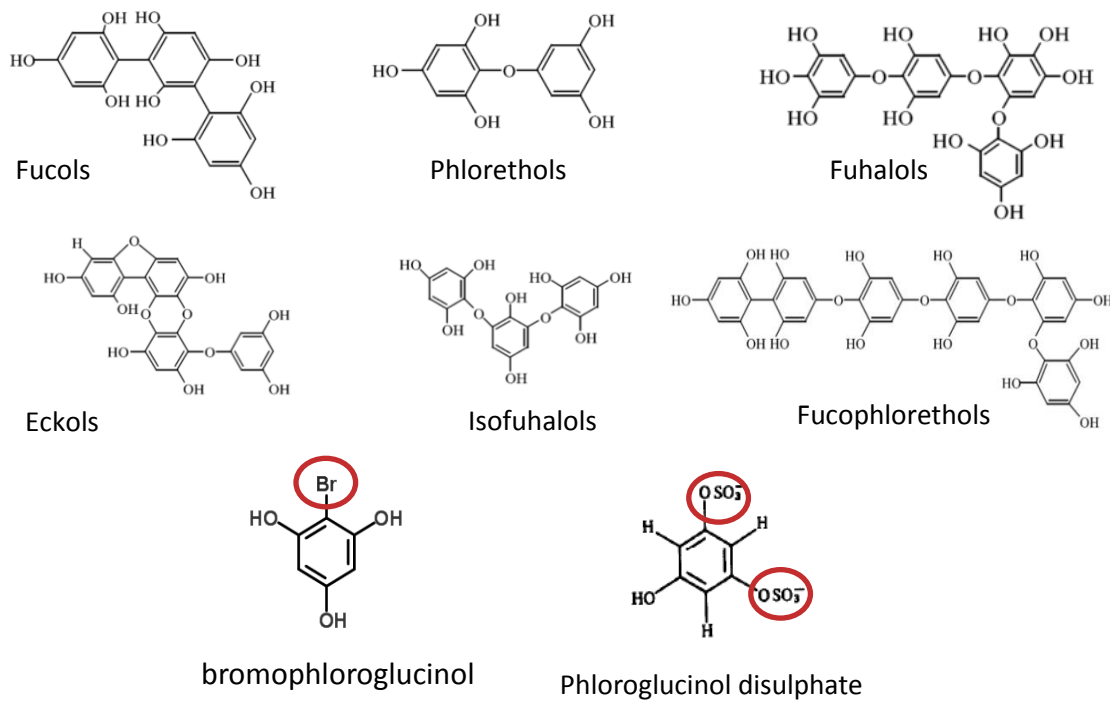


Figure 6: Illustration de la diversité structurale des phlorotannins issue de la condensation d'unités phloroglucinol et de l'intervention d'haloperoxidases ou de sulfotransférases.

La masse moléculaire des phlorotannins varie entre 126 Da et 650 kDa (Targett and Arnold, 1998), ce qui montre l'éventail de taille de ces composés synthétisés par les algues brunes. Tout comme chez les végétaux terrestres, les phlorotannins vont présenter des caractéristiques communes aux composés phénoliques, telles que la capacité à précipiter les protéines et les carbohydrates ou celle de se fixer aux ions métalliques (Ragan and Glombitza 1986).

Localisation cellulaire

Les phlorotannins sont localisés au sein des cellules des algues brunes sous forme soluble et polaire dans des vésicules nommées physodes, ainsi que dans la paroi cellulaire sous forme insoluble (Figure 7). La formation des physodes a été l'objet de nombreuses recherches depuis les travaux pionniers de cytologie de Crato à la fin du XIXème siècle (Crato 1892, 1893a, 1893b) puis de (Kylin 1912, 1918) et au cours des dernières décennies (Ragan, 1976; Arnold & Targett, 2003; Schoenwaelder & Clayton, 2000 ; Schoenwaelder, 2002, Schoenwalder, 2008). L'hypothèse qui avait d'abord été émise était que ces vésicules étaient maturés dans les chloroplastes ou par exocytose de leurs membranes, mais des études plus récentes suggèrent plutôt que leur formation dépend du réticulum endoplasmique et de l'appareil de Golgi (Schoenwaelder & Clayton, 2000). Les phlorotannins seraient d'abord séquestrés à l'intérieur des physodes avant d'être complexés à l'acide alginique de la paroi cellulaire (Bitton et al. 2006), par l'intervention de peroxydases tel que les vanadium bromoperoxydases (vBPO), ces enzymes pouvant même catalyser la formation de liaisons covalentes (Salgado et al. 2009b). Les phlorotannins pourraient également être exsudés dans le milieu extracellulaire (Carlson & Carlson, 1984; Jennings & Steinberg, 1994 ; Pavia & Toth, 2000 ; Koivikko & al., 2005 ; Shibata et al. 2006). Mais les travaux de Shibata et al. (2006) indiquent aussi que d'autres composés phénoliques comme des bromophénols sont exsudés par les algues brunes vivantes et que les tannins sont exsudés dans des conditions sub-léthales.

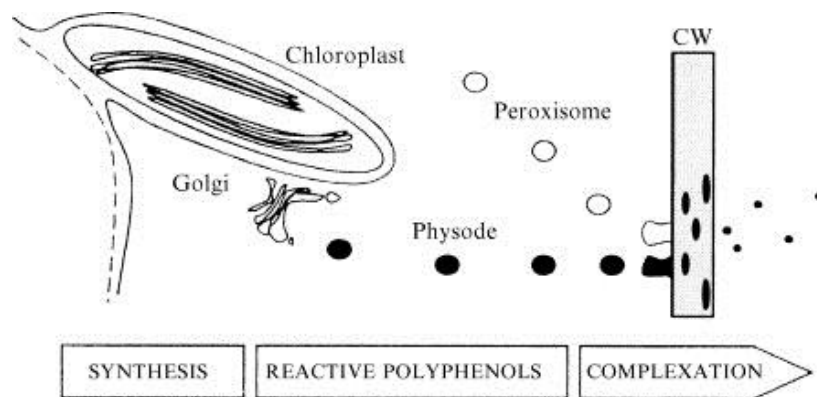


Figure 7 : Représentation schématique du modèle de localisation sub-cellulaire de la biosynthèse des phlorotannins illustrant la transition de ces composés au sein des physodes, de l'appareil de Golgi vers la paroi cellulaire. ([Arnold & Targett, 2003](#)).

Des études de localisation des physodes par coloration, telles que celles publiées par [Schoenwaelder en 2002](#), ont montré l'accumulation de phlorotannins au niveau de la paroi et ce dès les premiers stades de développement du zygote de Fucales (Figure 8), ainsi que lors de la fixation du zygote au substrat ([Tarakhovskaya 2013](#)). Sur la base d'études microscopiques, [Schoenwaelder et Clayton en 1998](#) ont également suggéré que les phlorotannins soient des composants structuraux des parois des algues brunes et joueraient un rôle important dans l'osmorégulation, notamment par leurs liaisons avec les alginates ([Schoenwaelder & Clayton, 1999](#)).

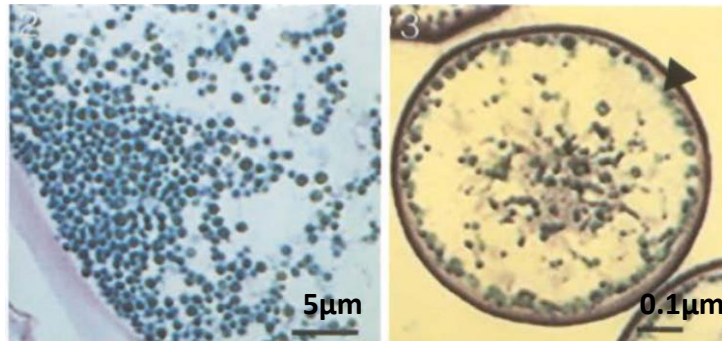


Figure 8 : Coupes fines colorées au bleu de toluidine d'un zygote d'*Himanthalia elongata* présentant une forte concentration en physodes au niveau de la paroi (à gauche) et d'un zygote d'*Hormosira banksii* (à droite) ([Schoenwaelder, 2002](#)).

Les composés phénoliques peuvent être liés par quatre types de liaisons différentes : hydrophobes, hydrogène, ioniques et covalentes (par ordre croissant de force de liaison) ([Appel 1993](#)). Des liaisons possibles entre la paroi (acide alginique) et les phlorotannins sont de type liaisons covalentes ester ou hémi-acétal (Figure 9), nécessitant des conditions fortes tel que des hydrolyses pour leur dégradation ([Koivikko et al. 2005](#)).

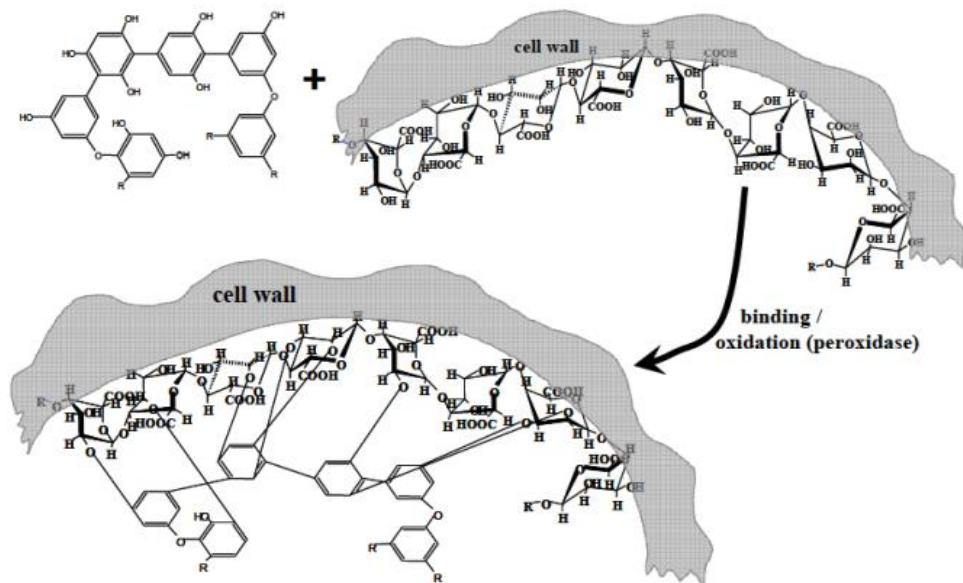


Figure 9 : Modèle présentant la complexation des phlorotannins à l'acide alginique par des liaisons de type covalentes. ([Koivikko 2008](#))

Fonctions

Les phlorotannins présents sous forme solubles peuvent représenter chez certaines algues jusqu'à 20 % de la matière sèche totale contre 4 % pour la partie insoluble pariétale ([Ragan and Glombitza 1986](#)). Il apparaît que la concentration en phlorotannins varie de façon considérable entre les espèces d'algues brunes (Phaeophyceae) ([Connan & al., 2004](#)) de même qu'au sein d'une même espèce. Ces variations pourraient provenir soit de réponses plastiques des algues à leur environnement, soit de divergences génétiques dans les populations ([Jormalainen and Honkanen 2004](#)), ou même des deux.

Les algues brunes évoluent dans un environnement changeant caractéristique des zones littorales. Les fortes intensités lumineuses, les variations de salinité, la dessiccation lors des

marées basses, l'eutrophisation, ou encore le broutage sont autant de facteurs auxquels les algues ont dû s'adapter. Pour cela un certain nombre de métabolites secondaires sont produits en réponse aux stress liés à cet environnement. Le stress est défini par l'impact de tous facteurs biotiques et/ou abiotiques qui affectent les «performances» individuelles, pouvant également affecter la population en réduisant la survie, la croissance et/ou la reproduction des individus ([Vinebrooke et al. 2004 ; Wahl et al. 2011](#)).

De nombreuses études se sont penchées sur l'implication des phlorotannins dans les mécanismes de défenses ([Ragan & Glombitza, 1986](#) ; [Potin et al. 2002](#)). Il a été montré que les phlorotannins possèdent des activités antioxydantes ([Wang et al. 2012](#)), antimicrobiennes, antifongiques et antibiotiques ([Lopes et al. 2012](#); [Sieburth & Conover, 1965](#); [Wikström & Pavia, 2004](#)). Des variations de leur concentration ont également pu être montrées face aux stress biotiques induits par les herbivores ([Yates & Peckol 1993](#); [Flöthe et al. 2014](#)) ou face aux stress abiotiques tels que les rayonnements UV ([Swanson & Druehl, 2002](#); [Pavia,et al. 1997](#)). Les phlorotannins peuvent ainsi être produits de manière constitutive ou inductible selon le type de stress appliqué ([Amsler and Fairhead 2006](#))

- Etude de l'effet d'un stress abiotique : les rayonnements UV

La zone médiolittorale est soumise à de fortes intensités lumineuses ainsi qu'aux rayonnements UV qui peuvent avoir des incidences majeures sur les organismes photosynthétiques des écosystèmes terrestres et marins ([Franklin and Forster 1997](#); [Caldwell et al. 1998](#); [Rozema J. 2002](#) ; [Häder et al. 2007](#)). Le spectre UV est divisé en trois grandes classes : les radiations UV-C (190-280 nm), UV-B (280-320 nm) et UV-A (320-400 nm). Les UV-C sont efficacement absorbés par l'atmosphère et n'atteignent pas la surface de la Terre ; Les UV-B ne représentent que 1,5% des irradiations totales reçues à la surface de la Terre mais sont fortement énergétiques et peuvent avoir des effets néfastes sur les végétaux; les UV-A sont moins énergétiques que les UV-B mais ils sont peu atténués par la couche d'ozone et peuvent pénétrer plus profondément dans les tissus végétaux. Dans les écosystèmes marins côtiers, la colonne d'eau atténue les radiations UV reçues par les macrophytes situés entre les basses mers de vives eaux et les pleines mers de mortes eaux. La profondeur à laquelle 90% des radiations UV-B et UV-A sont stoppées se situe entre 0,4 et 2 mètres de profondeur dans les zones côtières eutrophes et

jusqu'à 9 à 50 mètres dans les eaux claires (Franklin and Forster 1997). Sur nos côtes, le niveau médiolittoral est découvert deux fois par jour lors de la marée basse, c'est à ce moment que les radiations solaires et notamment les UV-B vont être les plus intenses et représenter un stress que l'on pourra qualifier de chronique. L'exposition d'organismes marins aux radiations UV a montré une dégradation des composants cellulaires (ADN, protéines, lipides, pigments) (Hollósy 2002; Holzinger and Lutz 2006), une réduction de la photosynthèse et de la biomasse (Franklin and Forster 1997; Caldwell et al. 1998) ainsi que des modifications de la structure des communautés de macrophytes (distribution verticale, compétition, interactions avec les herbivores) (Caldwell et al., 1998; Bischof et al., 2006). Les végétaux terrestres et les macroalgues ont développé divers mécanismes photoprotecteurs tels que la synthèse de composés phénoliques et les pigments pour réguler l'absorption, le transfert et l'utilisation de l'énergie des radiations UV, ainsi que pour éliminer les espèces réactives de l'oxygène produites (Figure 10). (Solovchenko and Merzlyak 2008)

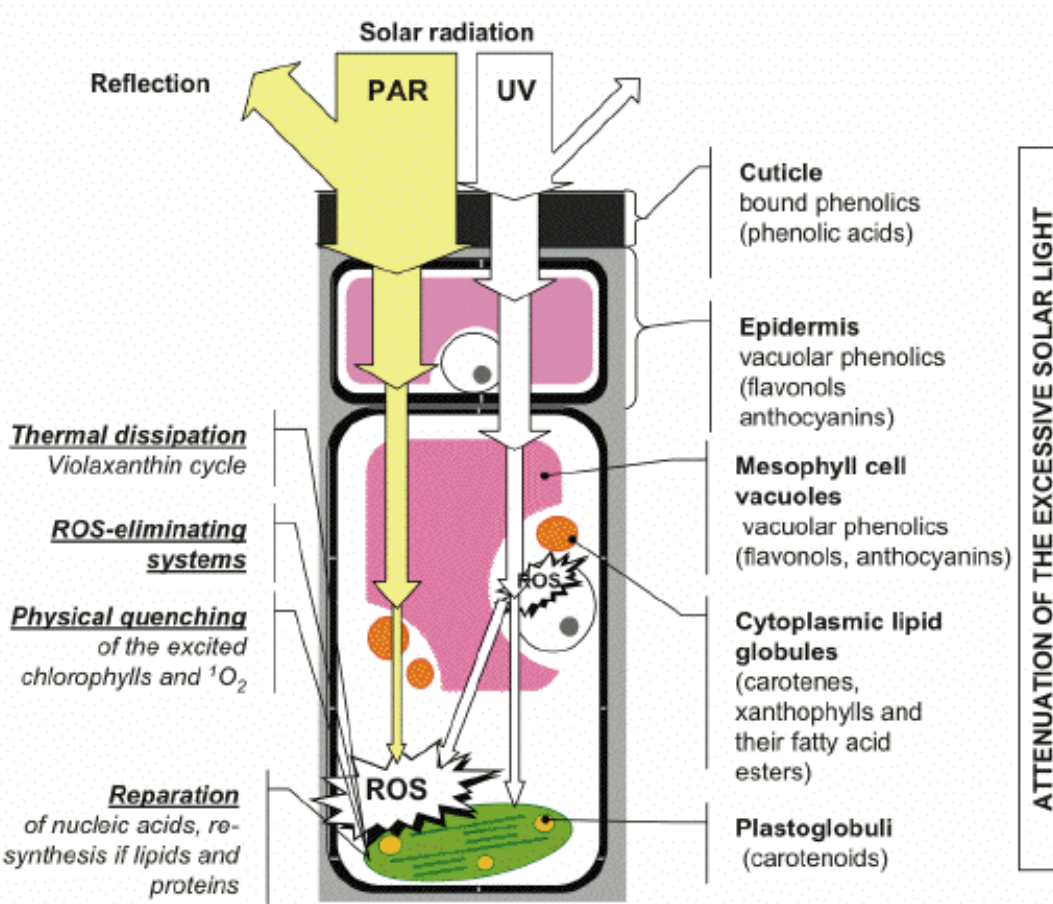


Figure 10 : Illustration des différentes étapes du stress photo-oxydant et des principaux mécanismes intervenant dans la photoprotection des végétaux à l'échelle cellulaire. ([Solovchenko and Merzlyak 2008](#)). PAR : Photosynthetically active radiation; ROS : Reactive Oxygen Species.

Ainsi, la synthèse de composés absorbant l'UV et présentant des activités antioxydantes, tels les caroténoïdes et les composés phénoliques chez les algues brunes et les végétaux terrestres, est une des réponses photo-protectrices possibles ([Cockell CS, 1999](#); [Rozema J., 2002](#); [Solovchenko & Merzlyak, 2008](#)).

Afin de tester cette hypothèse chez les algues brunes, plusieurs études ont quantifié les contenus en phlorotannins suite à une exposition des algues aux UV. La quantification la plus commune est réalisée sur des extraits de la fraction soluble des phlorotannins. Pour cela, différents solvants de type alcool (méthanol, éthanol, acétone) sont couramment utilisés en mélange avec de l'eau ([Waterman Peter G. 1994](#)). Les phlorotannins sont photosensibles, thermosensibles, ils s'oxydent rapidement et ont tendance à faire précipiter les protéines, ce qui demande de réaliser les extractions à l'obscurité, à une température inférieure à 40 °C et de favoriser une atmosphère inerte. Le choix des solvants va être dépendant de l'espèce d'algue choisie, l'article de [Koivikko et al. en 2005](#) présente une comparaison des teneurs mesurées en phlorotannins de *Fucus vesiculosus* en fonction du type de solvants utilisé. Pour exemple, l'utilisation d'un mélange acetone:eau (70:30) permet d'extraire un contenu en phlorotannins correspondant à 6 % du poids sec de l'algue contre seulement 1.5 % avec un mélange ethanol:eau (80:20).

En réalisant des quantifications par colorimétrie utilisant le réactif Folin Denis ou Folin Ciocalteu, il a été montré que face aux radiations UV-B les teneurs en phlorotannins solubles totaux pouvaient augmenter ([Swanson and Druehl 2002](#); [Pavia et al. 1997](#)), ou rester inchangées ([Henry and Van Alstyne 2004](#) ; [Hupel et al. 2011](#)).

- Etude de l'effet d'un stress biotique : le broutage

Les stress biotiques affectant les organismes peuvent être nombreux dans l'environnement marin, les interactions avec les parasites ou pathogènes, le développement d'épiphytes et d'épibioses (salissures marines ou biofouling), ou encore le broutage par les herbivores font l'objet d'un intérêt majeur dans l'étude des interactions entre les organismes marins.

L'implication des phlorotannins dans ces interactions biotiques pose encore à ce jour des questions. Plusieurs études ont pu montrer une augmentation des teneurs en phlorotannins

solubles, suite à un contact direct entre l’algue et l’herbivore (Yates and Peckol 1993), ou par un contact indirect médié par l’eau environnante d’une algue broutée (Toth and Pavia 2000).

Il a également été montré qu’il existait des variations de l’appétence de l’algue suite à un broutage ce qui suggère la mise en place de défenses afin de se prémunir d’une agression plus importante (Rohde et al. 2004, Flöthe et al. 2014 a, b). Dépendantes du brouteur et de l’algue, les interactions semblent être espèces-dépendantes (Yun et al. 2012). Dans le cas d’un contact direct ou indirect avec l’isopode *Idotea baltica*, il est observé une diminution de l’appétence pour *Fucus vesiculosus*. En revanche en présence du gastéropode *Littorina littorea*, seul un contact direct affecte l’appétence de l’algue (Rohde et al. 2004). Toutefois, le rôle déterrent des phlorotannins est discuté. Au vu de l’étude de Deal et al. (2003) utilisant un essai biologique de broutage par un oursin au long d’un processus de purification, l’activité déterrente proviendrait d’un galactolipide et non des phlorotannins. Il a néanmoins été montré très récemment que les phlorotannins joueraient bien un rôle dans les interactions algues-herbivores. Shibata et al. (2014) ont testé différents phlorotannins purifiés de l’algue brune *Ecklonia bicyclis* sur le comportement alimentaire du gastéropode *Turbo cornutus*. Cette étude a ainsi pu montrer qu’il y avait un effet significatif ($p<0,05$) des molécules Eckol, Fucofuroeckol A, Phlorofucofuroeckol A et Dieckol à une concentration de 0,1 µM sur le comportement alimentaire de *T. cornutus*. Il a également été montré que les composés phénoliques de faible polarité de type bromophenols (2,4-dibromophenol, 2,4,6-tribromophenol) étant majoritairement exsudés dans le milieu extérieur pendant la vie de l’algue (Shibata et al. 2006) présentaient une forte activité sur le comportement du gastéropode allant de la perte d’appétit à l’immobilisation jusqu’à la mort des individus.

Les mécanismes d’actions des phlorotannins sur les herbivores restent encore à explorer mais ces molécules pourraient ralentir la digestibilité de la nourriture par la précipitation des enzymes digestives ainsi rendues inactives. Cette action pourrait néanmoins chez certains herbivores être contrecarrée par la production de tensioactifs au sein du système digestif (Tugwell, S., Branch 1992) réduisant la complexation entre les phlorotannins et les protéines.

III. Connaissances acquises sur la synthèse des composés phénoliques:

Les composés phénoliques ou polyphénols sont des composés du métabolisme secondaire des végétaux. Ils constituent une famille de molécules organiques largement présentes dans le règne végétal. Tous ces composés sont caractérisés par la présence de plusieurs groupements phénoliques contenant le noyau phénol (Figure 11).

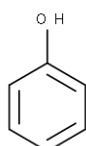


Figure 11 : Noyau phénol représentant la structure commune aux polyphénols

Les polyphénols sont subdivisés en trois grands groupes en fonction de leur structure : tout d'abord les flavonoïdes formés sur la base d'une unité flavanone présents chez les plantes terrestres, les tannins hydrolysables issus de la liaison entre l'acide gallique et un glucose présents chez les angiospermes et les algues vertes et enfin les phlorotannins construits sur la base d'unités phloroglucinol présents uniquement chez les algues brunes (Figure 12). Ces trois grands groupes présentent ainsi une multitude de structures et de fonctions d'importance capitale pour le métabolisme secondaire.

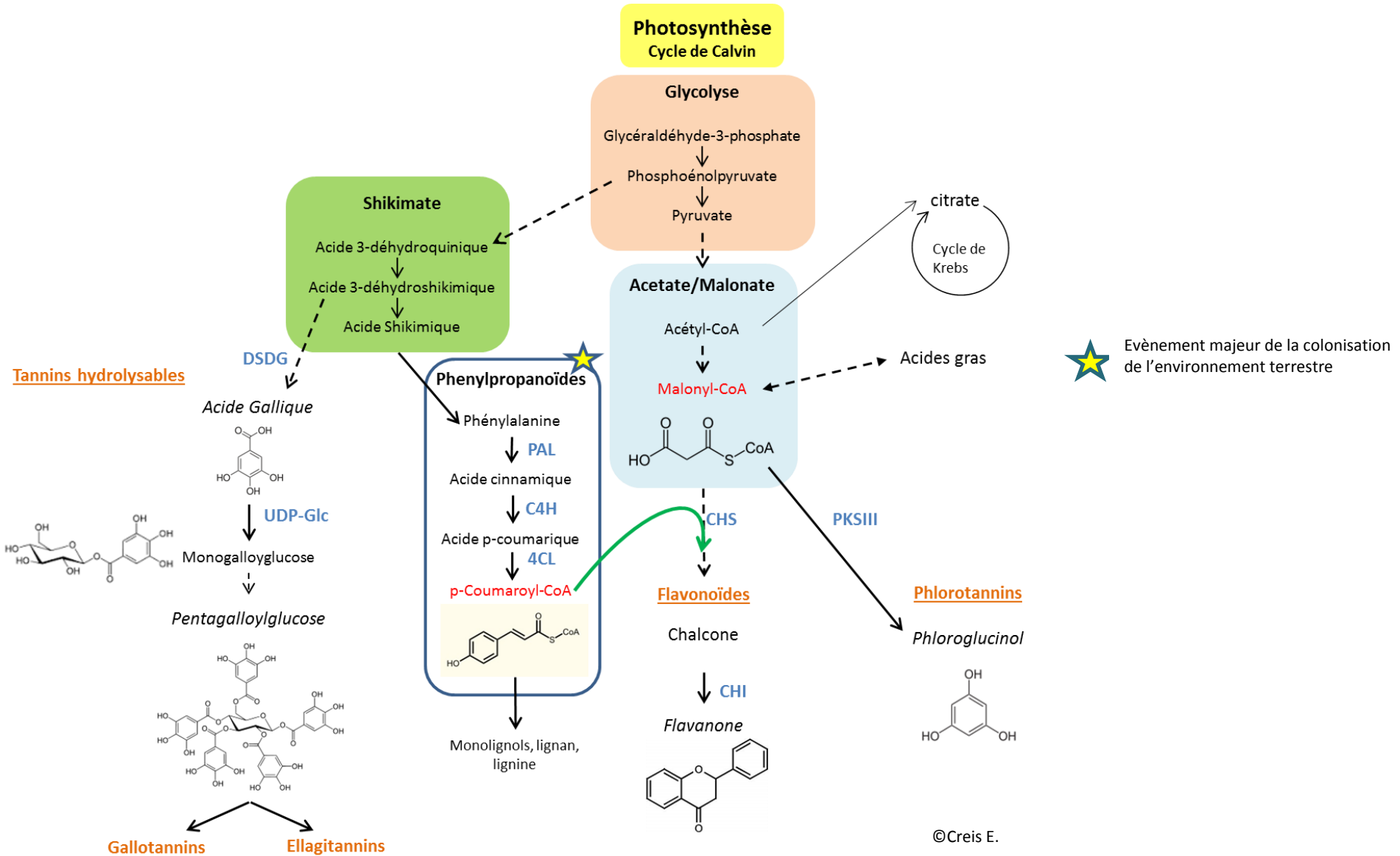


Figure 12 : Schéma représentant les principales voies de biosynthèse connues des composés phénoliques chez les végétaux. Modifié à partir de (Salminen and Karonen 2011). DSDG : déhydroshikimate déhydrogénase ; UDP-Glc : uridine diphosphate glucose ; PAL : phénylalanine ammonia-lyase ; C4H : cinnamate-4-hydroxylase ; 4CL : 4-coumaryl-coA-ligase ; CHS : chalcone synthase ; CHI : chalcone isomérase ; PKSIII : polycétide synthase

Chez les plantes terrestres : Les flavonoïdes

La voie de biosynthèse des composés phénoliques la plus étudiée dans le règne végétal est la voie des flavonoïdes chez les plantes terrestres. Cette voie est la résultante d'évènements majeurs de l'évolution tels que la sortie de l'eau ayant permis la colonisation de l'environnement terrestre. Chez les plantes, les composés phénoliques sont connus pour leur activité antioxydante, antimicrobienne, et pour leur pouvoir absorbant et filtrant contre les radiations UV (Cockell CS 1999; Rozema J. 2002) autant de fonctions indispensables pour la réussite de la colonisation de l'environnement terrestre.

Les premières spores fossiles attribuées à des plantes de type terrestre ont été retrouvées dans les sédiments datant d'il y a 450 millions d'années correspondant à la période de l'Ordovicien (Stewart, WN, & Rothwell 1993). C'est à ce même moment que le métabolisme des **phenylpropanoïdes** apparaît, il serait probablement issu d'un transfert latéral de gènes entre les bactéries du sol et les ancêtres des plantes (Emiliani et al. 2009) (Figure 12).

Ce métabolisme utilise la phénylalanine issue de la **voie du shikimate** à d'autres fins que la production de protéines. En effet, grâce à une phénylalanine ammonia-lyase (**PAL**) qui catalyse la conversion de l'acide aminé aromatique phénylalanine en acide cinnamique, puis à l'intervention d'une cinnamate-4-hydroxylase (**C4H**) et d'une 4-coumaryl-CoA-ligase (**4CL**), ce métabolisme produit du **p-coumaryl-coA**. Ce précurseur pourra ensuite être associé par l'intermédiaire d'une chalcone synthase (**CHS**) au **malonyl-CoA** issu de la **voie de l'acétate** pour former après cyclisation par une chalcone isomérase (**CHI**) la naringenin chalcone aussi appelée flavanone correspondant à la structure de base de tous les flavonoïdes (Figure 13A). Ces étapes cruciales ont ainsi permis l'émergence des composés que l'on connaît aujourd'hui comme faisant partie des flavonoïdes regroupant notamment les anthocyanes permettant la coloration des feuilles, fleurs et fruits des plantes (Cheynier et al. 2013) agissant également dans la communication à distance. On retrouve également les isoflavones, les flavones, impliquées dans la protection des plantes et également dans la stimulation des Rhizobiales formant par symbiose des nodosités permettant la fixation d'azote atmosphérique et sa transformation en ammonium directement assimilable par la plante. (Cooper 2007) (Figure 13B.)



Figure 13 : A. Flavanone, squelette de base des flavonoïdes. B. Exemple de nodulation retrouvée sur le système racinaire d'une légumineuse issu de la symbiose avec une bactérie de type rhizobium.

Si nous faisons le bilan des enzymes clés impliquées dans le métabolisme des composés phénoliques chez les plantes, nous retrouvons tout d'abord les enzymes initiatrices de la voie des flavonoïdes : **les chalcones synthases (CHS)** et les **chalcones isomérasées (CHI)**.

Les chalcones synthases (**CHS**) font partie du groupe des polyketides synthases de type III (PKS III) qui sont des enzymes clés chez les végétaux terrestres impliquant la synthèse de précurseurs de nombreux métabolites secondaires (flavones, flavonols, isoflavones, aurones, anthocyanines, phytoalexines de type stilbènes, etc..) mais aussi chez les bactéries, les champignons et quelques protozoaires comme l'indique l'arbre phylogénétique (Figure 14). Chez les plantes, les PKS III regroupent un grand nombre d'enzymes (chalcone synthases, PKS III, pyrone synthases,...) qui produisent une importante variété de produits différents à partir de la condensation d'unités malonyl-CoA et de différentes molécules « starters » tel que le coumaryl-CoA issu du métabolisme des phénylpropanoïdes ([Abe & Morita 2010](#)) (Figure 12).

La phylogénie des PKS III reportée Figure 14 montre une divergence importante entre deux groupes représentés d'un côté par les plantes et les bactéries et d'un autre côté par les champignons, les algues brunes, les amibes ou encore les actinobactéries.

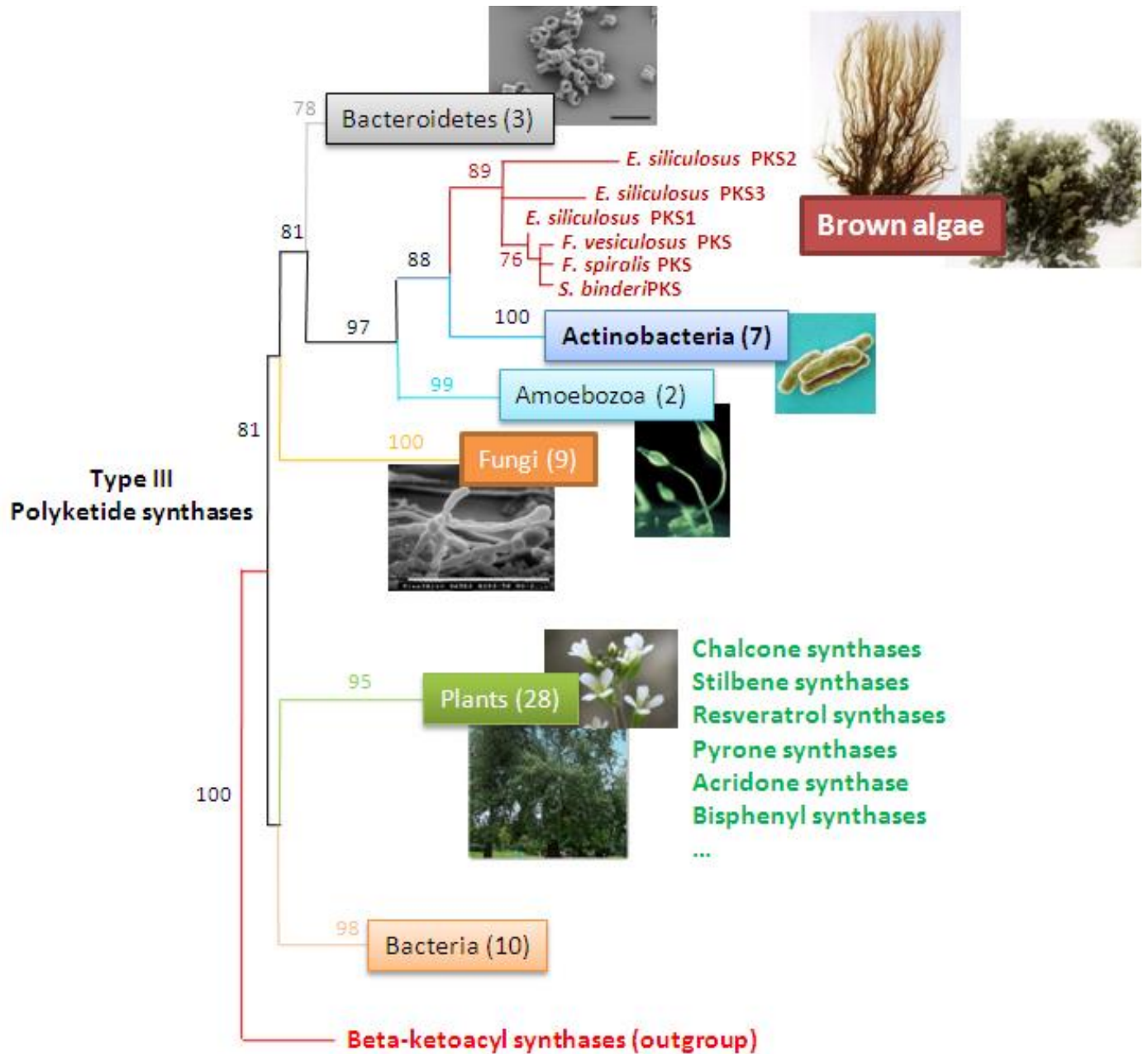


Figure 14 : Arbre phylogénétique représentatif de la diversité des PKS III dans l'arbre du vivant.

La phylogénie a été réalisée en maximum de vraisemblance avec PhyML, la valeur sur chaque branche représente son support et le nombre entre parenthèses correspond à la quantité d'espèces dans chaque sous-groupe (d'après Delage L.).

Les chalcones isomérasées (CHI) sont subdivisées en quatre grands types nommés ([Ralston et al. 2005](#), [Morita et al. 2014](#)): type I/CHI, type II/CHI, type III/FAP et type IV/ EFP (Figure 15)

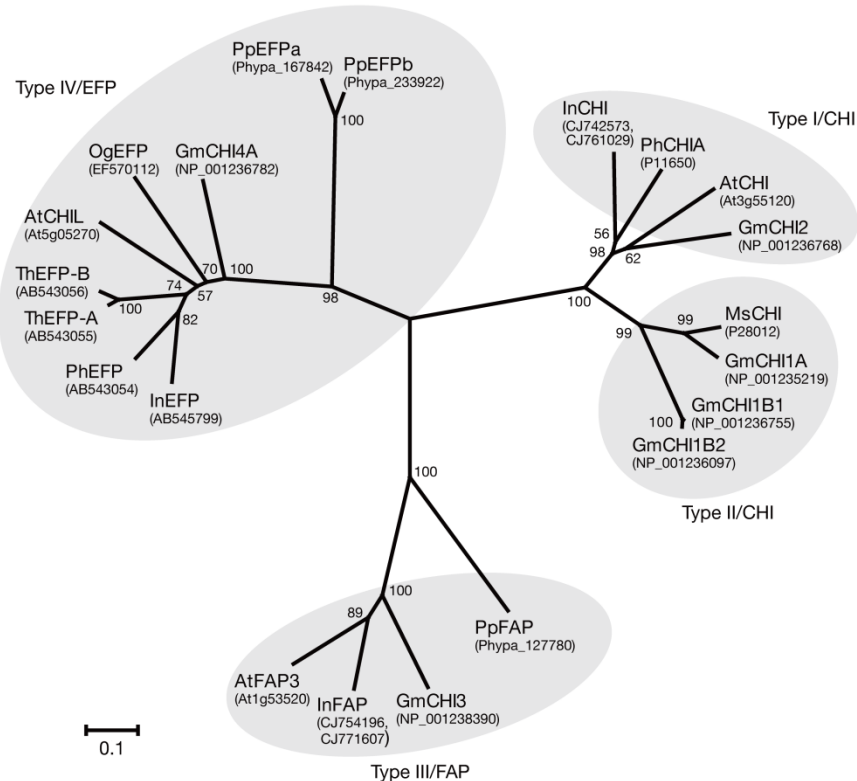


Figure 15: Classification des quatre types de chalcones isomérasées en fonction de leur activités connues ([Morita et al. 2014](#))

Le type I est présent uniquement chez les plantes vasculaires et participe à la formation des flavonoïdes en catalysant la cyclisation qui conduit à la transformation des chalcones en flavanones, précurseurs de la voie (Figure 16).

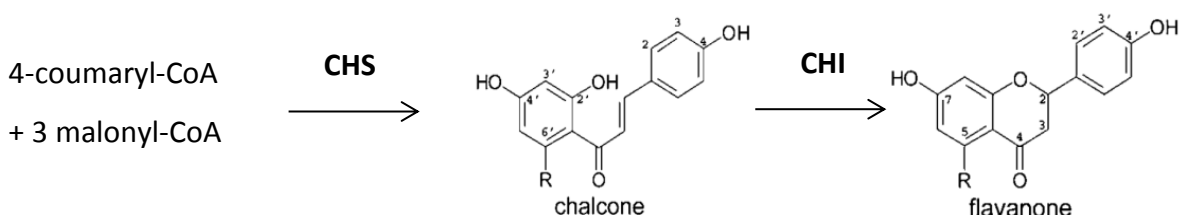


Figure 16: Schéma représentant la synthèse de flavanone à partir de la condensation d'unités coumaryl-coA et malonyl-coA par une chalcone synthase (CHS) puis par l'intermédiaire d'une chalcone isomérase (CHI) permettant la cyclisation de la chalcone.

Les chalcones isomérasées de *type II* sont quant à elles présentes chez les légumineuses et participent à la formation des isoflavonoïdes.

Le *type III* est retrouvé chez les plantes terrestres et les algues vertes. Trois protéines appartenant à cette classe III ont récemment été caractérisées chez *Arabidopsis* par [Ngaki et al., en 2012](#). Il avait été suggéré que ces gènes identifiés comme **chalcones isomérase-like** (CHIL) soient impliqués dans la voie de biosynthèse des flavonoïdes, mais leur caractérisation biochimique chez *Arabidopsis* a pu montrer que ces CHILs étaient en réalité des **Fatty Acid binding Proteins** (FAP) de trois classes différentes **1, 2 et 3**. Ce sont donc des protéines impliquées dans le métabolisme des acides gras. Ainsi, les chalcones isomérasées (CHI) uniquement retrouvées chez les plantes vasculaires seraient apparues récemment dans l'évolution des plantes terrestres et seraient issues d'une duplication de gène de CHIL (Figure 17).

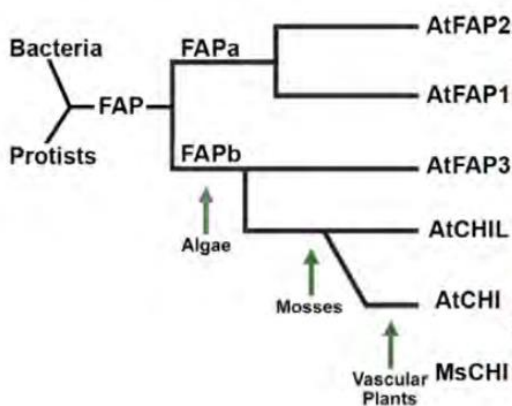


Figure 17: Phylogénie simplifiée des CHI présentant l'émergence des CHIL à partir du clade de AtFAP3, qui contient également des séquences d'algues, suivie de la différentiation des CHI chez les plantes vasculaires ([Ngaki et al., 2012](#)).

Enfin les chalcones isomérasées de *type IV* retrouvées uniquement chez les plantes terrestres ([Ralston et al. 2005](#)) ont récemment été montrées comme pouvant être impliquées dans la voie des flavonoïdes et notamment dans la pigmentation des fleurs par un mécanisme d'activation inconnu ([Morita et al. 2014](#)).

Suite à l'initiation de la voie de biosynthèse des flavonoïdes, d'autres enzymes vont intervenir et notamment apporter de nouvelles fonctionnalités aux molécules déjà produites, c'est le cas des **phénol-sulfotransférases**. Comme leur nom l'indique, ces enzymes ont la capacité de transférer un groupement sulfate depuis un donneur vers un groupement de type phénolique dans ce cas. Les sulfotransférases sont la plupart du temps des enzymes PAPS dépendantes, c'est-à-dire qu'elles vont utiliser le 3'-phosphate-5'-phosphosulfate (PAPS) comme donneur de groupement sulfate (Figure 18).

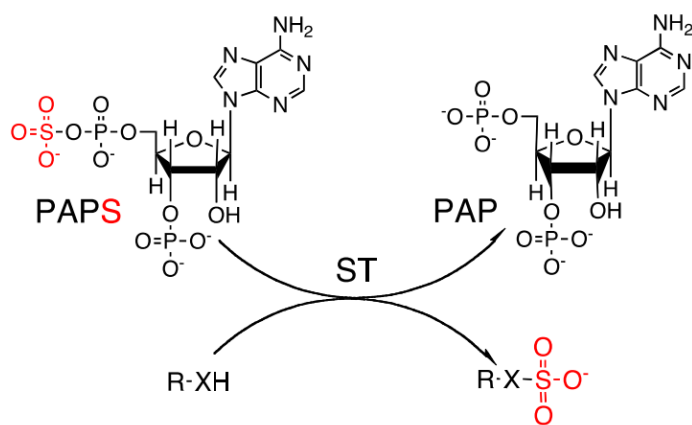


Figure 18: Représentation schématique de la réaction enzymatique d'une sulfotransférase (ST) utilisant le PAPS comme donneur de sulfate pour le transférer vers un accepteur, libérant ainsi le PAP (Paul et al. 2012).

Chez les mammifères, des phénol-sulfotransférases sont particulièrement bien étudiées. Leur activité de sulfatation peut être liée à la détoxification cellulaire et à la modulation d'activités biologiques sur des hormones stéroïdiennes ou des neurotransmetteurs. (Raffogianis 1997). Chez les plantes le rôle de la sulfatation reste encore méconnu malgré des efforts importants portés sur la caractérisation biochimique de ces enzymes utilisant notamment des flavonoïdes comme accepteur de sulfate (Varin, et al. 1992; Raffogianis 1997 ; Varin 2008 ; Hashiguchi et al. 2013; Hashiguchi et al. 2014).

Les **glycosyltransférases** vont également être des enzymes importantes dans le métabolisme des composés phénoliques non plus dans la synthèse de ces derniers mais dans leur stabilisation notamment au sein de vésicules ou dans leur détoxicification (Bowles et al. 2005). Ces enzymes vont agir par ajout d'un groupement carbohydrate ce qui va augmenter la solubilité des molécules dans l'eau, augmenter leur stabilité, réduire leur réactivité pouvant altérer leur activité biologique (Jones and Vogt 2014).

Chez les angiospermes et algues vertes : Les tannins hydrolysables

Une autre grande classe de composés phénoliques regroupe les tannins hydrolysables qui sont principalement retrouvés chez les angiospermes et les algues vertes. Ils sont construits sur la base structurale de l'acide gallique issu de la voie du shikimate (Figure 19).

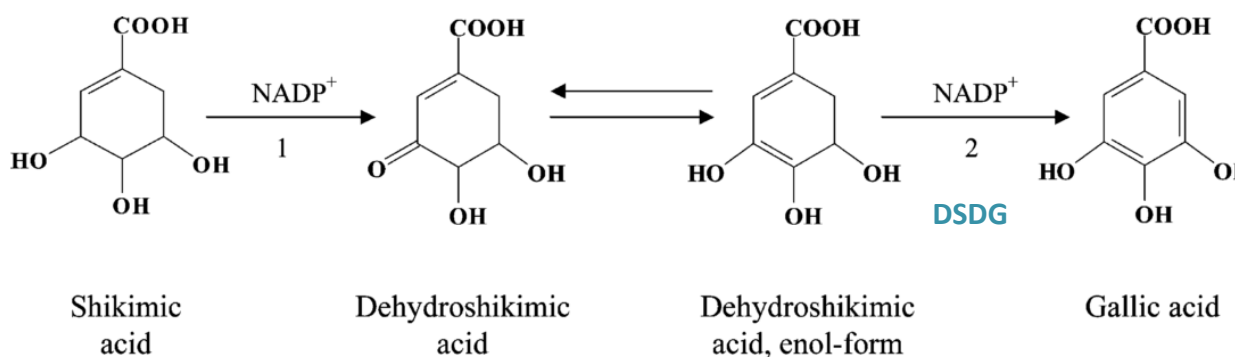


Figure 19 : Schéma représentant la conversion enzymatique de l'acide shikimique et de l'acide déydroshikimique en acide gallique. 1. Shikimate déhydrogénase 2. DSDG : Déhydroshikimate déhydrogénase d'après Ossipov et al. 2003.

L'acide gallique va ensuite être lié à un glucose par l'intermédiaire d'une uridine diphosphate glucose (UDP-Glc) transférase pour former un monogalloylglucose aussi appelé β -Glucogallin (Gross 2008) correspondant au monomère des gallotannins et ellagitannins (Mueller-Harvey

2001) (Figure 12). L'oligomérisation de ces tannins s'opère par des mécanismes de couplage oxydatif.

Chez les algues brunes : Les phlorotannins

Contrairement aux polyphénols des plantes terrestres, les enzymes de la voie de biosynthèse des phlorotannins ne sont pas connues à ce jour (Amsler and Fairhead 2006).

Les seules données disponibles au début de cette étude suggéraient que les phlorotannins pouvaient être formés par biosynthèse via la voie acétate-malonate aussi connue sous le nom de la voie des polycétides, par un processus qui pouvait impliquer une enzyme de type polyketide synthase de type III (Arnold and Targett 2002). L'annotation du premier génome d'une algue brune (Cock et al. 2010) a permis notamment d'identifier, par homologie de séquence avec les plantes terrestres, des gènes pouvant être impliqués dans le métabolisme des phlorotannins chez *Ectocarpus*. La voie du shikimate est aussi conservée chez *Ectocarpus* mais les enzymes clés telle que la PAL initiatrice de la voie des phénylpropanoïdes est absente. Comme vu précédemment, ceci souligne l'émergence du métabolisme des phénylpropanoïdes conduisant à la synthèse des flavonoïdes à partir de la colonisation terrestre par les végétaux de la lignée verte. D'autres enzymes clés pourraient cependant intervenir dans le métabolisme des phlorotannins notamment :

- ✓ 3 gènes homologues de polyketides synthases de type III (PKSIII)
- ✓ 2 gènes homologues de chalcones isomérases-like (CHIL)
- ✓ 4 gènes homologues d'aryl sulfotransférases (AST).
- ✓ 1 gène homologue d'une vanadium bromoperoxidase (v-BPO) pouvant intervenir dans la bromination et la complexation des phlorotannins avec les alginates de la paroi
- ✓ 1 gène homologue d'une UDP-glycosyltransférases (UGT) de la famille I qui regroupe toutes les UGTs qui modifient des composés phénoliques de plantes vasculaires.

IV. Contexte et objectifs du projet de thèse

Cette thèse s'inscrit dans la continuité du projet Phlorotan-ING de l'Axe 1 Génomique et chimie bleue 2009-2012 du GIS Europôle Mer. Financée par la Région Bretagne, cette thèse a été réalisée au sein de la Station Biologique de Roscoff en collaboration avec le laboratoire du LEMAR (UBO) à Brest. Deux collaborations internationales ont également été réalisées, la première avec le laboratoire Géomar à Kiel en Allemagne et la deuxième avec le département des Sciences Environnementales de la Faculté Agricole, de l'Université de Dalhousie à Truro au Canada.

Ce projet de thèse s'est articulé autour de deux principaux objectifs : Le premier consistait à poursuivre l'étude de la voie de biosynthèse des phlorotannins par la caractérisation biochimique d'enzymes recombinantes de l'algue brune modèle *Ectocarpus*. Le deuxième objectif était d'utiliser ces connaissances dans le but d'obtenir des outils biomoléculaires afin d'étudier l'implication des phlorotannins dans les mécanismes de défense chez les algues brunes.

Ce manuscript est présenté en deux parties, la première partie est divisée en trois chapitres présentant les travaux réalisés ou initiés sur l'étude et la caractérisation biochimique de six enzymes cibles, la polyketide synthase de type III (**Chapitre 1**), les deux chalcones isomérase-like (**Chapitre 2**) et les trois aryl-sulfotransférases (**Chapitre 3**). La deuxième partie est également présentée en trois chapitres, elle porte sur les études écophysiologiques réalisées sur le modèle *Fucus vesiculosus*. L'effet des rayonnements UV-B sera présenté dans le **Chapitre 4**, il sera suivi de l'étude portant sur l'effet du broutage par *Littorina littorea* (**Chapitre 5**), puis de la présentation d'un essai biologique permettant de tester des molécules d'intérêt sur l'attachement des littorines au substrat (**Chapitre 6**).

Partie 1 : Etude de la voie de biosynthèse des phlorotannins

Chapitre 1: Caractérisation de la Polyketide Synthase de type III d' <i>Ectocarpus</i>	29
Chapitre 2: Caractérisation biochimique et fonctionnelle de Chalcone Isomérases-like d' <i>Ectocarpus</i>	46
Chapitre 3: Etude préliminaire des aryl-sulfotransférases d' <i>Ectocarpus</i> : Surexpression des enzymes recombinantes.	73
Synthèse de la Partie 1.....	84

Chapitre 1: Caractérisation de la Polyketide Synthase de type III d'*Ectocarpus*.

Présentation de l'article :

Ce chapitre présente les résultats obtenus à l'issue du projet Phlorotan-ING sous forme d'un article publié dans Plant Cell en 2013. Ce projet finalisé au début de cette thèse a permis la caractérisation fonctionnelle d'une Polyketide synthase de type III d'*Ectocarpus*. La caractérisation biochimique et structurale de cette enzyme a permis de révéler son implication dans la première étape de la voie de biosynthèse des phlorotannins ie. : la synthèse du phloroglucinol. La validation de la fonction biologique *in vivo* a également pu montrer une corrélation entre l'expression du gène codant la PKS III et la synthèse du phloroglucinol lors de l'acclimatation d'une souche d'eau douce d'*Ectocarpus* à l'eau de mer.

Ma contribution à cet article m'a permis d'acquérir les connaissances techniques pour la surexpression et la purification d'enzymes recombinantes ainsi que pour l'extraction et la caractérisation par GC-MS des ligands associés aux protéines. Ces compétences ont ainsi pu être exploitées lors des deux études suivantes sur les chalcones isomérases-like et les aryl sulfotransférases d'*Ectocarpus*.

The Plant Cell, Vol. 25: 3089–3103, August 2013, www.plantcell.org © 2013 American Society of Plant Biologists. All rights reserved.

Structure/Function Analysis of a Type III Polyketide Synthase in the Brown Alga *Ectocarpus siliculosus* Reveals a Biochemical Pathway in Phlorotannin Monomer Biosynthesis^W

Laurence Meslet-Cladrière,^{a,b,c,1,2} Ludovic Delage,^{a,b,1} Cédric J.-J. Leroux,^d Sophie Goulitquer,^{a,b,d} Catherine Leblanc,^{a,b} Emeline Creis,^{a,b} Erwan Ar Gall,^c Valérie Stiger-Pouvreau,^c Mirjam Czjzek,^{a,b} and Philippe Potin^{a,b,3}

^a Centre National de la Recherche Scientifique, Unité Mixte de Recherche 7139, Station Biologique de Roscoff, 29688 Roscoff cedex, Brittany, France

^b Université Pierre et Marie Curie, Université Paris 6, Marine Plants and Biomolecules Laboratory, Unité Mixte de Recherche 7139, Station Biologique de Roscoff, 29688 Roscoff cedex, Brittany, France

^c Université Européenne de Bretagne, Université de Bretagne Occidentale, Laboratoire des Sciences de l'Environnement Marin, Unité Mixte de Recherche, Centre National de la Recherche Scientifique 6539, European Institute for Marine Sciences, 29280 Plouzané, Brittany, France

^d Centre de Ressources de Biologie Marine, MetaboMer and Structural Biology Core Facilities, Station Biologique de Roscoff, 29688 Roscoff cedex, Brittany, France

ORCID ID: 0000-0001-7358-6282 (P.P.).

Brown algal phlorotannins are structural analogs of condensed tannins in terrestrial plants and, like plant phenols, they have numerous biological functions. Despite their importance in brown algae, phlorotannin biosynthetic pathways have been poorly characterized at the molecular level. We found that a predicted type III polyketide synthase in the genome of the brown alga *Ectocarpus siliculosus*, PKS1, catalyzes a major step in the biosynthetic pathway of phlorotannins (i.e., the synthesis of phloroglucinol monomers from malonyl-CoA). The crystal structure of PKS1 at 2.85-Å resolution provided a good quality electron density map showing a modified Cys residue, likely connected to a long chain acyl group. An additional pocket not found in other known type III PKSs contains a reaction product that might correspond to a phloroglucinol precursor. In vivo, we also found a positive correlation between the phloroglucinol content and the PKS III gene expression level in cells of a strain of *Ectocarpus* adapted to freshwater during its reacclimation to seawater. The evolution of the type III PKS gene family in Stramenopiles suggests a lateral gene transfer event from an actinobacterium.

INTRODUCTION

Brown algal phenols attract considerable attention due to the wide variety of biological activities and potential beneficial health effects of these so-called phlorotannins (Stengel et al., 2011; Thomas and Kim, 2011). Phlorotannins are known only from brown algae (Phaeophyceae) and are structural analogs of condensed tannins, such as anthocyanidins and other flavonoid derivatives, a diverse class of metabolites with a vast array of functions in terrestrial plants (Dakora, 1995). They are also suggested to play multiple ecological roles in brown algae, such as antifouling substances (Sieburth and Conover 1965) and chemical defenses against herbivory (Toth and Pavia, 2000), in addition to providing

UV sunscreens to intertidal seaweeds (Amsler and Fairhead, 2006). Their chemical structure is based on aryl-aryl and/or diaryl ether linkages of phloroglucinol (1,3,5-trihydroxybenzene) units and is rather complex. Polymerization processes lead to a wide range of molecular sizes generally between 10 and 100 kD (Boettcher and Targett, 1993; McClintock and Baker, 2001; Le Lann et al., 2012).

Numerous dehydro-oligomers of phloroglucinol (fucols, fuhalols, phlorethols, fucophlorethols, and eckols) have been characterized by chemical analyses in the three past decades (Figure 1) and are essentially from Fucales (*Ascophyllum*, *Fucus*, and *Sargassum* species) and Laminariales (*Ecklonia* and *Eisenia* species) (Ragan and Glombitska, 1986; Amsler and Fairhead, 2006; Le Lann et al., 2012). These compounds, which can represent up to 25% dry weight, are found as soluble forms in cellular compartments (Amsler and Fairhead, 2006), as insoluble forms cross-linked to cell walls (Koivikko et al., 2005, 2007), and in extracellular exudates (Shibata et al., 2006). Phlorotannins accumulate especially in specialized secretion vesicles named physodes and may be synthesized in chloroplasts or endoplasmic reticulum (Schoenwaelder and Clayton, 1998; Arnold and Targett, 2002; Parys et al., 2007). Despite the importance of phlorotannins in brown algal biology and ecology, their corresponding biosynthetic pathways have been little characterized at the biochemical and molecular levels.

¹These authors contributed equally to this work.

²Current address: Université de Brest, Laboratoire Universitaire de Biodiversité et d'Ecologie Microbienne, Equipe d'accueil 3882, Technopôle Brest-Iroise, F-29280 Plouzane, France.

³Address correspondence to potin@sb-roscff.fr.

The author responsible for distribution of materials integral to the findings presented in this article in accordance with the policy described in the Instructions for Authors (www.plantcell.org) is: Philippe Potin (potin@sb-roscff.fr).

^WOnline version contains Web-only data.

www.plantcell.org/cgi/doi/10.1105/tpc.113.111336

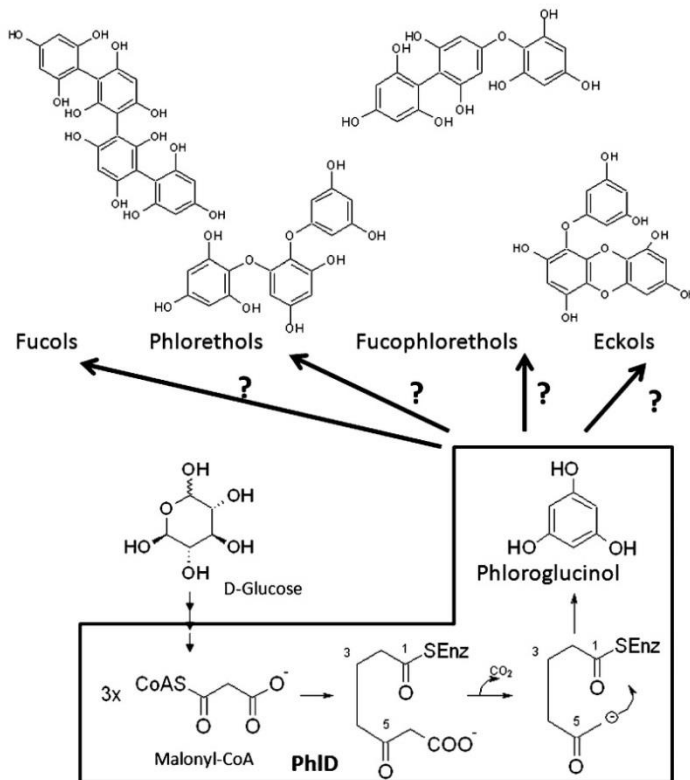


Figure 1. Chemical Structures of Phloroglucinol and Subunits of Four Different Structural Classes of Phlorotannins.

Boxed area shows the biosynthesis of a phloroglucinol by a bacterial type III PKS (PhID) in *P. fluorescens* from malonyl-CoA as the sole substrate. The polymerization steps of phloroglucinol (1,3,5-trihydroxybenzene) condensation are not known, and only the phloroglucinol synthesis from the acetate-malonate pathway was hypothesized by a process that may involve a polyketide synthase-type enzyme complex in brown algae.

Brown algal phlorotannins were proposed to be generated via the condensation of acetate and malonate units in a manner similar to the synthesis of fatty acids (Arnold and Targett, 2002; Amsler and Fairhead, 2006; Pelletreau and Targett, 2007; Pelletreau, 2008). In addition, other routes that produce aromatic compounds and tannins in land plants, such as the shikimate pathway and the phenylpropanoid pathway, have been suggested (Chen et al., 1997) as alternative conserved pathways and experimentally investigated without success in brown algae (Pelletreau, 2008). The sequential condensation of acetate and malonate units is catalyzed by type III polyketide synthase (PKS III; Abe and Morita, 2010), and the resulting polyketide chain could undergo cyclization and tautomerization to form phloroglucinol (Waterman and Mole, 1994). Previous work in bacteria has demonstrated the biosynthesis of phloroglucinol following this mechanism via the phloroglucinol synthase D (PhID; Figure 1), a PKS III from *Pseudomonas fluorescens* (Achkar et al., 2005; Zha et al., 2006). The PKS III protein family is specialized in the production of important secondary metabolites corresponding to aromatic polyketides that are of increasing economic interest (Abe and Morita, 2010). The biological roles of these molecules have been related to

defense (phytoalexins and antibiotics; Abe and Morita, 2010), development (differentiation factor; Sankaranarayanan, 2006), and pigmentation (chalcones and flavones; Abe and Morita, 2010).

PKS III proteins have been reported to date in many organisms, including bacteria, land plants, fungi, and amoebas. The best described are probably the chalcone synthases (CHSs) and stilbene synthases (STSs), which produce precursors of the flavonoid and stilbene pathways in terrestrial plants by catalyzing the sequential decarboxylative addition of three acetate units from malonyl-CoA to a *p*-coumaryl-CoA starter molecule derived from the general phenylpropanoid pathway (Pfeifer and Khosla, 2001). The first crystal structure of a PKS III was resolved for the alfalfa (*Medicago sativa*) CHS (Ferrer et al., 1999), and a dozen new structures have been described to date for plants (Abe and Morita, 2010) and bacteria (Austin et al., 2004a). Among them, a type III PKS from *Mycobacterium tuberculosis*, Mtu-PKS18, displays an unusual broad specificity for aliphatic long-chain acyl-CoA starter units (C6–C20) to produce tri- and tetra ketide pyrones (Sankaranarayanan et al., 2004).

The active state of PKS III enzymes is always found in dimeric form and they structurally and functionally differ from the

multimodular type I PKS and the multisubunit complexes of type II PKS (Pfeifer and Khosla, 2001). These structural studies revealed that the catalytic residues of PKS III are structurally conserved (Abe and Morita, 2010) and correspond to the catalytic triad (Cys-164, His-303, and Asn-336; following the numbering in alfalfa CHS). However, the active site cavity in each protein is drastically different, thus explaining the diversity of PKS III in terms of their substrate specificity and polyketide length (Jez et al., 2001). The amino acid residues in the active site of type III PKS (i.e., Thr-197, Gly-256, and Ser-338) (following numbering in CHS of alfalfa) are involved in the selectivity of starter substrate and control of product chain length (Ferrer et al., 1999; Jez et al., 2002; Abe et al., 2005a, 2005b).

The filamentous alga *Ectocarpus siliculosus* is becoming a reference model for studying brown algal biology (Charrier et al., 2008; Cock and Coelho, 2011) due to the molecular and genetic tools that have recently been made available, including a complete genome sequence (Cock et al., 2010). During the evolution of Eukarya, the Stramenopiles, the lineage that encompasses brown algae (Brown and Sorhannus, 2010), have been evolving for over a billion years independently compared with the most commonly studied multicellular eukaryotes comprising opisthokonts (represented by animals and fungi) and Plantae (red algae, green algae, and plants). Interestingly, the *E. siliculosus* genome was predicted to encode three PKS III, which like *P. fluorescens* PhID, may direct phloroglucinol biosynthesis (Cock et al., 2010). Moreover, one isoform of PKS III is highly represented in the expressed sequence tags libraries of *E. siliculosus*, probably reflecting a key role in a biosynthetic pathway (Cock et al., 2010). Previous attempts in the brown seaweed *Sargassum binderi* to characterize the biochemical function of a putative type III PKS failed to express a soluble active enzyme, and it was reported that a crude extract from a *Escherichia coli* recombinant clone incubated with malonyl-CoA yielded tetraketide pyrone but no phloroglucinol as products (Baharum et al., 2011). So far, the expression of recombinant soluble and active enzymes from brown algae remains highly challenging.

In this study, we provide phylogenetic, biochemical, and structural evidence that support a primary role of PKS1 in the condensation of malonyl-CoA to produce phloroglucinol, the direct precursor of phlorotannins unique to brown algae. We also link the phloroglucinol biosynthesis to physiological processes involved in the acclimation to salinity of a freshwater strain of *Ectocarpus*.

RESULTS

Phylogenetic Analysis of the Predicted *E. siliculosus* Type III PKS

Three genes encoding proteins similar to type III PKS (loci Esi0024_0032, Esi0110_0075, and Esi0046_0100 in the ORCAE database, named *E. siliculosus* (*Esi*) PKS1 [CBN76919.1], *Esi*PKS2 [CBJ48712], and *Esi*PKS3 [CBJ28635.1], respectively; <http://bioinformatics.psb.ugent.be/orcae/overview/Ects1>), were predicted during the annotation of the *Ectocarpus* genome (Cock et al., 2010). The amino acid sequences of *Esi*-PKS1 and *Esi*-PKS3 were highly similar to the PKS cDNA recently cloned in *S. binderi* that codes for a putative type III PKS. (Baharum et al., 2011). By

contrast, the *Esi*-PKS2 cDNA was only a partial sequence of the gene. Indeed, *Sb*-PKS and *Esi*-PKS1 open reading frames were 85% identical at the nucleotide level, and the two proteins of 414 amino acids in length shared 92% identical residues and up to 97% similar residues (see Supplemental Figure 1 online). A phylogenetic analysis was performed on 161 representative type III PKS proteins from eukaryotes and bacteria, including functionally characterized enzymes accepting a diversity of CoA thioester starter units. The global topology of the maximum likelihood tree showed major clades of PKS III, based on bootstrap analyses (Figure 2 and Supplemental Figure 1 online).

Clade I, supported by a bootstrap value of 82, contains only prokaryote enzymes from a large panel of bacterial groups (mainly belonging to cyanobacteria, proteobacteria, bacteroidetes, actinobacteria, and firmicutes). In clade I, none of the proteins have been functionally characterized, and most of them were discovered from environmental samples. Clade II corresponds to proteins from both eukaryotic and prokaryotic organisms and is clearly split into two well-supported groups. The first one contains only proteins from Amoebozoa (a sister lineage of opisthokonts), in which the PKS III steely 2 has been well characterized to produce acylphloroglucinols in vitro and in vivo (Sankaranarayanan, 2006). The second branch, strongly supported by a high bootstrap value of 99% leads to Actinobacteria proteins (in particular Corynebacteriaceae), such as Mtu-PKS18, which is closely related to PKS III of photosynthetic Stramenopiles (Ochrophyta) represented by two brown algae (*E. siliculosus* and *S. binderi*) and the pelagophyte *Aureococcus anophagefferens*.

Clade III contains exclusively prokaryotic proteins from actinobacteria, bacteroidetes, proteobacteria, and acidobacteria, but, in contrast with the first bacterial clade, this one contains numerous proteins that have been biochemically studied in the past 10 years. Most of the characterized enzymes are present in Actinobacteria, in particular *Streptomyces* species (1,3,6,8-tetrahydroxynaphthalene synthase [THNS], RppA and RppB, encoded in the same gene cluster and SrsA, and SrsB encoded in the same gene cluster in another species) and *Mycobacterium* species (PKS10 and PKS11). Another well-characterized PKS III activity has been described in the γ -proteobacterium *P. fluorescens* (PhID). The compounds produced by enzymes from the corresponding gene clusters have antibiotic function (napyradiomycine A in *Streptomyces coelicolor* and 2,4-diacylphloroglucinol in *P. fluorescens*; Bangera and Thomashow, 1999; Funa et al., 2002) or confer resistance to antibiotics (penicillin resistance in *Streptomyces lividans*; Funabashi et al., 2008) or virulence (complex lipids in *M. tuberculosis*; Waddell et al., 2005).

Finally, Clades IV, V, and VI, supported with lower bootstrap values, grouped together eukaryotic PKS III proteins belonging to fungi, Amoebozoa, and land plants. Among them, plant PKS III enzymes have only been well studied, especially those involved in the flavonoid pathway (Abe and Morita, 2010, Ferrer et al., 1999; Jez et al., 2001, 2002; Austin et al., 2004b).

Expression and Enzymatic Activities of Recombinant PKS1 Protein

To characterize the type III PKS function of PKS1, we produced the enzyme as recombinant protein with a His-tag tail at the

Partie 1 : Voie de biosynthèse des phlorotannins

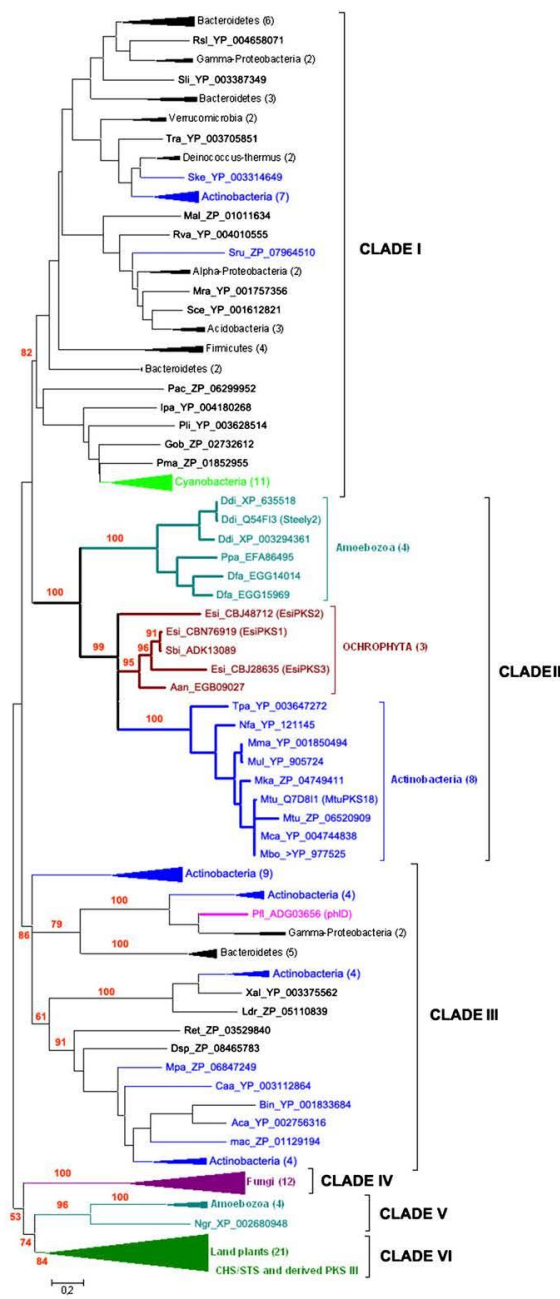


Figure 2. Unrooted Phylogenetic Tree of PKS III.

The phylogenetic tree presented here was constructed using the maximum likelihood approach. Numbers indicate the bootstrap values in the maximum likelihood analysis. The full listing of the aligned proteins is reported in Supplemental Data Set 1 and Supplemental Table 1 online. Rsl, *Runella slythiformis*; Sli, *Spirosoma linguale*; Tra, *Truepera radiovictrix*;

N terminus. In SDS-PAGE gels (see Supplemental Figure 2A online), the purified PKS1 migrated as a 40-kD protein, consistent with the predicted theoretical mass of 40.975 kD calculated without 34 amino acids of the putative N-terminal signal peptide. The identity of the purified protein was verified by matrix-assisted laser desorption/ionization-time-of-flight (MALDI-TOF) mass spectrometry (see Supplemental Figure 2B online). An additional band was detected on the SDS-PAGE; however, the dynamic light scattering analysis showed that a homogenous pure protein was present in the sample. Both results suggest that PKS1 forms a physiologically active, dimeric complex, as already shown for most type III PKS, including PKS18 (Sankaranarayanan et al., 2004).

Activity of the recombinant PKS1 protein was assayed in presence of various fatty acyl-CoA esters as starter substrates and malonyl-CoA as the extender molecule. We first employed ¹⁴C malonyl-CoA as a tracer to visualize radioactive products of condensation reaction. After extraction, compounds were fractionated by thin layer chromatography (TLC) and revealed by exposure to a phosphor imager plate (Figure 3A).

When nonradioabeled malonyl-CoA or acetyl-CoA was used as a starter molecule in the reaction mixture, only one radioactive product was observed (labeled "Band I" on Figure 3A) that was absent in the two negative controls consisting in incubations of ¹⁴C malonyl-CoA with boiled enzyme and without enzyme addition. When synthetic lauroyl-CoA (C16:0-CoA) and palmitoyl-CoA (C18:0-CoA) were used as starters (Figure 3A), additional reaction products were detected in incubation mixtures (labeled "Band II" on Figure 3A). The identity of some of the corresponding products was further investigated. For this purpose, similar experiments were conducted using nonradioactive malonyl-CoA as extender. With either acetyl-CoA or malonyl-CoA as starters, the major reaction TLC-separated product was scraped from the spot corresponding to "Band I" in the silica plate and extracted in methanol and was identified as phloroglucinol by liquid chromatography-electrospray ionization-mass spectrometry (LC-ESI-MS) analysis (Figures 3B and 3D) and confirmed by gas chromatography-mass spectrometry (GC-MS) using authentic standard (see Supplemental Figure 3 online).

A similar observation was previously described for the recombinant PhID enzyme from the bacteria *P. fluorescens* (Zha et al., 2006). By contrast, Baharum et al. (2011) did not observe phloroglucinol formation after incubation of brown alga *S. binderi* PKS in presence of various acyl-CoAs and proposed the formation of

Ske, *Sanguibacter keedieii*; Mal, *Maritimibacter alkaliphilus*; Rva, *Rhodomicromium vanniellii*; Sru, *Segniliparus rugosus*; Mra, *Methylobacterium radiotolerans*; Sce, *Sorangium cellulosum*; Pac, *Parachlamydia acanthamoebae*; Ipa, *Isosphaera pallida*; Pl, *Planctomyces limnophilus*; Gob, *Gemmata obscuriglobus*; Pma, *Planctomyces maris*; Ddi, *Dictyostelium discoideum*; Ppa, *Polysphondylium pallidum*; Dfa, *Dictyostelium fasciculatum*; Esi, *Ectocarpus siliculosus*; Sbi, *Sargassum binderi*; Aan, *Aureococcus anophagefferens*; Tpa, *Tsukamurella paucimetaabolita*; Nfa, *Nocardia farcinica*; Mma, *Mycobacterium marinum*; Mul, *Mycobacterium ulcerans*; Mka, *Mycobacterium kansasi*; Mtu, *Mycobacterium tuberculosis*; Mca, *Mycobacterium canetti*; Mbo, *Mycobacterium bovis*; Pfl, *Pseudomonas fluorescens*; Xal, *Xanthomonas albilineans*; Ldr, *Legionella drancourtii*; Ret, *Rhizobium etli*; Dsp, *Desmospora* sp.; Mpa, *Mycobacterium parascrofulaceum*; Caa, *Catenulispora acidiphila*; Bin, *Beijerinckia indica*; Aca, *Acidobacterium capsulatum*; mac, marine actinobacterium.

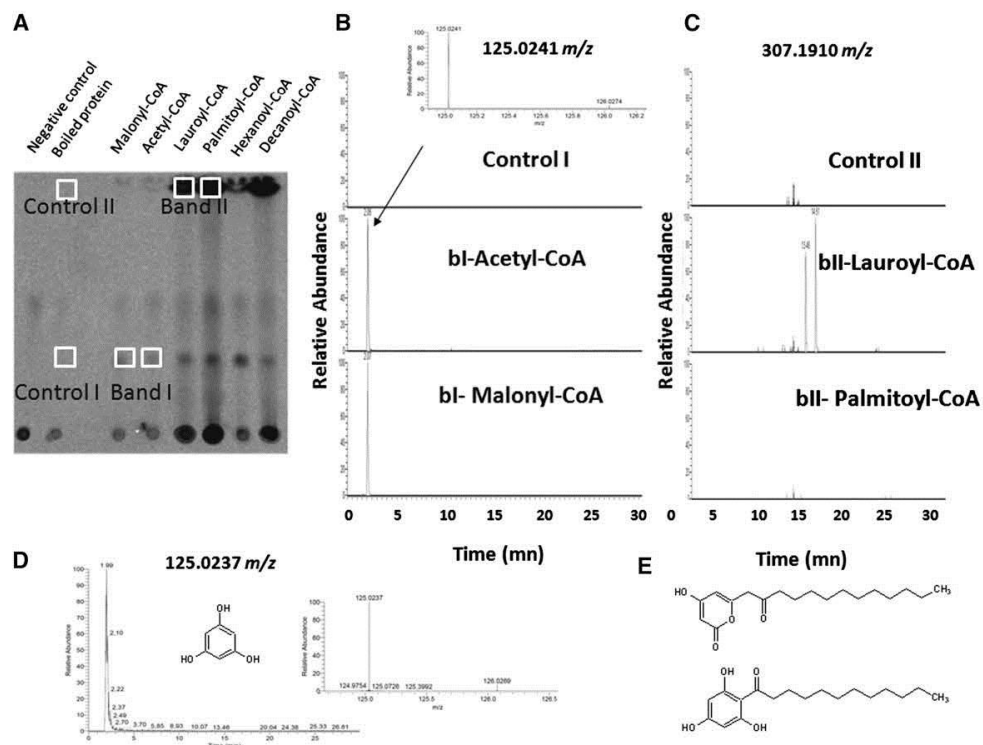


Figure 3. Identification of PKS1 Reaction Products by TLC Separation and UPLC-ESI-MS Analysis.

Recombinant protein was incubated with different CoA esters as starters and ¹⁴C-malonyl-CoA or unlabeled malonyl-CoA as extender. (A) TLC analysis of radiolabeled reaction products of PKS1, detected using a phosphor imager. Chemically synthesized CoA esters used as starters are indicated above each lane. No product was observed without addition of PKS1 (negative control) or after addition of boiled enzyme. Controls display only one radioactive spot, which corresponds to the unreacted ¹⁴C-malonyl-CoA at the origin of the migration. (B) Ultra-HPLC-ESI-MS chromatogram of a precursor ion at 125.0241 m/z of TLC-separated products corresponding to band I (bI), from incubation of unlabeled malonyl-CoA with acetyl-CoA or malonyl-CoA as starters, fitting with authentic phloroglucinol standard (see [D]). Inset displays the mass spectrum of the extracted ion at retention times (rt) 2.08 and 125.0241 m/z. The control I corresponds to an incubation of band I scraped from TLC in the lane corresponding to the incubation of boiled enzyme with malonyl-CoA as a starter and unlabeled malonyl-CoA as an extender. (C) Ultra-HPLC-ESI-MS chromatogram of a precursor ion at 307.1910 m/z of TLC-separated products corresponding to band II (bII), from incubation of unlabeled malonyl-CoA as extender with lauroyl-CoA and palmitoyl-CoA as starter molecules. The control II corresponds to an incubation of band II scraped from a TLC in the lane corresponding to the incubation of boiled enzyme with lauroyl-CoA as a starter and unlabeled malonyl-CoA as an extender. (D) Ultra-HPLC-ESI-MS chromatogram of a precursor ion at 125.0237 m/z of an authentic phloroglucinol standard. Insert displays the mass spectrum of the extracted ion at rt 2.10 min and 125.0237 m/z. (E) Putative structures corresponding to the formula C₁₈H₂₈O₄ and 307.1910 m/z are drawn corresponding to a tetraketide pyrone and an acylphloroglucinol, respectively.

triketide and tetraketide pyrone derivatives. In the presence of lauroyl-CoA, scraped from the spot corresponding to "band II" on the silica plate and extracted in methanol, only two major metabolites were detected by LC-ESI-MS analysis (Figure 3C; see Supplemental Figure 4 online). These two products feature the same [M-H]⁻ 307.1910 mass-to-charge ratio (*m/z*) at retention time (rt) 13.46 and 14.61 min with a putative identification as C₁₈H₂₈O₄ (Δ ppm -1.571). They are likely to be two different tetraketide derivatives from lauroyl-CoA: 1-(2,4,6-trihydroxyphenyl)-dodecan-1-one and 4-hydroxy-6-(2-oxotridecyl)-2H-pyran-2-one, that are also identified in ultra performance liquid chromatography (UPLC)-mass spectrometry (MS) analysis of whole incubation

medium (Figure 3E; see Supplemental Figure 4 and Supplemental Table 2 online). Moreover, they were not detected in the presence of palmitoyl-CoA (Figure 3C). This indicates that the enzyme formed specific metabolites depending on the acyl chain of the starter units of the reaction.

X-Ray Crystallographic Structure of *Ectocarpus* PKS1

To explore the potential structural basis for the observed substrate specificity and catalytic mechanism of PKS1, we solved its crystal structure. The structure of Esi-PKS1 was solved at 2.85-Å resolution using molecular replacement (Figure 4). The

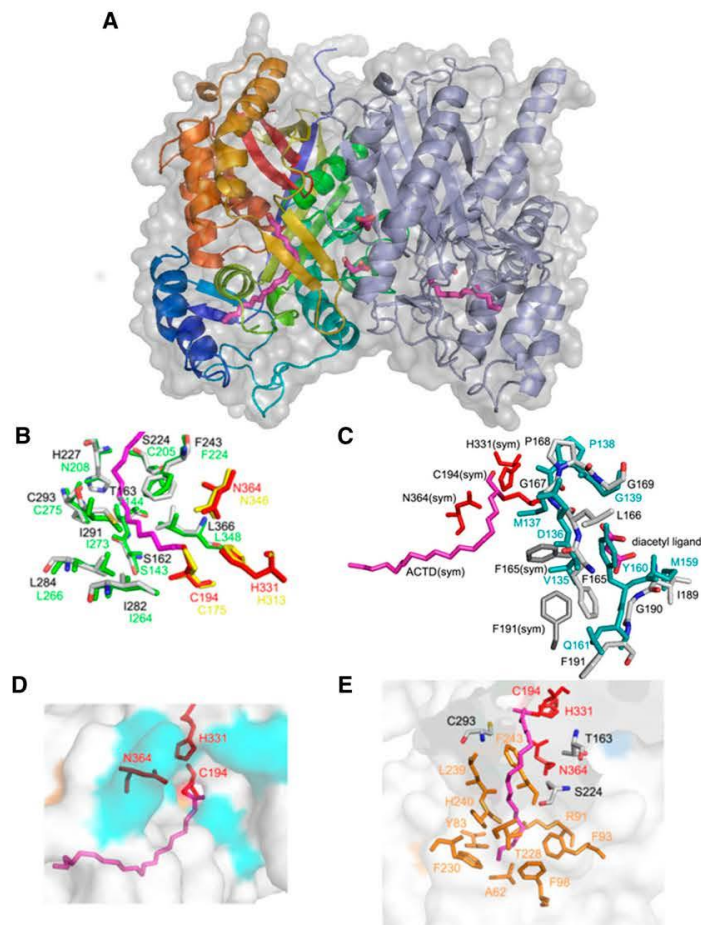


Figure 4. Overall Structure of Esi-PKS1 and Details of the Structural Insights of the Active Site and of the Tunnel for Binding of Long-Chain Acyl-CoAs.

(A) A ribbon representation of the dimeric Esi-PKS1 molecule superposed with its surface view. The two monomers are represented as ribbons that are rainbow-colored from the N terminus (blue) to the C terminus (red) for molecule A and gray for molecule B of the dimer.

(B) Superimposition of the initiation and elongation pocket of Esi-PKS1 (gray) and Mtu-PKS18 (green). Residues surrounding the substrate binding pocket in the tunnel region are labeled pinpointing the two differences between Esi-PKS1 and Mtu-PKS18, Ser-224/Cys-205 and His-227/Asn-208, respectively. These residues are likely important in the different catalytic machinery. Residue labels are gray and red for Esi-PKS1 and green and yellow for Mtu-PKS1.

(C) Structural basis for substrate specificity at the dimer interface (near the putative phloroglucinol product): Two successive GF stretches are present in each monomer, the second Phe (Phe-191) is in an atypical position. These residues are located in two adjacent loops near the surface of the enzyme, allowing the formation of a new pocket at the dimer interface. A product has been entrapped in the crystal structure that is represented as a diketide, given the resolution of the crystal structure.

(D) Surface view of the entrance of the substrate in the CoA binding site that is highlighted by the side chains of Cys-194, His-331, and Asn-364, which form the catalytic triad and the acyl binding site of CoA. Esi-PKS1 possesses a tunnel where long chain fatty acid acyl-CoA starter molecules can be inserted before ligation to the catalytic Cys and elongation by addition of acetate units provided from malonyl-CoA.

(E) Surface view and a close-up view of the residues surrounding the binding tunnel of the acyl-CoA starter where long fatty acid chains of starter acyl-CoA molecules can be inserted before ligation to the catalytic Cys-194.

space group of the crystals was determined to be $P_{2_1}2_12_1$, with unit cell dimensions $a = 61.3 \text{ \AA}$, $b = 83.4 \text{ \AA}$, and $c = 152.7 \text{ \AA}$ (Table 1). The asymmetric unit contains two molecules, giving a crystal volume per protein mass (V_M) of $2.39 \text{ \AA}^3 \text{ D}^{-1}$ and a solvent content of 48.5% by volume (Matthews, 1968).

The quaternary structure of PKS1 is a dimer, formed by two monomers present in the asymmetric unit of PKS1 crystal structure (Figure 4A). The dimeric arrangement is perfectly superimposable with those observed in other polyketide synthase crystal structures. In Figure 5, the primary sequence of PKS1 is

Table 1. Data Collection, Phasing, and Refinement Statistics for Esi-PKS1

Beamline at ESRF	ID23-I
Wavelength (Å)	0.979
Unit cell parameters (in Å)	a = 61.3, b = 83.4, c = 152.7
Space group	P2 ₁ 2 ₁ 2 ₁
Resolution range (Å)	49.4–2.85 (3.02–2.85) ^a
Number of observations	70,191 (1602)
Number of unique reflections	16,506 (2670)
Completeness (%)	91.7 (77.4)
<I/σ(I)>	8.5 (3.4)
Redundancy	4.2 (4.3)
R _{sym} ^b ; R _{point} ^c (%)	10.0 (33.3); 5.3 (17.7)
Map correlation coefficient (CC _{1/2})	0.994 (0.989)
Refinement statistics	
Resolution range	49.4–2.85
R factor (R _{free} on 5%)	21.2 (23.6)
Overall B factor (Å ²)	39.97
No. of protein atoms (mean B-factor in Å ²)	5,746 (A 42.2; B 39.4)
No. of ions/ligand atoms (mean B-factor in Å ²)	110 (21.6)
No. of solvent atoms (mean B-factor in Å ²)	345 (23.5)
Rms deviation in bond lengths (Å) ^d	0.01
Rms deviation in bond angles (°)	1.369
Ramachandran plot, most favored (%)	96.2
Ramachandran plot, additional allowed (%)	2.5

^aValues for the highest resolution shell are given in parenthesis.

^bR_{sym} = $\sum |I - I_{av}| / \sum |I|$, where the summation is over all symmetry-equivalent reflections.

^cR_{point} corresponds to the multiplicity weighted R_{sym}.

^dRms, root mean square.

compared with those of various other polyketide synthases and the residue positions are marked with respect to their secondary structure positions in the overall PKS fold. Structural alignment scores of several structures of type III PKSs deposited in the Protein Data Bank (PDB), computed by the Dali server, are provided in Supplemental Table 3 online.

A major part of the residues corresponding to the initiation and elongation pockets of the active site are identical between Esi-PKS1 and Mtu-PKS18 (Ser-143/Ser-162, Thr-144/Thr-163, Phe-224/Phe-243, Ile-264/Ile-282, Leu-266/Leu-284, Ile-273/Ile-291, and Cys-275/Cys-293). The superimposition of the two structures shows that the positions are also well conserved (Figure 4B), and globally the volume of the cavity is equivalent. Nevertheless, two of these amino acids differ (Cys-205/Ser-224 and Asn-208/His-227), suggesting that these residues may contribute to the functional specificity of cyclization exhibited by the two enzymes. The most evident change in Esi-PKS1 is the presence of His-227, which occupies more space than the equivalent Asn-208 in Mtu-PKS18. As it was described for Mtu-PKS18, Asn-208, Leu-266, and Leu-348 significantly affect the active site volume. Therefore, the presence of His-227 instead of an Asn residue might be crucial to produce acylphloroglucinols. For the synthesis of phloroglucinol, the cyclization of a shorter polyketide (triketide) should be more likely related to the proximal amino acids. This set of residues is completely identical, suggesting a fine-tuning of the production of the phloroglucinol core in Esi-PKS1, whereas

lactonization is found in Mtu-PKS18. For example, a Thr is responsible for either the Claisen cyclization C6→C1 giving rise to a phloroglucinol core in CHS or the aldol switch C2→C7 mechanism in STS (Austin et al., 2004b). The difference is due to the distance of the hydroxyl group oxygen that can activate a water molecule in the case of STS and a decarboxylation of the polyketide. However, the resolution of our structure is not sufficient to conclude more precisely on the reaction mechanism.

Similar to the presence of myristic acid in the crystal structure of PKS18 (Sankaranarayanan et al., 2004), the electron density in the active site of the Esi-PKS1 crystal structure revealed the presence of an aliphatic chain (Figure 6). The molecule was modeled as a C20 acyl group in order to match the electron density maxima that coincided well with chain length and distribution of double bonds of this acyl compound. The final structural model of Esi-PKS1 consists of 379 residues, representing residues 36 to 414 of each monomer, both of which bind an acetate ion and an arachidonyl group (ACTD group). The atomic distances of the acetate oxygen and the proximal Cys sulfur (Cys-194) are indicative of a covalent bond formation (Figures 4B, 4D, and 6). Moreover, the interpretation of the electron density suggests the presence of a malonic acid (MLA) that is practically superimposable with the positions of water molecules in PKS18 (pdbscode 1ted) and that comes to lie on the position of Tyr-165 in MsAPKS (pdbscode 1bq6). In addition to the amino acids and the two ligands of each monomer, the final Esi-PKS1 model contains 321 crystallographically defined water molecules.

The pocket accommodating the MLA ligand has a volume of 210 Å³ and is formed by Phe-128, Val-159, Phe-165, Leu-166, Leu-170, Leu-188, and Phe-191, close to the dimer interface. This interface displays an interesting feature, consisting of a cluster of two successive Gly and Phe (164 to 165 and 190 to 191) in each monomer. The second Phe (Phe-191) is in a constraint conformer. These residues, making an interface between the two pockets, seem to represent a barrier to ligand exit and entry (Figure 4C). We can also notice that residues Phe-230, Leu-366, and Gly-403 are additionally allowed or outlier regions of the Ramachandran plot, probably due to strong interactions with the ligand.

Most importantly and similar to Mtu-PKS18, Esi-PKS1 possesses a tunnel for insertion of long-chain acyl-CoA starter molecules to guide the ligation to the catalytic Cys and further elongation by addition of acetate units provided by malonyl-CoA. This pocket accommodating the ACTD ligand has a volume of 1300 Å³ and is formed by Ala-62, Tyr-83, Arg-91, Phe-93, Phe-98, Thr-163, Cys-194, Ser-224, Thr-228, Phe-230, Leu-239, His-240, Phe-243, Cys-293, His-331, and Asn-364 (Figure 4E). Within this pocket, three residues, Cys-175, His-313, and Asn-346 in the PKS18, form the catalytic triad that is conserved at the following positions in Esi-PKS1: Cys-194, His-331, and Asn-364 (Figure 4D).

Accumulation of Phloroglucinol and Correlation with PSK1 Transcripts in the Acclimation to Seawater of a Freshwater Strain of *Ectocarpus*

To further explore the biological relevance of phloroglucinol biosynthesis in *Ectocarpus*, methanol extracts prepared from two strains of *Ectocarpus* were analyzed by GC-MS for the presence of phloroglucinol. These strains are adapted to marine (*Ectocarpus*

Partie 1 : Voie de biosynthèse des phlorotannins

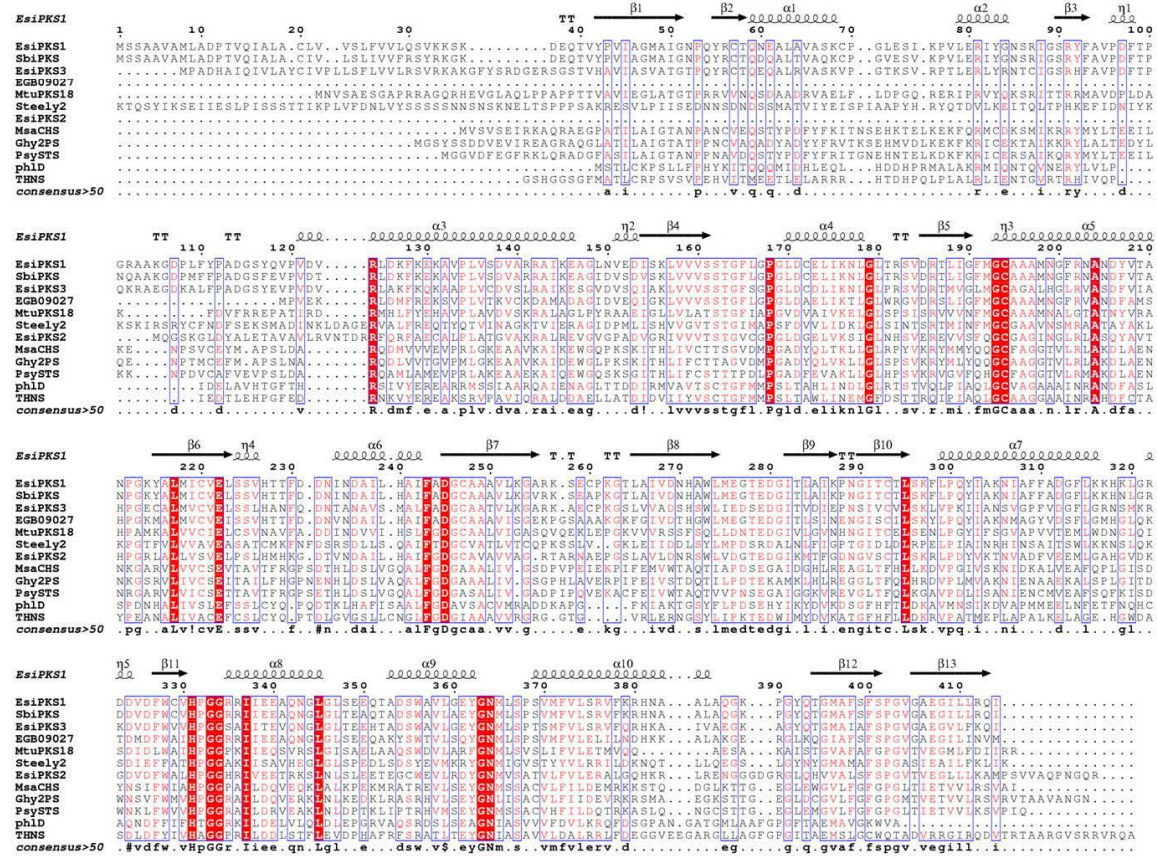


Figure 5. Structure Alignment of the Full Sequences of Esi-PKS1 and 11 Other PKS III Exhibiting Various Specificities of Products.

The sequences are compared with the secondary structures of Esi-PKS1. α -Helices and β -strands are represented above the alignment as helices and arrows, respectively, and β -turns are marked with TT.

[Ec] 32 genome-sequenced strain) and freshwater (Ec 371) environments, respectively, and were recently compared at a transcriptional and metabolic level to study the mechanisms that may allow the transition between these habitats (Dittami et al., 2012a). As shown in Supplemental Figure 3 online, phloroglucinol was identified from total ion chromatograms of extracts prepared from these isolates by extracted ion monitoring at a m/z of 342 and retention time of 46.8 min, and the corresponding mass spectra for the peaks revealed characteristic fragment ions supporting this identification and similar retention time as the authentic standard (see Supplemental Figure 3C online). Interestingly, absolute quantification revealed that the extract from the Ec 371 strain cultivated in freshwater exhibited a very low level of phloroglucinol compared with marine strain Ec 32 (Figure 7A). By contrast, when transferred in seawater, phloroglucinol accumulated in Ec 371 to a concentration that was comparable to those measured in the seawater strain Ec 32. To determine if the characterized Esi-PKS1 and the two other predicted PKS III

sequences in *Ectocarpus* exhibit expression patterns correlating with the accumulation of phloroglucinol (Figure 7), we examined microarray data recently published for these two strains of *Ectocarpus* (Dittami et al., 2012a). As shown in Figure 7B, the characterized Esi-PKS1 exhibited overexpression in the freshwater isolate Ec 371 reacclimated to seawater with a 244-fold increase (P value of 0.03). The two PKS III-like candidates, Esi-PKS2 and Esi-PKS3, did not show any significant changes of expression patterns (Dittami et al., 2012a).

DISCUSSION

Until now, it has not been possible to experimentally identify genes or enzymes responsible for phlorotannin biosynthesis in any species of brown algae (Arnold and Targett, 2002; Amsler and Fairhead, 2006; Pelletreau and Targett, 2007; Parys et al., 2007). Interestingly, homologs of some of the land plant flavonoid pathway genes were found in *Ectocarpus* genome, but these

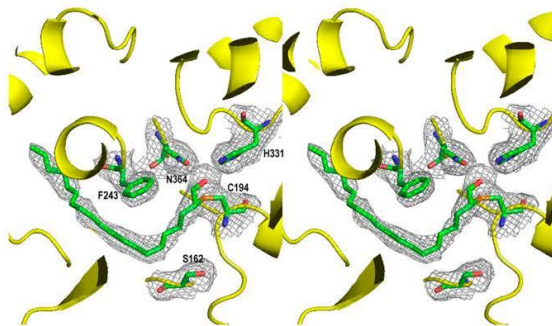


Figure 6. Wall-Eyed Stereo Representation of the Electron Density (2Fo-Fc Map; Cutoff Level 1 σ) Showing the Covalently Attached Aliphatic Ligand That Was Identified in the Catalytic Tunnel of Each Molecule of the Dimeric PKS.

The correlation coefficient when calculating an omit map of this ligand is 0.90.

are completely absent from diatom or green algal genomes (Cock et al., 2010). The shikimate pathway is also fully conserved in *Ectocarpus* genome, but some of the pathways that branch off the shikimate pathway in plants are absent, including routes for important compounds such as phenylpropanoids and salicylic acid (Cock et al., 2010). However, recent genomic approaches have predicted that several species of brown algae display gene homologs of type III polyketide synthases (Wong et al., 2007; Pearson et al., 2010; Baharum et al., 2011).

In this work, we demonstrate that similar to the bacterial enzyme PhID (Achkar et al., 2005; Zha et al., 2006), Esi-PKS1 functions as a phloroglucinol synthase, using the malonyl-CoA substrate. The differences in products produced from malonyl-CoA in Esi-PKS1 versus Sb-PKS (Baharum et al., 2011) might be a result of an overinterpretation of the HPLC and LC-ESI-MS profiles by

Baharum et al. (2011). Alternatively, it can be explained by interfering reactions due to the use of a recombinant protein that was only partially purified in the previous study. A major product of the incubation of Esi-PKS1 with malonyl-CoA as an extender and lauroyl-CoA as a starter molecule was also tentatively identified by LC-ESI-MS as an acylphloroglucinol or a tetraketide that are reminiscent of the phenolic lipids (Gerwick and Fenical, 1982) that have been proposed to be derived from various long-chain fatty acids, precursor of phloroglucinol derivatives in the brown seaweed *Zonaria tournefortii* (El Hattab et al., 2009).

As suggested by El Hattab et al. (2009), acylphloroglucinol derivatives could be generated by a polyketide-type biosynthesis beginning with the condensation of malonyl-CoA and acyl-CoA in order to furnish a tetraketide or a pentaketide intermediate. Therefore, as suggested by the production *in vitro* of long-chain acylphloroglucinol by recombinant Esi-PKS1, its homologs might be involved in the synthesis of long-chain acylphloroglucinol in orders of brown algae, such as Dictyotales and Fucales (Gerwick and Fenical, 1982; Wisespongand and Kuniyoshi, 2003), which are phylogenetically distant from the Ectocarpales. Presently, there is no report of the occurrence of acylphloroglucinols in *Ectocarpus*.

The crystal structure of Esi-PKS1 demonstrates that, similar to Mtu-PKS18 (Sankaranarayanan et al., 2004), Esi-PKS1 uses the tunnel created in the thiolase fold of the protein for substrate binding (Figure 4E). Interestingly, an additional cavity is found at the dimeric interface of Esi-PKS1 (Figures 4C and 8). In plant CHS or STS (Ferrer et al., 1999; Abe and Morita, 2010), this cavity is filled with a bulky aromatic amino acid instead of Gly-190 in Esi-PKS1. The absence of this bulky residue results in an additional cavity that allows the insertion of a small molecule. A product has been trapped in the crystal structure, but the electron density is not clear enough to unambiguously identify the nature of the molecule. We suggest that there is enough space to accommodate a phloroglucinol precursor. However, the resolution of the structure at 2.85 Å is too low to confirm this hypothesis. A diketide molecule (MLA) can be stably refined against the

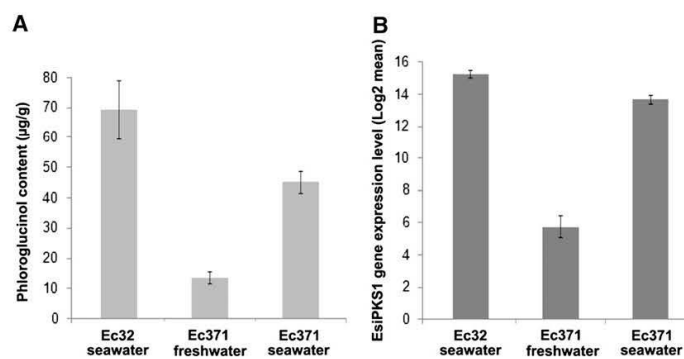


Figure 7. Phloroglucinol Accumulation and Expression Profiles of PKS1 in Two Isolates of *Ectocarpus* Adapted to Contrasting Environments.

(A) The phloroglucinol levels were determined by GC-MS analysis in methanol extracts prepared from the two isolates of *Ectocarpus*: marine Ec 32 cultured in undiluted seawater and freshwater Ec 371 in undiluted (saline stress) and highly diluted seawater (control).

(B) The relative expression levels of PKS1 determined by microarray analysis (Dittami et al., 2012a) were plotted for Ec 32 cultured in seawater and Ec 371, both in undiluted and highly diluted seawater. Relative changes are means of three replicates and error bars represent the corresponding standard deviations.

stramenopile oomycetes. However, a study has recently confirmed the presence of at least two different putative PKS III in *Pseudochattonella farcimen* from another class of ochrophytes, the Dicthyochophyta (Dittami et al., 2012b). These data corroborate the fact that a lateral transfer of PKS III gene has occurred after separation of diatoms from other ochrophytes, but before the divergence of brown algae with pelagophytes and dicthyochophytes. It was reported that several enzymes of major specific pathways found in brown algae and absent in diatoms (synthesis of mannitol, alginate, and hemicelluloses) are also derived from a lateral gene transfer involving an ancestral actinobacterium (Michel et al., 2010a, 2010b). It was proposed that a single massive transfer event allowed the acquisition of all these key genes and the emergence of brown algae. In addition, the phylogenetic tree suggests that the duplication of *E. siliculosus* PKS1 and PKS3 from an ancestral gene is very recent and posterior to the separation from *Aureococcus*, whereas PKS2 has been duplicated prior to this split (Figure 1). The acquisition of two genes of type III PKS (corresponding to Esi-PKS1 and Esi-PKS2) from actinobacteria that would imply a secondary loss in pelagophytes might also be possible.

In summary, this study deepens our understanding of the contribution of type III PKS in phlorotannin biosynthesis in *E. siliculosus* and provides structural insights into the specificity of PKS1 for phloroglucinol formation. Taken together, the above results suggest a conserved function of phlorotannin monomer biosynthesis for PSK1 and its orthologs in other brown algae and indicate that this function arose in Ochrophyta after the divergence of diatoms with the common ancestor of the other groups of photosynthetic stramenopiles, through a lateral gene transfer. This study also provides molecular tools to further investigate the regulation of phlorotannin biosynthesis, providing strong evidence that in vivo this type III PKS is also involved in the synthesis of phloroglucinol, the precursor of brown algal phlorotannins, and that the activation of this pathway is related to the acclimation and adaptation to salinity of euryhaline brown algae. Finally, it is likely that these tools will promote novel biotechnological developments to exploit the pharmaceutical potential of brown algal phenolic compounds.

METHODS

Chemicals

Malonyl-CoA, acetyl-CoA, hexanoyl-CoA, lauroyl-CoA, palmytoyl-CoA, decanoyl-CoA, phloroglucinol, vanillin, and all chemicals were purchased from Sigma-Aldrich. [2-¹⁴C] Malonyl-CoA (55 mCi/mmol) was purchased from Perkin-Elmer.

Algal Cultures and Saline Stress Experiments

The two strains used for these experiments were the *Ectocarpus siliculosus* marine strain Ec 32 (accession CCAP 1310/4, origin San Juan de Marcona, Peru) and the freshwater strain Ec 371 (accession CCAP 1310/196, origin Hopkins River Falls, Victoria, Australia). Cultures and experimental conditions were detailed previously (Dittami et al., 2012a). These experiments were done to study the acclimation of the freshwater strain, Ec 371, to saline stress. This strain was cultivated, during several months, in 100% seawater and in a mixture of 5% seawater and 95% distilled water with a final salinity of ~1.6 ppt. The Ec 32 strain was only cultivated in 100%

seawater and did not survive in 1.6 ppt medium. Samples for GC-MS analysis were obtained in similar conditions than the samples used for microarray experiments in previous experiments (Dittami et al., 2012a).

Bacterial Strains

Escherichia coli DH5α [fhuA2 Δ(argF-lacZ)U169 phoA glnV44 Δ(lacZ) M15 gyrA96 recA1 relA1 endA1 thi-1 hsdR17] (Stratagene) was used as a host strain for maintaining plasmids. For protein expression, *cis*-repressed pQE-80L (Qiagen) derivatives were transformed into *E. coli* BL21 (DE3) codon Plus RIPL [*E. coli* B F- ompT hsdS(r_B- m_B-) dcm+ Tet^r gal λ (DE3) endA Hte [argU ileY leuW Cam^r]] (Stratagene) containing extra copies for Arg, Ile, Pro, and Leu tRNAs.

Expression and Purification of Recombinant Proteins

The *E. siliculosus* PKS1 gene, locus Esi0024_0032 in the *Ectocarpus* ORCAE database (<http://bioinformatics.psb.ugent.be/webtools/bogas/> overview/Ectsi), was amplified by PCR with the corresponding cDNA n° LQ0AA5YM06FM1 as template, without signal peptide at the beginning (Cock et al., 2010). The pQE-80L (Qiagen) expression vector containing the isopropyl-β-D-thiogalactopyranoside-inducible bacteriophage T5 promoter was used to express all proteins. *E. siliculosus* was cloned using SphI and HindIII restriction sites and the following primers: PQECHSFowBis, 5'-GGCGGATCCGCATGCATGCCAAAGGACGAGCACGGTATACCCG-GTCATGCC-3', and pQECHSRev, 5'-GGCTAACGCTTTACTAGATCTG-CCTGAGAAGGATGCCCTCTGCC-3'. Expression constructs encode full-length proteins with a six-His tag on their N termini. The obtained clones were transformed into recombinant *E. coli* BL21-CodonPlus-RIPL cells (Stratagene) and then selected using Luria-Bertani solid medium, supplemented with 100 µg/mL of ampicillin. Protein expression was induced in ZIP medium (Studier, 2005) at 20°C. After 48 h of culture, induction was maintained by adding 0.5 mM isopropyl-β-D-thiogalactopyranoside (IPTG) at a temperature of 20°C for 2 h. Cells were then collected by centrifugation and resuspended in buffer A (20 mM Tris-HCl, pH 7.5, 300 mM NaCl, and 50 mM imidazole) supplemented with protease inhibitor mixture, lysozyme, and DNase. Cell lysis was performed by two passes on a French press to decrease viscosity of supernatants. Cellular debris was eliminated by centrifugation at 45,000g at 4°C during 90 min. All chromatographic procedures were performed on an Äkta Avant system at 20°C (GE Healthcare). Tagged proteins were purified on immobilized Ni-nickel tetradeinate absorbent (NTA) medium, according to the manufacturer's instructions (GE Healthcare), followed by purification on a Sephadryl-200 gel filtration column (GE Healthcare). All protein samples were analyzed for purity and integrity using 12% SDS-PAGE and by MALDI-TOF analyses (MetaboMER platform; SB Roscoff).

Dynamic light scattering analysis was performed using a DynaPro-801 molecular-sizing instrument (Structural Biology platform; SB Roscoff) equipped with a microsamper (Protein Solutions). A 50-µL sample was passed through a filtering assembly containing a 0.02-mm filter into a 12-µL chamber quartz cuvette. The data were analyzed using the Dynamics 4.0 and DynaLS software.

Enzyme Assays

TLC

Experiments were performed by individually testing five different starter acyl-CoAs at 200 µM (acetyl-CoA, hexanoyl-CoA, lauroyl-CoA, palmytoyl-CoA, and decanoyl-CoA) in an assay mixture of 500 µL containing also 20 µM [2-¹⁴C] malonyl-CoA (55 mCi/mmol), 50 µg of purified enzyme, 50 mM Tris HCl, pH 7.5, and 1 mM EDTA (final concentrations). Incubations were performed at room temperature for 1 or 3 h and stopped by adding 10 µL of 37% HCl. The products were then extracted with 1 mL of ethyl

acetate and separated by TLC (Merck Art. 1.11788 silica gel 60 F254; ethyl acetate/hexane/AcOH 65:25:5, v/v/v). Radioactive signals were detected and quantified with a Typhoon imaging system (Molecular Dynamics-GE Healthcare).

GC-MS

Assays were performed as described for TLC. An internal standard of 2.50 µg of vanillin was added. Samples were vortexed for 5 min and centrifuged at 1000g for 5 min. The organic phase was transferred to a glass vial and evaporated under a stream of nitrogen. Trimethylsilyl-ethers were formed by addition of 100 µL acetonitrile and 100 µL of bis(trimethylsilyl) trifluoroacetamide (Sylon-BFT^R) for 60 min at 60°C and evaporated under a stream of nitrogen. Metabolites were resuspended in 100 µL hexane and analyzed by GC-MS in the EI mode on an Agilent GC 6890 coupled to a 5973 MS detector (Agilent) and equipped with a DB-5MS column (30 m × 0.25 mm i.d. × 0.25-µm film thickness; J and W Scientific, Agilent). Temperatures of the injection port and interface were 250 and 280°C, respectively; those of the ion source and MS analyzer were set at 230 and 150°C, respectively. The samples were injected in splitless mode. The oven temperature was first set at 60°C for 5 min and then raised at 10°C/min to 100°C, elevated at 1°C/min to 150°C, and finally elevated at 290°C at the rate of 8°C/min and held for 5 min. The compounds were ionized by electron impact at 70 eV energy. Analytes were detected by total ion current from *m/z* 50 to 850.

LC-MS

The products were separated by reverse-phase U-HPLC (Dionex Ultimate 3000) on a Acclaim RSLC 120, C18, 2.2 µm (2.1 × 100 mm) column at a flow rate of 250 µL/min. Gradient elution was performed with water and acetonitrile, both containing 1% acetic acid, from 20 to 100% acetonitrile in 25 min. Elution was monitored by a multichannel UV detector at 280 or 360 nm. Online LC-ESI-MS spectral analyses were performed using a Thermo LTQ Orbitrap Discovery. Identification of the enzyme reaction products was performed by direct comparison with the authentic compounds or proposed from accurate *m/z* determination and fragmentation patterns.

Crystallization, Data Collection, Structure Determination, and Refinement

PKS1 crystals were grown by the hanging drop vapor diffusion method at room temperature (19°C) in 4.5-µL drops containing a 2:1 mixture of 7 mg/mL protein and crystallization buffer (0.1 M Bicine, pH 8, and 18% polyethylene glycol 6000).

Prior to data collection, the crystals were rapidly soaked in a cryo-buffer that was identical to the reservoir solution supplemented with 10% glycerol and subsequently frozen in a nitrogen gas stream at 100K. X-ray diffraction data were then collected from PKS1 crystals at 100K on beamline ID23-1 at the European Synchrotron Radiation Facilities (ESRF; Grenoble, France) using an ADSC Quantum Q315r charge-coupled device detector. The crystals were rotated through 110° with a 1° oscillation range per frame at a wavelength of 0.979 Å. All raw data were processed using the program Mosflm (Leslie, 2006), and the resultant data were merged and scaled using the program Scala (Evans, 2006). All further data collection statistics are given in Table 1. Potential models for structure solution by molecular replacement were selected by a sequence search using BLAST (Altschul et al., 1990) against the PDB sequence database, indicating that the crystal structure of 1ted was the best model (see Supplemental Table 3 online). Consequently, we used the protein coordinates of the dimeric unit of 1ted as a search model to solve the structure of PKS1 by molecular replacement, which was performed with the program Molrep (Vagin and Teplyakov, 2010). A single solution with a weighted R-factor of

0.53 and a correlation coefficient of 0.34 was obtained using the complete data set at 2.85-Å resolution.

The starting phases obtained with Molrep were subsequently used to automatically build the initial model using ARP/wARP and REFMAC (Murshudov et al., 1997; Perrakis et al., 1999) as part of the CCP4 suite (Potterton et al., 2003, 2004). The initial electron density map was displayed with Coot (Emsley et al., 2010). Roughly 70% of the helices were constructed by the automatic procedure. The subsequent manual adjustment and model building was performed with Coot and alternated with refinement cycles using REFMAC. Water molecules were added automatically with the REFMAC-ARP/wARP option and visually verified, one by one, using Coot. The phasing and final refinement statistics are given in Table 1.

Molecular Phylogenetic Analysis of PKS III Sequences

The unrooted maximum likelihood phylogenetic tree and evolutionary analyses were conducted using MEGA5 (Tamura et al., 2007). A preliminary step was done to find the best-fit model among 48 different amino acid substitution models where the WAG+G+I was selected. The tree with the highest log likelihood (~38977,7031) is shown in Figure 2. Initial trees for the heuristic search were obtained automatically as follows. When the number of common sites was <100 or less than one-fourth of the total number of sites, the maximum parsimony method was used; otherwise, the BIONJ method with MCL distance matrix was used. A discrete gamma distribution was used to model evolutionary rate differences among sites (five categories; +G, parameter = 2.3239). The rate variation model allowed for some sites to be evolutionarily invariable ([+I], 3.9969% sites). The analysis involved 160 amino acid sequences. All positions containing gaps and missing data were eliminated. There were a total of 219 positions in the final data set.

Accession Numbers

Sequence data from this article can be found in the ORCAE *Ectocarpus* database (Sterck et al., 2012) (<http://bioinformatics.psb.ugent.be/orcae/overview/Ects1>) or GenBank/EMBL data libraries under the following accession numbers: *EsiPKS1* (CBN76919.1), *EsiPKS2* (CBJ48712), and *EsiPKS3* (CBJ28635.1), respectively. Accession numbers for the sequences used in the phylogenetic analysis of Figure 2 are provided in Supplemental Figure 1 online. Accession numbers are also labeled on the alignment in Figure 5. The coordinates and structure factors of Esi-PKS1 structure have been deposited in the Protein Data Bank (www.pdb.org; PDB ID 4b0n). Raw data and publicly available Gene Ontology annotations for the *Ectocarpus* microarrays are available at <http://www.sb-roscff.fr/UMR7139/ectocarpus/transcriptomics/>.

Supplemental Data

The following materials are available in the online version of this article.

Supplemental Figure 1. Full Alignment Used to Draw the Phylogenetic Tree of Figure 1.

Supplemental Figure 2. SDS-PAGE of Recombinant PKS1 from *E. siliculosus* and MALDI-TOF Mass Spectrometry Spectrum of the Purified Recombinant PKS1.

Supplemental Figure 3. GC-MS Chromatograms of Phloroglucinol-TMS Products.

Supplemental Figure 4. U-HPLC-ESI-MS Chromatograms.

Supplemental Table 1. Accession Numbers, Organismal Origin, and Short Name of the Organism of the Proteins That Were Aligned to Construct the Phylogeny of Figure 2.

acetate and separated by TLC (Merck Art. 1.11798 silica gel 60 F254; ethyl acetate/hexane/AcOH 65:25:5, v/v/v). Radioactive signals were detected and quantified with a Typhoon imaging system (Molecular Dynamics-GE Healthcare).

GC-MS

Assays were performed as described for TLC. An internal standard of 2.50 µg of vanillin was added. Samples were vortexed for 5 min and centrifuged at 1000g for 5 min. The organic phase was transferred to a glass vial and evaporated under a stream of nitrogen. Trimethylsilyl-ethers were formed by addition of 100 µL acetonitrile and 100 µL of bis(trimethylsilyl) trifluoroacetamide (Sylon-BFT[®]) for 60 min at 60°C and evaporated under a stream of nitrogen. Metabolites were resuspended in 100 µL hexane and analyzed by GC-MS in the EI mode on an Agilent GC 6890 coupled to a 5973 MS detector (Agilent) and equipped with a DB-5MS column (30 m × 0.25 mm i.d. × 0.25-µm film thickness; J and W Scientific, Agilent). Temperatures of the injection port and interface were 250 and 280°C, respectively; those of the ion source and MS analyzer were set at 230 and 150°C, respectively. The samples were injected in splitless mode. The oven temperature was first set at 60°C for 5 min and then raised at 10°C/min to 100°C, elevated at 1°C/min to 150°C, and finally elevated at 290°C at the rate of 8°C/min and held for 5 min. The compounds were ionized by electron impact at 70 eV energy. Analytes were detected by total ion current from *m/z* 50 to 850.

LC-MS

The products were separated by reverse-phase U-HPLC (Dionex Ultimate 3000) on a Acclaim RSLC 120, C18, 2.2 µm (2.1 × 100 mm) column at a flow rate of 250 µL/min. Gradient elution was performed with water and acetonitrile, both containing 1% acetic acid, from 20 to 100% acetonitrile in 25 min. Elution was monitored by a multichannel UV detector at 280 or 360 nm. Online LC-ESI-MS spectral analyses were performed using a Thermo LTQ Orbitrap Discovery. Identification of the enzyme reaction products was performed by direct comparison with the authentic compounds or proposed from accurate *m/z* determination and fragmentation patterns.

Crystallization, Data Collection, Structure Determination, and Refinement

PKS1 crystals were grown by the hanging drop vapor diffusion method at room temperature (19°C) in 4.5-µL drops containing a 2:1 mixture of 7 mg/mL protein and crystallization buffer (0.1 M Bicine, pH 8, and 18% polyethylene glycol 6000).

Prior to data collection, the crystals were rapidly soaked in a cryo-buffer that was identical to the reservoir solution supplemented with 10% glycerol and subsequently frozen in a nitrogen gas stream at 100K. X-ray diffraction data were then collected from PKS1 crystals at 100K on beamline ID23-1 at the European Synchrotron Radiation Facilities (ESRF; Grenoble, France) using an ADSC Quantum Q315r charge-coupled device detector. The crystals were rotated through 110° with a 1° oscillation range per frame at a wavelength of 0.979 Å. All raw data were processed using the program Mosflm (Leslie, 2006), and the resultant data were merged and scaled using the program Scala (Evans, 2006). All further data collection statistics are given in Table 1. Potential models for structure solution by molecular replacement were selected by a sequence search using BLAST (Altschul et al., 1990) against the PDB sequence database, indicating that the crystal structure of 1ted was the best model (see Supplemental Table 3 online). Consequently, we used the protein coordinates of the dimeric unit of 1ted as a search model to solve the structure of PKS1 by molecular replacement, which was performed with the program Molrep (Vagin and Teplyakov, 2010). A single solution with a weighted R-factor of

0.53 and a correlation coefficient of 0.34 was obtained using the complete data set at 2.85-Å resolution.

The starting phases obtained with Molrep were subsequently used to automatically build the initial model using ARP/wARP and REFMAC (Murshudov et al., 1997; Perrakis et al., 1999) as part of the CCP4 suite (Potterton et al., 2003, 2004). The initial electron density map was displayed with Coot (Emsley et al., 2010). Roughly 70% of the helices were constructed by the automatic procedure. The subsequent manual adjustment and model building was performed with Coot and alternated with refinement cycles using REFMAC. Water molecules were added automatically with the REFMAC-ARP/wARP option and visually verified, one by one, using Coot. The phasing and final refinement statistics are given in Table 1.

Molecular Phylogenetic Analysis of PKS III Sequences

The unrooted maximum likelihood phylogenetic tree and evolutionary analyses were conducted using MEGA5 (Tamura et al., 2007). A preliminary step was done to find the best-fit model among 48 different amino acid substitution models where the WAG+G+I was selected. The tree with the highest log likelihood (-38977.7031) is shown in Figure 2. Initial trees for the heuristic search were obtained automatically as follows. When the number of common sites was <100 or less than one-fourth of the total number of sites, the maximum parsimony method was used; otherwise, the BIONJ method with MCL distance matrix was used. A discrete gamma distribution was used to model evolutionary rate differences among sites (five categories; +G, parameter = 2.3239). The rate variation model allowed for some sites to be evolutionarily invariable ([+I], 3.9969% sites). The analysis involved 160 amino acid sequences. All positions containing gaps and missing data were eliminated. There were a total of 219 positions in the final data set.

Accession Numbers

Sequence data from this article can be found in the ORCAE *Ectocarpus* database (Sterck et al., 2012) (<http://bioinformatics.psb.ugent.be/orcae/>) or GenBank/EMBL data libraries under the following accession numbers: *EsiPKS1* (CBN76919.1), *EsiPKS2* (CBJ48712), and *EsiPKS3* (CBJ28635.1), respectively. Accession numbers for the sequences used in the phylogenetic analysis of Figure 2 are provided in Supplemental Figure 1 online. Accession numbers are also labeled on the alignment in Figure 5. The coordinates and structure factors of Esi-PKS1 structure have been deposited in the Protein Data Bank (www.pdb.org; PDB ID 4b0n). Raw data and publicly available Gene Ontology annotations for the *Ectocarpus* microarrays are available at <http://www.sb-roscoff.fr/UMR7139/ectocarpus/transcriptomics/>.

Supplemental Data

The following materials are available in the online version of this article.

Supplemental Figure 1. Full Alignment Used to Draw the Phylogenetic Tree of Figure 1.

Supplemental Figure 2. SDS-PAGE of Recombinant PKS1 from *E. siliculosus* and MALDI-TOF Mass Spectrometry Spectrum of the Purified Recombinant PKS1.

Supplemental Figure 3. GC-MS Chromatograms of Phloroglucinol-TMS Products.

Supplemental Figure 4. U-HPLC-ESI-MS Chromatograms.

Supplemental Table 1. Accession Numbers, Organismal Origin, and Short Name of the Organism of the Proteins That Were Aligned to Construct the Phylogeny of Figure 2.

Supplemental Table 2. Formula and Chemical Structures of the Products Identified by UPLC-MS Analysis in the Incubation of Malonyl-CoA with Different Starter Molecules.

Supplemental Table 3. Structural Alignment Scores of Several Structures of Type III PKS Deposited in the PDB Database, Computed by the Dali-Server.

Supplemental Data Set 1. Text File of the Sequences and Alignment Used for the Phylogenetic Analysis Shown in Figure 2 and Supplemental Figure 1 Online.

ACKNOWLEDGMENTS

Crystal structure determination was performed at the crystallography platform of the Station Biologique de Roscoff, supported by the Centre National de la Recherche Scientifique and Université Pierre et Marie Curie, Paris 06. We are indebted to the staff of the ESRF (Grenoble, France), beamlines ID23-1 and BM30A, for technical support during data collection and treatment. We thank Thierry Tonon for providing biological material and access to microarrays data before publication and for helpful discussions and advice, Fanny Gaillard for MALDI-TOF mass spectrometry analysis, and Laurence Darteville for technical assistance. This project was supported by a Grant-in-Aid for Scientific Research from Groupement d'Intérêt Scientifique Europole MER to V.S.-P. and P.P. (Phlorotann'ING project). L.M.-C. and S.G. were also partly supported by the project IDEALG (ANR-10-BTBR-04-02) "Investissements d'avenir, Biotechnologies-Bioresources." We also thank Groupement d'Intérêt Scientifique BiogenOuest for supporting MetaboMER facilities through the CORSAIRE metabolomics network.

AUTHOR CONTRIBUTIONS

P.P., V.S.-P., E.A.G., C.L., and M.C. designed research. L.M.-C., L.D., S.G., M.C., and C.J.-J.L. performed research. S.G., C.J.-J.L., E.C., and M.C. contributed new reagents/analytic tools. L.M.-C., L.D., S.G., M.C., C.J.-J.L., C.L., and P.P. analyzed data. L.M.-C., L.D., M.C., and P.P. wrote the article.

Received March 11, 2013; revised June 3, 2013; accepted August 7, 2013; published August 27, 2013.

REFERENCES

- Abe, I., and Morita, H.** (2010). Structure and function of the chalcone synthase superfamily of plant type III polyketide synthases. *Nat. Prod. Rep.* **27:** 809–838.
- Abe, I., Oguro, S., Utsumi, Y., Sano, Y., and Noguchi, H.** (2005a). Engineered biosynthesis of plant polyketides: Chain length control in an octaketide-producing plant type III polyketide synthase. *J. Am. Chem. Soc.* **127:** 12709–12716.
- Abe, I., Utsumi, Y., Oguro, S., Morita, H., Sano, Y., and Noguchi, H.** (2005b). A plant type III polyketide synthase that produces pentaketide chromone. *J. Am. Chem. Soc.* **127:** 1362–1363.
- Achkar, J., Xian, M., Zhao, H., and Frost, J.W.** (2005). Biosynthesis of phloroglucinol. *J. Am. Chem. Soc.* **127:** 5332–5333.
- Altschul, S.F., Gish, W., Miller, W., Myers, E.W., and Lipman, D.J.** (1990). Basic local alignment search tool. *J. Mol. Biol.* **215:** 403–410.
- Amsler, C.D., and Fairhead, V.A.** (2006). Defensive and sensory chemical ecology of brown algae. *Adv. Bot. Res.* **43:** 1–91.
- Arnold, T.M., and Targett, N.M.** (2002). Marine tannins: The importance of a mechanistic framework for predicting ecological roles. *J. Chem. Ecol.* **28:** 1919–1934.
- Austin, M.B., Bowman, M.E., Ferrer, J.L., Schröder, J., and Noel, J.P.** (2004b). An aldol switch discovered in stilbene synthases mediates cyclization specificity of type III polyketide synthases. *Chem. Biol.* **11:** 1179–1194.
- Austin, M.B., Izumikawa, M., Bowman, M.E., Udwary, D.W., Ferrer, J.L., Moore, B.S., and Noel, J.P.** (2004a). Crystal structure of a bacterial type III polyketide synthase and enzymatic control of reactive polyketide intermediates. *J. Biol. Chem.* **279:** 45162–45174.
- Baharum, H., Morita, H., Tomitsuka, A., Lee, F.C., Ng, K.Y., Rahim, R.A., Abe, I., and Ho, C.L.** (2011). Molecular cloning, modeling, and site-directed mutagenesis of type III polyketide synthase from *Sargassum binderi* (Phaeophyta). *Mar. Biotechnol. (NY)* **13:** 845–856.
- Bangera, M.G., and Thomashow, L.S.** (1999). Identification and characterization of a gene cluster for synthesis of the polyketide antibiotic 2,4-diacetylphloroglucinol from *Pseudomonas fluorescens* Q2-87. *J. Bacteriol.* **181:** 3155–3163.
- Berglin, M., Delage, L., Potin, P., Vilter, H., and Elwing, H.** (2004). Enzymatic cross-linking of a phenolic polymer extracted from the marine alga *Fucus serratus*. *Biomacromolecules* **5:** 2376–2383.
- Bitton, R., Berglin, M., Elwing, H., Colin, C., Delage, L., Potin, P., and Bianco-Peled, H.** (2007). The influence of halide-mediated oxidation on algae-barn adhesives. *Macromol. Biosci.* **7:** 1280–1289.
- Boettcher, A.A., and Targett, N.M.** (1993). Role of polyphenolic molecular size in reduction of assimilation efficiency in *Xiphister mucosus*. *Ecology* **74:** 891–903.
- Brown, J.W., and Sorhannus, U.** (2010). A molecular genetic timescale for the diversification of autotrophic stramenopiles (Ochrophyta): Substantive underestimation of putative fossil ages. *PLoS ONE* **5:** e12759.
- Charrier, B., Coelho, S.M., Le Bail, A., Tonon, T., Michel, G., Potin, P., Kloareg, B., Boyen, C., Peters, A.F., and Cock, J.M.** (2008). Development and physiology of the brown alga *Ectocarpus siliculosus*: Two centuries of research. *New Phytol.* **177:** 319–332.
- Chen, Y., Yan, X., and Fan, X.** (1997). A hypothesis on Phaeophyceae polyphenols: Their structural unit and mechanism of the formation (in Chinese with English summary). *Oceanol. Limnol. Sin.* **28:** 225–232.
- Cock, J.M., and Coelho, S.M.** (2011). Algal models in plant biology. *J. Exp. Bot.* **62:** 2425–2430.
- Cock, J.M., et al.** (2010). The *Ectocarpus* genome and the independent evolution of multicellularity in brown algae. *Nature* **465:** 617–621.
- Dakora, F.D.** (1995). Plant flavonoid: Biological molecules for useful exploitation. *Aust. J. Phys.* **22:** 87–99.
- Dittami, S.M., Gravot, A., Goultquer, S., Rousvoal, S., Peters, A.F., Bouchereau, A., Boyen, C., and Tonon, T.** (2012a). Towards deciphering dynamic changes and evolutionary mechanisms involved in the adaptation to low salinities in *Ectocarpus* (brown algae). *Plant J.* **71:** 366–377.
- Dittami, S.M., Riisberg, I., John, U., Orr, R.J., Jakobsen, K.S., and Edvardsen, B.** (2012b). Analysis of expressed sequence tags from the marine microalga *Pseudochattocella farcimen* (Dictyochophyceae). *Protist* **163:** 143–161.
- El Hattab, M., Bouzidi, N., Ortalo-Magne, A., Daghbouche, Y., Richou, M., Chitour, S.E., de Reviers, B., and Piovetti, L.** (2009). Eicosapentaenoic acid: Possible precursor of the phloroglucinol derivatives isolated from the brown alga *Zonaria tournefortii* (J.V. Lamouroux) Montagne. *Biochem. Syst. Ecol.* **37:** 55–58.
- Emsley, P., Lohkamp, B., Scott, W.G., and Cowtan, K.** (2010). Features and development of Coot. *Acta Crystallogr. D Biol. Crystallogr.* **66:** 486–501.
- Evans, P.** (2006). Scaling and assessment of data quality. *Acta Crystallogr. D Biol. Crystallogr.* **62:** 72–82.

- Ferrer, J.L., Jez, J.M., Bowman, M.E., Dixon, R.A., and Noel, J.P.** (1999). Structure of chalcone synthase and the molecular basis of plant polyketide biosynthesis. *Nat. Struct. Biol.* **6:** 775–784.
- Funa, N., Ohnishi, Y., Ebizuka, Y., and Horinouchi, S.** (2002). Alteration of reaction and substrate specificity of a bacterial type III polyketide synthase by site-directed mutagenesis. *Biochem. J.* **367:** 781–789.
- Funabashi, M., Funa, N., and Horinouchi, S.** (2008). Phenolic lipids synthesized by type III polyketide synthase confer penicillin resistance on *Streptomyces griseus*. *J. Biol. Chem.* **283:** 13983–13991.
- Gerwick, W., and Fenical, W.** (1982). Phenolic lipids from related marine algae of the order Dictyotales. *Phytochemistry* **21:** 633–637.
- Jez, J.M., Bowman, M.E., and Noel, J.P.** (2001). Structure-guided programming of polyketide chain-length determination in chalcone synthase. *Biochemistry* **40:** 14829–14838.
- Jez, J.M., Bowman, M.E., and Noel, J.P.** (2002). Expanding the biosynthetic repertoire of plant type III polyketide synthases by altering starter molecule specificity. *Proc. Natl. Acad. Sci. USA* **99:** 5319–5324.
- Kim, S.S., et al.** (2010). LAP6/POLYKETIDE SYNTHASE A and LAP5/POLYKETIDE SYNTHASE B encode hydroxyalkyl α -pyrone synthases required for pollen development and sporopollenin biosynthesis in *Arabidopsis thaliana*. *Plant Cell* **22:** 4045–4066.
- Koivikko, R., Loponen, J., Honkanen, T., and Jormalainen, V.** (2005). Contents of soluble, cell-wall-bound and exuded phlorotannins in the brown alga *Fucus vesiculosus*, with implications on their ecological functions. *J. Chem. Ecol.* **31:** 195–212.
- Koivikko, R., Loponen, J., Pihlaja, K., and Jormalainen, V.** (2007). High-performance liquid chromatographic analysis of phlorotannins from the brown alga *Fucus vesiculosus*. *Phytochem. Anal.* **18:** 326–332.
- Le Lann, K., Connan, S., and Stiger-Pouvreau, V.** (2012). Phenology, TPC and size-fractioning phenolics variability in temperate Sargassaceae (Phaeophyceae, Fucales) from Western Brittany: Native versus introduced species. *Mar. Environ. Res.* **80:** 1–11.
- Leslie, A.G.** (2006). The integration of macromolecular diffraction data. *Acta Crystallogr. D Biol. Crystallogr.* **62:** 48–57.
- Matthews, B.W.** (1968). Solvent content of protein crystals. *J. Mol. Biol.* **33:** 491–497.
- McClintock, J.B., and Baker, B.J.** (2001). Marine Chemical Ecology. (Boca Raton, FL: CRC Press).
- Michel, G., Tonon, T., Scornet, D., Cock, J.M., and Kloareg, B.** (2010a). Central and storage carbon metabolism of the brown alga *Ectocarpus siliculosus*: Insights into the origin and evolution of storage carbohydrates in Eukaryotes. *New Phytol.* **188:** 67–81.
- Michel, G., Tonon, T., Scornet, D., Cock, J.M., and Kloareg, B.** (2010b). The cell wall polysaccharide metabolism of the brown alga *Ectocarpus siliculosus*: Insights into the evolution of extracellular matrix polysaccharides in Eukaryotes. *New Phytol.* **188:** 82–97.
- Mizuuchi, Y., Shimokawa, Y., Wanibuchi, K., Noguchi, H., and Abe, I.** (2008). Structure function analysis of novel type III polyketide synthases from *Arabidopsis thaliana*. *Biol. Pharm. Bull.* **31:** 2205–2210.
- Murshudov, G.N., Vagin, A.A., and Dodson, E.J.** (1997). Refinement of macromolecular structures by the maximum-likelihood method. *Acta Crystallogr. D Biol. Crystallogr.* **53:** 240–255.
- Nyvall, P., Corre, E., Boisset, C., Barbeyron, T., Rousvoal, S., Scornet, D., Kloareg, B., and Boyen, C.** (2003). Characterization of mannuronan C-5-epimerase genes from the brown alga *Laminaria digitata*. *Plant Physiol.* **133:** 726–735.
- Parys, S., Rosenbaum, A., Kehraus, S., Reher, G., Glombitzka, K.-W., and König, G.M.** (2007). Evaluation of quantitative methods for the determination of polyphenols in algal extracts. *J. Nat. Prod.* **70:** 1865–1870.
- Pearson, G.A., Hoarau, G., Lago-Leston, A., Coyer, J.A., Kube, M., Reinhardt, R., Henckel, K., Serrão, E.T., Corre, E., and Olsen, J.L.** (2010). An expressed sequence tag analysis of the intertidal brown seaweeds *Fucus serratus* (L.) and *F. vesiculosus* (L.) (Heterokontophyta, Phaeophyceae) in response to abiotic stressors. *Mar. Biotechnol.* (NY) **12:** 195–213.
- Pelletreau, K.N.** (2008). The Application of Molecular Tools towards the Study of Brown Algal Chemical Ecology and the Production of Phlorotannins. PhD dissertation (University of Delaware, Newark).
- Pelletreau, K.N., and Targett, N.M.** (2007). New perspectives for addressing patterns of secondary metabolites in marine macroalgae. In *Algal Chemical Ecology*, C.D. Amsler, ed (Berlin: Springer-Verlag), pp. 121–146.
- Perrakis, A., Morris, R., and Lamzin, V.S.** (1999). Automated protein model building combined with iterative structure refinement. *Nat. Struct. Biol.* **6:** 458–463.
- Pfeifer, B.A., and Khosla, C.** (2001). Biosynthesis of polyketides in heterologous hosts. *Microbiol. Mol. Biol. Rev.* **65:** 106–118.
- Potterton, E., Briggs, P., Turkenburg, M., and Dodson, E.** (2003). A graphical user interface to the CCP4 program suite. *Acta Crystallogr. D Biol. Crystallogr.* **59:** 1131–1137.
- Potterton, L., McNicholas, S., Krissinel, E., Gruber, J., Cowtan, K., Emsley, P., Murshudov, G.N., Cohen, S., Perrakis, A., and Noble, M.** (2004). Developments in the CCP4 molecular-graphics project. *Acta Crystallogr. D Biol. Crystallogr.* **60:** 2288–2294.
- Ragan, M.A., and Glombitzka, K.W.** 1986. Phlorotannins, brown algal polyphenols. In *Progress in Phycological Research*, F.E. Round and D.J. Chapman, eds (Bristol, UK: Biopress), pp. 129–241.
- Sankaranarayanan, R.** (2006). A type III PKS makes the DIFFerence. *Nat. Chem. Biol.* **2:** 451–452.
- Sankaranarayanan, R., Saxena, P., Marathe, U.B., Gokhale, R.S., Shanmugam, V.M., and Rukmini, R.** (2004). A novel tunnel in mycobacterial type III polyketide synthase reveals the structural basis for generating diverse metabolites. *Nat. Struct. Mol. Biol.* **11:** 894–900.
- Schoenwaelder, M.E.A., and Clayton, M.N.** (1998). Secretion of phenolic substances into the zygote wall and cell plate in embryos of *Homosira* and *Acropora* (Fucales, Phaeophyceae). *J. Phycol.* **34:** 969–980.
- Shibata, T., Hama, Y., Miyasaki, T., Ito, M., and Nakamura, T.** (2006). Extracellular secretion of phenolic substances from living brown algae. *J. Appl. Phycol.* **18:** 787–794.
- Sieburth, J.M.C., and Conover, J.T.** (1965). *Sargassum* tannin, an antibiotic which retards fouling. *Nature* **208:** 52–53.
- Stengel, D.B., Connan, S., and Popper, Z.A.** (2011). Algal chemodiversity and bioactivity: Sources of natural variability and implications for commercial application. *Biotechnol. Adv.* **29:** 483–501.
- Sterck, L., Billiau, K., Abeel, T., Rouzé, P., and Van de Peer, Y.** (2012). ORCAE: Online resource for community annotation of eukaryotes. *Nat. Methods* **9:** 1041.
- Studier, F.W.** (2005). Protein production by auto-induction in high density shaking cultures. *Protein Expr. Purif.* **41:** 207–234.
- Tamura, K., Dudley, J., Nei, M., and Kumar, S.** (2007). MEGA4: Molecular Evolutionary Genetics Analysis (MEGA) software version 4.0. *Mol. Biol. Evol.* **24:** 1596–1599.
- Thomas, N.V., and Kim, S.K.** (2011). Potential pharmacological applications of polyphenolic derivatives from marine brown algae. *Environ. Toxicol. Pharmacol.* **32:** 325–335.
- Toth, G.B., and Pavia, H.** (2000). Water-borne cues induce chemical defense in a marine alga (*Ascophyllum nodosum*). *Proc. Natl. Acad. Sci. USA* **97:** 14418–14420.
- Vagin, A., and Teplyakov, A.** (2010). Molecular replacement with MOLREP. *Acta Crystallogr. D Biol. Crystallogr.* **66:** 22–25.

- Waddell, S.J., Chung, G.A., Gibson, K.J., Everett, M.J., Minnikin, D.E., Besra, G.S., and Butcher, P.D.** (2005). Inactivation of polyketide synthase and related genes results in the loss of complex lipids in *Mycobacterium tuberculosis* H37Rv. *Lett. Appl. Microbiol.* **40**: 201–206.
- Waterman, P.G., and Mole, S.** (1994). Analysis of Plant Metabolites, Methods in Ecology Series. (Oxford, UK: Blackwell).
- Wisespongand, P., and Kuniyoshi, M.** (2003). Bioactive phloroglucinols from the brown alga *Zonaria diesingiana*. *J. Appl. Phycol.* **15**: 225–228.
- Wong, T.K.-M., Ho, C.-L., Lee, W.-W., Rahim, R.A., and Phang, S.-M.** (2007). Analyses of expressed sequence tags (ESTs) from *Sargassum binderi* (Phaeophyta). *J. Phycol.* **43**: 528–534.
- Zha, W., Rubin-Pitel, S.B., and Zhao, H.** (2006). Characterization of the substrate specificity of PhID, a type III polyketide synthase from *Pseudomonas fluorescens*. *J. Biol. Chem.* **281**: 32036–32047.

Chapitre 2: Caractérisation biochimique et fonctionnelle de Chalcone Isomérases-like d'*Ectocarpus*.

Présentation de l'article :

Ce chapitre présente l'étude menée sur les deux Chalcones isomérases-like d'*Ectocarpus*.

La caractérisation biochimique des protéines recombinantes a été couplée à la caractérisation fonctionnelle sur le modèle plante *Arabidopsis*. Suite aux découvertes récentes sur cette classe de protéines ayant montré l'implication des CHI de type III dans le métabolisme des acides gras plutôt que dans le métabolisme des composés phénoliques chez les plantes, nous avons réorienté notre stratégie de caractérisation fonctionnelle par la collaboration avec l'équipe du Dr. Balakrishnan Prithiviraj du Département des Sciences Environnementales, à Truro au Canada. Cette étude est la première à présenter la complémentation d'*Arabidopsis* avec des gènes d'algues, apportant ainsi de nouvelles opportunités notamment pour la caractérisation des enzymes clés du métabolisme des phlorotannins chez les algues brunes.

Article en préparation

Chalcone isomerase-like proteins from the brown alga Ectocarpus are fatty-acid binding proteins that complement AtCHIL1 mutant of Arabidopsis thaliana.

Emeline Creis^{a,b,1}, Pramod Rathor^{c,1}, Ludovic Delage^{a,b}, Laurence Meslet-Cladière^{a,b,2}, Catherine Leblanc^{a,b}, Erwan Ar Gall^d, Balakrishnan Prithiviraj^c, Philippe Potin^{a,b,3}

^aSorbonne Universités, UPMC Univ Paris 06, UMR 8227, Integrative Biology of Marine Models, Station Biologique de Roscoff, CS 90074, F-29688, Roscoff cedex, Brittany, France

^bCNRS, UMR 8227, Integrative Biology of Marine Models, Station Biologique de Roscoff, CS 90074, F-10 29688, Roscoff cedex, Brittany, France.

^cDepartment of Environmental Sciences, Faculty of Agriculture, Dalhousie University, P.O. Box 550, Truro, Canada

^dUniversité Européenne de Bretagne, Université de Bretagne Occidentale, Laboratoire des Sciences de l'Environnement Marin, Unité Mixte de Recherche 6539, Centre National de la Recherche Scientifique, Institut Européen d'Etudes Marines-IUEM, 29280 Plouzané, Brittany, France

Corresponding authors :

Dr Philippe Potin, LBI2M, UMR 8227 CNRS/UPMC-Paris6, Station Biologique, CS90074, 29688 ROSCOFF Cedex, France; Phone: 33+(0)2-98-29-23-75
Fax: 33+(0)2-98-29-23-85 E-mail :potin@sb-roscuff.fr

Dr Balakrishnan Prithiviraj Department of Environmental Sciences, Faculty of Agriculture, Dalhousie University, P.O. Box 550, Truro, Canada
E-mail: bprithiviraj@dal.ca; Fax: +1-902-893-1404 ; Tel: +1-902-893-6643

Abstract

Phlorotannins are known only from brown algae and are structural analogues of flavonoid derivatives from vascular plants. Until recently, it has not been possible to experimentally identify genes or enzymes responsible for any other steps in phlorotannin biosynthesis than a phloroglucinol synthase. We found that the chalcone isomerase-like proteins EsiCHIL1 and EsiCHIL2 from the brown alga *Ectocarpus* are ancestral proteins in the family of chalcone isomerase fold proteins. EsiCHIL1 and EsiCHIL2 lack the catalytic amino acids of the *bona fide* Chalcone isomerases (CHI) from vascular plants. We used transgenic plants of the null mutants AtCHIL1 of *Arabidopsis thaliana*. Indeed, they function as fatty-acid binding proteins closely related to the FAP3 family recently characterized in *Arabidopsis* for their biochemical and structural features. A microscale thermophoresis analysis of recombinant proteins revealed preferential interaction of EsiCHIL1 with palmitoyl CoA (C16 CoA) $K_d = 31.2\mu M \pm 3.7\mu M$ than for palmitic acid (C16) $K_d = 153\mu M \pm 1.83\mu M$. In contrast, no affinity was detected with C18 compounds. qRT-PCR analysis of At5G05270 (AtCHIL-1) expression confirmed that *Atchil-1* is a knockdown line. Therefore, it was used to investigate the potential function of EsiCHIL1 by complementation in *AtCHIL-1*. The complementation will be soon confirmed by studying how the defects associated with *Atchil-1* deficiency are reversed. The subcellular localization study in tobacco plants revealed also that YFP-EsiCHIL-1 was localized in the chloroplast, similar to the localization of FAP3 proteins in *Arabidopsis*.

From these results, we conclude that EsiCHILs are Fatty-Acid binding proteins, and their function is likely conserved among diverse family of Ochrophyta. Further experiments are required to confirm the complementation of *Arabidopsis* CHI-fold proteins mutant, *AtCHIL-1* and also mutants of the FAP3 family.

Introduction

Phlorotannins are a diverse set of phenolic polymers synthesized by brown algae, and similar to the well-characterized biosynthesis of terrestrial plant tannins from alcoholic monomers, phlorotannins are produced by polymerization of phloroglucinol (1,3,5-trihydroxybenzene) monomer units in a variety of combinations. However, the biosynthetic pathway for phlorotannin biosynthesis is poorly characterized, and has been variously proposed to be via condensation of acetate and malonate units, by the shikimate pathway, or by the phenylpropanoid pathway ([Pelletreau, 2008](#)). A major advance in our understanding of phlorotannin biosynthesis was made by identifying and characterizing PKS1, a type III polyketide synthase in the brown alga *Ectocarpus* ([Meslet-Cladière et al., 2013](#)). It was shown that PKS1 catalyzes the synthesis of phloroglucinol monomers from malonyl-CoA, thus identifying a major step in phlorotannin biosynthesis.

Until this recent report of a type III Polyketide synthase having a function of phloroglucinol synthase ([Meslet-Cladière et al., 2013](#)), it has not been possible to experimentally identify genes or enzymes responsible for any other step in phlorotannin biosynthesis in any species of brown algae ([Arnold & Targett, 2002](#); [Amsler & Fairhead, 2006](#); [Pelletreau &Targett, 2008](#); [Parys et al., 2007](#)). Interestingly, homologs of some of the land plant flavonoid pathway genes were found in *Ectocarpus* genome but these are completely absent from diatom or green algal genomes ([Cock et al., 2010](#)). The shikimate pathway is also fully conserved in *Ectocarpus* genome but some of the pathways that branch off the shikimate pathway in plants are absent, including routes for important compounds such as phenylpropanoids and salicylic acid ([Cock et al., 2010](#)).

In the flavonoid pathway, chalcone Isomerase (CHI) enzymes (EC 5.5.1.6) catalyse the intramolecular and stereospecific cyclization of chalcones to chiral flavanones by a Michael addition reaction. The CHI super-family comprises four types of CHI proteins ([Ralston et al., 2005](#), [Morita et al., 2014](#)). Type I and II proteins are *bona fide* CHI having CHI enzymatic activity (Figure 2.1). Type I proteins are ubiquitous in vascular plants and are responsible for flavonoid biosynthesis (Figure 2.1), whereas type II enzymes appear to be legume-specific and are involved in isoflavonoid production. Type III proteins are found widely in both land plants and

green algae, fungi and bacteria whereas type IV proteins are found in land plants only ([Ralston et al., 2005](#); [Ngaki et al., 2012](#)). CHI-like homologues in green algae, fungi and bacteria lack both key catalytic residues and the chalcone-binding site of *bona fide* CHI. Three type III proteins in *Arabidopsis* were recently shown to be fatty acid-binding proteins (FAPs) localized to plastids ([Ngaki et al., 2012](#)), whereas the function of type IV CHI proteins seems to be related to the enhancement of flavonoid production and flower pigmentation in the Japanese morning glory (*Ipomoea nil*) ([Morita et al. 2014](#)).

The filamentous brown alga *Ectocarpus* is an upcoming model system for algal biology and metabolism ([Cock and Coelho, 2012](#)). Interestingly, the *Ectocarpus* genome was predicted to encode two CHI-like proteins, which may participate in phlorotannin biosynthesis or may be involved in other metabolic pathways ([Cock et al., 2010; 2012](#)).

In the present work, we demonstrate that similar to the *Arabidopsis* CHIL of type III family ([Ralston et al., 2005](#); [Ngaki et al , 2012](#)), Esi-CHIL1 and CHIL2 function as fatty-acid binding proteins. Their heterologous expression in *Arabidopsis* *AtCHIL1*-null mutant, as well as subcellular localization of YFP-EsiCHIL1 in tobacco plants was attempted to elucidate their biological function.

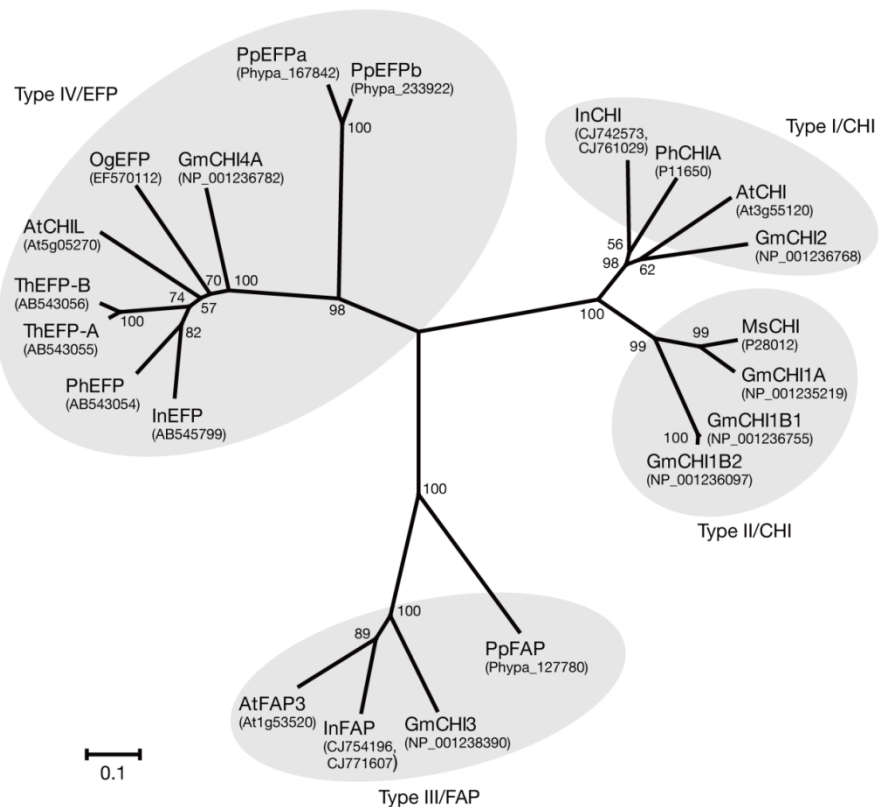


Figure 2.1: Comparison of the EFP protein (Enhancer of Flavonoid Production) with its relatives
([Morita et al., 2014](#))

Materials and Methods:

Ectocarpus EsiCHILs characterization

Molecular Phylogenetic Analysis of EsiCHIL1 and EsiCHIL2 sequences:

86 sequences of homologues of EsiCHIL1 and EsiCHIL2 were gathered by PSI-BLAST from the National Center for Biotechnology Information NR database, followed by iterative profile hidden Markov model building and searches against public protein, expressed sequence tag and genome sequence databases. These sequences were aligned by MUSCLE and manually edited by JALVIEW resulting in the selection of 119 informative positions. This curated alignment was submitted to PhyML analysis using a bootstrapping procedure of 100 replicates and the WAG+G substitution model. Then the phylogenetic tree was customized into MEGA 5.03.

Modelization of tridimensional structure:

Structural models of EsiCHILs were realized by Swiss-Model (swissmodel.expasy.org) using the PDB entries 4DOL-A and 1FM7-A for AtFAP3 (At = *Arabidopsis thaliana*) and MsCHI (Ms= *Medicago sativa*), respectively. Main amino acids residues were customized with Chimera 1.6.2.

Expression and purification of recombinant proteins:

The *Ectocarpus* CHIL1 (Esi0184_0004) and CHIL2 (Esi0475_007) genes were amplified by PCR with the corresponding cDNA as templates. The pQE-80L (Qiagen) expression vector containing the isopropyl- β -D-thiogalactopyranoside-inducible bacteriophage T5 promoter was used to express all proteins. EsiCHIL1 was cloned using KpnI and HindIII restriction sites and the following primers: PQECHIL1Forw: 5'-GGATGGTACCGCCGACGTAACGGAAGGGCCACCAAGATA-3' and PQECHIL1Rev: 5'-GGATAAGCTTTACTAACGCTCCAGAAGGGCCGCAAC-3'. EsiCHIL2 was cloned using SphI and HindIII restriction sites and the following primers: PQECHIL2Forw: 5'-GGATGCATGCATGGCGGACCGGGCTACGGCTTCAACG-3' and PQECHIL2Rev: 5'-GGATAAGCTTTAGCTGCCAGGAACGCGGGCAC-3'.

Expression constructs encode full-length proteins with a six-His tag at their N termini. The obtained clones were transformed into recombinant *E. coli* BL21-CodonPlus-RIPL cells (Stratagene) and then selected using Luria-Bertani (LB) solid medium, supplemented with 100 µg/mL of ampicillin. Protein expression was induced in 500 mL Graffinity medium, a LB medium containing ampicillin 200 µg·µL⁻¹ and 0.25% glucose. Culture was incubated at 37°C until reaching an absorbance at 600 nm = 2, after which an equivalent volume of cold LB medium containing 0.6% lactose, 20 mM Hepes pH 7.0, and 1 mM IPTG was added and the culture was incubated for 18 h at 20 °C. Cells were then collected by centrifugation and resuspended in buffer A (20 mM Tris-HCl, pH 7.5, 300 mM NaCl, and 10 mM imidazole) supplemented with protease inhibitor mixture, lysozyme, and DNase. Cell lysis was performed by two passes on a French press to decrease viscosity of supernatants. Cellular debris was eliminated by centrifugation at 45,000 g at 4 °C during 90 min. All chromatographic procedures were performed on an Äkta Avant system at 20 °C (GE Healthcare). Tagged proteins were purified by affinity on immobilized Ni-nickel tetradeinate absorbent (NTA) medium using an imidazole gradient from 10 mM to 500 mM, according to the manufacturer's instructions (GE Healthcare), followed by purification on a Sephadryl-200 gel filtration column (GE Healthcare) with buffer containing 20 mM Tris-HCl, pH 7.5 and 300 mM NaCl. All protein samples were analyzed for purity and integrity using 12 % SDS-PAGE and chemiluminescent western blot detection using the kit Bio-Rad Clarity western ECL with anti-his tag antibodies.

Dynamic light scattering analysis was performed using a DynaPro-801 molecular-sizing instrument (Structural Biology platform; SB Roscoff) equipped with a microsampler (Protein Solutions). A 50 µL sample was passed through a filtering assembly containing a 0.02 mm filter into a 12 µL chamber quartz cuvette. The data were analyzed using the Dynamics 4.0 and DynaLS software.

Analysis of fatty-acid binding by EsiCHIL1 and EsiCHIL2 fold protein

Bound ligands were extracted from proteins while stirring samples continuously during 10 min using 10 µL of HCl 37 % mixed with 1 mL of ethyl acetate. The upper aqueous phase was collected and dried under N₂ at 40 °C before derivation by Sylon BFT and acetonitrile (V/V) 60 °C

1 hour. The derivated extract was then dried under N₂ and re-suspended in 100 µL hexane for GC-MS analysis.

GC-MS was operated in the EI mode on an Agilent GC 6890 coupled to a 5973 MS Detector (Agilent, Les Ulis, France) and equipped with a DB-5MS column 30 m × 0.25 mm inner diameter × 0.25 µm film thickness (J and W Scientific, Agilent). Temperatures of the injection port and interface were 250 and 280°C respectively; those of the ion source and MS analyzer were set at 230 and 150°C respectively. The samples were injected in splitless mode. The oven temperature was first set at 60°C for 5 min, then raised at 10 °C/min to 100 °C, elevated at 1 °C/min to 150 °C and finally elevated at 290 °C at the rate of 8 °C/min and held for 5 min. The compounds were ionized by electron impact at 70 eV energy. Analytes were detected by total ion current from *m/z* 50 to 850.

Microscale thermophoresis (MST) binding assays

The microscale thermophoresis (MST) assays consisted in the detection of changes in the hydration shell, charge or size of molecules by measuring changes of the mobility of molecules in microscopic temperature gradients ([Seidel et al. 2013](#)). In this study, the affinity of EsiCHILs for different substrates was tested.

The first assay was performed in the buffer used for the purification of recombinant proteins by Sephadryl-200 gel filtration supplemented by Tween 20 (0.05%). Recombinant protein was incubated with a substrate at different concentrations between 500 µM to 15 nM then the samples were loaded into MST NT-Label Free hydrophilic glass capillaries and the MST analysis was performed using the Monolith NT. Label Free.

In the second MST experiment 10 µM of proteins of interest were labeled with a fluorescent dye NT-647 using Monolith NT™ Protein Labeling Kits. The dye carries a reactive NHS-ester group that modifies primary amines as they are present in amino acids like lysine. We have kept the concentration of NT-647 labeled EsiCHIL1 constant, while the concentration of the non-labeled substrate was varied between 500 µM – 15 nM. After a short incubation the samples were loaded into MST NT.115 standard glass capillaries and the MST analysis was performed using the Monolith NT.115.

Arabidopsis mutant complementation and protein localization experiments in tobacco plants.

T-DNA insertion lines and mutant growth

Seeds of AtCHIL1 T-DNA insertion line (of At5G05270) were obtained from ???? the Arabidopsis Biological Resource Center

Quantitative reverse transcription - polymerase chain reaction analysis

To test whether T-DNA insertion mutant of *AtCHIL1* is knockout or knockdown, the expression of *AtCHIL1* was quantified, using qRT-PCR. Leaf samples were collected from wild type and mutant plants. Samples were flash frozen in liquid nitrogen and stored at -80 °C until processed. The samples were powdered in liquid nitrogen using a pre-chilled mortar and pestle. Approximately 60-80 mg of sample was used for total RNA extraction, with some modification to the method described by Chomczynski and Sacchi, (1987). The alteration to the protocol was made at the step after adding the 500 µl of Isopropanol. The initial protocol was to incubate the samples at room temperature for 10 minutes and instead of this, the samples were incubated at -20 °C for 15 minutes, which increased the yield and quality of RNA. The pellet was dissolved in 50 µl of DEPC (Diethylpyrocarbonate) water and gently mixed by using the bench top vortex. RNA concentrations were assessed using the Nanodrop 2000 Spectrophotometer (Thermo Scientific, Ontario, Canada). Two micrograms of RNA was treated with 2 units of RQ1 DNase (Promega, Ontario, Canada), according to the manufacturer's instructions, to eliminate any DNA contamination. The total volume of the reaction was made to 10 µl, using the DEPC water. The DNase-treated RNA was converted to cDNA, using an Applied Biosystems High Capacity cDNA Synthesis Kit (Applied Biosystems Ontario, Canada), according to the manufacturer's protocol. RT-PCR was performed using the EconoTaq® PLUS GREEN Master Mix (Lucigen, Ontario, Canada) with gene specific primers and *ACTIN* as the endogenous control on MJ Mini™ Personal Thermal Cycler (Bio-Rad, Ontario, Canada). The relative transcript levels were determined by Real-Time polymerase chain reaction, using the gene specific primers and *ACTIN* as the endogenous control, on the StepOne™ Real-Time PCR system (Applied Biosystems, Ontario, Canada), using

SYBR green (Applied Biosystems). Gene specific primer sequences were designed using Primer 3 Plus Software.

Subcellular localization and generation of transgenic lines

The cds clones of *EsiCHIL1* and *EsiCHIL2* were obtained as described above. Plasmid DNA concentrations were assessed using the Nanodrop 2000 Spectrophotometer (Thermo Scientific, Ontario, Canada). To clone the complete gene of interest, PCR was performed using the Takara master mix (Clontech, San Francisco, USA) with attB primers and plasmid DNA on MJ Mini™ Personal Thermal Cycler (Bio-Rad, Ontario, Canada). The attb PCR product was restriction digested with *Dpn1* (Invitrogen, Ontario, Canada) and purified by using 30% PEG 8000/30mM MgCl₂. The attB PCR product, which has attB sites, was cloned into pDONR221, which has attP sites, by the BP recombination reaction using the BP Clonase™ II Gateway®, following the manufacturer's instructions to create the entry clone containing the gene of interest (Gateway® Technology with Clonase II, Invitrogen, ON, Canada). The BP recombination reaction was then transformed into *E.coli* DH5α competent cells by the heat shock method, as described by the manufacturer's protocol.

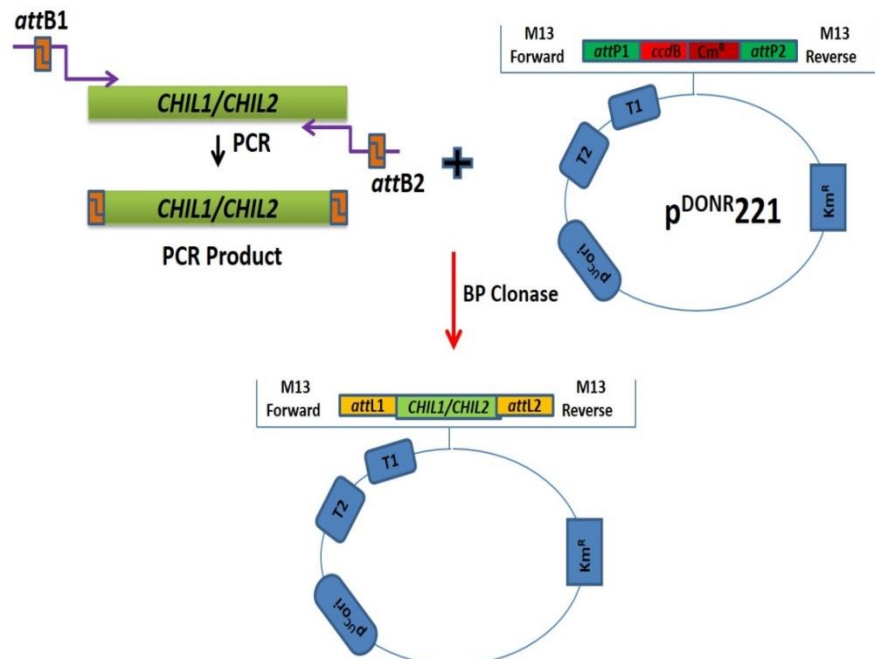


Figure 2.2: Scheme of the principle of the BP Clonase II Gateway strategy

The transformed cells were diluted to 1/10 and 1/100, and 100 µl of each was plated on pre-warmed LB plates containing kanamycin, 50 µg.ml⁻¹ and incubated at 37 °C overnight. The positive entry clones appeared on the plates the next day. Then, 10 positive entry clones were randomly inoculated in LB medium containing 50 µg.ml⁻¹ kanamycin and incubated overnight at 37 °C at 200 RPM. Plasmid DNA was isolated from the entry clones and concentration was assessed as described earlier. The approximate size of the entry clone was verified by running 2 µl of plasmid DNA on a 0.8% agarose gel in 1X TBE buffer along with GeneRuler 1Kb DNA ladder (Thermo Scientific, Ontario, Canada), at 80 V for 90 minutes.

To confirm the insert for gene of interest (*CHIL1/CHIL2*), PCR was performed with gene specific primers as described earlier. To generate the transformation vector, pEarleyGate104 (N-YFP; Earley, 2006) was obtained from ABRC (Columbus, OH, USA). The positive entry clone containing *attL* sites and complete sequence of the gene of interest were linearized by restriction digestion with *pVU1*, which cuts the kanamycin gene and, then cloned into pEarleyGate104 (N-YFP), containing *attR* sites, by LR recombination reaction using the LR Clonase™ II Gateway® (Figures 2.2 and 2.3), following the manufacturer's instructions to create the expression clone containing the gene of interest (Gateway® Technology with Clonase II, Invitrogen, ON, Canada). The LR reaction was transformed into *E.coli* DH5α cells, and the transformed cells diluted and plated, as discussed earlier in this section. The approximate size of the expression clone was confirmed as previously described. The insert for the gene of interest was confirmed by performing a PCR using gene specific primers as mentioned earlier.

Partie 1 : Voie de biosynthèse des phlorotannins

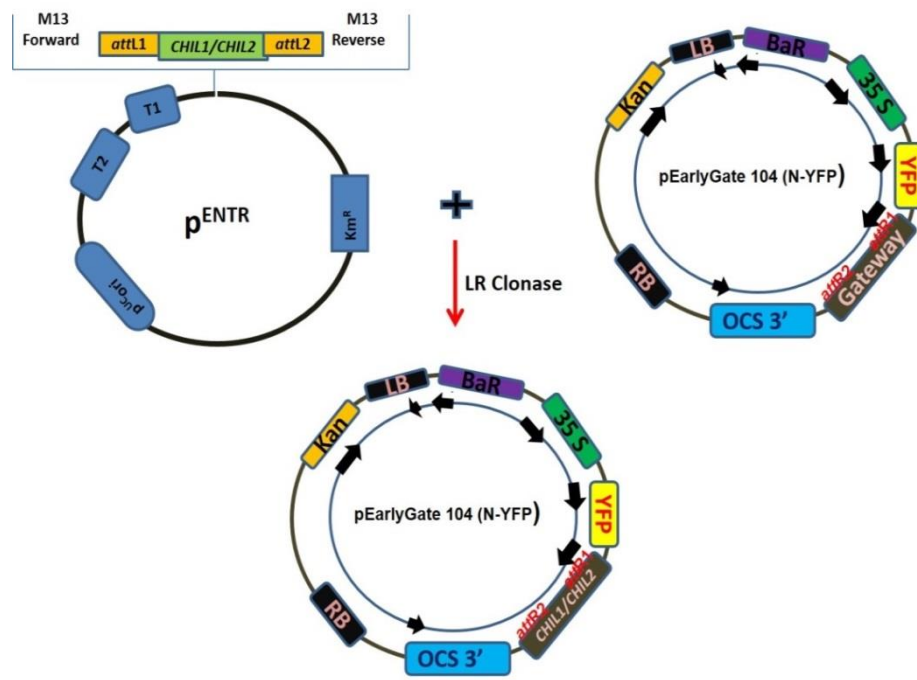


Figure 2.3: Scheme representing the following steps in the LR Clonase II Gateway strategy

The expression clone containing the gene of interest was transformed into *Agrobacterium* strain GV310 (pMB90) using the freeze and thaw method as described by Hofgen and Willmitzer (1988). The transformed cells were plated on LB plates containing 50 µg.ml⁻¹ of kanamycin, and 50 µg.ml⁻¹ of gentamycin. The plates were incubated at 28 °C for 3 days. After 3 days, colony PCR was performed to confirm the insert. The recombinant *Agrobacterium* strain carrying the gene of interest was transformed to flowering Col-0 plants, using the floral dip method, as described by Clough and Steven (1998). Seeds were collected from the floral dipped transgenic plants, planted in the Jiffy peat pellets (Jiffy, NB, Canada), and placed in a growth chamber set at 22 °C with a 16-h light/8-h dark cycle, and a light intensity of 100 µmol.m⁻²s⁻¹. After 10 days of growth, the plants were sprayed with 250 µM ammonium glufosinate (Sigma, Ontario, Canada) as the expression clone harbored the *Basta* resistant gene and ammonium glufosinate is the active ingredient of *Basta*. After one week, plants started to turn yellow and then they were again sprayed with ammonium glufosinate, as mentioned above. After this, only positive plants survived, and gene expression was confirmed as described earlier by excising one leaf from each positive plant.

Transient expression of CHIL1 in Tobacco

To study subcellular localization of *CHIL1*, the organ specific markers for mitochondria (MT), Golgi bodies (GB), chloroplasts (Chl), endoplasmic reticulum (ER), plastids (PT) and peroxisomes (PX) were obtained from ABRC (Columbus, OH, USA; Nelson, 2007). The markers were streaked on LB plates containing 50 µg.ml⁻¹ kanamycin and plates were incubated at 37 °C overnight. Next day, one colony was selected from each plate by sterile loop, transferred in to 5 ml LB liquid medium containing 50 µg.ml⁻¹ kanamycin, and incubated at 37 °C for overnight at 200 RPM (revolution per minute). Plasmid DNA was isolated and concentration was accessed as described in previous section. Plasmid DNA for each marker was transformed to *Agrobacterium* strain GV310 (pMB90), and positive clones were selected as described in the previous section. To study the co-localization, tobacco plants were grown in the pots filled with promix and maintained in controlled conditions as mentioned in the earlier section. When plants were one month old, and leaves were large enough to infiltrate them, they were used in the experiment. Transformed vector pEarelyGate104 (N-YFP) carrying the gene of interest in *Agrobacterium* and organ specific markers in *Agrobacterium* were grown in liquid LB medium containing 50 µg.ml⁻¹ of kanamycin, and 50 µg.ml⁻¹ of gentamycin at 28 °C at 200 RPM until it reached an OD₆₀₀ of 0.8. The cells were collected by centrifugation, and rinsed with sterile water and re-centrifuged. The cells were re-suspended in infiltration medium prepared as described by ([Sparkes, et al. 2006](#)). The final 0.1 (OD₆₀₀) of expression clone and 0.1 (OD₆₀₀) of above mentioned organ specific markers was mixed well and co-infiltrated in cleaned tobacco leaves as described by [Sparkes et al., \(2006\)](#). After 24 and 48 hrs the leaves were cut into pieces and examined for co-localization using a confocal microscope (Carl Zeiss, Ontario, Canada), at the CMDI (center for molecular digital imaging) Dalhousie University, Halifax.

Fatty Acid analysis

The samples of fatty acids were extracted by following a protocol using barium hydroxide hydrolysis as described by ([Markham et al. 2006](#)); ([Bonaventure et al. 2003](#)); ([Moon, S. & Nikolau 2009](#)) 100 mg of fresh tissue or 5 mg of seeds were used for fatty acid extraction. The samples were flash frozen in liquid nitrogen and grounded into fine powder. The samples were

transferred into a micro centrifuge tube and 20 µl of internal standard (heptadecanoic acid C17:0, 2 mg.ml⁻¹ in chloroform) and 1 ml of barium hydroxide was added. The samples were completely homogenized. The homogenized samples were transferred into glass vials and 550 µl of 1, 4 dioxane (Sigma, ON, Canada) was added. The glass vials were closed tightly and incubated at 110 °C for 24 hours. The samples were acidified by adding 6 drops of 6 M HCl and extracted twice with hexane (3 ml each). The samples were centrifuged at 6000 RPM for 10 minutes and the hexane layer was transferred into a new glass tube. The sample was dried under nitrogen and it was methylated using 2 ml of HCl : methanol (1:1) at 80 °C for 1 hour. The methylation was followed by two extractions in hexane (2 ml each) and samples were dried under nitrogen gas. The samples were acetylated using 1ml of acetonitrile (Sigma, ON, Canada) and 70 µl of bis-(trimethylsilyl) trifluoroacetamide at 60 °C for 20 minutes. This solvent was evaporated under nitrogen gas and samples were suspended in 200 µl of chloroform. The chloroform dissolved samples were subjected for fatty acid analysis using gas chromatography (Bruker, ON, Canada) with the FAME standard from C8: C24.

Results and discussion

Phylogenetic study of EsiCHILs :

To assess the evolutionary relationship between *Ectocarpus CHILs* and the already established CHIL phylogeny published recently by [Ngaki et al. \(2012\)](#) and [Morita et al. \(2014\)](#), a combined multiple alignment and phylogenetic analysis was conducted. The results are shown in Figure 2.4. We identified 6 major clades. Two clades display essentially sequences from Stramenopile CHI-like proteins (CHIL1 and CHIL2 respectively) and CHIL2-type sequences are the closest related sequences, from CHI-like proteins from green algae and cryptophytes that were hypothesized as ancestral Fatty Acid Binding Proteins. A group that was considered as the green alga FAP proteins by [Ngaki et al \(2012\)](#) encompasses *Arabidopsis FAP3* sequences and is here called Viridiplantae FAP3. Another unlabeled clade encompasses sequences from vascular plants that are the bona fide CHI enzymes, whereas the second is composed of FAP1 proteins from vascular plants and Chlorophyceae. It appears clearly from this phylogeny that sequences from Stramenopiles belong to a distinct family of FAP proteins than the others FAP1, 2 and 3 and are more closely related to the FAP3 clade from Viridiplantae. They are more distant from the clade of bona fide CHI and CHIL from terrestrial plants that correspond to type I, type II and type IV, respectively, in the nomenclature of [Ralston et al. \(2005\)](#)

Modelization of tridimensional structure

After modelization of the EsiCHIL proteins (Figure 2.5), the superposition between AtFAP3 and EsiCHILs reveals a global conservation of the whole structure, and particularly in the β -hairpin. In contrast, the superposition of AtFAP3 and MsCHI shows divergent β -hairpin structure. In addition, the main amino acids involved in the binding of substrates for AtFAP3 are conserved in EsiCHILs, four of five residues are identical the Lysine (K), Arginine (R), Alanine (A) and Tyrosine (Y) and the last one Phenylalanine (F) is replaced by a Methionine (M) in EsiCHIL1 and by a Valine (V) in EsiCHIL2. In contrast, all these residues are different between MsCHI and AtFAP3 as shown previously ([Ralston et al., 2005; Ngaki et al., 2012](#)).

Partie 1 : Voie de biosynthèse des phlorotannins

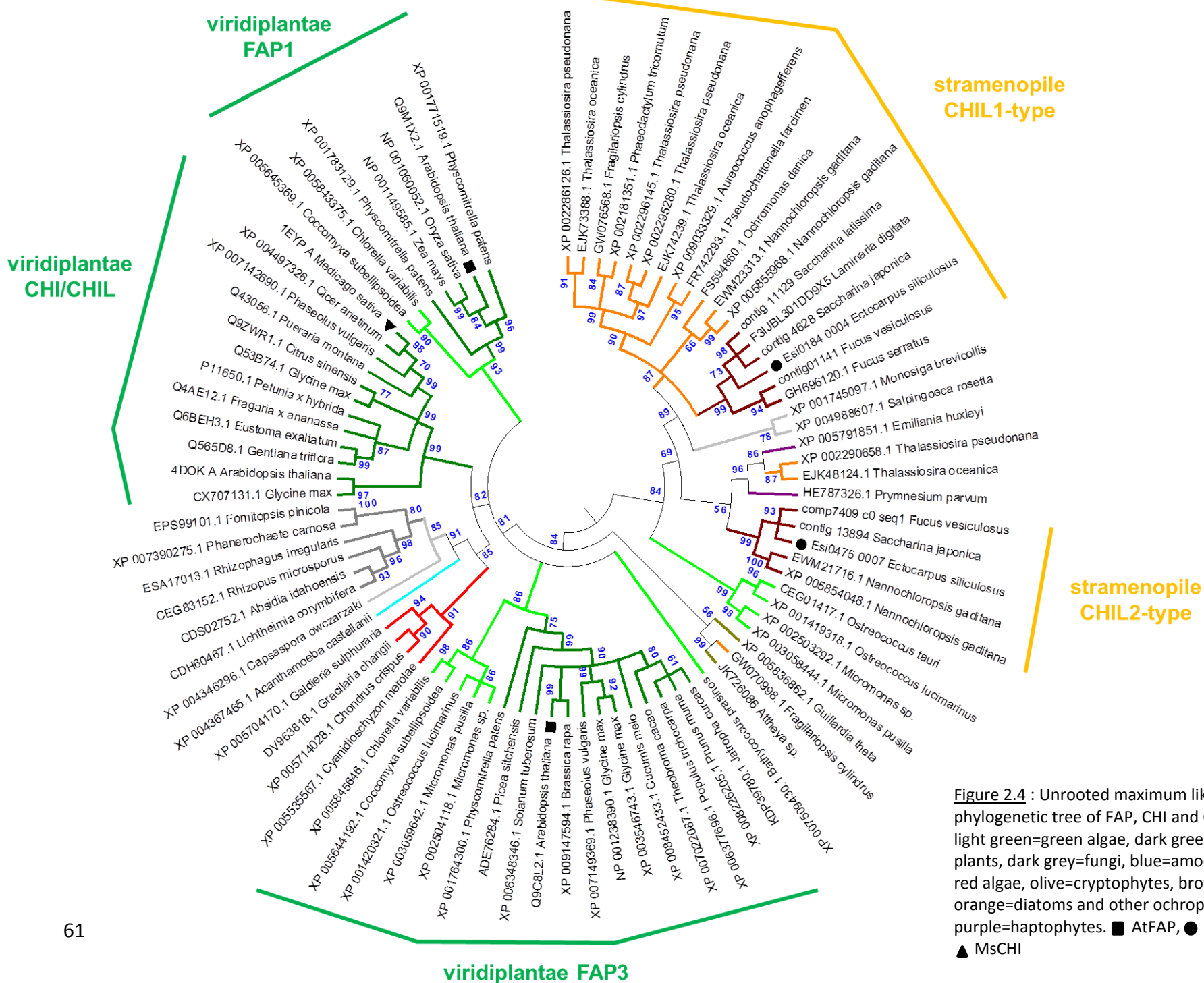


Figure 2.4 : Unrooted maximum likelihood phylogenetic tree of FAP, CHI and CHIL proteins. light green=green algae, dark green=terrestrial plants, light grey=fungi, blue=amoebozoans, red=red algae, olive=cryptophytes, brown=brown algae, orange=diatoms and other ochrophytes, purple=haptophytes. ■ AtFAP, ● EsiCHIls, ▲ MsCHI

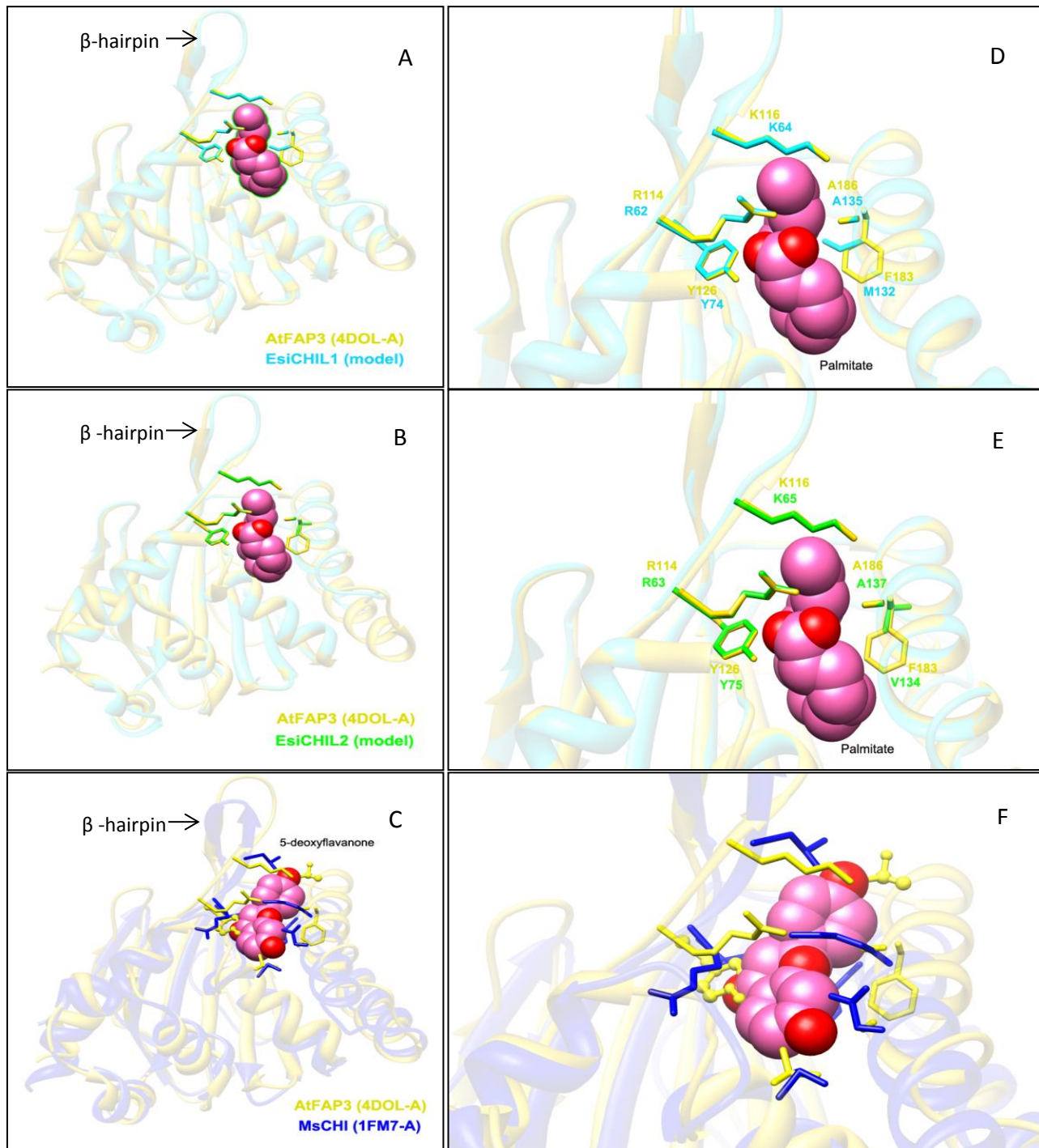


Figure 2.5: A. A model of the superposition of AtFAP3 and EsiCHIL1, B. Superposition of AtFAP3 and EsiCHIL2, C. Superposition of AtFAP3 and MsCHI. D.E.F. panels represent a respective focus of A.B.C showing the main residues implicated in the binding. Pink molecule corresponding to palmitate in A.B.D.E. panels, and to 5-deoxyflavanone in C.F. panels.

Purification of recombinant enzymes

EsiCHIL1 and EsiCHIL2 were purified by affinity on Ni-NTA column (GE Healthcare) and by Sephadryl-200 gel filtration column (Figure 2.6). We obtain after electrophoresis migration in denaturing condition (SDS-PAGE) for the EsiCHIL1 purification by gel filtration (Figure 2.6A) a major band corresponding to a protein of 24kDa (Figure 2.6B) confirmed by western blot using the His-tag antibody (Figure 2.6C). For EsiCHIL2 a major band is observed after the purification step by gel filtration (Figure 2.6D) at 21.5 kDa, but some aggregations stay on the top of Coomassie blue-stained gel (Figure 2.6E).

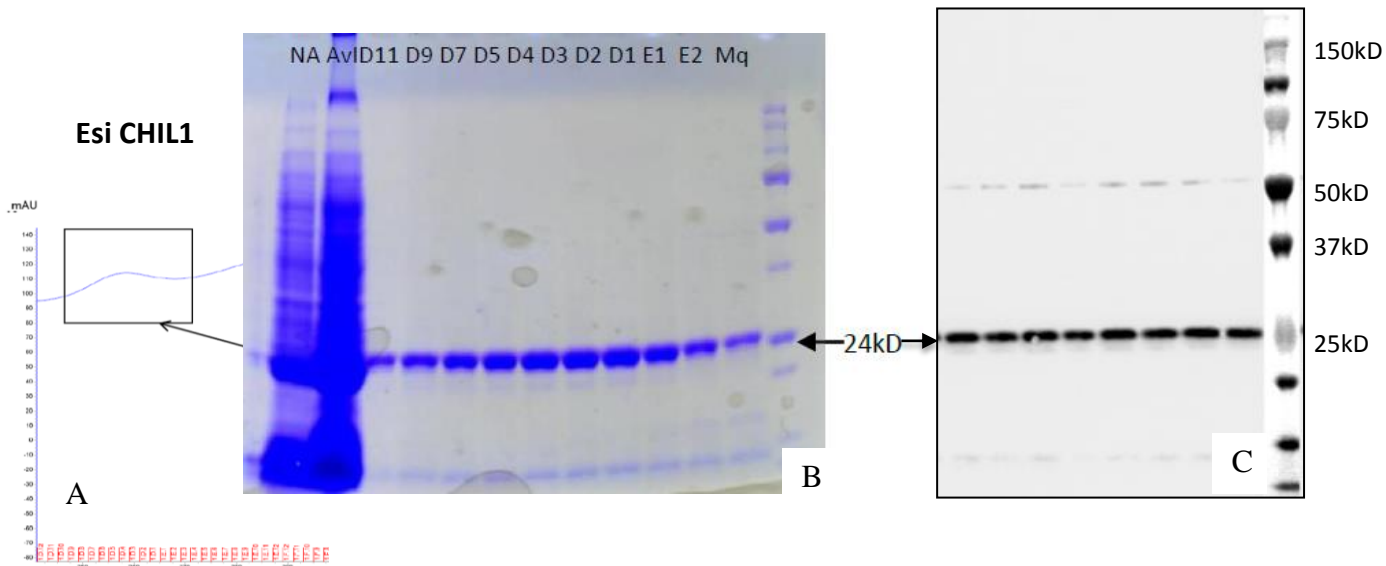


Figure 2.6: A. Chromatogram corresponding to the absorbance in UV (mAU) during the purification by gel filtration of recombinant EsiCHIL1. B) SDS-PAGE of recombinant EsiCHIL1 from *E. siliculosus*. Lane 1: Fraction non retained by the column; lane 2: crude extract before purification; lane 3-12: Fractions of the proteins eluted during the purification by IMAC affinity. lane 13: Molecular weight marker (15-150 kDa); Arrows point at the bands. C. Western-blots corresponding to SDS-PAGE gel revelation by anti-histag antibodies.

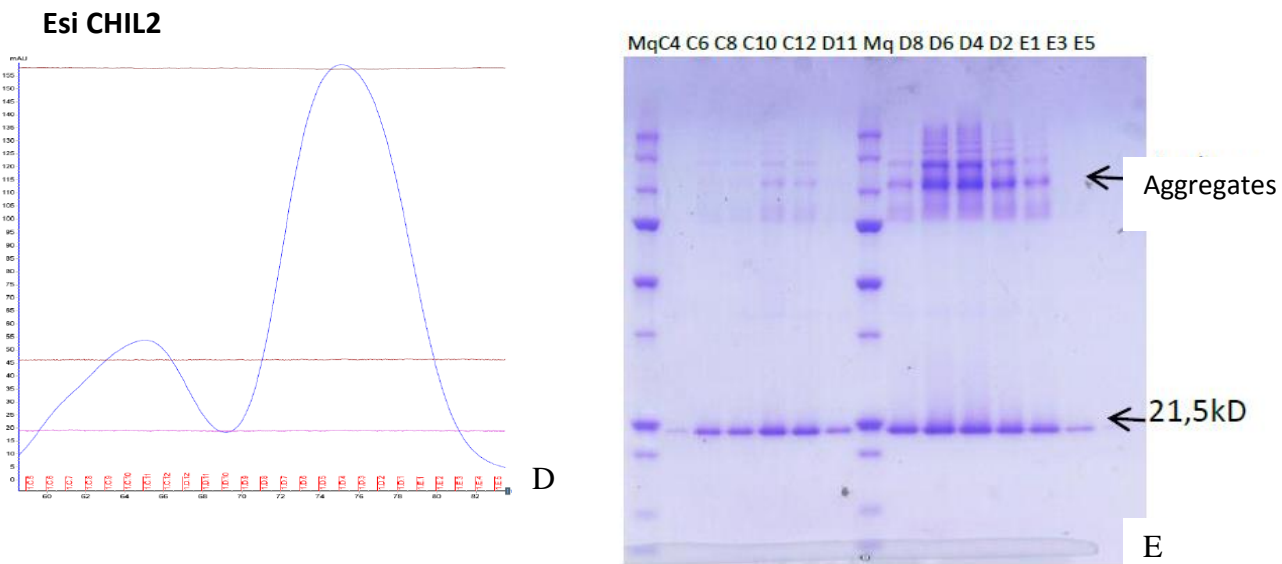


Figure 2.6: D. Chromatogram corresponding to the absorbance in UV (mAU) during the purification by gel filtration of EsiCHIL2. E. SDS-PAGE gel colored by Coomassie blue corresponding to fractions collected during the purification.

Analysis of fatty-acid binding by CHIL1 and CHIL2 proteins

After organic acid extraction and derivation of compounds bound to the recombinant proteins, GC-MS chromatograms were obtained. By comparing the control containing the buffer, with protein extracts, we can identify different fatty acids that were trapped in the protein (Figure 2.7). These free fatty acids originated from *E Coli* and were kept by EsiCHIL1 or EsiCHIL2 during the production of the recombinant proteins in *E. coli* cultures.

Partie 1 : Voie de biosynthèse des phlorotannins

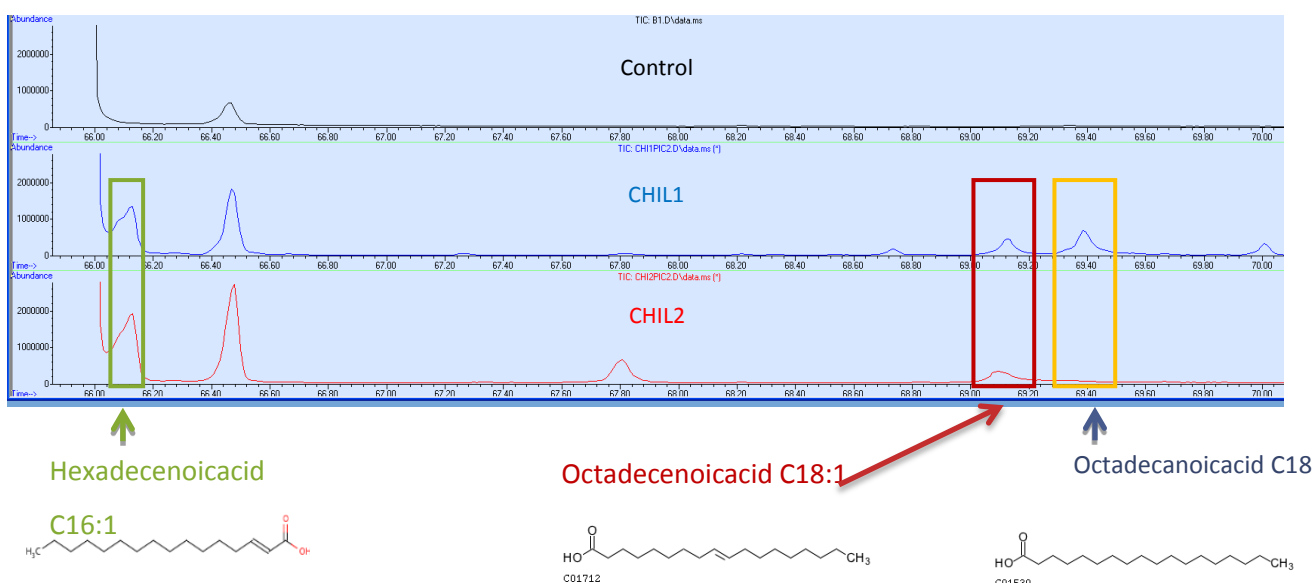


Figure 2.7: Analysis of ligands associated with purified recombinant Esi-CHIL proteins separated and detected by GC-MS. GC-MS chromatograms of ethyl acetate extracts from purification buffer (control) and Esi-CHIL1 and Esi-CHIL2, respectively..

Microscale thermophoresis (MST) binding assays

The microscale thermophoresis analysis revealed a differential interaction between EsiCHIL1 and substrates (Table 2.1). We found a preferential interaction of EsiCHIL1 with palmitoyl coA (C16 CoA) $K_d = 31.2\mu M +/- 3.7\mu M$ than for palmitic acid (C16) $K_d = 153\mu M +/- 1.83\mu M$. In contrast, no affinity was detected with C18 (Table 1).

Table 2.1: Results of microscale thermophoresis between EsiCHIL1 and different substrates expressed by the calculation of the constant of dissociation in (K_d).

Substrate	Source Fluorescence	MST measured Dissociation constant (K_d)
C18:1	NT647	No K_d
C18:2	NT647	No K_d
C18:3	NT647	No K_d
C16:0	NT647	$153\mu M +/- 1.83\mu M$
C16 CoA	NT647	$31.2\mu M +/- 3.7\mu M$

Molecular characterization of AtCHIL-1 expression in *Arabidopsis*

qRT-PCR analysis of At5G05270 (*AtCHIL-1*) expression revealed that *Atchil-1* is a knockdown line.

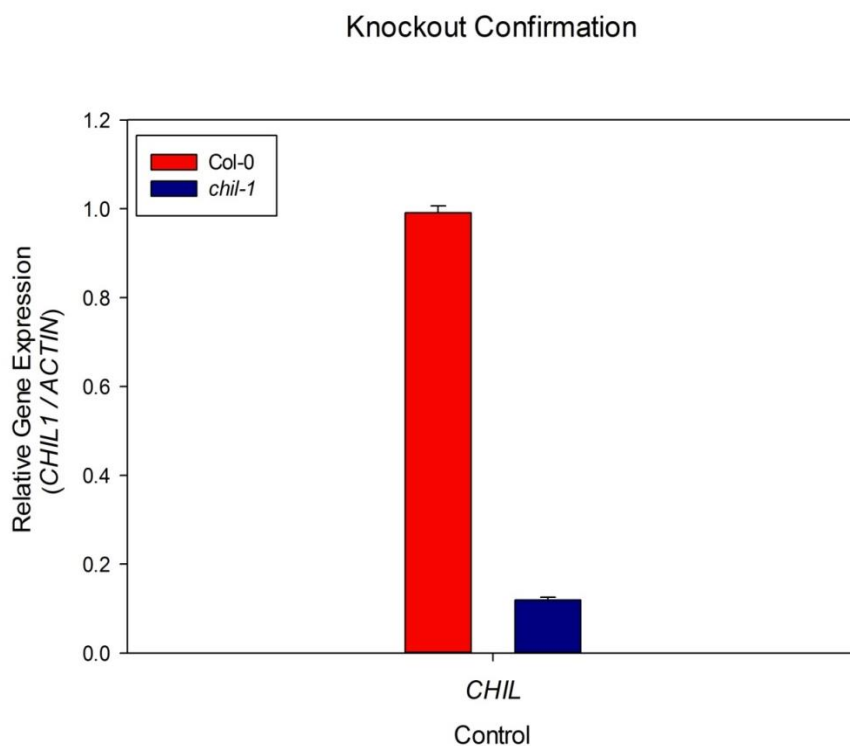


Figure 2.8: Relative gene expression in T-DNA insertion line of *Arabidopsis thaliana* *CHIL1* and the *Col-0* wild type. The expression of *CHIL1* gene is normalized to the geometric mean of the expression of actin. Values represent means of three independent replicates and bars represent the SE.

Subcellular localization of *EsiCHIL1* in tobacco cells.

To study the localization of *EsiCHIL-1* protein in the plant cell, the gene was cloned into the plant transformation vector (pEarleyGate104-N-YFP, Earley, 2006) using Gateway Technology (Gateway® Technology with Clonase II, Invitrogen, ON, Canada), and the plasmid was incorporated into *Agrobacterium*. The subcellular localization of YFP tagged *EsiCHIL-1* protein was examined in tobacco leaves through confocal microscopy as described by (Sparkes et al. 2006). The subcellular localization study revealed that YFP-*EsiCHIL-1* was localized in the

chloroplast. (Nelson et al. 2007) reported the use of this chloroplast marker for subcellular localization studies. The images (Figure 2.9) were taken at different magnification (40X and 60X) and on different planes. The round oval shape is the chloroplast of tobacco cell.

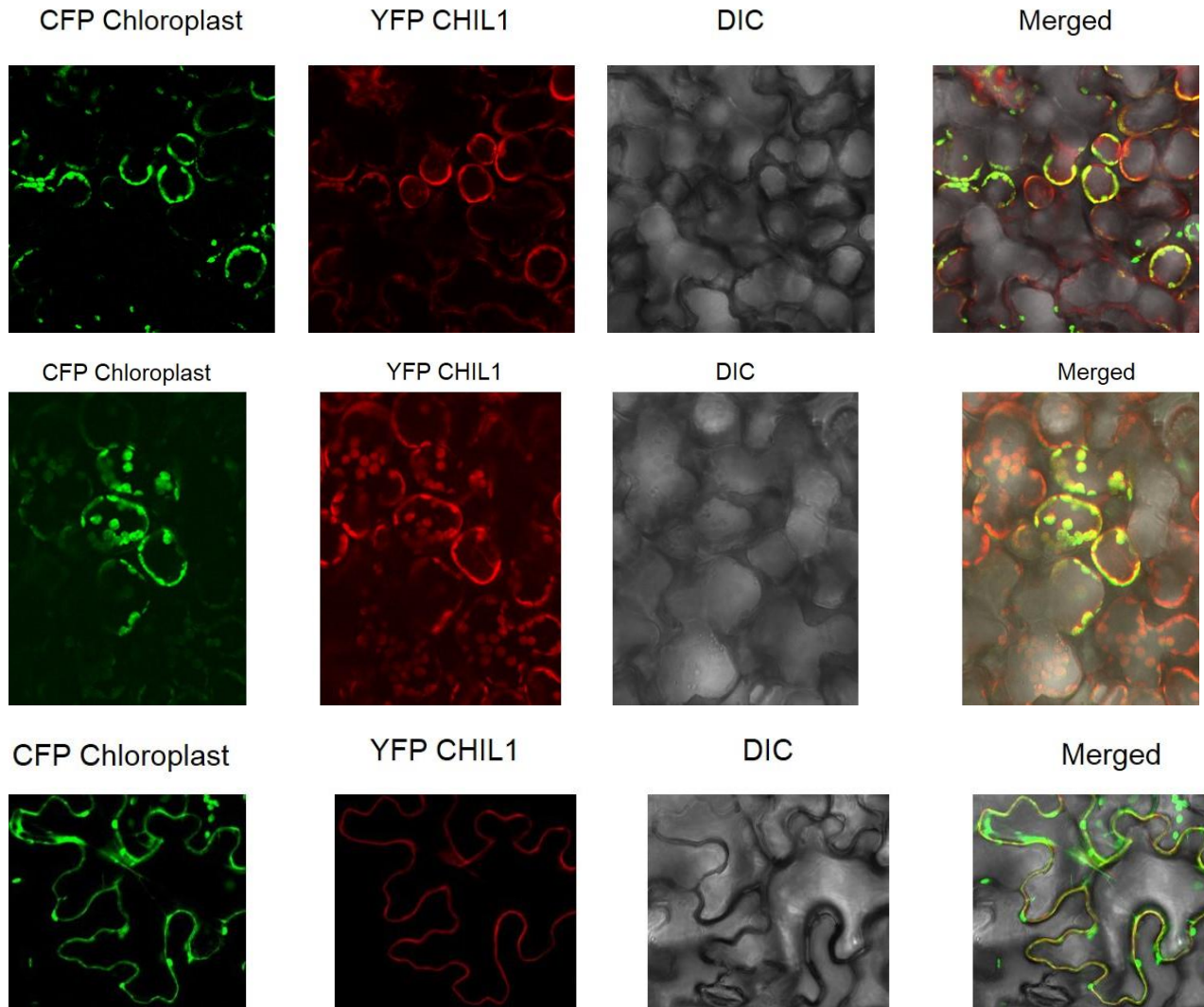


Figure 2.9: Subcellular localisation of *EsiCHIL1* in tobacco cells. Confocal images of a water infiltrated leaf of *Nicotiana* displayed in false colour. **A-D:** Confocal section through the palisade parenchyma of a water-infiltrated leaf of a *Esi-CHIL1-YFP* overexpressing plant **A,E,I:** Chlorophyll autofluorescence, **B,F,J:** YFP fluorescence, **C,G,K:** DIC Images, **D,H,L:** Merged images of chlorophyll, YFP fluorescence with a DIC image.

Overexpression of EsiCHIL-1 and Esi-CHIL-2 in Arabidopsis

EsiCHIL-1 was overexpressed in the wild type plants as described by (Clough and Bent 1999), to further study the phenotype of overexpression lines. In this study, two overexpression lines (*chil1-1*, *chil1-2*) were identified by qRT-PCR for *EsiCHIL1* and *chil2-1* and *chil2-2* for *EsiCHIL2*. In wild type (Col-0) plants, no expression was detected for both *EsiCHIL1* and *EsiCHIL2* (Figure 2.10).

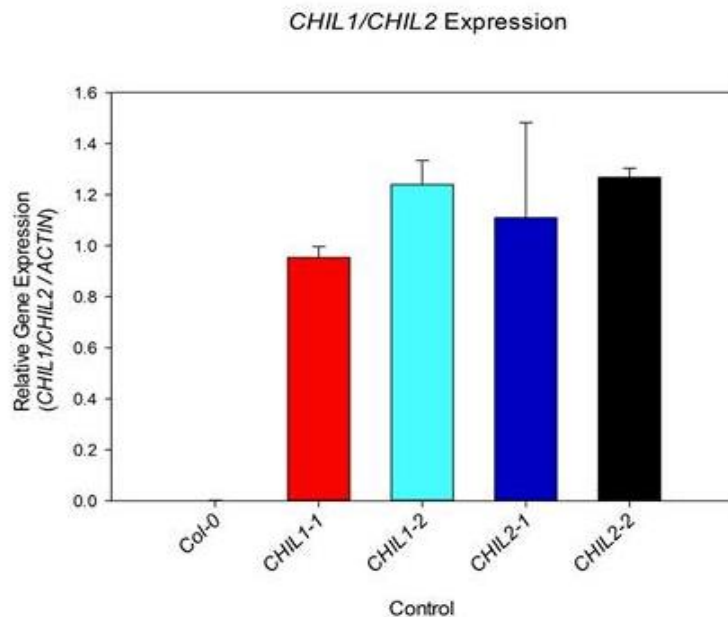


Figure 2.10: Relative gene expression in transgenic lines of *Arabidopsis thaliana* for *Esi-CHIL1* and *Esi-CHIL2* genes. The expression of a gene is normalized to the geometric mean of the expression of actin. Values represent means of three independent replicates and bars represent the SE.

Fatty acids analysis

In fatty acid analysis, the difference in concentration of C14:0 to C18:3 fatty acids was observed in wild type and *AtCHIL* mutant. The tables 2.2, 2.3 and 2.4 display the retention time, area and height for peaks of standard and plant samples.

Table 2.2: Fatty Acid Methyl Esterified (FAME) Standard C8 to C24

Name	Rt	Height	area
C8:0	6.37	202246.4	5512.6
C10:0	8.64	136294.9	5732.7
C12:0	12.66	96055.1	5762
C14:0	17.96	72196.3	5583.2
C16:0	24.26	80251.3	7514.1
C16:1	25.15	38133.2	3271.1
C18:0	30.81	51378.7	5334.1
C18:1	31.58	32180	3377.8
C18:2	33.47	27938.9	3318.2
C18:3	36.45	23876.6	3306.9
C20:0	39.87	29415.6	5131.8
C22:0	54.28	22217.2	5002.9
C22:1	55.84	14456.6	3196
C24:0	70.16	10781.1	4232.1

Table 2.3: Fatty acids in wild type leaf

Name	Rt	Height	area
C14:0	17.9	3866.2	278.7
C16:0	24.23	52152.1	4542.9
C18:0	30.76	30203	2972.6
C18:1	31.56	13645.6	1700.2
C18:2	33.44	17469.7	2060.6
C18:3	36.46	35318.6	5033.5

Table 2.4: Fatty acids in *AtCHIL1* mutant leaf

Name	Rt	Height	area
C14:0	0	0	0
C16:0	24.2	27049.5	2244.6
C18:0	30.74	14622.8	1415.8
C18:1	31.53	6082.8	691.2
C18:2	33.41	11030.3	1282.6
C18:3	36.43	22384.5	3121.7

Conclusion and prospects

Phlorotannins are known only from brown algae and are structural analogues of condensed tannins such as anthocyanidins and other flavonoid derivatives from vascular plants. Therefore, we hypothesized that the conserved chalcone isomerase-like proteins encoded in the *Ectocarpus* genome may also act in a potential step in phlorotannin biosynthesis. We found that the CHI-like proteins EsiCHIL1 and EsiCHIL2 from the brown alga *Ectocarpus* are ancestral proteins in the family of chalcone isomerase fold proteins. They function as fatty-acid binding proteins closely related to the FAP3 family recently characterized in *Arabidopsis* for their biochemical and structural features ([Ngaki et al., 2012](#)). By modelization, EsiCHILs were shown to have conserved important structural features with AtFAPs that participate in fatty-acid binding. The expression of GFP-fused Esi-CHIL1 in tobacco plants revealed that the protein is targeted to the chloroplast similar to the localization of AtFAPs proteins ([Ngaki et al., 2012](#)). Overexpression of *EsiCHIL1/2* was confirmed in *Arabidopsis* transgenic lines. The complementation of an *AtCHIL1* null mutant was attempted from an *Arabidopsis* T-DNA insertion line and the phenotypes of the complemented plants will soon become available. However, further developments are required using at least another T-DNA insertion line for the *Atfap3* proteins ([Ngaki et al. 2012](#)), because the *AtCHIL1* is not closely related to EsiCHIL1/2 proteins and belongs to the clade of type IV CHI-like proteins, which seems to have evolved novel functions than FAPs related to specific secondary metabolism in mosses and vascular plants ([Morita et al. 2014](#)). Ongoing work involves, i) Overexpression of *EsiCHIL1/2* in *AtCHIL1* mutants and other mutant lines; ii) The selection of homozygous transgenic lines; iii) GC experiments for quantifying fatty acids in wild type, *AtCHIL1* mutant and in *EsiCHIL1/2* overexpression lines and iv) global phenotypic characterization of *EsiCHIL1/2* transgenic lines.

From the available results, it is likely that CHILs proteins participate in fatty-acid metabolism in *Ectocarpus* and are not directly involved in phlorotannin biosynthesis.

References :

- Amsler CD, Fairhead VA (2006) Defensive and Sensory Chemical Ecology of Brown Algae. In: Callow JA (ed) Inc. Adv. Plant Pathol. Academic Press, pp 1–91
- Arnold TM, Targett NM (2002) Marine Tannins: The Importance of a Mechanistic Framework for Predicting Ecological Roles. *J Chem Ecol* 28:1919–1934.
- Bonaventure G, Salas J (2003) Disruption of the FATB gene in *Arabidopsis* demonstrates an essential role of saturated fatty acids in plant growth. *Plant Cell* ... 15:1020–1033. doi: 10.1105/tpc.008946.2
- Chapman E, Best MD, Hanson SR, Wong C-H (2004) Sulfotransferases: structure, mechanism, biological activity, inhibition, and synthetic utility. *Angew Chem Int Ed Engl* 43:3526–48. doi: 10.1002/anie.200300631
- Clough SJ, Bent AF (1999) Floral dip : a simplified method for *Agrobacterium*-mediated transformation of *Arabidopsis thaliana*. *Plant J* 16:735–743.
- Cock JM, Sterck L, Rouzé P, et al. (2010) The *Ectocarpus* genome and the independent evolution of multicellularity in brown algae. *Nature* 465:617–21. doi: 10.1038/nature09016
- Dombrovski L, Dong A, Bochkarev A, Plotnikov AN (2006) Crystal structures of human sulfotransferases SULT1B1 and SULT1C1 complexed with the cofactor product adenosine-3'- 5'-diphosphate (PAP). *Proteins* 64:1091–4. doi: 10.1002/prot.21048
- Gidda SK, Varin L (2006) Biochemical and molecular characterization of flavonoid 7-sulfotransferase from *Arabidopsis thaliana*. *Plant Physiol Biochem* 44:628–36. doi: 10.1016/j.plaphy.2006.10.004
- Glombitza K-W, Knoss W (1992) Sulphated phlorotannins from the brown alga *Pleurophycus gardneri*. *Phytochemistry* 31:279–281.
- Hirschmann F, Krause F, Papenbrock J (2014) The multi-protein family of sulfotransferases in plants: composition, occurrence, substrate specificity, and functions. *Front Plant Sci* 5:556. doi: 10.3389/fpls.2014.00556
- Jakoby W, Ziegler D (1990) The enzymes of detoxication. *J Biol Chem* 265:20715–20718.
- Knoss W, Glombitza K-W (1993) A phenolsulphatase from the marine brown alga *Cystoseira tamariscifolia*. *Phytochemistry* 32:1119–1123.
- Markham JE, Li J, Cahoon EB, Jaworski JG (2006) Separation and identification of major plant sphingolipid classes from leaves. *J Biol Chem* 281:22684–94. doi: 10.1074/jbc.M604050200
- Martiny VY, Carbonell P, Lagorce D, et al. (2013) In silico mechanistic profiling to probe small molecule binding to sulfotransferases. *PLoS One* 8:e73587. doi: 10.1371/journal.pone.0073587
- Meslet-Cladire L, Delage L, J.-J. Leroux C, et al. (2013) Structure/Function Analysis of a Type III Polyketide Synthase in the Brown Alga *Ectocarpus siliculosus* Reveals a Biochemical Pathway in Phlorotannin Monomer Biosynthesis. *Plant Cell* 25:3089–3103. doi: 10.1105/tpc.113.111336
- Michel G, Tonon T, Scornet D, et al. (2010) The cell wall polysaccharide metabolism of the brown alga *Ectocarpus siliculosus*. Insights into the evolution of extracellular matrix polysaccharides in Eukaryotes. *New Phytol* 188:82–97. doi: 10.1111/j.1469-8137.2010.03374.x
- Moon, S. & Nikolau BJ (2009) Plantmetabolomics Platform2: fatty acids. In: <http://www.plantmetabolomics.org>.
- Morita Y, Takagi K, Fukuchi-Mizutani M, et al. (2014) A chalcone isomerase-like protein enhances flavonoid production and flower pigmentation. *Plant J* 78:294–304. doi: 10.1111/tpj.12469
- Negishi M, Pedersen LG, Petrotchenko E, et al. (2001) Structure and function of sulfotransferases. *Arch Biochem Biophys* 390:149–57. doi: 10.1006/abbi.2001.2368

- Nelson BK, Cai X, Nebenführ A (2007) A multicolored set of in vivo organelle markers for co-localization studies in Arabidopsis and other plants. *Plant J* 51:1126–36. doi: 10.1111/j.1365-313X.2007.03212.x
- Ngaki MN, Louie G V, Philippe RN, et al. (2012) Evolution of the chalcone-isomerase fold from fatty-acid binding to stereospecific catalysis. *Nature* 485:530–3. doi: 10.1038/nature11009
- Parys S, Rosenbaum A, Kehraus S, et al. (2007) Evaluation of quantitative methods for the determination of polyphenols in algal extracts. *J Nat Prod* 70:1865–70. doi: 10.1021/np070302f
- Pelletreau KN, Targett NM, Patterns I (2008) New Perspectives for Addressing Patterns of Secondary Metabolites in Marine Macroalgae. 121–146.
- Ragan, Glombitza (1986) Phlorotannins, brown algal polyphenols. *Prog Phycol Res Round FE Chapman DJ (ed)* Biopress Ltd Bristol 129–241.
- Ralston L, Subramanian S, Matsuno M, Yu O (2005) Partial Reconstruction of Flavonoid and Isoflavonoid Biosynthesis in Yeast Using Soybean Type I and Type II Chalcone Isomerases. *Plant Physiol* 137:1375–1388. doi: 10.1104/pp.104.054502
- Seidel SAI, Dijkman PM, Lea WA, et al. (2013) Microscale thermophoresis quantifies biomolecular interactions under previously challenging conditions. *Methods* 59:301–15. doi: 10.1016/j.ymeth.2012.12.005
- Sparkes I a, Runions J, Kearns A, Hawes C (2006) Rapid, transient expression of fluorescent fusion proteins in tobacco plants and generation of stably transformed plants. *Nat Protoc* 1:2019–25. doi: 10.1038/nprot.2006.286
- Steevensz AJ, Mackinnon SL, Hankinson R, et al. (2012) Profiling Phlorotannins in Brown Macroalgae by Liquid Chromatography-High Resolution Mass Spectrometry. *Phytochem Anal* 23:547–553. doi: 10.1002/pca.2354
- Varin L, Chamberland H, Lafontaine JG, Richard M (1997) The enzyme involved in sulfation of the turgorin, gallic acid 4-O-(-D-glucopyranosyl-6'-sulfate) is pulvini-localized in *Mimosa pudica*. *Plant J* 12:831–837.
- Varin L, DeLuca V, Ibrahim RK, Brisson N (1992) Molecular characterization of two plant flavonol sulfotransferases. *Proc Natl Acad Sci* 89:1286–1290. doi: 10.1073/pnas.89.4.1286
- Vreeland V, Waite JH, Epstein L (1998) Minireview-polyphenols and oxidases in substratum adhesion by marine algae and mussels. *J Phycol* 34:1–8. doi: 10.1046/j.1529-8817.1998.340001.x
- Welling M, Ross C, Pohnert G (2011) A desulfatation-oxidation cascade activates coumarin-based cross-linkers in the wound reaction of the giant unicellular alga *Dasycladus vermicularis*. *Angew Chem Int Ed Engl* 50:7691–4. doi: 10.1002/anie.201100908
- Welling MA (2010) The Role of Sulfated Metabolites in the Wound Response of Siphonous Green Algae.

Chapitre 3: Etude préliminaire des aryl-sulfotransférases d'*Ectocarpus*: Surexpression des enzymes recombinantes.

Introduction

Lors des travaux pionniers de [Ragan et Glombitza \(1986\)](#) portant sur l'étude des structures chimiques des phlorotannins, plusieurs structures de phlorotannins sulfatés de petite masse moléculaire ont été décrites (Figure 3.1 ; [Glombiza & Knoess, 1992](#)).

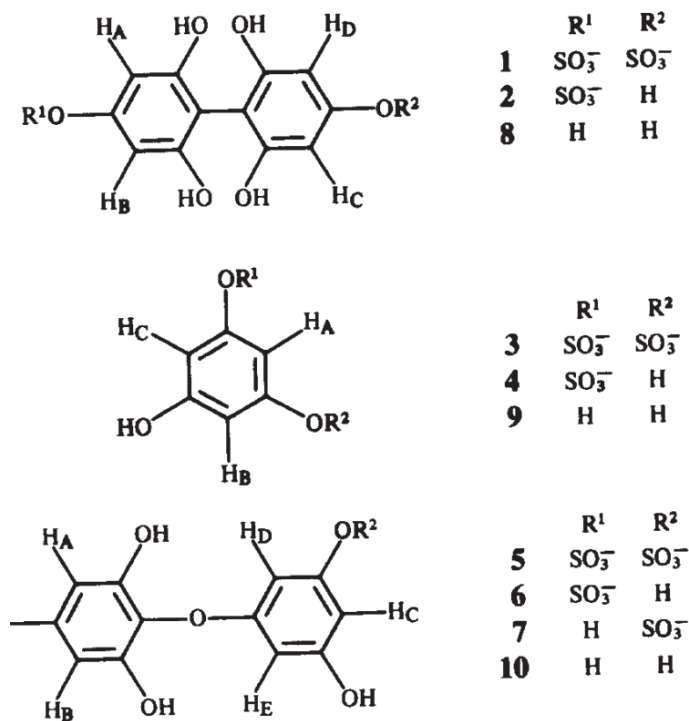


Figure 3.1: Structures chimiques de phlorotannins sulfatés ([Glombitza and Knoss 1992](#))

La sulfatation des composés phénoliques a largement été étudiée chez les mammifères mais beaucoup moins chez les végétaux ([Negishi et al. 2001](#) ; [Chapman et al. 2004](#) ; [Dombrovski et al. 2006](#)) ; ([Varin et al. 1992](#) ; [Hirschmann et al. 2014](#)). Cette sulfatation est réalisée sous l'action de sulfotransférases (ST), qui pour la majorité utilisent le 3'-phosphoadenosine 5'-phosphate (PAPS) comme donneur de sulfate. Les acides aminés codants les régions de fixation de ce substrat sont très conservés et sont représentées par quatre principales régions (Figure 3.2).

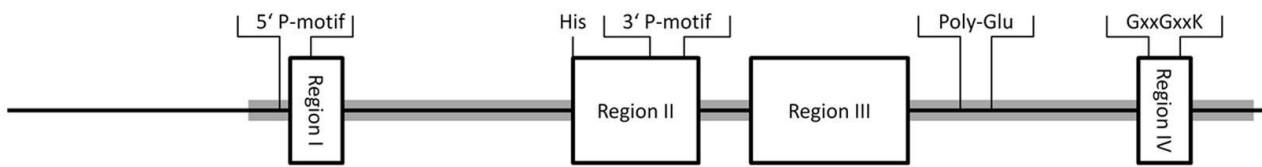


Figure 3.2 : Régions conservées entre les sulfotransférases PAPS dépendantes (issu de Hirschmann et al. 2014).

Il existe deux types de sulfotransférases, celles associées à la membrane et celles qui se situent dans le cytosol (Chapman et al. 2004). Ces deux classes peuvent agir sur différents substrats, la première classe associée aux membranes agit sur des macromolécules tel que les protéines, les peptides ou encore les glycosaminoglycanes (Niehrs et al. 1994). La seconde classe cible les petites molécules organiques de structures chimiques très diverses telles que les flavonoïdes, les stéroïdes ou les xénobiotiques (Hirschmann et al. 2014). L'addition d'un groupement sulfate sur ce type de molécule, augmente la solubilité des composés, réduit leur réactivité facilitant ainsi leur compartimentation pouvant permettre leur excréption (Jakoby and Ziegler 1990 ; Martiny et al. 2013; Chapman et al. 2004).

Chez certaines algues vertes, la sulfatation de métabolites secondaires a été décrite (Welling 2010). Dans des cellules intactes de l'algue siphonée *Dasycladus vermicularis* ces auteurs ont décrit le 6,7-dihydroxycoumarine-3-sulfate, un dérivé stable hydroxylé et sulfaté de coumarine benzopyrone. Cette sulfatation a été montrée comme pouvant prévenir l'oxydation des hydroxycoumarines dans la cellule, ce qui pourrait être comparable à la glycosylation ou la glutathionylation utilisés dans les cellules eucaryotes pour inactiver des composés hydroxylés réactifs et permettre leur compartimentation cellulaire. La sulfatation pourrait également jouer ce rôle pour certains métabolites de plantes terrestres (flavonoïdes, glucosinolates) ou d'algues brunes (phlorotannins). Ensuite, sous l'action de sulfatasées non caractérisées, qui sont libérées lorsque les cellules de *D. vermicularis* sont endommagées, il se forme de la 3,6,7-trihydroxycoumarine qui sera immédiatement polymérisée par pontage oxydatif (Welling et al. 2011). Une activité sulfatase a aussi été caractérisée chez *Cystoseira tamariscifolia* et présente une spécificité pour les composés phénoliques (Knoss and Glombitza 1993).

Lors de l'annotation experte du génome d'*Ectocarpus*, 15 gènes différents codant pour des sulfotransférases (STs) ont été identifiés ([Cock et al. 2010](#)). Leur analyse phylogénétique réalisée par [Michel et al. \(2010\)](#) a révélé qu'ils appartenaient à cinq clades principaux dans l'arbre phylogénétique reproduit sur la Figure 3.3.

Un premier groupe de quatre protéines (Esi0028_0011, Esi0197_0021, Esi0197_0023 et Esi0442_0008) est apparenté aux aryl STs animales, ainsi qu'aux STs de plantes caractérisées pour leur implication dans les voies de biosynthèse de différents métabolites secondaires (e.g. glucosinolates, flavonoïdes, sulfohydroxyjasmonate). Aussi, ces auteurs ont émis l'hypothèse que ces STs du Clade A pourraient être actives sur des composés phénoliques, comme les phlorotannins sulfatés précédemment caractérisés ([Ragan and Glombitza 1986](#), [Glombitza and Knoss 1992](#) ; [Vreeland et al. 1998](#), [Potin et Leblanc, 2006](#)) et /ou des flavonoïdes ([Varin, et al., 1997](#)). Les autres clades comprennent des séquences apparentées à des protéines de fonction moins bien caractérisée de bactéries (Esi0289_0025, Clade B) ou à diverses familles de sulfotransférases agissant sur des sucres, notamment sur des glycosphingolipides ou des glycosaminoglycans comme les héparanes, indiquant que ces enzymes seraient impliquées dans la sulfatation des fucanes chez les algues brunes ([Michel et al., 2010](#)).

Afin de poursuivre la caractérisation des enzymes pouvant intervenir dans la voie de biosynthèse des phlorotannins, le but de cette étude est de caractériser la fonction biochimique des trois sulfotransférases d'*Ectocarpus* appartenant au Clade A, AST1 (Esi0442_0008), AST2 (Esi0197_0023) et AST3 (Esi0028_0011) en utilisant les outils de surexpression d'enzymes recombinantes en condition hétérologue chez *E. coli*.

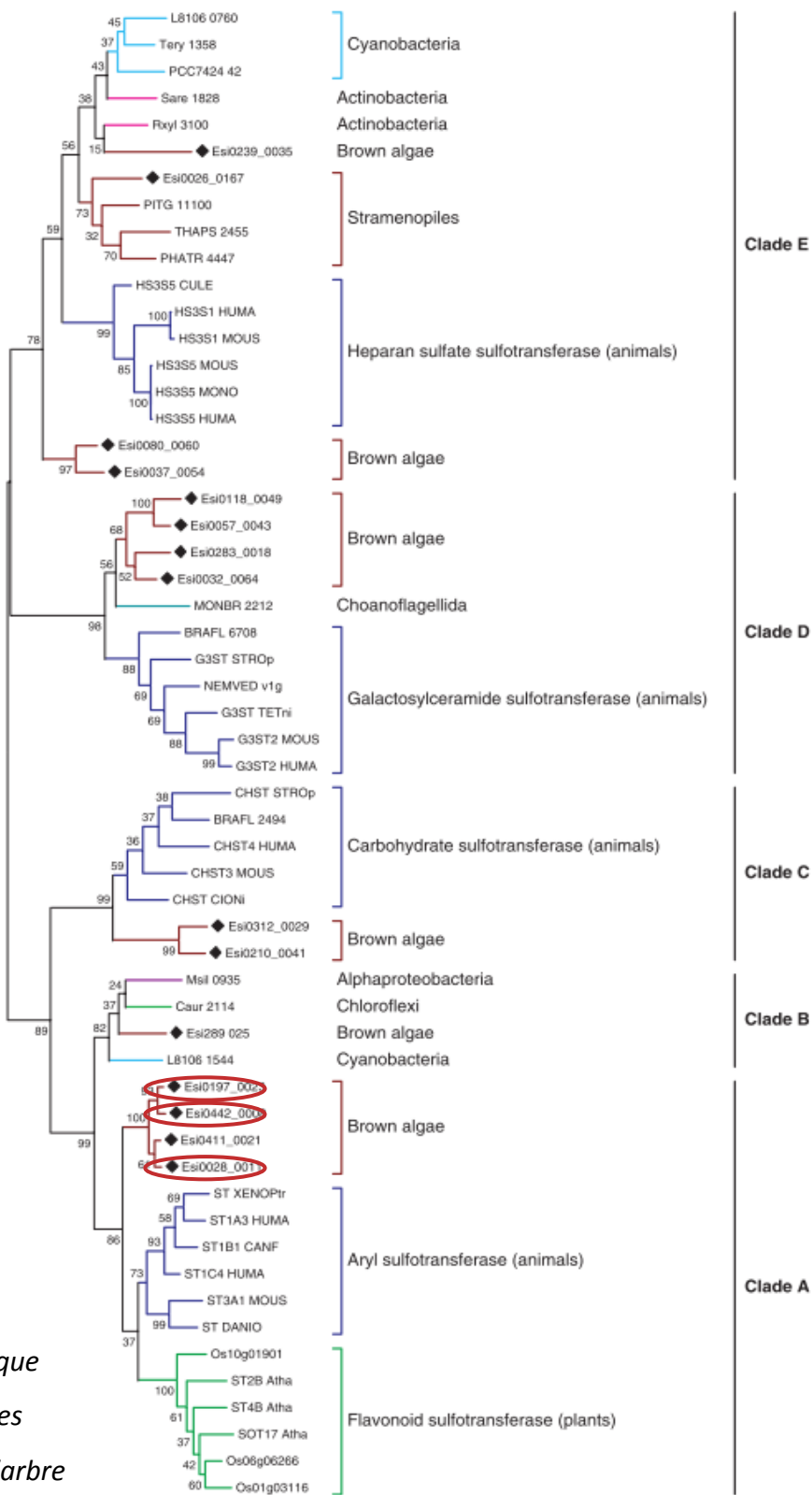


Figure 3.3: Arbre phylogénétique représentatif de la diversité des sulfotransférases (STs) dans l'arbre du vivant (Michel et al. 2010b)

Matériel et Méthodes

Clonage des aryl sulfotransferases (AST) d'Ectocarpus :

Les trois gènes (Esi0028_0011, Esi0197_0023 et Esi0442_0008) identifiés comme étant des homologues d'aryl sulfotransférases actives sur des composés phénoliques ont été clonés conformément aux instructions indiquées par le kit In-Fusion® HD Cloning (Clontech). Les amorces utilisées pour l'amplification des gènes par PCR sont reportées dans le tableau 3.1.

Tableau 3.1: Séquences nucléotidiques des amorces utilisées pour le clonage des AST dans le vecteur d'expression pQE80L. La séquence en rouge correspond au site de restriction SphI/HindIII précédé de 15pb correspondantes au vecteur pQE80L.

Nom Locus	Code banque ADNC	Nom	Séquences des amorces pour le clonage dans pQE80L	Taille de la protéine attendue (kD)
Esi0442_0008	LQ0AAB8YA20FM1.SCF	EsiAST1_1	ACCATCACGGATCCGCA TGC ACCCCTAACCTGGT GAACGGTGTCTACCAG	34
		EsiAST1_2	TCAGCTAATTAAGCTTCT AGGGCATGACGAGTCCT TCCCCG	
Esi0197_0023	LQ0AAB58YO20FM1.SCF	EsiAST2_1	ACCATCACGGATCCGCA TGC ATGTCGTCCTCCGA TGGGAGAAAGATTATG	38
		EsiAST2_2	TCAGCTAATTAAGCTTCT AGGGCATGACGAGCCCT TCCCCGAAG	
Esi0028_0011	LQ0AAB64YH02FM1.SCF	EsiAST3_1	ACCATCACGGATCCGCA TGC ATGGAAGGTGCATC CAAGATGAGCAGCCAG	39
		EsiAST3_2	TCAGCTAATTAAGCTTTC ACATGACCAATCCCTCC CCGAAGTCC	

Le vecteur pQE80-L a été utilisé afin de permettre la surexpression des protéines recombinantes. Il est caractérisé par la présence d'un tag codant pour une queue poly-histidines devant le site de clonage, ce qui permet l'expression d'une protéine de fusion possédant une étiquette de six résidus His en N-terminal. Ce plasmide possède un gène de régulation transcriptionnelle (*LacIq*) synthétisant des répresseurs de l'initiation de la transcription se fixant sur LacO. Cependant, un ajout d'IPTG inactive les répresseurs induisant ainsi l'initiation de la transcription à partir des promoteurs LacO. Ce plasmide porte le gène de résistance à l'ampicilline pour la sélection de clones transformants.

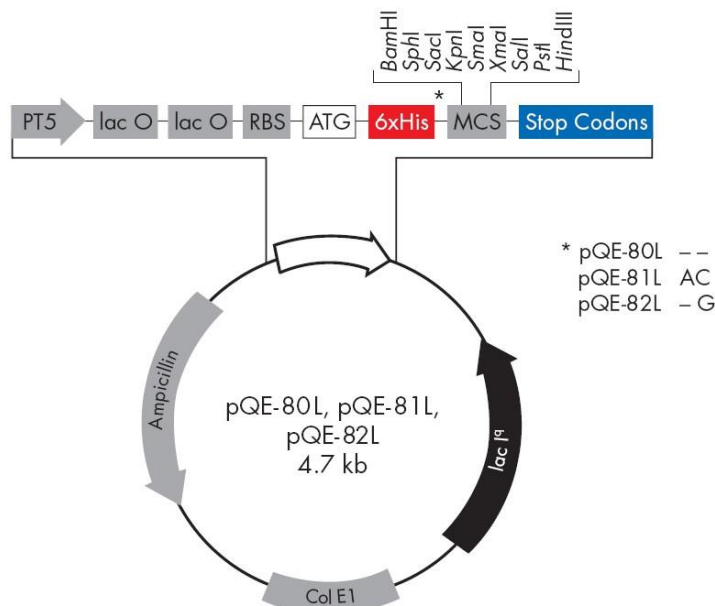


Figure 3.4 : Schéma présentant les caractéristiques du plasmide pQE80L (Qiagen)

Après le clonage de chaque gène d'intérêt dans le vecteur d'expression pQE80L, les cellules compétentes Stellar Competent Cells fournies par le kit ont été transformées puis étalées sur boîte LB agarose contenant l'antibiotique ampicilline. Après une nuit à 37 °C, plusieurs colonies ont été ciblées puis l'ADN a été extrait à l'aide du kit PureYieldTM Plasmid Miniprep System (Promega). Une partie de l'ADN a ensuite été digérée avec les enzymes de restriction SphI/HindIII et une migration sur gel d'agarose a permis de vérifier la taille de l'insert. Une fois la taille de l'insert contrôlée, le plasmide recombinant non digéré contenant le gène d'intérêt a

été transformé dans les cellules BL21-CodonPlus(DE3)-RIPL (Stratagene) permettant la surexpression des protéines recombinantes.

Génotype : *E. coli* B F⁻ompThsdS(rB⁻mB⁻) dcm⁺Tetrgalλ(DE3) endAHte [argUproLCamr] [argUileYleuWStrep/Specr].

Surexpression des protéines recombinantes

Afin de permettre la surexpression des enzymes recombinantes, les cellules recombinantes BL21 Codon Plus –RIPL contenant le plasmide transformé ont été mises en culture dans le milieu LB-amp supplémenté de 0.5 mM d’IPTG pour les cultures induites (In) à 37°C sous agitation durant 1 heure.

Chaque culture a ensuite été centrifugée afin de récupérer le culot bactérien contenant les protéines d’intérêt.

Purification et analyses des protéines

Les culots bactériens sont lysés puis les protéines sont purifiées par affinité en suivant les indications du kit GE Healthcare His SpinTrap sur une colonne contenant du nickel possédant une affinité avec l’étiquette 6-Histidines de nos protéines recombinantes. Après chargement du lysat et lavage de la colonne avec le tampon d’équilibration contenant 20 mM Tris-HCl, 8 M urée, 500 mM NaCl, 5 mM imidazole, pH 8.0 + 1 mM β-mercaptoproethanol , deux élutions sont réalisées avec le tampon d’élution contenant 20 mM Tris-HCl, 8 M urée, 500 mM NaCl, 500 mM imidazole, pH 8.0 + 1 mM β-mercaptoproethanol. L’imidazole possédant une affinité plus forte avec le nickel de la colonne qu’avec les histidines de notre protéine, cette dernière est éluée.

Les protéines sont analysées par électrophorèse sur gel dénaturant SDS-PAGE et par Western-blot par immuno-révélation avec les anticorps anti-histidines et le kit Bio-Rad Clarity western ECL.

Résultats

Alignement de séquences

Suite à l'alignement des séquences d'*Ectocarpus* avec les séquences d'*Aureococcus anophagefferens* et *Homo sapiens*, nous observons une bonne conservation des domaines I et IV caractéristiques du site de fixation du PAPS. Ainsi les sulfotransférases d'*Ectocarpus* semblent pouvoir utiliser le PAPS comme donneur de sulfate (Figure 3.5).

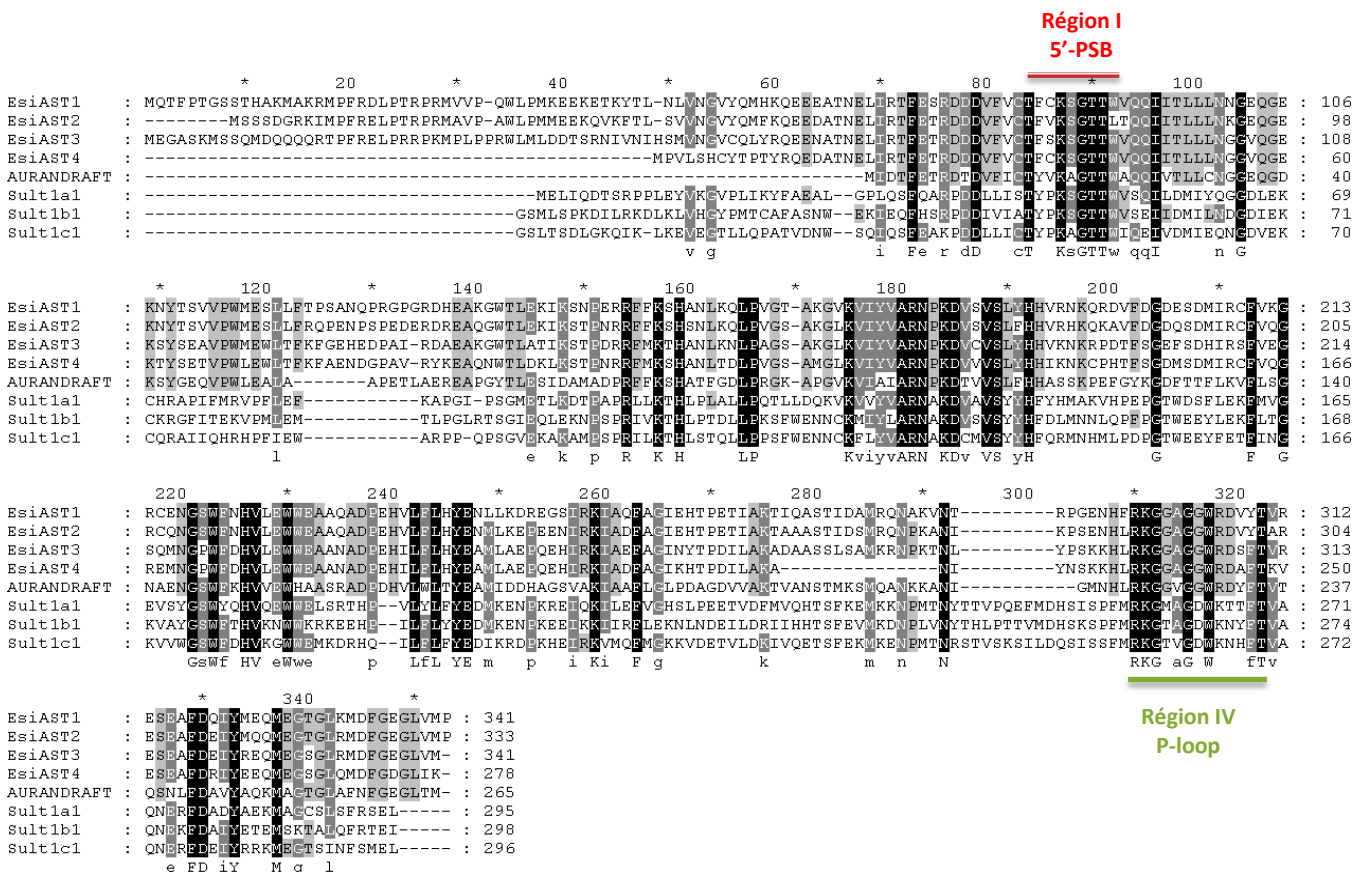


Figure 3.5: Représentation des domaines conservés Région I et IV, représentatives des sulfotransférases dépendantes du PAPS chez *Ectocarpus* (EsiAST1, 2, 3), *Aureococcus anophagefferens* (AURANDRAFT) et *Homo sapiens* (Sulta1, b1, c1).

Surexpression des AST recombinantes

Les premiers tests de surexpression des trois AST d'*Ectocarpus* du Clade A montrent une expression des protéines dans les cultures induites en comparaison avec les cultures non induites avec l’IPTG (Figure 3.6A). Les protéines différemment exprimées se retrouvent aux tailles attendues respectivement 34kD pour AST1, 38kD pour AST2 et 39kD pour AST3, ce qui est confirmé par le test de purification et le western blot révélant uniquement les protéines portant l’étiquette histidine (Figure 3.6B).

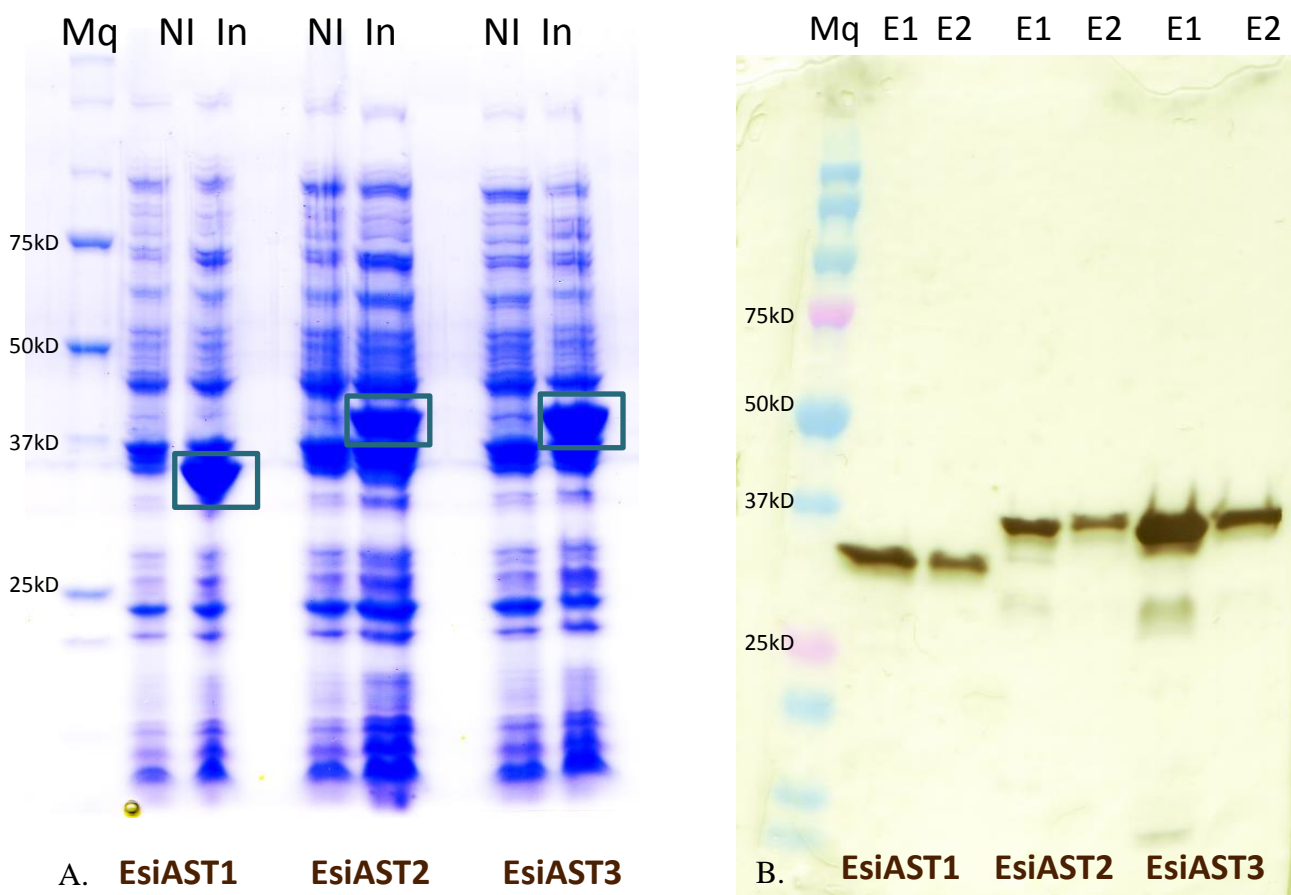


Figure 3.6: A. Gel SDS-PAGE coloré au bleu de coomassie révélant les protéines présentes dans l’extrait total des cultures non induites NI et induites In par l’IPTG. B. Western Blot après hybridation d’un anti-corps anti-His, présentant le marqueur de taille coloré Mq, les deux élutions E1 et E2 du test de purifications des trois AST révélé à l’ECL.

Discussion et Perspectives

Les premiers résultats obtenus dans cette étude ont tout d'abord révélé que les trois sulfotransférases *d'Ectocarpus* appartenant au Clade A présentaient des régions conservées représentatives des sulfotransférases utilisant le PAPS comme donneur de sulfate.

L'expression en condition hétérologue chez *E.coli* des trois protéines s'est révélée concluante. En effet une surexpression des protéines est bien observée en condition induite par l'IPTG, de plus les protéines sont produites sous forme soluble ce qui facilitera leur purification. Afin de caractériser la fonction biochimique de ces trois protéines, nous testerons dans un premier temps la spécificité pour le PAPS en parallèle de dosages des activités de sulfatation sur des composés phénoliques endogènes (phloroglucinol, difucol, diphloretol) des algues brunes.

Des méthodes de chromatographie UPLC-MS par HILIC ([Steevensz et al. 2012](#)), développées dans la partie II de ce manuscript, devraient pouvoir s'adapter à la caractérisation des produits de réaction de ces enzymes qui seront plus polaires après sulfatation. Ces méthodes transposées à l'échelle semi-préparative pourront aussi contribuer à la préparation de certains substrats d'oligomères de phlorotannins.

Après une caractérisation biochimique approfondie de ces 3 STs *d'Ectocarpus*, il sera intéressant d'étudier les relations structure/fonction de ces enzymes pour déterminer leurs spécificités. Il a été montré que la sulfatation des flavonoïdes pouvait être spécifique de certains composés ([Gidda and Varin 2006](#)). Pour exemple l'AtST3a *d'Arabidopsis* présente une affinité plus importante pour les composés de type flavonol plutôt que flavone. Ainsi, l'étude structurale approfondie des trois protéines permettra d'orienter la caractérisation biochimique et ainsi de connaître la spécificité des substrats utilisés par ces enzymes.

D'autre part, il sera particulièrement intéressant d'étudier la régulation de ces STs *in vivo* dans un contexte écophysiologique, notamment sur un modèle comme *Ectocarpus*, en comparant l'acclimatation et l'adaptation à la salinité ([Dittami et al. 2011](#)). En effet, il s'avère que dans ces conditions la synthèse des phlorotannins est fortement activée comme vu dans le chapitre 1 et que la synthèse de composés sulfatés pourraient bien jouer un rôle important dans cette acclimatation ([Dittami et al., 2011](#)).

Synthèse de la Partie 1

Au travers des caractérisations biochimiques finalisées ou initiées pour ces trois catégories d'enzymes, la connaissance de la voie de biosynthèse des phlorotannins chez *Ectocarpus* reste encore très partielle. Une seule étape, a été élucidée avant le début de ce travail de thèse, il s'agit de la production du phloroglucinol qui est le précurseur monomérique de tous les types d'oligomères de phlorotannins par la polyketide synthase de type III (EsiPKS1) d'*Ectocarpus* (**Chapitre 1**).

Les protéines de type chalcone isomérase-like identifiées dans le génome d'*Ectocarpus* ne présentent aucune activité enzymatique sur du phloroglucinol ou des substrats de plantes comme la naringénine. En effet, ces protéines ne possèdent pas les acides aminés catalytiques des chalcone isomérasées de plantes vasculaires qui permettent la production des précurseurs de flavanones ([Ralston et al. 2005](#)). En revanche nous avons pu montrer que les deux chalcones isomérasées-like d'*Ectocarpus* appartenaient aux chalcones isomérasées de type III aussi appelées FAP impliquées dans la fixation aux acides gras ([Ngaki et al. 2012](#)). La caractérisation biochimique a révélé la présence d'acides gras de type C16 et C18 au sein des protéines recombinantes, et les premiers tests de substrat présentent une spécificité d'EsiCHIL1 pour le C16-CoA. La caractérisation fonctionnelle de ces enzymes étant actuellement en cours chez *Arabidopsis* nous connaîtrons très prochainement leur spécificité.

La caractérisation biochimique des sulfotransférases d'*Ectocarpus* présentant une séquence très conservée avec celles des sulfotransférases de flavonoïdes de plantes ou les phénols sulfotransférases animales est encore trop partielle pour conclure sur l'activité enzymatique et la spécificité de ces protéines. Les travaux de caractérisation biochimique de certains oligomères de phlorotannins qui ont été effectués dans le cadre de cette thèse (Partie 2 Chapitre 4) vont permettre d'utiliser de nouveaux outils pour caractériser les produits sulfatés de ces activités.

Cependant, grâce à ces connaissances acquises sur les enzymes étudiées et principalement à l'étude finalisée de la PKSIII, l'utilisation de nouveaux outils moléculaires en écophysiologie est aujourd'hui possible pour étudier les fonctions biologiques et écologiques des phlorotannins, c'est ce que nous présenterons en deuxième partie de ce manuscript.

Partie II: Ecophysiolologie : étude de l'implication des phlorotannins dans la réponse aux stress biotiques et abiotiques chez *Fucus vesiculosus*

<i>Contexte général :</i>	87
<i>Chapitre 4 : Implication des phlorotannins dans la réponse à une irradiation chronique aux UV-B.</i>	89
<i>Chapitre 5 : Effet du stress biotique du brouteur <i>Littorina littorea</i> sur la synthèse de phlorotannins chez <i>Fucus vesiculosus</i>.</i>	119
<i>Chapitre 6: Essai biologique : test de molécules d'intérêt sur le comportement et l'attachement au substrat des Littorines</i>	1387
<i>Synthèse de la Partie 2</i>	162

Contexte général :

Fucus vesiculosus est une macroalgue brune appartenant à l'ordre des Fucales. Cette espèce est très largement présente sur les côtes Nord Ouest et Nord Est Atlantique, en Mer Baltique, et Mer du Nord (Figure 20). *F.vesiculosus* constitue une biomasse importante et se répartit sous forme de ceinture algale au niveau médiolittoral. Cette espèce est pérenne et vit environ 3 ans en se développant principalement sur les zones rocheuses en modes semi-battu et abrité.



Figure 20: Répartition géographique de l'algue brune *Fucus vesiculosus*

Caractérisée par la présence de vésicules aérières le long de son thalle lui permettant une bonne flottabilité dans la colonne d'eau (Figure 21), *F. vesiculosus* est adaptée à de fortes variations environnementales, ce qui en fait un bon modèle d'étude pour la compréhension des mécanismes de défense et d'interactions avec l'environnement.

Pour étudier ces mécanismes, et en particulier l'implication des phlorotannins dans la



Figure 21 : *Fucus vesiculosus* L.

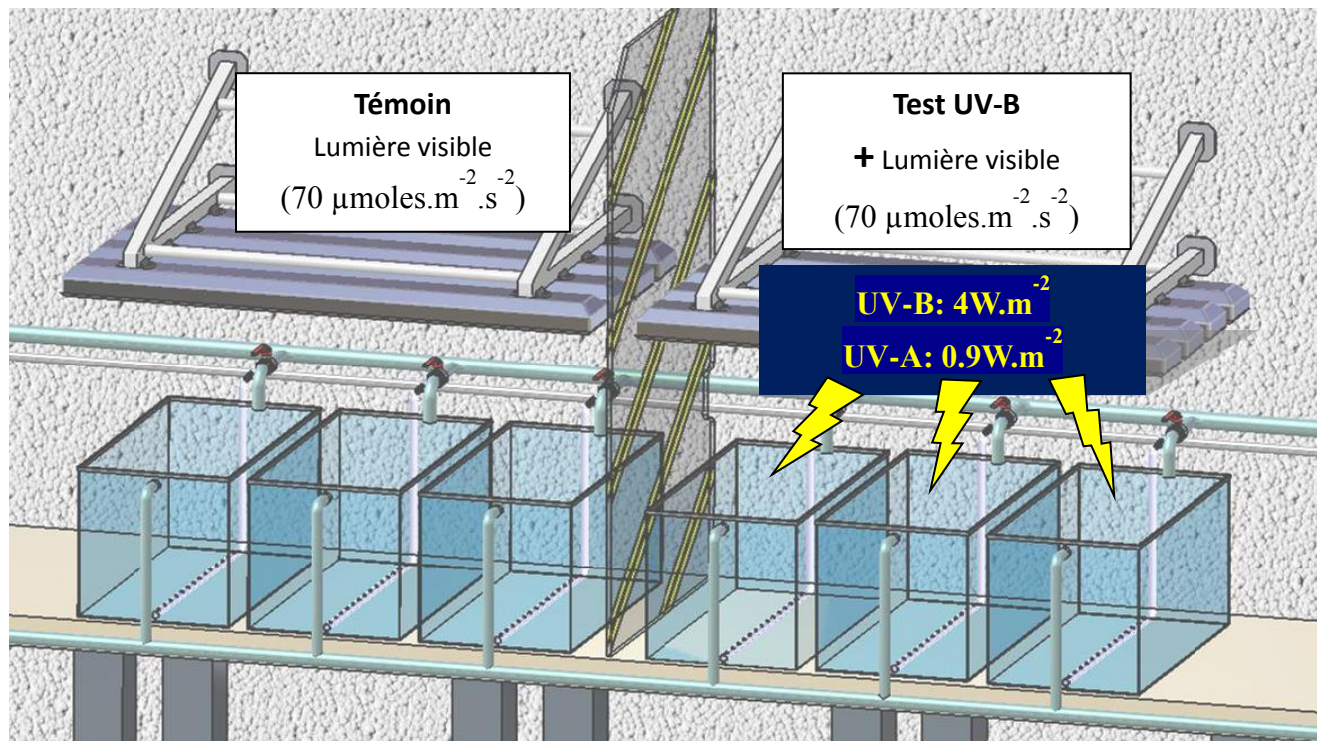
réponse aux stress environnementaux, nous avons choisi de tester l'effet d'un stress abiotique représenté par de fortes radiations UV-B (**Chapitre 4**) ainsi que l'effet d'un stress biotique induit par la présence du brouteur *Littorina littorea* (**Chapitre 5**).

La première expérimentation rapportée ci-après a été menée au laboratoire du Lémar de l'IUEM à Plouzané (Université de Brest). Cette étude a consisté à tester l'hypothèse de l'effet d'un rayonnement UV-B chronique sur la production de phlorotannins chez *Fucus vesiculosus*. L'implication des phlorotannins dans la réponse aux UV-B étant un sujet controversé dans la littérature, nous avons choisi d'utiliser de nouveaux outils biomoléculaires en complément à la quantification globale des phlorotannins.

Grâce aux connaissances acquises sur l'algue brune modèle *Ectocarpus*, ainsi qu'aux ressources génomiques aujourd'hui disponibles notamment sur le modèle *Fucus vesiculosus*, ([Pearson et al. 2010](#) ; [Flöthe et al. 2014a](#) ; [Flöthe et al. 2014c](#)), nous avons suivi l'expression de gènes d'intérêt pouvant coder pour des enzymes intervenant dans la synthèse des phlorotannins lors de la cinétique UV-B.

Afin de valider cette nouvelle approche, nous avons ensuite collaboré avec le Dr. Florian Weinberger du laboratoire Géomar de Kiel en Allemagne, afin d'étudier l'effet du broutage du gastéropode *Littorina littorea* sur *Fucus vesiculosus*. Cette collaboration a également été l'occasion de tester un essai biologique (**Chapitre 6**) permettant de mesurer *in vitro* l'effet d'extraits et de molécules, ici le phloroglucinol, sur le comportement et l'attachement au substrat de *Littorina littorea*.

Chapitre 4 : Implication des phlorotannins dans la réponse à une irradiation chronique aux UV-B.



Article soumis à Plos One, révisions mineures en cours, janvier 2015.

Constitutive or inducible protective mechanisms against UV-B radiation in the brown alga *Fucus vesiculosus*? A study of gene expression and phlorotannin content responses.

Creis Emeline^{1,2}, Delage Ludovic^{1,2}, Charton Sophie^{1,2}, Goulitquer Sophie³, Leblanc Catherine^{1,2}, Potin Philippe^{1,2*}, Ar Gall Erwan^{4*}

¹Sorbonne Universités, UPMC Univ Paris 06, UMR 8227, Integrative Biology of Marine Models, Station Biologique de Roscoff, CS 90074, F-29688, Roscoffcedex, Brittany, France

²CNRS, UMR 8227, Integrative Biology of Marine Models, Station Biologique de Roscoff, CS 90074, F-29688, Roscoff cedex, Brittany, France

³Centre de Ressources de Biologie Marine, MetaboMer Mass Spectrometry Core Facility, CNRS FR2424, Station Biologique de Roscoff, 29688 Roscoffcedex, Brittany, France

⁴Université Européenne de Bretagne, Université de Bretagne Occidentale, Laboratoire des Sciences de l'Environnement Marin, Unité Mixte de Recherche, Centre National de la Recherche Scientifique 6539, Institut Européen d'Etudes Marines-IUEM, 29280 Plouzané, Brittany, France

Corresponding authors:

Dr Philippe Potin, LBI2M, UMR 8227 CNRS/UPMC-Paris6, Station Biologique, CS90074, 29688 ROSCOFF Cedex, Brittany, France; Phone: 33+(0)2-98-29-23-75
Fax: 33+(0)2-98-29-23-85 E-mail :potin@sb-roscocco.fr

Dr Erwan Ar Gall, LEMAR UMR 6539 CNRS/UBO/IFREMER/IRD, Institut Européen d'Etudes Marines-IUEM, Place Nicolas Copernic, 29280 Plouzané, Brittany, France.
Phone: 33+(0)2-98-49-87-92, E-mail :erargall@univ-brest.fr

Abstract

A role as UV sunscreens has been suggested for phlorotannins, the phenolic compounds which accumulate in brown algae in response to a number of external stimuli and take part in cell wall structure. After exposure of the intertidal brown alga *Fucus vesiculosus* to artificial UV-B radiation, we examined its physiological responses by following the transcript level of the *pksIII* gene encoding a phloroglucinol synthase, likely to be involved in the first step of phlorotannins biosynthesis. We also monitored the expression of three targeted genes, encoding a heat shock protein (*hsp70*), which is involved in global stress responses, an aryl sulfotransferase (*ast*), which could be involved in the sulfation of phlorotannins, and a vanadium bromoperoxidase (*vopo*), which can potentially participate in the scavenging of Reactive Oxygen Species (ROS) and in the cross-linking and condensation of phlorotannins. We investigated whether transcriptional regulation of these genes is correlated with an induction of phlorotannin accumulation by establishing metabolite profiling of purified fractions of low molecular weight phlorotannins. Our findings demonstrated that a high dose of UV-B radiation induces a significant overexpression of *hsp70* after 12 and 24 hours following the exposure to the UV-B treatment, compared to control treatment. The physiological performance of algae quantified by the photosynthetic efficiency (Fv/Fm) was slightly reduced. However UV-B treatment did not induce the accumulation of soluble phlorotannins in *F. vesiculosus* during the kinetics of four weeks, correlated with no induction of the *pksIII* gene expression. By using molecular tools to further investigate the regulation of phlorotannin biosynthesis, we provide here complementary approaches to global quantifications currently used in studies of phenolic compounds in brown algae.

Introduction

The marine environment is highly contrasted from tidal zone to deeper waters. Based on tidal influence, ecological factors shape seaweed communities. The intertidal zone of cold and temperate rocky shores exposed to regular and extreme changes in abiotic conditions ([Davison and Pearson 1996](#)) is largely colonized by brown algae (mainly Fucales), which are especially experience to large variations of solar radiation, desiccation and osmotic stress during low tide. To resist and survive in this extreme environment, brown algae have acquired specific physiological traits during their independent evolution from the other major eukaryotic groups. As members of the Phylum Stramenopiles, brown algae have diverged over a billion years ago from land plants, red and green algae (Archaeplastida) and also from fungi and animals (Opisthokonts)([Baldauf 2008](#)). This independent evolution has given way to many novel features with regard to their metabolism and cell biology.

One of these metabolic originalities is the synthesis of phenolic compounds which are specific to Phaeophyceae, namely phlorotannins. These metabolites are synthesized from the acetate-malonate pathway. The monomer synthesis consists in the condensation of malonyl-CoA units by a Polyketide Synthase of type III (PKS III) ([Meslet-Cladiere et al. 2013](#)) leading to the formation of phloroglucinol (1,3,5-trihydroxybenzene) units. However further steps in the biosynthesis leading to the oligomerization of phloroglucinol units and condensation of high molecular weight phlorotannins still remain un-elucidated. Numerous studies have suggested that vanadium-dependent haloperoxidases may be involved in phlorotannin oxidative condensation ([Berglin et al. 2004 ; Salgado et al. 2009; Bitton et al. 2006](#)) and probably play a major role in the processes leading to reactive oxygen species (ROS) detoxification ([Roeder et al. 2005](#)). The expert annotation of the *Ectocarpus* genome has also provided other candidates for phlorotannin biosynthesis such as arylsulfotransferases ([Cock et al. 2010](#)), which could be involved in the water solubility and stabilization of phenolic compounds ([Harborne 1975](#)). Similarly to land plant polyphenols, the phlorotannins are likely to possess important ecological roles. Indeed phlorotannin contents in Phaeophyceae exhibit plasticity in their responses to a large variety of environmental factors, such as light, and nutrient availability, ultraviolet

radiation and the intensity of grazing (Arnold and Targett 1998 ; Amsler and Fairhead 2006 ; Jormalainen et al. 2003).

These metabolites occur under different forms in algal cells, soluble in cellular compartments like physodes (Ragan 1976 ; Schoenwaelder 2008) and in extracellular exudates (Shibata et al. 2006), or insoluble cross-linked into the cell walls (Koivikko et al. 2005). This apparent diversity of location, chemical speciation and functions of phlorotannins has currently been poorly explored. Therefore, even though global estimations of soluble phenol pools have been provided up to date (Breton et al. 2011), precise quantification of total phlorotannin contents in these different compartments still remains a challenge.

In this present study, we focused on the potential effect of UV-B on synthesis of phlorotannins. Impacts of UV-B can be multiple (Bischof et al. 2006), from DNA damage -inhibition of DNA replication or mutations-, to photosynthetic apparatus impairment -decrease of CO₂-fixation, production of (ROS)- (Renger et al. 1989 ; Allen et al. 1997). During acclimation to UV radiation, a reduction in the degree of photo-inhibition is commonly observed in brown algae. Such an effect may be explained either by activation of the antioxidative response, or by the formation of UV-screening compounds (Lesser 1996) and an increase in the activity of repairing enzymes. Phlorotannins are able to absorb UV radiation, mainly UV-C and partly UV-B, with maxima at 195 nm and 265 nm (Ragan and Glombitza 1986 ; Pavia et al. 1997 ; Henry and Van Alstyne 2004) making them good candidates for UV protection. Similarly to tannins from land plants, phlorotannins expose a high antioxidant activities, essential for the scavenging of toxic ROS, such as superoxide anion radicals produced by harmful UV-B radiation. However, results of previous studies are contrasted regarding the role of phlorotannins in brown algal responses upon UV radiations (Pavia et al. 1997 ; Henry and Van Alstyne 2004 ; Swanson and Druehl 2002 ; Hupel et al. 2011a ; Wahl et al. 2011).

In this context, our study has the aim to study the chronic exposition of UV-B on physiological performance of *F.vesiculosus* by an original approach, combining targeted transcriptomic and quantification of phenolic compounds. The expression of target genes was monitored for a gene encoding the PKSIII enzyme responsible for the synthesis of phloroglucinol, the precursor of phlorotannins pathway, and for three other genes potentially involved in stress responses and

phlorotannin modifications. The quantification of soluble phlorotannin content was completed with metabolite profiling of purified fractions of low molecular weight.

Material and methods:

Ethics Statement

The scientific research and collecting permits were obtained for the described field studies from the Maritime Affairs Authorities at DDTM29 (Department of Finistère, Brittany, France).

Algal material and experimental design

Fucus vesiculosus was collected in October 2011 in the Bay of Brest near St Anne du Portzic (48.361591°N,-4.554375°W) at Plouzané (Brittany, France), thoroughly washed with filtered seawater and assigned in 40 liters tanks with a permanent renewal of both seawater and bubbled air. Three tanks were used as control with a permanent white light intensity of 70 $\mu\text{moles.m}^{-2}.\text{s}^{-2}$ (Philips Master TL-D 36W/840) and three tanks were used for UV-B stress with the same white light intensity plus an additional UV-B illumination of 4,9 W.m^{-2} UV-B and 0.09 W.m^{-2} UV-A (UV-B Q-Panel 313 nm). Each treatment was isolated from each other with dark sheets. The kinetic study lasted four weeks with 13 successive sampling points: after 0, 1, 3, 6, 12, 24, 36, 48, 72 hours, and 1, 2, 3, 4 weeks. The sampling consisted in the collection of one thallus in each tank, so three thalli under control treatment and three thalli under UV-B treatment.

Fluorescence measurements and sampling

Photosynthetic efficiency was measured to determine the maximum quantum yield of PS II (F_v/F_m) by pulse amplitude modulated (PAM) fluorescence as Junior PAM Walz (Germany), with optical fiber and optical head as measuring units. Thalli were dark-adapted for 5 min prior to three independent measurements. After fluorescence assessment, total fresh tissues were cut

off from three thalli of each condition, then frozen in liquid nitrogen and stored at -80°C before freeze-drying.

Ribonucleic acid (RNA) extraction

The RNA extraction protocol was adapted from [Apt & Grossman \(1993\)](#), [Apt et al. \(1995\)](#) and [Pearson et al. \(2006\)](#). 50 mg dry weight (DW) of freeze-dried tissue were grounded for 5min at 6500rpm at room temperature using a mixer-mill (Precellys 24, Bertin Technologies) in 2 mL Eppendorf tubes with ceramic beads supplied. Extraction buffer consisted of Tris-EDTA (100 mMTris, 50 mM EDTA, pH 7.5, with 1.5 M NaCl and 2 % CTAB). Immediately prior to extraction, 500 mM of DTT was added as antioxidant from a 1 M stock dissolved in water. Extraction buffer was added to the tissue (1.5 mL per 50 mg dry weight) and the suspension was mixed vigorously by vortexing. After 15 min of extraction on ice, the mixture was centrifuged at 10000 g for 20 min at 4 °C. The upper aqueous phase was transferred to a new tube and 1 volume of chloroform:isoamyl alcohol (24:1 v/v) was added, vortexed vigorously and centrifuged at 10000 g for 20 min at 4 °C. The upper aqueous phase was transferred to a new tube and 0.2 volume of absolute ethanol was added gently and mixed by rocking the tube. Ethanol addition resulted in the precipitation of polysaccharides ([Fang G, Hammar S 1992](#)). A second chloroform extraction was then carried out under the same conditions and the aqueous phase was carefully removed. RNA was precipitated with 0.4 volumes of 12 M LiCl in the presence of 1 % (v/v) β-mercaptoethanol as antioxidant. Precipitation was performed overnight at -20 °C. The RNA was collected by centrifugation at 10000 g for 30 min at 4 °C, the RNA pellet was dried up (10 – 20 min on ice) and then re-suspended in 500 µL RNase-free water. The RNA was extracted with an equal volume of phenol-chloroform:isoamylalcohol (24:1 v/v) (1:1) and centrifuged at 10000 g for 15 min at 4 °C. The resulting pellet was washed by 1 volume of chloroform:isoamyl alcohol (24:1 v/v) in order to remove the phenol. RNA was re-precipitated with 2 volumes ethanol, 0.3 M sodium acetate and re-suspended in 20 µL of sterile H₂O. The RNA was treated with RNase-free DNase-I according to the manufacturer's instructions (Qiagen) to remove any contaminating desoxyribonucleic acid (DNA). The concentration of RNA was assessed using a

NanoDrop 2000 spectrophotometer (ThermoScientific), and the quality was assessed on a 2 % agarose gel by running the gel electrophoresis at 80 - 100 V.

Quantitative Real-time PCR (qRT- PCR)

The reverse transcription (RT) was performed on 250 ng of total RNA, with 1 µL DT18 (100 µM). The reaction mixture was incubated at 70 °C for 5 min. Following the incubation the master mixture, which contains 5 µL Improm II Buffer 5X (Promega), 4 µL MgCl₂ (25 mM), 1 µL dNTP mix (10 mM), 0.5 µL RNAsine, 2.5 µL Nuclease free water and 1 µL of ImProm-II™ Reverse Transcriptase (Promega) was added. The reaction mixture was incubated at 25 °C for 5 min, the extension was carried out at 42 °C for 60 min, and the RT was inactivated by heating at 70 °C for 15 min. Finally, the total complementary DNA (cDNA) was diluted at 1 ng/µL to perform the reverse transcription polymerase chain reaction (qRT-PCR) which was carried out using *ef1.alpha* and *tuaas* endogenous control on the LightCycler® 480 multiwell plate 96, on a LightCycler® 480 Real-Time PCR System (Roche Diagnostics, Mannheim, Germany) in three technical replicates. The final reaction volume was made to 10 µL, using 5 µL of the LightCycler® 480 SYBR Green Master mix (Roche Diagnostics, Mannheim, Germany) with 2.5 µL of cDNA (1 ng.µL⁻¹) or *F. vesiculosus* cesium chloride-purified genomic DNA (gDNA) for quantification, 0.5 µL of each primer (10 µM) (Table1) and 1.5 µL water.

The cycling program for PCR quantification was as follows: 5 min denaturation at 95 °C, followed by 45 cycles of 95 °C for 10 s, 60 °C for 15 s, and 72 °C for 15 s.

Gene expression study

Primer pairs were designed using Primer3plus (<http://primer3plus.com/cgi-bin/dev/primer3plus.cgi>).

The design of a set of primers (Table 4.1) was based on expressed sequence tag (EST) clones from cDNA libraries from desiccated *F. vesiculosus* and *F. serratus* (Pearson et al. 2010). For the *pksIII* gene, the EST available from *F. vesiculosus* corresponded to the three prime untranslated region (3'UTR) (Pearson et al. 2010) those function were not assigned. In order to identify this gene the 3'end part of the cDNA sequence was obtained using rapid amplification of cDNA ends

(RACE) approaches. The 3'end sequence was cloned using the protocol developed by ([Scotto-Lavino et al. 2006](#)).

Table 4.1: Primers used for the qRT-PCR analysis on control and UV-B conditions.

Gene	Forward	Reverse	Amplicon Length (bp)	Tm °C	Accession number	References
<i>ef1.alpha</i>	TGCGTACAATCGCATTG	CGAACATGAAGGACAGTT GC	198	58	GH706096	EST (Pearson et al. 2010)
<i>tua</i>	GTCACACCGATGTAGAGGA	GGCTTCCAGACAATTACCC	96	58	GH702736	EST (Pearson et al. 2010)
<i>pks</i>	TTGCACGTATGCTCTGTTGC	GCGCGAATAACCTGATGG	135	60	GH706741	EST (Pearson et al. 2010)
<i>vbpo</i>	CCAAGGCCGTCGAGTCATATC	GCACTTACTGCAATCCAATG TAC	129	59	comp9395_c0_seq3	I.Kruse, personal communication
<i>hsp70</i>	AGATCGAGGAGATTGACTAGA TGG	CGACTTGCATCACACATATC G	161	60	GH704979	EST (Pearson et al. 2010)
<i>ast6</i>	GACCCTCCCTGATCTTCC	CCAGATGCGGTCAATTAC	83	59	GH702197	EST (Pearson et al. 2010)

Phlorotannin extraction and semi-purification

100 mg dry weight (DW) of freeze-dried tissue were grounded for 5 min at 6500 rpm at room temperature, using a mixer-mill (Precellys 24, Bertin Technologies) in 2 mL Eppendorf tubes with metal beads supplied. Extraction buffer consisted of methanol: water (80:20) at pH 4.3. Extraction was performed three times successively on the powder in dark at 40 °C during 30 min with agitation in a thermomixer (Eppendorf). The extract was centrifuged 10 min at 10000 g and the supernatant was removed. Methanol was evaporated in a speed-vacuum concentrator miVac Duo Concentrator (miVac, Genevac Limited, Ipswich, UK) at 40 °C and the total extract was lyophilized and weighed.

In order to purify the total extract, the protocol developed by ([Steevensz et al. \(2012\)](#)) was tested on 3 g of powder with 30 mL of methanol: water (80:20) at pH 4.3. After three consecutive extractions at 40 °C with agitation, the methanol was removed with a Büchi Rotovapor R-114 with a B-480 water heater set at 35 °C. Then the extract was defatted three to four times using

dichloromethane (1:1 v/v) partitioning and fractionated using a C18 Sep-Pak cartridge (6 cc; 500 mg), which had been preconditioned with 12 mL methanol followed by 18 mL Milli Q (mQ) water. A sample (200 – 300 mg) of the freeze-dried aqueous fraction was dissolved in 200 mL mQ water for fractionation on the DionexAutoTrace[®] 280 SPE (Thermo Scientific) and eluted with 20 mL methanol. Samples were dried under N₂, freeze-dried and weighed.

Quantification of soluble phlorotannins

The quantification of total soluble phlorotannins in the extracts was performed using the adapted Folin-Ciocalteu method (Van Alstyne 1995) with phloroglucinol used as standard (Sigma). Each sample was re-suspended in 1 mL methanol:water (80:20) at pH 4.3 and diluted to reach a concentration of 1 mg.mL⁻¹. Quantification was carried out using multiwell plates (Nunc UV-Star 96 wells), 20 µL of extract (1 mg.mL⁻¹) were added to 40 µL of Na₂CO₃ 20 %, 130 µL MQ water and 10 µL Folin-Ciocalteu reagent (Sigma). The reaction was incubated at 70°C during 10 min with a cover in a thermocycler and the absorbance of the solutions was then measured at 750 nm in multiwell plates on a Safire²Tecan Multi-detection Microplate reader.

Ultrahigh-pressure liquid chromatography coupled to mass spectrometry conditions for profiling of purified phlorotannins

Ultrahigh-pressure liquid chromatography was performed in the same conditions described by Steevensz et al. (2012)(Steevensz et al. 2012) using an Ultimate 3000 (Dionex). Mass spectrometry analyses were performed on LTQ-Orbitrap Discovery (Thermo Scientific). Separations were achieved using a Waters UPLC BEH Amide 1.7 µm (2.1 x 100mm) column, 5 µL injections and a flow-rate of 400 µL.min⁻¹. Mobile phase A was composed of 10.0 mM ammonium acetate adjusted to pH 9.0 with ammonium hydroxide and mobile phase B was acetonitrile. The gradient consisted of an initial hold at 5 % mobile phase A for 1 min, followed by a linear gradient to 35 % A in 16 min, followed by re-equilibration for 5 min at 5 % A, for a total run time of 22 min. In the negative ion mode, the electrospray voltage was set to 3.42 kV, the capillary voltage to 45 V, and the tube lens offset to 130 V. The sheath and auxiliary gas flows (both nitrogen) were set to 5 arbitrary units (a.u.), and the drying gas temperature was set

to 300 °C. Mass spectra were recorded from 50 m/z up to 1000 m/z at a resolution of 30 000 (FWHM at m/z 400) acquired in the centroid mode.

Following their acquisition by Xcalibur® software (Thermo Fisher Scientific), metabolomic fingerprints were deconvoluted to allow the conversion of the three-dimensional raw data (m/z, retention time, ion current) to time- and mass-aligned chromatographic peaks with associated peak areas. Massmatrix File Conversion was used to convert the original Xcalibur data files (*.raw) to a more exchangeable format (*.mzXML). Data processing was then performed using the open-source Workflow4metabolomics.org. CentWave was used for the peak picking. The interval of *m/z* value was set to 0.1, the signal to noise ratio threshold was set to 10, the group band-width was set to 10 and the minimum fraction was set to 0.75. Obiwarp was used for retention time correction with profstep set to 0.1.

Statistical analyses

All data obtained under the different experiments and conditions were analyzed using one-way analysis of variance (one-way ANOVA p < 0.05). Mean comparisons were made using LSMEANS test with significant differences reported at p < 0.05. All statistical analyses were done using R version 3.0.1 (R Development Core Team 2010) with R packages ([Maxime Hervé 2014](#)),([Russell V. Lenth 2014](#)).

Results

Effect of UV-B chronic exposure on the physiological fitness of *Fucus vesiculosus*

In our experimental conditions, the UV-B condition corresponded to a UV-B dose approximately two times more important than in full sunlight at noon in spring in Brittany ([Hupel et al. 2011b](#)). This condition was likely to affect the alga physiological performance. In order to control this performance, changes in the optimal quantum yield (Fv/Fm) of apical parts of the *F. vesiculosus* thallus were measured after different times of exposure to UV-B radiation (Figure 4.1). During the first 3 days of UV-B exposure, no significant difference appeared compared to the control conditions. However, after one week and four weeks of chronic exposure, the

maximum efficiency of PSII was significantly more affected by UV-B radiation in comparison with control conditions (ANOVA pvalue = 0.040; LSMEANS 0.05), with a slight reduction during the whole kinetics.

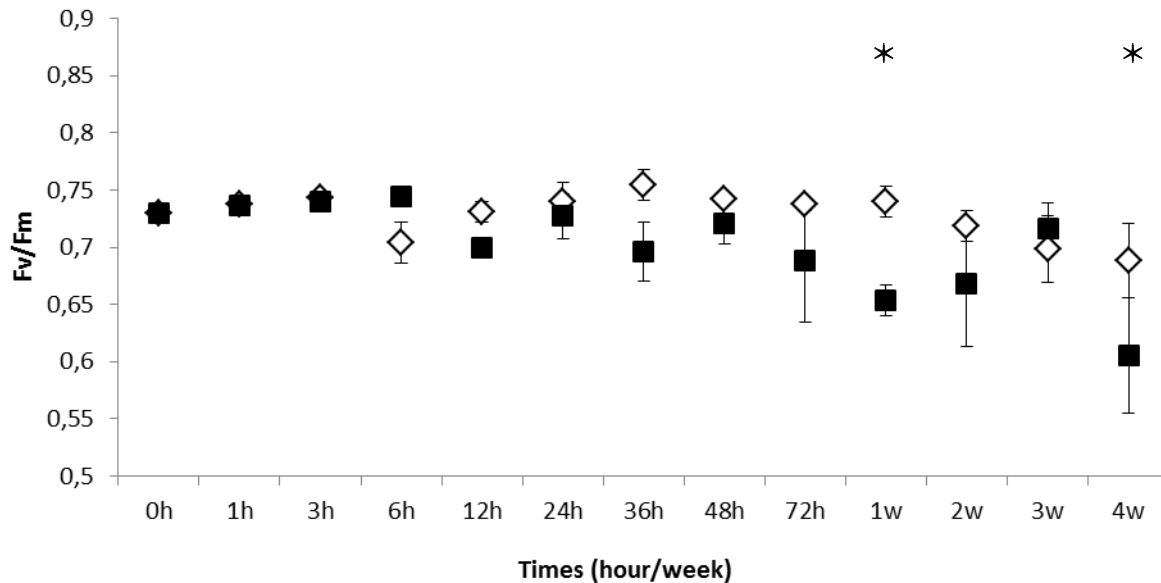
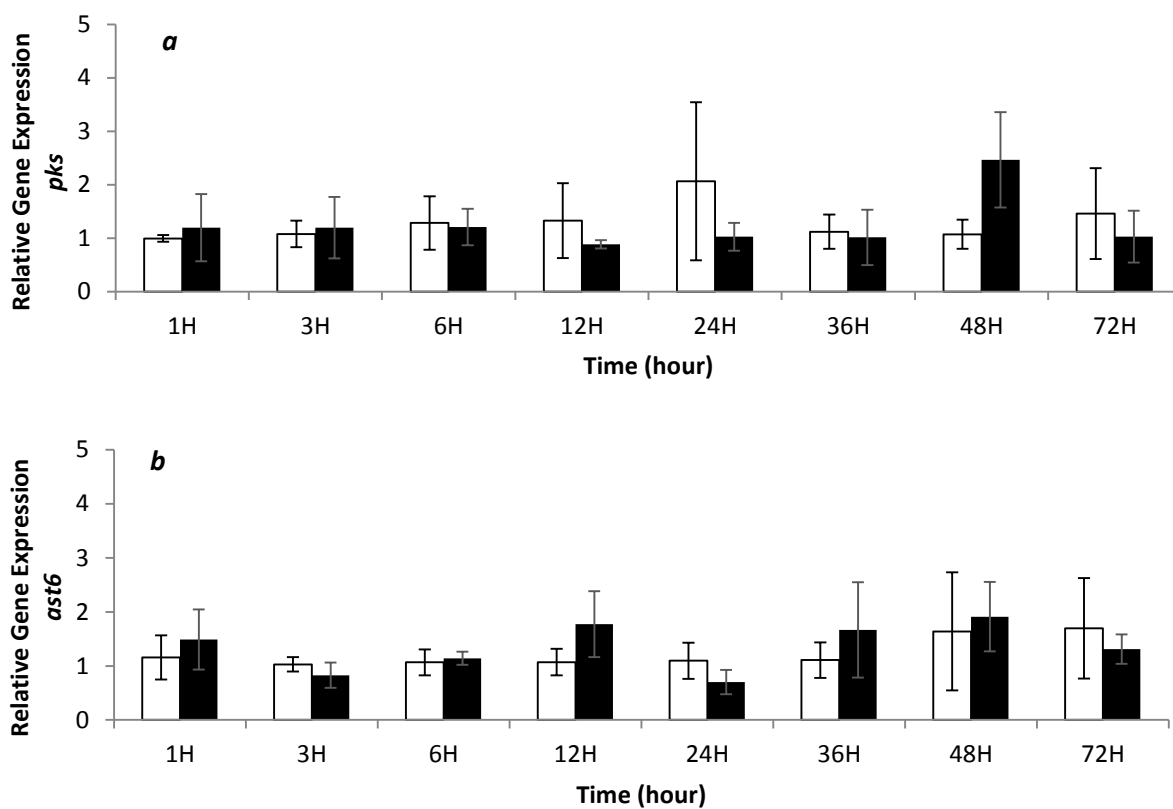


Figure 4.1: Photosynthesis efficiency of *Fucus vesiculosus* under chronic exposure to UV-B radiation during 4 weeks. The optimal quantum yield (F_v/F_m) of apical parts of *F. vesiculosus* thalli was measured through imaging PAM fluorimetry during exposure to PAR (controls, white losanges) and UV-B stress condition (black squares). Values represent means of three independent replicates and bars represent the SE. Statistically significant differences (LSMEANS 0.05) between treatments are indicated by stars (*).

Gene expression

A large number of ESTs available in the databases for *Fucus* spp. correspond to 3'UTR regions. Therefore, before designing primer sequences for qRT-PCR, we cloned a larger partial cDNA of a *pksIII*/gene from *F. vesiculosus* in order to confirm the identity of the coding region of this sequence with other *pksIII*/genes, including a biochemically characterized PKSIII enzyme, such as *EsiPKS1* from the brown alga *E. siliculosus* (Meslet-Cladiere et al. 2013). The cDNA of *F.vesiculosus* cloned covered 67.5 % of the total sequence of *EsiPKS1* with 1726 bp fragment.

The corresponding amino acid sequence was 98.3 % identical to the PKS1 from *Ectocarpus* (GenBank™ accession no: CBN76919) and exhibited significant similarities to algal and bacterial *pksIII* (Supporting Information, Figures. S1 - S3). The expression kinetics of *pksIII*, *ast6*, *hsp70* and *vbpo* genes was monitored by qRT-PCR (Figure 4.2). The relative expression of *pksIII* and *ast6* genes showed no significant regulation of these genes during UV-B exposure, expression levels ranged from 1 to 2.5 in fold-change. However an effect of UV-B treatment was detected for *hsp70* gene (ANOVA, pvalue = 0.00376). In fact, *hsp70* gene (Figure 4.2C) was over-expressed four times at 12h and eight times at 24h in UV-B condition compared to control. Despite a relative expression more variable than *pksIII* and *ast6* gene, the relative expression of *vbpo* (Figure 4.2D) ranged from 0.6 to 6.47 did not show any significant difference between control and UV-B treatment due to a high inter-individual variability.



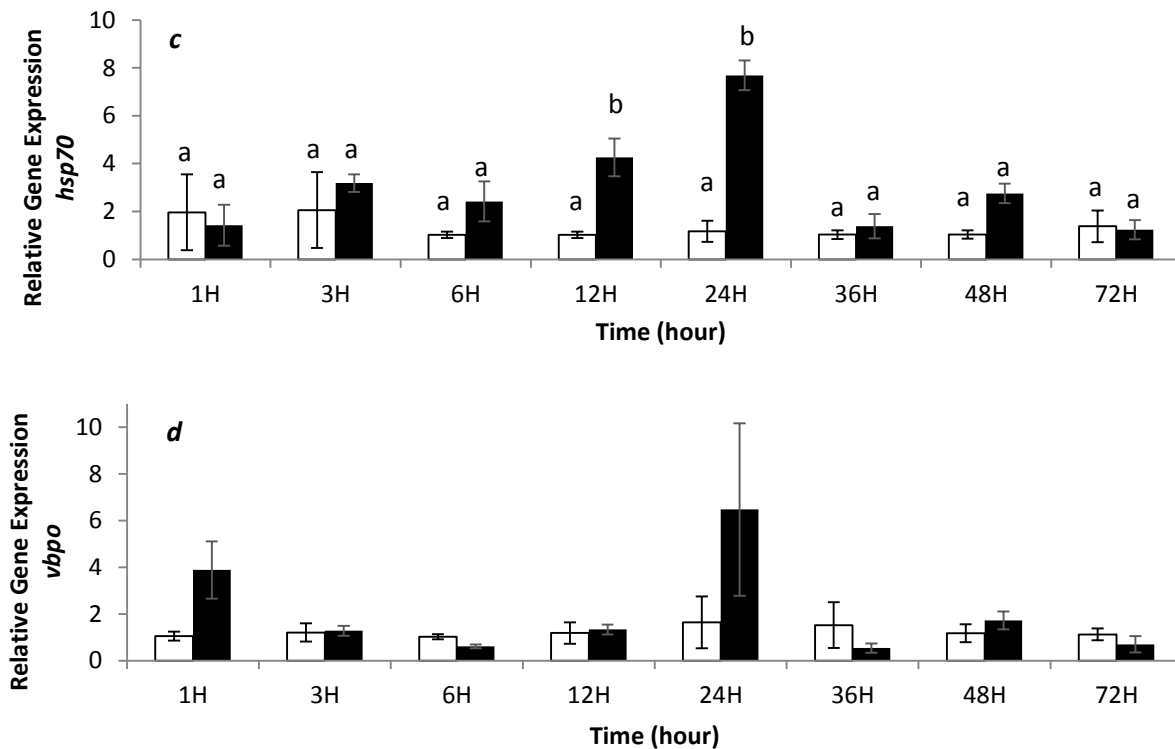


Figure 4.2: Relative gene expression in *Fucus vesiculosus* in controlled condition (white square) and exposed to UV-B (black square) during 72 hours are presented for *pksIII* a), *ast6* b), *hsp70* c), and *vbpo* d). The expression of a gene is normalized to the geometric mean of the expression of 2 reference genes (*ef1 alpha*, *tua*) in the same algal sample and to the mean of its expression in the three control algae at each time point. Values represent means of three independent replicates and bars represent the SE. Letters indicate significant difference (LSMEANS 0.05).

Phenol contents:

The total soluble phenol concentrations were measured by Folin-Ciocalteu method in methanolic extracts of the *Fucus vesiculosus* thallus, sampled after different times of exposure to UV-B radiation, and compared to those of control algae (Figure 4.3). The concentration of soluble phlorotannins ranged from 12 to 23 mg.g⁻¹ DW, according to the phloroglucinol standard curve and the standard deviation (SD) calculated on three biological replicates, and showed a large variability between individuals. Indeed, the statistical analysis of the results revealed no

significant difference between control and UV-B treatment (ANOVA, pvalue = 0.7381) and no effect of the kinetics (ANOVA, pvalue = 0.0696).

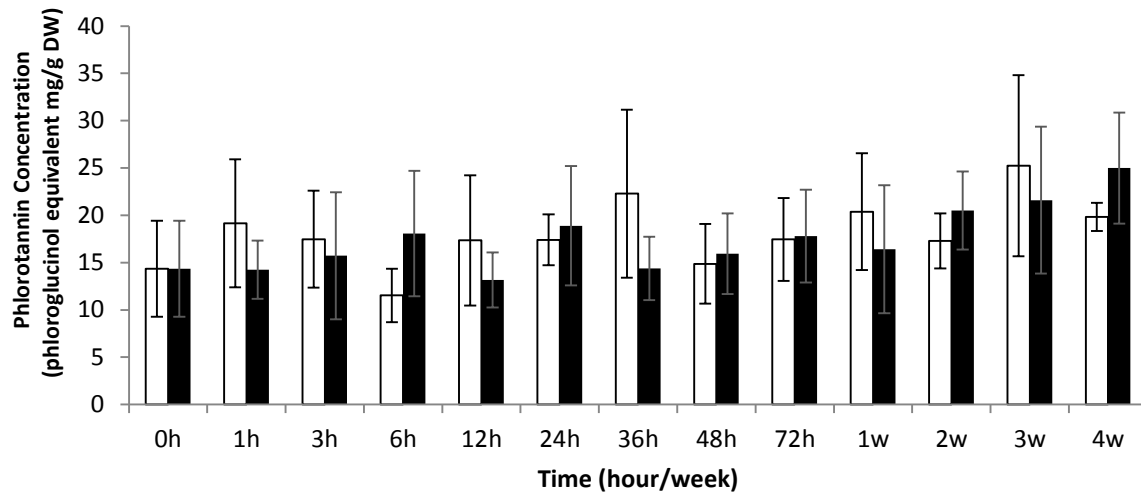


Figure 4.3: Quantification of total soluble phenol contents ($\text{mg equivalent phloroglucinol.g}^{-1} \text{DW}$) before purification in controlled condition (white square) and exposed to UV-B (black square). Values represent means of three independent replicates and bars represent the SD.

In semi-purified fractions (Figure 4.4), soluble phenol concentrations were in the range 3 – 8.9 $\text{mg.g}^{-1} \text{DW}$ equivalent phloroglucinol, indicating a significant loss of compounds during the semi-purification process. The quantification of semi-purified fractions pointed out a significant effect of kinetics (ANOVA, pvalue = 0.001), with the lowest concentration in algae sampled after 24 hours of UV-B treatment ($2.81 \text{ mg.g}^{-1} \text{DW}$) and the most concentrated extract in those collected after 2 weeks of UV-B treatment ($8.93 \text{ mg.g}^{-1} \text{DW}$). A light but significant effect of UV-B treatment was also detected (ANOVA, pvalue < 0.1) and we observed a decrease of phenolic content from $5.9 \text{ mg.g}^{-1} \text{DW}$ equivalent phloroglucinol in control algae to $2.81 \text{ mg.g}^{-1} \text{DW}$ for treated algae with UV-B at 24 hours.

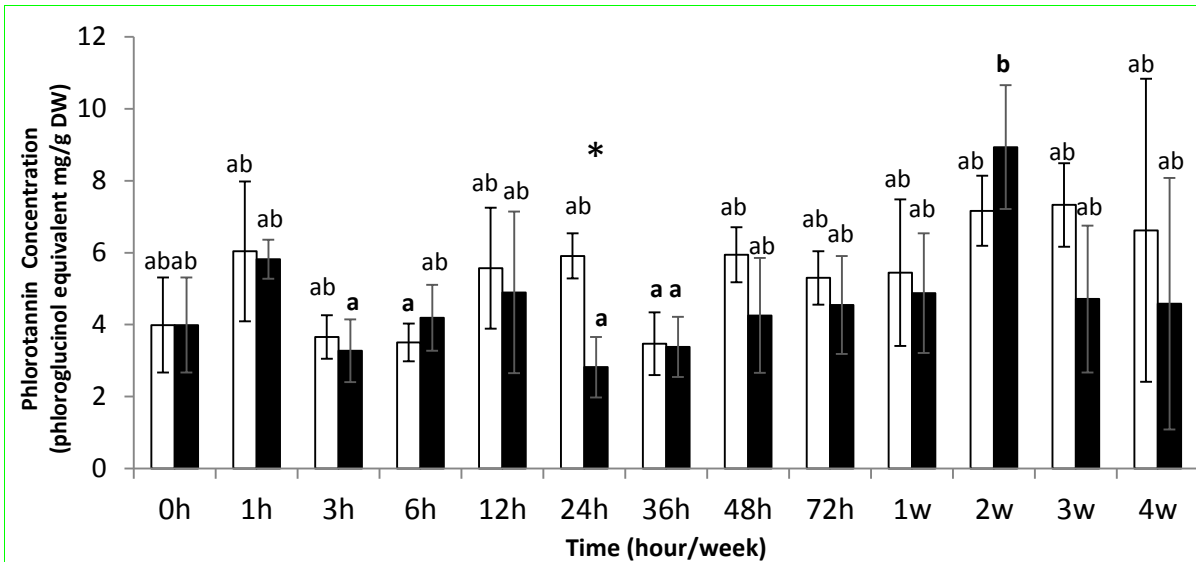


Figure 4.4: Quantification of soluble phenol contents in semi-purified phlorotannins fractions (mg equivalent phloroglucinol.g⁻¹ DW) in controlled condition (white square) and exposed to UV-B (black square). Values represent means of three independent replicates and bars represent the SD. Mean with different letters indicate significant difference between all samples along the kinetic (LSMEANS 0.05). Star (*) indicate significant difference between control and UV-B treatment (LSMEANS 0.05).

Profiling of purified phlorotannins

The U-HPLC-ESI-MS analyses of purified extracts evidenced several degrees of polymerization of phlorotannins from DP3 to DP7 (data not shown). However, after quantification of DP3 to DP7, no significant difference has been observed between control and UV-B treatment during the kinetic study (ANOVA pvalue = 0.84667). Figure 4.5 represents the chromatograms of an extraction of the precursor ion at *m/z* 621.0882 corresponding to a DP5 oligomer of phlorotanninin a control (Figure 4.5a) and UV-B treatment (Figure 4.5b) after two weeks. At least four isomers were detectable but no significant difference in their distribution and quantification upon UV treatment has been established compared to control treatment.

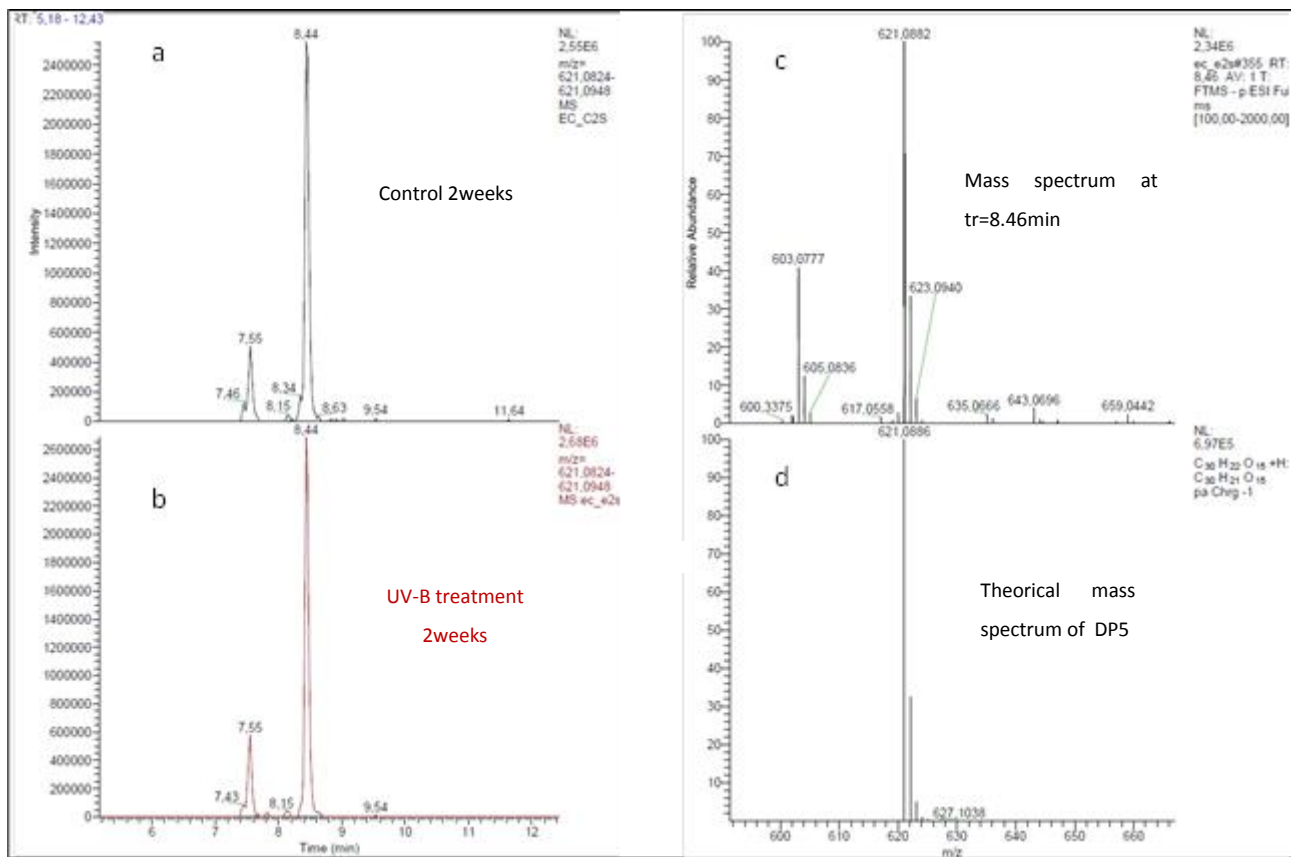


Figure 4.5: Ultra-HPLC-ESI-MS chromatogram of a precursor ion at m/z 621.0886 corresponding to a DP5 oligomer of phlorotannin in semi-purified fractions extracted from control a) and UV-B treated algae b) after 2 weeks. Mass spectrum from the chromatogram identified as DP5 c). The theoretical mass spectrum of DP5: $C_{30}H_{21}O_5$ in the negative ion mode ($[M-H]^- = 621.0886\text{ }m/z$) d).

Discussion

In order to cope with high levels of UV-B radiation, algae of the intertidal zone have developed strategies to survive and adapt in this fluctuating environment (Häder and Figueroa 1997). In terrestrial plants, both constitutive and inducible protection have been reported (Jansen et al. 2010). UV-B radiations affect algae at different levels from degradation of the photosynthetic apparatus to DNA damage. However, the cumulative potential effects of this chronic stress on intertidal seaweeds at low tide are poorly understood (Henry and Van Alstyne 2004).

To address this question, we applied molecular and chemical analytical tools which could bring a major step forward in seaweed physiology ([Bischof et al. 2006](#)). This study monitored the expression profile of targeted genes involved in the stress responses of brown algae and in the metabolism of phlorotannins.

Recent approaches on gene expression applied to ecophysiological studies in brown algae used global transcriptomics based on DNA microarrays or EST sequencing, which provide large amounts of information on the expression of thousands genes with less than 35 – 40 % of them which can be attributed to a putative function. A large amount of genes hence remains with unknown physiological roles. In Fucales, recent studies followed the gene expression changes upon grazing in *F. vesiculosus* ([Flöthe et al. 2014b](#), [Flöthe et al. 2014c](#)) or desiccation stress in *Fucus* spp. ([Pearson et al. 2010](#)). These studies provided a large overview of gene categories that are regulated in response to these challenges. However, activation of specific pathways involved in both defense and dessication tolerance remains to be investigated. Such a global transcriptomics was not yet attempted to specifically monitor gene expression in a brown alga in response to UV radiation.

A targeted approach was recently attempted to evaluate the responses to thermal stress in *F.serratus* ([Jueterbock et al. 2014](#)). This study measured specifically the stress response to common-garden heat stress (20 °C – 36 °C), by using both photosynthetic performance and transcriptomic upregulation of heat shock protein genes, including *hsp70* in *F. serratus* from four European populations. In the same way, our choice in this study was to show the expression variation of targeted genes implicated in global and specific stress responses during three days of treatment with UV-B radiation. We studied the expression of genes such as *hsp70* which is involved in global stress responses, *pksIII* which is the homologous of the gene encoding a phloroglucinol synthase in *E. siliculosus* ([Meslet-Cladiere et al. 2013](#)) (Supporting information), *ast6* encoding an aryl sulfotransferase and *vypo* encoding a vanadium bromoperoxidase, that are interesting candidates for their implication in phlorotannin modification and scavenging of harmful ROS, respectively.

Our analysis using qRT-PCR has evidenced a significant effect of UV-B treatment on the expression level of *hsp70* at 12h and 24h, and a while no significant difference in the expression

of the three other genes was detected. In our study the non-induction of the *pksII* seems to be correlated with the non-induction of *vbpo* and *ast6* genes which encode proteins potentially implicated in modification of phlorotannins. However the presence of multigenic families in brown algae has been reported for the *vbpo* (Roeder et al. 2005) and *ast* (Michel et al. 2010) that could reveal a potential presence of constitutive and inducible genes in these families. The maximum capacity of the PSII seemed to be affected only after 1 week of chronic radiation, suggesting that photosynthetic efficiency of *F. vesiculosus* remained globally stable in culture, with a relative good tolerance of this species to UV-B radiation in opposition to the sensitivity of Laminariales (Gomez and Huovinen 2010). The quantification of photosynthetic efficiency (Fv/Fm) gave values ranging from 0.6 to 0.75, which are comparable to results previously reported in fucoids (Nielsen et al. 2003).

Regarding contrasted responses in the implication of phlorotannins in response to UV-B radiation reported in the literature, we performed a quantitative and qualitative study of soluble algal phenol contents during a longer period of exposure (four weeks). In our study, high intensity (4.9 W.m^{-2}) of UV-B did not induce the accumulation of soluble phlorotannins in *F. vesiculosus* tissues after four weeks. Contents ranged from 12 to 23 mg.g^{-1} DW in the total methanolic extract, still comparable to levels found in others Fucales (Connan et al. 2004).

To complete this global quantification, we tested the hypothesis that the proportion of low molecular weight versus high molecular weight phlorotannins may shift upon UV exposure. Indeed the phlorotannin profiling can give more physiological information than the total phenol content (Koivikko et al. 2008). We purified phlorotannins following a procedure involving U-HPLC-MS analysis, recently developed by Steevensz et al. 2012. Phenol concentrations in semi-purified fractions were in the range $3 - 9 \text{ mg.g}^{-1}$ DW equivalent phloroglucinol, indicating a significant loss of compounds during the semi-purification process. However, a significant effect of kinetics has been detected (Figure 4.4) that could indicate a significant variation in the extraction efficiency of semi-purified phlorotannins. The use of U-HPLC separation gave access to several degrees of polymerization (DP), from DP3 to DP7, with a good resolution but no significant difference in their distribution and quantification upon UV treatment has been established compared to control treatment (Figure 4.5).

Previous reports suggested that responses of brown algae to UV stress were dependent of species, seasons and the development stage of thalli. In fact, a study in the Fucales *Ascophyllum nodosum* ([Pavia et al. 1997](#)) has shown an increment of 30 % of phlorotannin content after two weeks of exposure to UV-B radiation at 0.6 W.m^{-2} . In contrast in embryos and juveniles of *Fucus gardneri* ([Henry and Van Alstyne 2004](#)), no effect of UV-B has been detected on the phlorotannins content during a treatment of three weeks. Seasonal variations of phenol contents have been also demonstrated in *Fucus vesiculosus* ([Connan et al. 2004](#)), with the highest levels in spring like in the Laminariales *Lessonia nigrescens* ([Gomez and Huovinen 2010](#)), with significant increase of phlorotannin content during UV exposure in summer, when the development of sporophytes is optimal. Regarding these results, we can hypothesize that the induction of phlorotannin synthesis may require particular conditions. Other stimuli than UV-B, such as those provided by physical damage have previously shown a phlorotannin production over 20 % in *Fucus distichus* in less than 2 weeks ([Van Alstyne 1988](#)).

By combining biochemical and molecular approaches, we can now assert that the lack of accumulation of soluble phlorotannins over the kinetics is related to the lack of over-expression of the gene encoding for PKSIII and others genes potentially related to phlorotannin modifications (*ast6, vbpo*). From our data, we cannot exclude a turn-over of some phenols ([Arnold and Targett 2000](#)) potentially insolubilized in the cell walls or secreted that would not require transcriptional activation of the *pksIII* gene for *de novo* synthesis. However, this hypothesis points also that the capacity of acclimation of *F. vesiculosus* to drastic UV exposure could involve constitutive mechanisms, as already shown in terrestrial plants ([Bieza and Lois 2001](#)).

In summary, this work highlights the adaptation of *Fucus vesiculosus* to elevated UV-radiation in the intertidal zone. Taken together, the above results suggest a constitutive accumulation of phlorotannins occurring during the development of *F. vesiculosus*, rather than inducible processes. It is likely that phenols provide in these species efficient UV-sunscreens, as deduced from the relative stability of the physiological performance under strong UV-B exposure. In this context, the use of molecular tools to further investigate the regulation of phlorotannin biosynthesis appears particularly complementary of global quantifications and will be suitable to

follow developmental changes in the phlorotannin synthesis or responses to biotic stress in brown algae.

Supporting information

Figure. S1: Nucleotide alignment of the *Fucus vesiculosus* cDNA sequence with Fucus EST sequences.

Figure. S2: Nucleotide alignment of the brown algal PKS III coding sequences.

Figure. S3: Protein sequence alignment of the brown algal PKS III with a bacterial counterpart.

Partie 2 : Implication des phlorotannins dans la réponse aux stress biotiques et abiotiques chez *F.vesiculosus*

FvePKS_FWp :	*	20	*	40	*	60	*	80	*	100	:	-
FvePKS_RVp :	-----										:	-
FvePKS_clo :	ACTGCGAGCTGATCAAGAACCTGGCCTACCCGCTCCGTGGACCGTACTCTCATCGGTTCATGGGGTGCGCCGCGGCATGAACGGCTTCCGCAACGCGAACG :	105										
FvePKS_GH7 :	-----										:	-
FsePKS_GH7 :	-----										:	-
FvePKS_FWp :	*	120	*	140	*	160	*	180	*	200	*	-
FvePKS_RVp :	-----										:	-
FvePKS_clo :	ACTTCGTGACTGCCAACCCGGCAAGTACGCCCTGATGATCTGCGTCGAGCTTCCTCGGTGCACACGACCTTCGACGACAACATCAACGACGCCATCCTCCACG :	210										
FvePKS_GH7 :	-----										:	-
FsePKS_GH7 :	-----										:	-
FvePKS_FWp :	220	*	240	*	260	*	280	*	300	*	-	-
FvePKS_RVp :	-----										:	-
FvePKS_clo :	CAATCTCGCCGATGGGTGCGCCGCCGTGCTCAAGGGTATCAAGAAGTCCGAGGCCCCAAGGGAACCTGGGATCGTCGACAACCACCGCTGGCTCATGG :	315										
FvePKS_GH7 :	-----										:	-
FsePKS_GH7 :	-----										:	-
FvePKS_FWp :	320	*	340	*	360	*	380	*	400	*	420	-
FvePKS_RVp :	-----										:	-
FvePKS_clo :	AGGGCACCGAGGATGGCATCACCTCGCGATCAAGCCCCACGGCATCACCTGCACTCTCTAAGTTCTGCCAGTACATGCCAAGAACATCGCTTCTTCG :	420										
FvePKS_GH7 :	-----										:	-
FsePKS_GH7 :	-----										:	-
FvePKS_FWp :	*	440	*	460	*	480	*	500	*	520	:	-
FvePKS_RVp :	-----										:	-
FvePKS_clo :	CCGACGGCTTCTCAAGAACGACAACCTGGCGCGATGACGTTGACTTCTGGTGCACCCGGGGACGCCGTATCATCGAGGAGGCGCAGAACGGCTCG :	525										
FvePKS_GH7 :	-----										:	-
FsePKS_GH7 :	-----							CGCAGAACGGCTCG :	15			
FvePKS_FWp :	*	540	*	560	*	580	*	600	*	620	*	-
FvePKS_RVp :	-----										:	-
FvePKS_clo :	GCCTCACGGAGGAGCAGACCGCGGATTCTGGGGCGGTGCTTGCCGAGTACGGGAACATGCTTCACCGTCGGTGTGTTGTGCTGTCAGGGTGTCAAGCGCC :	630										
FvePKS_GH7 :	-----							CGGTGATGTTGTGCTGTCAGGGTGTCAAGCGCC :	36			
FsePKS_GH7 :	GCCTCACGGAGGAGCAGACCGCGGACTCTGGGGCGGTGCTTGCCGAGTACGGGAACATGCTTCGCCATCGGTGATGTTGTGCTGTCAGGGTGTCAAGCGCC :	120										

Partie 2 : Implication des phlorotannins dans la réponse aux stress biotiques et abiotiques chez *F.vesiculosus*

FvePKS_FWp :	-----	640	*	660	*	680	*	700	*	720	*	-----	:	-	
FvePKS_RVp :	-----												:	-	
FvePKS_clo :	ACAAACGCCCGCCTCGCGCAAGGGAAAGCCTGGCTACCAGACCGGCATGGCGTTCCTCGTTTCCCCGGCGTGGCGCCGAGGGTATCCTCTCAAGCAGCTCTAAA												:	735	
FvePKS_GH7 :	ACAAACGCCCGCCTCGCGCAAGGGAAAGCCTGGCTACCAGACCGGCATGGCGTTCCTCGTTTCCCCGGCGTGGCGCCGAGGGTATCCTCTCAAGCAGCTCTAAA												:	141	
FsePKS_GH7 :	ACAAACGCCCGCCTCGCGCAAGGAAGCCTGGCTACAAGACCGGCATGGCGTTCCTCGTTTCCCCGGCGTGGCGCCGAGGGTATTCTCTCAAGCAGCTCTAAA												:	225	
FvePKS_FWp :	-----	740	*	760	*	780	*	800	*	820	*	840	:	-	
FvePKS_RVp :	-----												:	-	
FvePKS_clo :	AGAAGCGCGAAAGGATTGGAGTTGCGACACACCTCCGAGTAGTACATAACTGGAGGGGTGTCAAGCGGAGAAAGGCCATCGTATAC---TGTAGTCACCGATGCG												:	837	
FvePKS_GH7 :	AGAAGCGCGAAAGGATTGGAGTTGCGACACA-CTCCGAGTAGTACATAACTGGAGGGGTGTCAAGCGGAGAAAGGCCATCGTATAC---TGTAGTCACCGATGCG												:	242	
FsePKS_GH7 :	AGGAGCGCGAAAGGATTGGAGATTGCGACACG-CTCCGAGTAGTACATAACTGGAGGGGTGTTCGGCGGAGAAAGGCCATCGTATACTGTTGAGTCACCGATGCG												:	329	
FvePKS_FWp :	-----	*	860	*	880	*	900	*	920	*	940	:	21		
FvePKS_RVp :	-----												:	-	
FvePKS_clo :	ATCCCACATCACACCCGAGGTGGGCACGGGTCAAGCTCGTTTGCGATGTTGCACGTATGTCCTGTCGTAAGGTTT												:	942	
FvePKS_GH7 :	ATCCCACATCACACACGAGTTGGGCACGGGTCAAGCTCGTTTGCGATGTTGCACGTATGTCCTGTCGTAAGGTTT												:	347	
FsePKS_GH7 :	ATCCCACATCACACCCGAGTTGGGCACGGGTCAAGCTCGTTTGCGATGTTGCACGTATGTCCTGTCGTAAGGTTT												:	434	
ttgcacgtatgtctctgttgc															
FvePKS_FWp :	-----	*	960	*	980	*	1000	*	1020	*	1040	*	-----	:	-
FvePKS_RVp :	-----												:	18	
FvePKS_clo :	ATGTTTC-GGAGCCAGCGTTTGTCACATTGTTGAGCGACAACACTCGAGCGGTCCCATCAGGTATTGCGCGCAGCCCCATTGTTGCTGATGGCGCACCGA												:	1046	
FvePKS_GH7 :	ATGTC-TC-GGAGCCAGCGTTTGTCACATTGTTGAGCGACAACACTCGAGCGGTCCCATCAGGTATTGCGCGCAGCCCCATTGTTGCTGATGGCGCACCGA												:	451	
FsePKS_GH7 :	ATGTC-TCGGGAGCCAGCGTTGTCACATTGTTGAGCGACAACACTCGAGCGGTCCCATCAGGTATTGCGCGCAGCCCCATTGTTGCTGATGGCGCACCGA												:	496	
ccatc															
FvePKS_FWp :	-----	1060	*	1080	*	1100	*	1120	*	1140	*	-----	:	-	
FvePKS_RVp :	-----												:	-	
FvePKS_clo :	AACAAATGCGGCAGGGATTGGGGCGAGTGAAATCTCGCGCAACGACCGTGTATTCTTGTGACAAGCTATCAGTTACTCTTGCCTGAGATTCTGGGCC												:	1151	
FvePKS_GH7 :	AACAAATGCGGCAGGGATTGGGGCGAGTGAAATCTCGCGCAACGACCGTGTATTCTTGTGACAAGCTATCAGTTACTCTTGCCTGAGATTCTGGGCC												:	556	
FsePKS_GH7 :	-----												:	-	
FvePKS_FWp :	-----	1160	*	1180	*	1200	*	1220	*	1240	*	1260	:	-	
FvePKS_RVp :	-----												:	-	
FvePKS_clo :	ACTTTAGAAGCGATTCCCAGTCCCTTTTATGGGTGCATCGCAAGCGTCTTCCCCCCCAGCACCGCTTCCCTCTTAACGGGTGGTCATTGCGCACCAC												:	1256	
FvePKS_GH7 :	ACTTTAGAAGCGATTCCCAGTCCCTTTTATGGGTGCATCGCAAGCGTCTTCCCCCCCAGCACCGCTTCCCTCTTAACGGGTGGTCATTGCGCACCAC												:	661	
FsePKS_GH7 :	-----												:	-	

Partie 2 : Implication des phlorotannins dans la réponse aux stress biotiques et abiotiques chez *F. vesiculosus*

* 1280 * 1300 * 1320 * 1340 * 1360	: -	: -	: -	: -	: -	: -	: -	: -	: -
FvePKS_FWp :	-	-	-	-	-	-	-	-	-
FvePKS_RVp :	-	-	-	-	-	-	-	-	-
FvePKS_clo :	TGGGCTTCTCCCTCTCGAAAAAGAGAGTTGGTGTCCAAGTTGAAGTACGGTGGCATTGGTGATGCCGAAAGATATGTCCTGCACGTGTGGC	: 1361							
FvePKS_GH7 :	TGGGCTTCTCCCTCTCGAAAAAGAGAGTTGGTGTCCAAGTTGAAGTACGGTGGCATTGGTGATGCCGAAAGATATGTCCTGCACGTGTGGC	: 766							
FsePKS_GH7 :	-	-	-	-	-	-	-	-	-
* 1380 * 1400 * 1420 * 1440 * 1460 * 1480									
FvePKS_FWp :	-	-	-	-	-	-	-	-	-
FvePKS_RVp :	-	-	-	-	-	-	-	-	-
FvePKS_clo :	AGAACAGGGGAAGCCCAATAGCTTCTATATAACTCCAGTA	CTGCTGTTGCGGTAGCGCGTGC	GTTGTCTTGAGGTTGGCGGGTAC	CTTGTGGT	TTGAGGTTGGCGGGTAC	CTTGTGGT	TTGAGGTTGGCGGGTAC	CTTGTGGT	TTGAGGTTGGCGGGTAC
FvePKS_GH7 :	AAAACAAGGGA								
FsePKS_GH7 :	-	-	-	-	-	-	-	-	-
* 1480 * 1500 * 1520 * 1540 * 1560 * 1580									
FvePKS_FWp :	-	-	-	-	-	-	-	-	-
FvePKS_RVp :	-	-	-	-	-	-	-	-	-
FvePKS_clo :	CAAAACGTTTGTGGTCGTGCTGTATATTGATCGTACGATTGTA	CTGTTGGGT	CACAA	CGGGTGTGGAGGGTCGT	CGCGAGTGGTAGCGTT	CACTTG	CGGGTGTGGAGGGTCGT	CGCGAGTGGTAGCGTT	CACTTG
FvePKS_GH7 :	-	-	-	-	-	-	-	-	-
FsePKS_GH7 :	-	-	-	-	-	-	-	-	-
* 1580 * 1600 * 1620 * 1640 * 1660 * 1680									
FvePKS_FWp :	-	-	-	-	-	-	-	-	-
FvePKS_RVp :	-	-	-	-	-	-	-	-	-
FvePKS_clo :	CTGCGGAGGAGGCAGGAATATG	TAGTTATTTCGTTGGGTGCGGTTTATCGCCTG	TACCATCGGGACATGTGGATCGTC	GTCAATTGGCAAAC	AC	ACT	CGGGACATGTGGATCGTC	GTCAATTGGCAAAC	AC
FvePKS_GH7 :	-	-	-	-	-	-	-	-	-
FsePKS_GH7 :	-	-	-	-	-	-	-	-	-
* 1700 * 1720 *									
FvePKS_FWp :	-	-	-	-	-	-	-	-	-
FvePKS_RVp :	-	-	-	-	-	-	-	-	-
FvePKS_clo :	ACCTCGCTCGATGATAATGAA	ATATTTCTCNTAAAAAAAAA	AAAAA	AAAAA	AAAAA	AAAAA	AAAAA	AAAAA	AAAAA
FvePKS_GH7 :	-	-	-	-	-	-	-	-	-
FsePKS_GH7 :	-	-	-	-	-	-	-	-	-

Figure. S1: Nucleotide alignment of the brown algal PKS III coding sequences.

Nucleotide alignment of the *Fucus vesiculosus* cDNA sequence with *Fucus* EST sequences.

qPCR forward primer (FvePKS_FWp), qPCR reverse primer (FvePKS_RVp), partial cDNA sequence cloned from *F. vesiculosus* (FvePKS_clo), *F. vesiculosus* EST of GH706741 GenBank accession (FvePKS_GH7), *F. serratus* EST of GH701018 GenBank accession (FsePKS_GH7). The positions sharing a conservation of 100, 80 and 60% are respectively shaded in black, dark grey and light grey.

Partie 2 : Implication des phlorotannins dans la réponse aux stress biotiques et abiotiques chez *F.vesiculosus*

FsePKS :	-----	* 20 * 40 * 60 * 80 * 100 * 120	: -
FvePKS :	-----		: -
SbiPKS :	ATGTCTTCAGCAACTGTTGCTATGTTGGGGATCCCACCGTGCAGATGCCCTGGCTTGATCGTGCCTCCCTCATCGTGGTATTCGGTCTACCGAAGGGAAAGGATGAGCAGACCGTCT		: 124
EsiPKS1 :	ATGTCTTCAGCAACTGTTGCTATGTTGGGGATCCCACCGTGCAGATGCCCTGGCTGACCCGACTGTCAGATCGCTCTGGCTGGTGTCTCTTCGTTGTGCTGCAGTCGGTCAAAAGTCCAAGGACGAGCACGGTAT		: 124
FsePKS :	-----	* 140 * 160 * 180 * 200 * 220 * 240	: -
FvePKS :	-----		: -
SbiPKS :	ACCCCGTCATCGCGGGGATGGGATCGGCAACCCCTCAGTACCGGTGCACCCAGGACCAGGGCTCACGGTCGCTCAGAAGTGCCCTGGCGTGGAGTCGCTGAAGCCAGTGCTCGAGCGAATCTA		: 248
EsiPKS1 :	ACCCGGTCATCGCCGGGATGCCATCGGCAACCCGCACTACCGCTGCACGCAGAACGAGGCCCTCGCGTCGCCTCAAAGTGCCCCGGCTCGAGTCCATCAAGGCCGTTCTCGAGCGCATCTA		: 248
FsePKS :	-----	* 260 * 280 * 300 * 320 * 340 * 360 * 380	: -
FvePKS :	-----		: -
SbiPKS :	CGGAAACTCCCGCATCGGCACCGATACTTCGCCGTGCCGGACTTTACTCCCACCCAGGCTGCCAAGGGGACCCATTGTTCTCCCGCCAGGGCAGCTTGAGGTGCCGTGGACACCGC		: 372
EsiPKS1 :	CGGCAACTCGGCATCGGCACCGCTACTTCGCCGTGCCGGACTTCACCCCCGGCAAGGGCGGCCAACCCCTTCTAACCGGGCAGCTAACAGGTGCCGTGGACGTCCGG		: 372
FsePKS :	-----	* 400 * 420 * 440 * 460 * 480 * 500	: -
FvePKS :	-----		: -
SbiPKS :	CTCGACAAGTTCAAGGAGAAGGGGTTCCCTCGTTCCGACGTCGCTCGCCGCCATTAAAGGAGGGGGGATCGATGTGTCGACGTGTCGAAGCTCGTCGTCGTCTACCGGTTTC		: 496
EsiPKS1 :	CTGGACAAGTTCAAGGAGAAGGGCTCCGCTGGTGTCCGACGTCGCCGCCGCGCCATCAAGGAGGCCGCGCTGAACGTCGAGGACATCTCAAGCTCGTCGTCGTCTCCACCGGATTC		: 496
FsePKS :	-----	* 520 * 540 * 560 * 580 * 600 * 620	: -
FvePKS :	-----		: -
SbiPKS :	ACTGGAGCTGATCAAGAACCTGGCCTCACCGCTCCGTGGACCTACTCTCATCGGTTCATGGGGTGCGCCGGCCATGAACGGCTTCCGAAACGCGAACGACTT		: 109
EsiPKS1 :	TCGGCCCCGGCTGGACTCGCAGCTTATCAAGAACCTCGCCCTCACCGCTCTGTCGACCCACTCTCATCGGTTCATGGGAATGGCTGCCGCATGAACGGCTTCCGAAACGCGAACGACTT		: 620
FsePKS :	-----	* 640 * 660 * 680 * 700 * 720 * 740	: -
FvePKS :	-----		: -
SbiPKS :	CGTTACCGCAAAACCTGGCAAGTACGCCCTGATGATCTCGCTCGAGCTTCCCTCGGTGCACACGACCTTCGACGACAATCAACGACGCCATCTCCACGCATCTCGCCGATGGGTGCC		: 233
EsiPKS1 :	CGTCACCGCCAACCCGGAAAGTACGCCCTGATGATCTCGCTCGAGCTTCCCTCGGTGCACACGACCTTGACGACAATCAACGACGCCATCTCCACGCATCTCGCCGACGGTGGGCC		: 744
FsePKS :	-----	cgt ac gc aaccggg aagtacgc ct atgatctcgct gagct tcctc gtgcacac acctt ga gacaatcaacgacgc atc t cacgc atcttcgcccga gg tgcgcc	: 744

Partie 2 : Implication des phlorotannins dans la réponse aux stress biotiques et abiotiques chez *F.vesiculosus*

FsePKS :	-----	*	760	*	780	*	800	*	820	*	840	*	860	:	-
FvePKS :	GCCGCCGTGCTCAAGGGTATCAAAGAAGTCGGAGGCCCAAGGGAAACCTGGCGATCGTCGACAACCACCGTGGCATGGAGGCACCGAGGATGGCATCACCCCTCGCGATCAAGGCCAACG	357													
SbiPKS :	GCTGCCGTGCTAAAGGGTGTCAAGGAAGTCGGAGGCCCAAGGGAAACCTGGCTATCGTGACAACCACCGTGGCATGGAGGCACCGACGGCATCACCCCTCGCCATCAAGGCCAACG	868													
EsiPKS1 :	GCTGCCGTGCTCAAGGGAGCAGGAAGTGGAGTGGCCCCAAGGGAAACCTCGCTATCGTGACAACCACCGTGGCATGGAGGCACCGAGGACGAATCACCCCTGCTATCAAGGCCAACG gc gccgtgt aaggg ca gaagtc gag ccccaagggaacacct gc atcgt gacaaccacccgtggcatggaggg accggaga gg atcacccct gc atcaagcc aacg	868													
FsePKS :	-----	*	880	*	900	*	920	*	940	*	960	*	980	:	-
FvePKS :	GCATCACCTGCACACTCTCTTAAGTTCTGCCCAAGTACATGCCAACAGACATCGCGTCTTGCGGACGGCTTCCTCAAGAACCTCGGCCGATGACGTTGACTTCTGGTGCCTGCA	481													
SbiPKS :	GTATCACCTGCACCCCTGTCCAAGTTCTGCCCAAGTACATGCCAACAGATATGCCCTCTTGCGGACGGTTCTCAAGAACCTCGGCCGATGACGTTGACTTCTGGTGCCTGCA	992													
EsiPKS1 :	GCATCACCTGCACCCCTGTCCAAGTTCTGCCCAAGTACATGCCAACAGACATCGCGTCTTCGCGGACGGCTTCCTCAAGAACAGCTGGACGGACGACGTTGACTTCTGGTGCCTGCA g atcacctgcac ct tc aagttctt ccccaagtacatcgccaagaa atcgc ttctt gc gacgg ttccctaagaagcacaat ctcgg cg ga gacgttacttctggtgctgtca	992													
FsePKS :	-----	1000	*	1020	*	1040	*	1060	*	1080	*	1100	*	:	95
FvePKS :	CCCCGGGGACCCGTATCATCGAGGAGGCCAGAACCGGGCTCGGCCACCGGAGGACACCCGGGATTCGTGGCGGTGCTTGCGAGTACGGAAACATGCTTTCACCGTCTGGTATGTTT	605													
SbiPKS :	CCCCGGAGGACCCGCATCATCGAGGAGGACAGAACCGGGCTTGGCTCACGGAGGCTCAACCCGGGACTCGTGGCGGTGCTTGCGAGTACGGAAACATGCTTTCACCGTCTGGTATGTT	1116													
EsiPKS1 :	CCCCGGAGGCCACGTATCATCGAGGAGGCCAGAACCGGGCTTGGCTCTCGAGGAGGACACCCGGGACTCGTGGCGGTGCTGGGGAGTACGGAAACATGCTTCACCGTCTGGTATGTT ccccgg gg cg cg atcatcgaggaggCgCAGAACGGgCT GGCCTaCGGAGGAgCAGAACCGGGAcTCGTGGCGGTGCTtGccGAGTACGG AACATGCTtTC CC TC GTgATGTT	1116													
FsePKS :	GTGCTCTCCAGGGTGTTCAGGCCAACACGCCGCGCTGGCCAAGGAAGCCATGGCTACAGACCGGGATGGCGTTCTCGTTTTCGCCCCGGGGTGGGCGCGAGGGTATTCTCTCAAGGAGC	219													
FvePKS :	GTGCTCTCCAGGGTGTTCAGGCCAACACGCCGCGCTGGCCAAGGAAGCCATGGCTACAGACCGGGATGGCGTTCTCGTTTTCGCCCCGGGGTGGGCGCGAGGGTATTCTCTCAAGGAGC	729													
SbiPKS :	GTGCTCTAGGGTGTTCAGGCCAACACGCCGCGCTGGCCAAGGAAGCCGGCTACAGACCGGGATGGCGTTCTCGTTTTCGCCCCGGGGTGGGCGCGAGGGTATTCTCTCAAGGAGC	1240													
EsiPKS1 :	GTGCTCTAGGGTGTTCAGGCCAACACGCCGCGCTGGCCAAGGAAGCCGGCTACAGACCGGGATGGCGTTCTCGTTTTCGCCCCGGGGTGGGCGCGAGGGTATTCTCTCAAGGAGC GtGCTgTC AGGGTgTTCAAGGCCAACACGCCGCGCTcGCgCAaGG AAGCC GGCTACcAGACcGG ATGGCGTTCTC TT TC CCgGG GT GGcGC GAgGGtATcCtCTCA GCAG	1240													
FsePKS :	TCTAA :	224													
FvePKS :	TCTAA :	734													
SbiPKS :	TTTAA :	1245													
EsiPKS1 :	TCTAG :	1245													
	TcTAa														

Figure. S2: Nucleotide alignment of the brown algal PKS III coding sequences.

Fucus serratus GH701018 (FsePKS), partial cDNA sequence cloned from *Fucus vesiculosus* (FvePKS), *Sargassum binderi* HM245964 (SbiPKS), *Ectocarpus siliculosus* Esi0024_0032 ORCAE Id (EsiPKS1). The positions sharing a conservation of 100, 75 and 50% are respectively shaded in black, dark grey and light grey.

Partie 2 : Implication des phlorotannins dans la réponse aux stress biotiques et abiotiques chez *F.vesiculosus*

MtuPKS18 :	MNVSAESGAPRRAQRHVGGLAQI-----PPAPPTTVAVIEGLATGT PRRVVNGSDAADRVAELFLDPGQRERIPRVYQKSRTTRMAV-----DPLDAKFDFVERREPA	: 100
FsePKS :	-	: -
FvePKS :	-	: -
SbiPKS :	--MSSAAVAMLADPTVQIALACIVLSSLIVVFRSYRKGKDEQT VY PVIA GMAIGN PQYRCT QDQALTVAQKCPGVESVKPVLERIYGN S RIGS RYFA VP DFT PNQA AKGDPMFF PADGSF E VPV	: 121
EsiPKS1 :	--MSSAAVAMLADPTVQIALACLVVSLEVVLQSVKKSKDEQT VY PVIA GMAIGN PQYRCT QNEALAVASKCPGLESIKPVLERIYGN S RIGS RYFA VP DFT PGRAAKGDPLFYPADGSYQVPV	: 121
SjaPKS :	--MSSPVVAMLTPEPSVQIALACVVLSSLVRLSLQSKDEQT VY PVIA GMAIGN PQYRCT QDEALAVATKCPGLPSIKPVLERIYGN S RIGS RYFA IPDFT PSQA AKGDPMFF PADGSYEV VPV	: 121
SlapKS :	-	: -
MtuPKS18 :	TIRDRMHLFYEHAVPLAVDVS KRALAGLPYRAAEIGLLV LATSTGFIAPGV DVAIVKE LGLSPSI SRV VNF MGCAAMN ALGT AT NY VR AH AMK ALV CIE LCS VNA F ADD IN D VVI HSLF	: 224
FsePKS :	-	: -
FvePKS :	-	: -
SbiPKS :	DT--RLDKFKEKAVPLVSDVARRAIKEAGIDVSDVSKL VVV SSTGFLGPGLDCE LIK NGLTR SVDR LI GFMG CAA AMNGFRN AND FVT ANEG KY ALMICVELSSVHTT FDDNINDA IHLA IF	: 72
EsiPKS1 :	DV--RLDKFKEKAVPLVSDVARRAIKEAGLNVEDISKL VVV SSTGFLGPGLDCE LIK NGLTR SVDR LI GFMG CAA AMNGFRN AND YVT ANEG KY ALMICVELSSVHTT FDDNINDA IHLA IF	: 243
SjaPKS :	DT--RLDKFKEKAVPLVSDVARRAIKEAGLDVSDISKL VVV SSTGFLGPGLDCE LIK NGLTR SVDR LI GFMG CAA AMNGFRN AND YVT ANEG KY ALMICVELSSVHTT FDDNINDA IHLA IF	: 243
SlapKS :	--EKA VPLVSDVARRAIKEAGLDVSDISKL VVV SSTGFLGPGLDCE LIK NGLTR SVDR LI GFMG CAA AMNGFRN AND YVT ANEG KY ALMICVELSSVHTT FDDNINDA IHLA IF	: 114
k lgl s r fm gca amn a v a p al cel sv f d ind h f		
MtuPKS18 :	GDGCAA ALV I GAS QVQ EKLE PCK VV VRS S ESQL LDN T EDGIV LG NHNG IT C ELS EN LPGY I FSG VAP VTE M LWD NG LQ I S D ID I MAIHP GCE KIIIEQS VRS LGI SA BLAQ S WDV LARFGNML	: 348
FsePKS :	-	: 25
FvePKS :	ADGCAA AVLKG I K-SEAPK CT LAIVDNHAWLME GTEDG I TLAI KPN G I CTL SKFL P OYIA K NIA FFADGFLK KHNL GRDD DV D FWC VHPG CRRIEEA QN GL LT E QT A DS WA VL AEY GNML	: 195
SbiPKS :	ADGCAA AVLKG V R-KSEAPK CT LAIVDNHAWLME GTEDG I TLAI KPN G I CTL SKFL P OYIA K NIA FFADGFLK KHNL GRDD DV D FWC VHPG CRRIEEA QN GL LT E QT A DS WA VL AEY GNML	: 366
EsiPKS1 :	ADGCAA AVLKG AR-KSECPK CT LAIVDNHAWLME GTEDG I TLAI KPN G I CTL SKFL P OYIA K NIA FFADGFLK KHNL GRDD DV D FWC VHPG CRRIEEA QN GL LT E QT A DS WA VL AEY GNML	: 366
SjaPKS :	ADGCAA AVMKG AR-KSECPK CT LAIVDNHAWLME GTEDG I TLAI KPN G I CTL SKFL P OYIA K NIA FFADGFLK KHNL GRDD DV D FWC VHPG CRRIEEA QN GL LT E QT A DS WA VL AEY GNML	: 366
SlapKS :	ADGCAA AVI KG AR-KSECPK CT LAIVDNHAWLME GTEDG I TLAI KPN G I CTL SKFL P OYIA K NIA FFADGFLK KHNL GRDD DV D FWC VHPG CRRIEEA QN GL LT E QT A DS WA VL AEY GNML	: 237
dg ca v g l t edgi 1 n gitc ls lp yi a 1 1 d d w h pgg i ie qn gl G63 ee qt Ad s Wa VL e 5 GNML		
MtuPKS18 :	SVSLIFVLET MVQQAESAKA----ISTGVAFAFGPGVTVEGMIFDIIRR	: 393
FsePKS :	SPSVMF VLS RVF KRHN A ALAQ KGP GYKTGM AF SF SPG V GAEG ILL KQL	: 73
FvePKS :	SPSVMF VLS RVF KRHN A ALAQ KGP GYQTGM AF SF SPG V GAEG ILL KQL	: 243
SbiPKS :	SPSVMF VLS RVF KRHN A ALAQ KGP GYQTGM AF SF SPG V GAEG ILL KQL	: 414
EsiPKS1 :	SPSVMF VLS RVF KRHN A ALAQ KGP GYQTGM AF SF SPG V GAEG ILL KQL	: 414
SjaPKS :	SPSVMF VLS RVF KRHN A ALAE G KGP GYKTGM AF SF SPG V GAEG ILL KQL	: 414
SlapKS :	SPSVMF VLS RVF KRHN A ALAE G KGP GYKTGM AF SF SPG V GAEG ILL KQL	: 285
SpS66FVLsr6fk rhna A1a gkpgy TG6AFsFs PGVga EG6L1 q6		

Figure. S3: Protein sequence alignment of the brown algal PKS III with a bacterial counterpart.

Mycobacterium tuberculosis P9WPF0 (MtuPKS18), translated sequence of *Fucus serratus* GH701018 (FsePKS), translated sequence of *Fucus vesiculosus* (FvePKS), *Sargassum binderi* ADK13089 (SbiPKS), *Ectocarpus siliculosus* Esi0024_0032 (EsiPKS1), translated sequence of *Saccharina japonica* contig_6991 (SjaPKS), translated sequence of *Saccharina latissima* contig_4304 (SjaPKS). The residues sharing 100, 80 and 60% identity are respectively shaded in black, dark grey and light grey.

References

1. Davison IR, Pearson GA (1996) Stress tolerance in intertidal seaweeds. *J Phycol* 32: 197–211.
2. Baldauf SL (2008) An overview of the phylogeny and diversity of eukaryotes. *J Syst Evol* 46: 263–273.
3. Meslet-Cladiere L, Delage L, J.-J. Leroux C, Goulitquer S, Leblanc C, et al. (2013) Structure/Function Analysis of a Type III Polyketide Synthase in the Brown Alga *Ectocarpus siliculosus* Reveals a Biochemical Pathway in Phlorotannin Monomer Biosynthesis. *Plant Cell* 25: 3089–3103.
4. Berglin M, Delage L, Potin P, Vilter H, Elwing H (2004) Enzymatic cross-linking of a phenolic polymer extracted from the marine alga *Fucus serratus*. *Biomacromolecules* 5: 2376–2383.
5. Salgado LT, Cinelli LP, Viana NB, Tomazetto de Carvalho R, de Souza Mourão PA, et al. (2009) a Vanadium Bromoperoxidase Catalyzes the Formation of High-Molecular-Weight Complexes Between Brown Algal Phenolic Substances and Alginates. *J Phycol* 45: 193–202.
6. Bitton R, Ben-Yehuda M, Davidovich M, Balazs Y, Potin P, et al. (2006) Structure of algal-born phenolic polymeric adhesives. *Macromol Biosci* 6: 737–746.
7. Roeder V, Collén J, Rousvoal S, Corre E, Leblanc C, et al. (2005) Identification of Stress Gene Transcripts in *Laminaria Digitata* (Phaeophyceae) Protoplast Cultures By Expressed Sequence Tag Analysis1. *J Phycol* 41: 1227–1235.
8. Cock JM, Sterck L, Rouzé P, Scornet D, Allen AE, et al. (2010) The *Ectocarpus* genome and the independent evolution of multicellularity in brown algae. *Nature* 465: 617–621.
9. Harborne JB (1975) Flavonoid sulphates: A new class of sulphur compounds in higher plants. *Phytochemistry* 14: 1147–1155.
10. Arnold TM, Targett NM (1998) Quantifying in Situ Rates of Phlorotannin Synthesis and Polymerization in Marine Brown Algae. *J Chem Ecol* 24: 577–595.
11. Amsler CD, Fairhead VA (2006) Defensive and Sensory Chemical Ecology of Brown Algae. In: Callow JA, editor. Incorporating Advances in Plant Pathology. Advances in Botanical Research. Academic Press, Vol. 43. pp. 1–91.
12. Jormalainen V, Honkanen T, Koivikko R, Eränen J (2003) Induction of phlorotannin production in a brown alga: defense or resource dynamics? *Oikos* 103: 640–650.
13. Ragan MA (1976) Physodes and the Phenolic Compounds of Brown Algae. Composition and Significance of Physodes in vivo. *Bot Mar* 19: 145–154.
14. Schoenwaelder MEA (2008) The Biology of Phenolic Containing Vesicles. *Algae* 23: 163–175.
15. Shibata T, Hama Y, Miyasaki T, Ito M, Nakamura T (2006) Extracellular secretion of phenolic substances from living brown algae. *J Appl Phycol* 18: 787–794.
16. Koivikko R, Loponen J, Honkanen T, Jormalainen V (2005) Contents of soluble, cell-wall-bound and exuded phlorotannins in the brown alga *Fucus vesiculosus*, with implications on their ecological functions. *J Chem Ecol* 31: 195–212.
17. Breton F, Cérantola S, Ar Gall E (2011) Distribution and radical scavenging activity of phenols in *Ascophyllum nodosum* (Phaeophyceae). *J Exp Mar Bio Ecol* 399: 167–172.
18. Bischof K, Gómez I, Molis M, Hanelt D, Karsten U, et al. (2006) Ultraviolet radiation shapes seaweed communities. *Rev Environ Sci Bio/Technology* 5: 141–166.

19. Renger G, Völker M, Eckert HJ, Fromme R, Hohm-Veit S, et al. (1989) On the mechanism of Photosystem II deterioration by UV-B irradiation. *Photochem Photobiol* 49: 97–105.
20. Allen DJ, McKee IF, Farage PK, Baker NR (1997) Analysis of limitations to CO₂ assimilation on exposure of leaves of two *Brassica napus* cultivars to UV-B. *Plant, Cell Environ* 20: 633–640.
21. Lesser MP (1996) Acclimation of phytoplankton to UV-B radiation : oxidative stress and photoinhibition of photosynthesis are not prevented by UV-absorbing compounds in the dinoflagellate *Prorocentrum micans*. *Mar Ecol Prog Ser* 132: 287–297.
22. Ragan, Glombitzka (1986) Phlorotannins, brown algal polyphenols. *Prog Phycol Res Round FE Chapman* DJ (ed) Biopress Ltd Bristol: 129–241.
23. Pavia H, Cervin G, Lindgren (1997) Effects of UV-B radiation and simulated herbivory on phlorotannins in the brown alga *Ascophyllum nodosum*. *Mar Ecol Prog Ser* 157: 139–146.
24. Henry BE, Van Alstyne KL (2004) Effects of uv radiation on growth and phlorotannins in *Fucus gardneri* (Phaeophyceae) juveniles and embryos. *J Phycol* 40: 527–533.
25. Swanson AK, Druehl LD (2002) Induction, exudation and the UV protective role of kelp phlorotannins. *Aquat Bot* 73: 241–253.
26. Hupel M, Lecointre C, Meudec A, Poupart N, Gall EA (2011) Comparison of photoprotective responses to UV radiation in the brown seaweed *Pelvetia canaliculata* and the marine angiosperm *Salicornia ramosissima*. *J Exp Mar Bio Ecol* 401: 36–47.
27. Wahl M, Jormalainen V, Eriksson BK, Coyer JA, Molis M, et al. (2011) Stress ecology in fucus: abiotic, biotic and genetic interactions. *Adv Mar Biol* 59: 37–105.
28. Apt KE, Grossman AR (1993) Characterization and transcript analysis of the major phycobiliprotein subunit genes from *Aglaothamnion neglectum* (Rhodophyta). *Plant Mol Biol* 21: 27–38.
29. Apt KE, Clendennen SK, Powers DA, Grossman AR (1995) The gene family encoding the fucoxanthin chlorophyll proteins from the brown alga *Macrocystis pyrifera*. *Mol Gen Genet* 246: 455–464.
30. Pearson G, Lago-Leston A, Valente M, Serrão E (2006) Simple and rapid RNA extraction from freeze-dried tissue of brown algae and seagrasses. *Eur J Phycol* 41: 97–104.
31. Fang G, Hammar S GR (1992) A quick and inexpensive method for removing polysaccharides from plant genomic DNA. *Biotechniques* 13: 52–56.
32. Pearson G, Hoarau G, Lago-Leston A, Coyer J, Kube M, et al. (2010) An Expressed Sequence Tag Analysis of the Intertidal Brown Seaweeds *Fucus serratus*(L.) and *F. vesiculosus* (L.) (Heterokontophyta, Phaeophyceae) in Response to Abiotic Stressors. *Mar Biotechnol* 12: 195–213.
33. Scotto-Lavino E, Du G, Frohman M a (2006) 3' end cDNA amplification using classic RACE. *Nat Protoc* 1: 2742–2745.
34. Steevensz AJ, Mackinnon SL, Hankinson R, Craft C, Connan S, et al. (2012) Profiling Phlorotannins in Brown Macroalgae by Liquid Chromatography-High Resolution Mass Spectrometry. *Phytochem Anal* 23: 547–553.
35. Van Alstyne K (1995) Comparison of three methods for quantifying brown algal polyphenolic compounds. *J Chem Ecol* 21: 45–58.
36. R Development Core Team (2010) R: A Language and Environment for Statistical Computing. R Found Stat Comput Vienna Austria 0: {ISBN} 3–900051–07–0.
37. Maxime Hervé (2014) RVAideMemoire: Diverse basic statistical and graphical functions.
38. Russell V. Lenth (2014) lsmeans: Least-Squares Means. R package version 2.11. <http://CRAN.R-project.org/package=lsmeans>.

39. Hupel M, Poupart N, Gall EA (2011) Development of a new in vitro method to evaluate the photoprotective sunscreen activity of plant extracts against high UV-B radiation. *Talanta* 86: 362–371.
40. Häder D, Figueroa FL (1997) Photoecophysiology of Marine Macroalgae. *Photochem Photobiol* 66: 1–14.
41. Jansen M a K, Martret B Le, Koornneef M (2010) Variations in constitutive and inducible UV-B tolerance; dissecting photosystem II protection in *Arabidopsis thaliana* accessions. *Physiol Plant* 138: 22–34.
42. Flöthe CR, Molis M, John U (2014) Induced resistance to periwinkle grazing in the brown seaweed *Fucus vesiculosus* (Phaeophyceae): molecular insights and seaweed-mediated effects on herbivore interactions. *J Phycol* 50: 564–576.
43. Flöthe CR, Molis M, Kruse I, Weinberger F, John U (2014) Herbivore-induced defence response in the brown seaweed *Fucus vesiculosus* (Phaeophyceae): temporal pattern and gene expression. *Eur J Phycol* 49: 356–369.
44. Jueterbock A, Kollias S, Smolina I, Fernandes JMO, Coyer JA, et al. (2014) Thermal stress resistance of the brown alga *Fucus serratus* along the North-Atlantic coast: acclimatization potential to climate change. *Mar Genomics* 13: 27–36.
45. Michel G, Tonon T, Scornet D, Cock JM, Kloareg B (2010) The cell wall polysaccharide metabolism of the brown alga *Ectocarpus siliculosus*. Insights into the evolution of extracellular matrix polysaccharides in Eukaryotes. *New Phytol* 188: 82–97.
46. Gomez I, Huovinen P (2010) Induction of Phlorotannins During UV Exposure Mitigates Inhibition of Photosynthesis and DNA Damage in the Kelp *Lomentaria nigrescens*. *Photochem Photobiol* 86: 1056–1063.
47. Nielsen HD, Brownlee C, Coelho SM, Brown MT (2003) Inter-population differences in inherited copper tolerance involve photosynthetic adaptation and exclusion mechanisms in *Fucus serratus*. *New Phytol* 160: 157–165.
48. Connan S, Goulard F, Stiger V, Deslandes E, Ar Gall E (2004) Interspecific and temporal variation in phlorotannin levels in an assemblage of brown algae. *Bot Mar* 47: 410–416.
49. Koivikko R, Eränen JK, Loponen J, V. J (2008) Variation of phlorotannins among three populations of *Fucus vesiculosus* as revealed by HPLC and colorimetric quantification. *J Chem Ecol* 34: 57–64.
50. Van Alstyne K (1988) Herbivore Grazing Increases Polyphenolic Defenses in the Intertidal Brown Alga *Fucus Distichus*. *Ecology* 69: 655–663.
51. Arnold TM, Targett NM (2000) Evidence for metabolic turnover of polyphenols in tropical brown algae. *J Chem Ecol* 26: 1393–1410.
52. Bieza K, Lois R (2001) An *Arabidopsis* mutant tolerant to lethal ultraviolet-B levels shows constitutively elevated accumulation of flavonoids and other phenols. *Plant Physiol* 126: 1105–1115.

Chapitre 5 : Effet du stress biotique du brouteur *Littorina littorea* sur la synthèse de phlorotannins chez *Fucus vesiculosus*



GEOMAR

Article en préparation

Short-term variations in the metabolism of phlorotannins in response to the herbivore Littorina littorea in the brown alga Fucus vesiculosus.

Authors:

Creis Emeline^{1,2}, Vallet Laurent, Delage Ludovic^{1,2}, Leblanc Catherine^{1,2}, Kruse Inken⁴, Ar Gall Erwan³, Weinberger Florian⁴, Potin Philippe^{1,2}

¹Sorbonne Universités, UPMC Univ Paris 06, UMR 8227, Integrative Biology of Marine Models, Station Biologique de Roscoff, CS 90074, F-29688, Roscoff cedex, Brittany, France

²CNRS, UMR 8227, Integrative Biology of Marine Models, Station Biologique de Roscoff, CS 90074, F-10 29688, Roscoff cedex, Brittany, France.

³Université Européenne de Bretagne, Université de Bretagne Occidentale, Laboratoire des Sciences de l'Environnement Marin, Unité Mixte de Recherche UM6539, Centre National de la Recherche Scientifique 6539, European Institute for Marine Studies, 29280 Plouzané, Brittany, France

⁴GEOMAR Helmholtz-Zentrum für Ozeanforschung, Marine Ecology Division, DüsternbrookerWeg 20, D-24105 Kiel, Germany

Corresponding authors:

Dr Philippe Potin, LBI2M, UMR 8227 CNRS/UPMC-Paris6, Station Biologique, CS90074, 29688 ROSCOFF Cedex, France, Brittany, ; Phone: 33+(0)2-98-29-23-75
Fax: 33+(0)2-98-29-23-85 E-mail :potin@sb-roscoff.fr

Dr Erwan Ar Gall, LEMAR UMR 6539 CNRS/UBO/IFREMER/IRD, Institut Européen d'Etudes Marines-IUEM, Place Nicolas Copernic, 29280 Plouzané, France, Brittany.
Phone: 33+(0)2-98-49-87-92, E-mail :erargall@univ-brest.fr

Introduction:

Phlorotannins are polyphenolic compounds specifically produced by brown algae. They present a large variety of structures from phloroglucinol monomer (1,3,5-trihydroxybenzene) to polymeric complex forms. Issued of the acetate-malonate pathway, phloroglucinol is produced by a Polyketide synthase of type III (PKSIII) by the condensation of malonyl-CoA units ([Meslet-Cladiere et al. 2013](#)). Despite little available knowledge on the biosynthesis pathway of these metabolites, previous studies underlined the role of phlorotannins in primary and secondary metabolism. Phlorotannins occur in soluble form in vesicles named physodes, in insoluble form cross-linked with alginates in the cell-wall, or they can be exuded in the extra-cellular environment ([Arnold & Targett 2003 ; Shibata et al. 2006](#)). Involved in the formation of cell walls during the early development of the fucoid zygote, polyphenol molecules carrying numerous hydroxyl groups facilitate the adsorption and adhesion of zygotes to the substrate via the formation of rigid structures by cross-links in the adhesive material ([Tarakhovskaya 2013](#)). In these primary stages, phlorotannins are essential for the construction of this protective wall between intra and extracellular compartments. Phlorotannins are also considered as defense molecules ([Ragan and Glombitza 1986 ; Potin et al. 2002](#)). They present antioxidant (Wang et al. 2012), antifungal, or antibacterial activities ([Lopes et al. 2012](#)) and they take part in the absorption of UV radiations ([Swanson and Druhl 2002](#)). Moreover, they can deter grazers by their ability to precipitate proteins like digestive enzymes ([S.Tugwell & G.M.Branch 1992](#)). In terrestrial plants, tannins have been occasionally called "quantitative" defenses ([Feeny 1976](#)) and may interfere with nutrient acquisition by herbivores and so playing the role of "digestibility reducer" defenses ([Rhoades & Cates 1976](#)) but the mechanisms of interaction are actually poorly understood.

[Coleman et al. \(2007\)](#) have shown that the treatment of *Ascophyllum nodosum* tissues by an α -amylase potentially occurring in the saliva of marine grazers induces an increase in the production of phlorotannins after 2 weeks. The direct effect of grazing has also been demonstrated in *Fucus vesiculosus* with a significant increase of phlorotannins contents after 3 days ([Yates and Peckol 1993](#)). To reduce energy costs allocated to defense, specific strategies

have been developed by organisms to adapt to the extent of grazing. Rapid and efficient specific responses are the best strategy to optimize defenses (Stamp 2003). In this context, a recent study has shown in the brown alga that *Fucus vesiculosus* responds to grazing by short chemical pulses to repel herbivores (Flöthe et al. 2014c). However, the repelling effect of phlorotannins is the subject to controversy. As pointed out by a guided separation bioassay in *F.vesiculosus* showing that galactolipids deter sea urchin herbivory and not phlorotannins (Deal et al. 2003). Nevertheless, a 300 µg.mL⁻¹ concentration of phloroglucinol is enough to affect the behavior of *Littorina littorea* with a reduction of *F.vesiculosus* palability of 40% or more (Weinberger et al. unpublished). The same concentration significantly increases the creeping velocity of *L.littorea*, whereas a tenfold dose of phloroglucinol promotes the detachment of the grazers from an artificial substrate.

In this context, this study followed complementary strategies to study the short term effects of the presence of the periwinkle snail *Littorina littorea*, on the production of phlorotannins in *Fucus vesiculosus*. In order to obtain an overview of phlorotannin-mediated defense to grazing, this study investigated the relative expression of targeted genes potentially involved in phlorotannin metabolism and/or stress during 3 days of treatment, in combination with the assessment of soluble phlorotannin content over a period of 3 weeks.

Material and methods:

Ethics Statement

Relevant permissions were obtained for observational and field studies from the German governmental authorities at.....

Biological materials and experimental design

Fucus vesiculosus plants were freshly collected from the littoral zone of Kiel Fjord at Kiekut (N54.448117°, E9.872275°) and *Littorina littorea* individuals were fished on a rocky shore at Mönkeberg (N54.352866°, E10.177580°). Induction experiments were run in a constant temperature chamber (15 ° C) during August 2013 at the Leibniz-Institute of Marine Sciences (IfM-GEOMAR) in Kiel, Germany.

Thalli were thoroughly washed with filtered seawater, weighted in order to calculate the adequate number of *Littorina* individuals per gr of fresh tissue to be assigned into each aquarium. The experimental set-up consisted of a flow-through system of 90 transparent plastic aquaria (2.9 L) with a permanent renewal of both seawater and bubbled air. Ambient water was obtained from the nearby Kiel Fjord, filtered (1.2 µm) and stored in a tank (150 L) before supply to the aquaria, which were individually regulated with roller clamps to give a constant flow rate. Light was provided by fluorescent tubes (OSRAM FLUORA L 36 W/77 25X1), which were mounted in parallel above the aquaria, so that total irradiance was $14.24 \pm 0.04 \text{ W.m}^{-2}$ with a light/dark period of 14/10 hours. In order to prevent escape of *Littorina*, aquaria were covered with a metal grid. The acclimatization of *F.vesiculosus* lasted 1 week and *L.littorea* individuals were kept in an aquarium without food for 3 days before the induction experiment.

In each treatment aquarium we applied 37 mg DW of snails per gram of algal FW, as estimated from the shell diameter, using a regression formula between both parameters (Hammann et al 2013).

The kinetic study lasted 3 weeks with successive sampling points of five replicates for each condition.

RNA extraction

The RNA extraction protocol was adapted from [Apt & Grossman \(1993\)](#), [Apt et al. \(1995\)](#) and [Pearson et al. \(2006\)](#). 50 mg dry weight (DW) of freeze-dried tissue were ground for 5min at 6500rpm at room temperature using a mixer-mill (Precellys 24, Bertin Technologies) in 2 mL Eppendorf tubes with ceramic beads supplied. Extraction buffer consisted of Tris-EDTA (100 mMTris, 50 mM EDTA, pH 7.5, with 1.5 M NaCl and 2% CTAB). Immediately prior to extraction, 500mM of DTT was added as antioxidant from a 1M stock dissolved in water. Extraction buffer was added to the tissue (1.5 mL per 50 mg dry weight) and the suspension was mixed vigorously by vortexing. After 15 min of extraction on ice, the mixture was centrifuged at 10,000 g for 20min at 4 °C. The upper aqueous phase was transferred to a new tube and 1 volume of chloroform:isoamyl alcohol (24:1 v/v) was added, vortexed vigorously and centrifuged at 10,000 g for 20 min at 4 °C. The upper aqueous phase was transferred to a new tube and 0.2 volumes of absolute ethanol were added gently and mixed by rocking the tube. Ethanol addition resulted in the precipitation of polysaccharides ([Fang & Hammar 1992](#)). A second chloroform extraction was then carried out under the same conditions and the aqueous phase was carefully removed. RNA was precipitated with 0.4 volumes of 12 M LiCl in the presence of 1 % (v/v) β-mercaptoethanol as antioxidant. Precipitation was performed overnight at -20 °C. The RNA was collected by centrifugation at 10,000 g for 30 min at 4 °C, the RNA pellet was dried (10–20 min on ice) and then re-suspended in 500 µL RNase-free water. The RNA was extracted with an equal volume of phenol-chloroform:isoamylalcohol (24:1 v/v) and centrifuged at 10,000g for 15 min at 4 °C. The resulting pellet was washed with 1 volume of chloroform:isoamyl alcohol (24:1 v/v) in order to remove the phenol. RNA was re-precipitated with 2 volumes ethanol, 0.3 M sodium acetate and re-suspended in 20 µL of sterile H₂O. The RNA was treated with RNase-free DNase-I according to the manufacturer's instructions (Qiagen) to remove any contaminating DNA.

RNA was stored at -80°C after determining its purity and concentration using a NanoDrop 2000 spectrophotometer (ThermoScientific) (A260/280), and its integrity by agarose gel electrophoresis.

Quantitative Real-time PCR (qRT-PCR)

Reverse transcription (RT) was performed in 10 µL on 250 ng total RNA, with 1 µL dT18 oligonucleotide (100 µM). The reaction mixture was denatured at 70 °C for 5 min. Then the master mixture containing 5 µL Improm II Buffer 5X (Promega), 4 µL MgCl₂ (25 mM), 1 µL dNTP mix (10 mM), 0.5 µL RNAsine, 2.5 µL Nuclease free water and 1 µL of ImProm-II™ Reverse Transcriptase (Promega) was added. The reaction mixture was pre-incubated at 25 °C for 5 min, the extension was carried out at 42 °C for 60 min, and the RT was inactivated by heating at 70 °C for 15 min. Finally, the total cDNA was diluted to 1 ng.µL⁻¹ to perform the qRT-PCR. qRT-PCR was carried out using the LightCycler® 480 multiwell plate 96, on a LightCycler® 480 Real-Time PCR System (Roche Diagnostics, Mannheim, Germany) in three technical replicates, using 5 µL of the LightCycler® 480 SYBR Green Master mix (Roche Diagnostics, Mannheim, Germany) with 2.5 µL cDNA (1 ng.µL⁻¹) or genomic DNA (gDNA) for quantification, 0.5 µL of each primer (10µM) and 1.5 µL water for a final volume of 10µL.

The cycling program for PCR quantification was run as follows: 5 min denaturation at 95 °C, followed by 45 cycles of 95 °C for 10 s, 60 °C for 15 s, and 72 °C for 15 s. Melting curves were also programmed from 65 °C to 97 °C in order to verify the absence of multiple amplifications.

Gene expression study

Primer pairs were designed using the program Primer3plus (<http://primer3plus.com/cgi-bin/dev/primer3plus.cgi>).

The design of primer sets (Table 5.1) was based on EST clones originated from cDNA libraries of desiccated *F. vesiculosus* and *F. serratus* (Pearson et al. 2010) and from a microarray study (personnal communication Inken Kruse).

Table 5.1: Primers used for the qRT-PCR analysis on control and grazing conditions.

Gene	Forward	Reverse	Amplicon Length (bp)	Tm °C	Accession number	References
<i>ef1.alpha</i>	TGCGTACAATCGCATTG	CGAAACATGAAGGACAG TTGC	198	58	GH706096	EST (Pearson et al. 2010)
<i>tua</i>	GTCACACCGATGTAGAGGA	GGCTTCCAGACAATTACC C	96	58	GH702736	EST (Pearson et al. 2010)
<i>pks</i>	TTGCACGTATGTCTCTGTT GC	GCGCGAATAACCTGATGG	135	60	GH706741	EST (Pearson et al. 2010)
<i>vypo</i>	CCAAGGCCGTCGAGTCATA TC	GCACTTACTGCAATCCAA TGTAC	129	59	comp9395_c0 _seq3	I.Kruse, personal communication
<i>hsp70</i>	AGATCGAGGAGATTGACT AGATGG	CGACTTGCATCACACATA TCG	161	60	GH704979	EST (Pearson et al. 2010)
<i>ast6</i>	GACCCTCCCTGATCTTCC	CCAGATGCGGTCAATTCA C	83	59	GH702197	EST (Pearson et al. 2010)
<i>X22181</i>	TGGTCGAGACGGAGGAA G	TGCACTTCAAGCTTACT CTTGC	132	60	unpublished	I.Kruse, personal communication
<i>Cyp450</i>	TAACGACATGGCTCAAAT CAC	ACACAACAAACACCCACA C	84	59	unpublished	I.Kruse, personal communication

Phlorotannin extraction

100mg dry weight (DW) of freeze-dried tissue were ground for 5 min at 6500rpm at room temperature, using a mixer-mill (Precellys 24, Bertin Technologies) in 2 mL Eppendorf tubes with metal beads supplied. Extraction buffer consisted of methanol: water (80:20) at pH 4.3. Extraction was performed 3 times successively on the powder in dark at 40°C during 30 min with agitation in a thermomixer (Eppendorf). The extract was centrifuged 10 min at 10,000g and the supernatant was removed. Methanol was evaporated in a speed-vacuum concentrator miVac Duo Concentrator (miVac, Genevac Limited, Ipswich, UK) at 40°C and the total extract was lyophilized and weighed.

Quantification of soluble phlorotannins

The quantification of total soluble phlorotannins in the extracts was performed using the adapted Folin-Ciocalteu method (Van Alstyne 1995) with phloroglucinol used as standard

(Sigma). Each sample was re-suspended in 1 mL methanol:water (80:20) at pH 4.3 and diluted to reach a concentration of 1 mg.mL^{-1} . Quantification was carried out using multiwell plates (Nunc UV-Star 96 wells), 20 μL of extract (1 mg.mL^{-1}) was added to 40 μL of Na_2CO_3 20%, 130 μL MQ water and 10 μL Folin-Ciocalteu reagent (Sigma). The reaction was performed at 70°C during 10 min with a cover in a thermocycler and the absorbance of the solutions was then measured at 750 nm in multiwell plates on a Safire²Tecan Multi-detection Microplate reader.

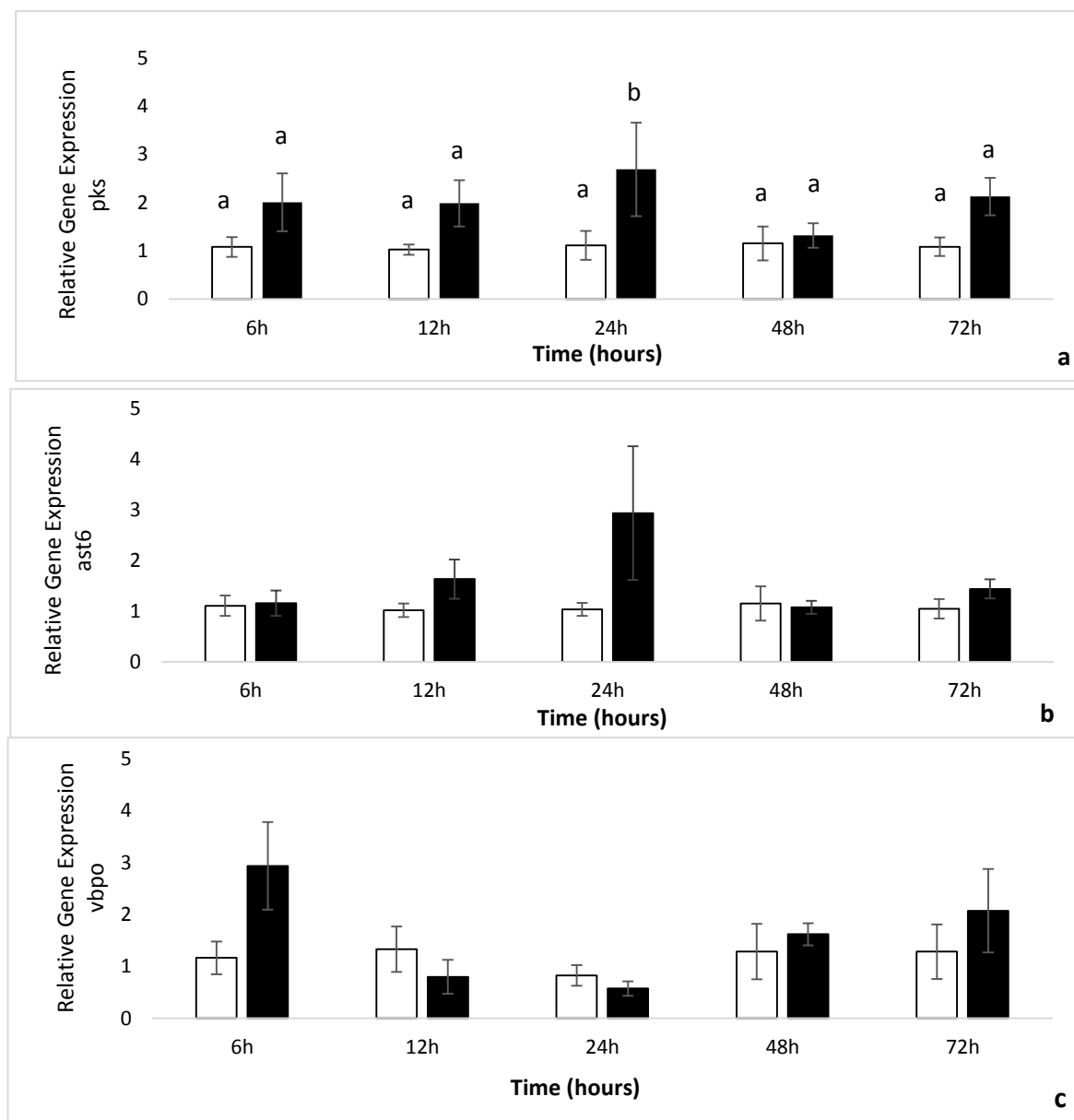
Statistical analyses

All values obtained in the different experiments and conditions were analyzed using one-way analysis of variance (one-way ANOVA $p<0.05$, $p < 0.1$). Mean comparisons were made using LSMEANS test with significant differences reported at $p<0.05$. All statistical analyses were done using R version 3.0.1 (R Development Core Team 2010) with R packages RVAideMemoire ([Maxime Hervé 2014](#)), and LSMEANS ([Russell V. Lenth 2014](#)).

Results:

Gene expression:

The expression kinetics of *pksIII*, *ast6*, *hsp70*, *vbpo*, *X22181*, *cyp450* genes were monitored by qRT-PCR (Figure 5.1). The relative expression of *pks* and *X22181* genes showed a significant regulation during grazing at 24hours, *pks* gene was overexpressed 2.6-fold (p-value = 0.0189) and *X22181* gene was overexpressed 9-fold (p-value = 0.0032) in grazing condition compared to control. However no significant effect of grazing was detected for *hsp70*, *ast6*, *vbpo*, and *cyp450* genes.



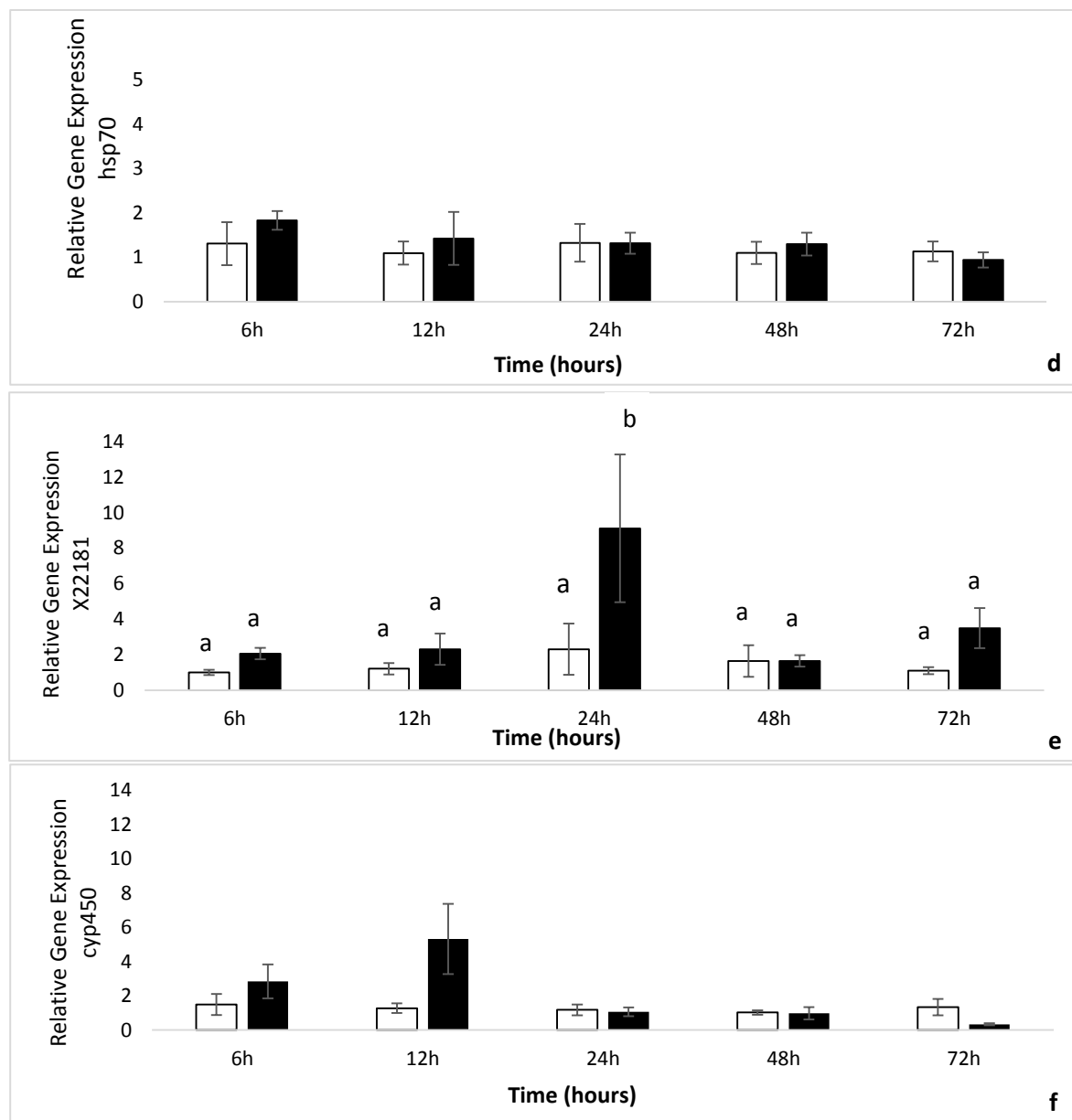


Figure 5.1: Relative gene expression in *Fucus vesiculosus* in controlled condition (white square) and exposed to grazing condition (black square) during 72 hours for a) *pksIII*, b) *ast6*, c) *vbpo* d) *hsp70*, e) *X22181*, f) *cyp450*. The expression of a gene is normalized to the geometric mean of the expression of 2 reference genes (*ef1 alpha*, *tua*) in the same algal sample and to the mean of its expression in the three control algae at each time point. Values represent means of five independent replicates and bars represent the SE. Letters indicate significant differences (LSMEANS 0.05).

Phenol contents:

Soluble phlorotannin contents ranged from 18 to 26 mg.g⁻¹ DW according to the phloroglucinol standard curve. An effect of grazing has been detected along the kinetics (Anova, p-value < 0.1) and an increment of 7 mg.g⁻¹ DW of phlorotannin contents was observed at 12 hours in the presence of grazers compared to the control (LSMEANS, p-value = 0.023) (Figure 5.2).

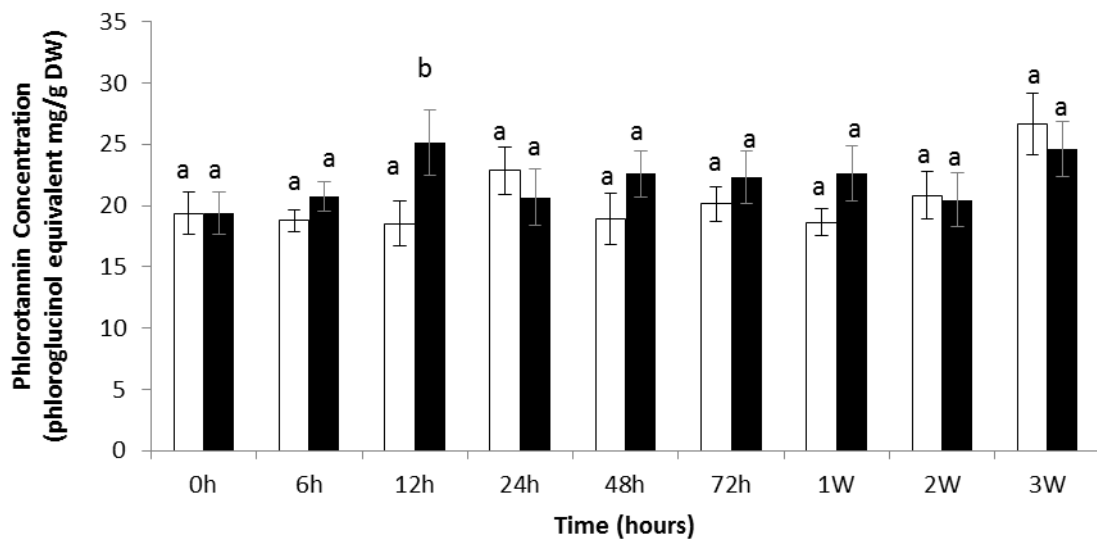


Figure 5.2: Quantification of total soluble phenol contents (mg equivalent phloroglucinol.g⁻¹ DW) in methanolic extracts in controlled conditions (white squares) and exposed to grazing (black square). Values represent means of five independent replicates and bars represent the SE. "a" and "b" letters indicate significant differences between control and grazing treatment (LSMEANS 0.05).

Discussion:

In *Fucus vesiculosus*, recent studies using global transcriptomics based on DNA microarrays or EST sequencing followed the gene expression changes upon grazing by the gastropod *Littorina littorea* ([Flöthe et al., 2014a](#)) or the crustacean isopod *Idotea baltica* ([Flöthe et al., 2014b](#)). These studies provided a large overview of gene categories that are regulated in response to the challenges with these two types of herbivores. However, activation of specific pathways involved in both defense and grazing tolerance remains to be investigated.

In this study, our choice was to show the expression variation of targeted genes implicated in global and specific responses to grazing during three days of treatment. The study of the expression of genes by qRT-PCR revealed that the *pksIII* gene encoding an homolog of EsiPKS1 Phloroglucinol Synthase ([Meslet-Cladiere et al. 2013](#)) was overexpressed 2.6-fold after 24 hours in grazing condition. As we can see in Figure 5.1a, there was a tendency toward the overexpression in grazing condition starting at 6 hours with a significant difference appearing after 24 hours. Regarding the expression of others genes, we also found an overexpression of the gene X22181 (unknown function) at 24 hours which has already been identified as a gene involved in grazing stress in a previous microarray study ([Flöthe 2014b](#)). However, the *hsp70* gene shows no differential expression in this study compared to our previous study on UV-B stress in *F.vesiculosus* ([Creis et al., 2015 submitted](#)), in which *hsp70* gene was overexpressed 4-fold at 12 hours and 8-fold at 24 hours of treatment, suggesting a stress dependent response. Concerning the *vbpo* gene encoding a vanadium bromoperoxidase, which can participate in the scavenging of ROS and in cross linking of phlorotannins to the cell wall ([Bitton et al. 2006 ; Salgado et al. 2009](#)), we observed a differential but not significant expression at 6 hours in grazing condition. As members of multigenic families, *ast* and *vbpo* genes need to be further investigated in order to better understand metabolic pathways of phlorotannin biosynthesis.

In our experiment, we sampled the total thallus even though generally only the surface is damaged by grazers. Therefore we took the risk of getting a potentially diluted defense pattern of *F. vesiculosus*, yet more consistent at a whole plant approach. After only 12 hours of grazing treatment (Figure 5.2), the pool of soluble phlorotannins slightly but significantly increased,

supporting the hypothesis of a rapid perception of eliciting signals followed by a quick mobilization of oligo- and poly-phenols at the whole thallus level. To date, we have no information about the number of PKS III genes and the sub-cellular localization the corresponding proteins in *Fucus vesiculosus*. In the same way, we focused only on the quantification of soluble phenols, and provided no information about both contents of insoluble (cell-wall) phlorotannins and excreted fractions. Consequently, no correlation can be established yet between the expression of the *pksIII* gene and the phloroglucinol turn-over in *F.vesiculosus*. Nevertheless, we evidenced the rapid activation of phlorotannin synthesis in *F.vesiculosus* in the presence of molluscan grazers, in agreement with previous studies and supporting the idea that herbivory may trigger the production of phlorotannins in the genus *Fucus* ([Targett and Arnold 1998](#)). In this context, an increase of phenol contents has been demonstrated in *Fucus distichus* after 2 weeks of grazing by *Littorina sitkana* ([Van Alstyne 1988](#)) and in *Fucus vesiculosus* after 2 weeks in the presence of *Littorina littorea* ([Yates and Peckol 1993](#)). In conclusion, phlorotannins seem to play an important role in interactions between algae and herbivores but more information is needed about the biosynthesis pathway of these metabolites to understand these mechanisms. To further investigate the mechanisms involved in defense responses, it will be necessary to develop and to characterize more precisely the biosynthesis pathway of phlorotannins and also the enzymes and metabolites implicated.

References

- Allen DJ, McKee IF, Farage PK, Baker NR (1997) Analysis of limitations to CO₂ assimilation on exposure of leaves of two *Brassica napus* cultivars to UV-B. *Plant, Cell Environ* 20:633–640.
- Van Alstyne K (1995) Comparison of three methods for quantifying brown algal polyphenolic compounds. *J Chem Ecol* 21:45–58.
- Van Alstyne K (1988) Herbivore Grazing Increases Polyphenolic Defenses in the Intertidal Brown Alga *Fucus Distichus*. *Ecology* 69:655–663.
- Amsler CD, Fairhead VA (2006) Defensive and Sensory Chemical Ecology of Brown Algae. In: Callow JA (ed) Inc. Adv. Plant Pathol. Academic Press, pp 1–91
- Apt KE, Clendennen SK, Powers DA, Grossman AR (1995) The gene family encoding the fucoxanthin chlorophyll proteins from the brown alga *Macrocystis pyrifera*. *Mol Gen Genet* 246:455–464.
- Apt KE, Grossman AR (1993) Characterization and transcript analysis of the major phycobiliprotein subunit genes from *Aglaothamnion neglectum* (Rhodophyta). *Plant Mol Biol* 21:27–38.
- Arnold TM, Targett NM (2000) Evidence for metabolic turnover of polyphenols in tropical brown algae. *J Chem Ecol* 26:1393–1410.
- Arnold TM, Targett NM (2003) To grow and defend: lack of tradeoffs for brown algal phlorotannins. *Oikos* 100:406–408.
- Arnold TM, Targett NM (1998) Quantifying in Situ Rates of Phlorotannin Synthesis and Polymerization in Marine Brown Algae. *J Chem Ecol* 24:577–595.
- Baldauf SL (2008) An overview of the phylogeny and diversity of eukaryotes. *J Syst Evol* 46:263–273.
- Berglin M, Delage L, Potin P, et al. (2004) Enzymatic cross-linking of a phenolic polymer extracted from the marine alga *Fucus serratus*. *Biomacromolecules* 5:2376–83.
- Bieza K, Lois R (2001) An *Arabidopsis* mutant tolerant to lethal ultraviolet-B levels shows constitutively elevated accumulation of flavonoids and other phenols. *Plant Physiol* 126:1105–15.
- Bischof K, Gómez I, Molis M, et al. (2006) Ultraviolet radiation shapes seaweed communities. *Rev Environ Sci Bio/Technology* 5:141–166.
- Bitton R, Ben-Yehuda M, Davidovich M, et al. (2006) Structure of algal-born phenolic polymeric adhesives. *Macromol Biosci* 6:737–46.
- Breton F, Cérantola S, Ar Gall E (2011) Distribution and radical scavenging activity of phenols in *Ascophyllum nodosum* (Phaeophyceae). *J Exp Mar Bio Ecol* 399:167–172.
- Cock JM, Sterck L, Rouzé P, et al. (2010) The *Ectocarpus* genome and the independent evolution of multicellularity in brown algae. *Nature* 465:617–21.

Partie 2 : Implication des phlorotannins dans la réponse aux stress biotiques et abiotiques chez *F.vesiculosus*

- Coleman R a., Ramchunder SJ, Moody a. J, Foggo a. (2007) An enzyme in snail saliva induces herbivore-resistance in a marine alga. *Funct Ecol* 21:101–106.
- Connan S, Goulard F, Stiger V, et al. (2004) Interspecific and temporal variation in phlorotannin levels in an assemblage of brown algae. *Bot Mar* 47:410–416.
- Davison IR, Pearson GA (1996) Stress tolerance in intertidal seaweeds. *J Phycol* 32:197–211.
- Deal MS, Hay ME, Wilson D, Fenical W (2003) Galactolipids rather than phlorotannins as herbivore deterrents in the brown seaweed *Fucus vesiculosus*. *Oecologia* 136:107–14.
- Fang G, Hammar S GR (1992) A quick and inexpensive method for removing polysaccharides from plant genomic DNA. *Biotechniques* 13:52–56.
- Flöthe CR, Molis M, John U (2014a) Induced resistance to periwinkle grazing in the brown seaweed *Fucus vesiculosus* (Phaeophyceae): molecular insights and seaweed-mediated effects on herbivore interactions. *J Phycol* 50:564–576.
- Flöthe CR, Molis M, Kruse I, et al. (2014b) Herbivore-induced defence response in the brown seaweed *Fucus vesiculosus* (Phaeophyceae): temporal pattern and gene expression. *Eur J Phycol* 49:356–369.
- Gomez I, Huovinen P (2010) Induction of Phlorotannins During UV Exposure Mitigates Inhibition of Photosynthesis and DNA Damage in the Kelp *Lessonia nigrescens*. *Photochem Photobiol* 86:1056–1063.
- Häder D, Figueroa FL (1997) Photoecophysiology of Marine Macroalgae. *Photochem Photobiol* 66:1–14.
- Harborne JB (1975) Flavonoid sulphates: A new class of sulphur compounds in higher plants. *Phytochemistry* 14:1147–1155.
- Henry BE, Van Alstyne KL (2004) Effects of uv radiation on growth and phlorotannins in *Fucus gardneri* (Phaeophyceae) juveniles and embryos. *J Phycol* 40:527–533.
- Hupel M, Lecointre C, Meudec A, et al. (2011a) Comparison of photoprotective responses to UV radiation in the brown seaweed *Pelvetia canaliculata* and the marine angiosperm *Salicornia ramosissima*. *J Exp Mar Bio Ecol* 401:36–47.
- Hupel M, Poupart N, Gall EA (2011b) Development of a new in vitro method to evaluate the photoprotective sunscreen activity of plant extracts against high UV-B radiation. *Talanta* 86:362–71.
- Jansen M a K, Martret B Le, Koornneef M (2010) Variations in constitutive and inducible UV-B tolerance; dissecting photosystem II protection in *Arabidopsis thaliana* accessions. *Physiol Plant* 138:22–34.
- Jormalainen V, Honkanen T, Koivikko R, Eränen J (2003) Induction of phlorotannin production in a brown alga: defense or resource dynamics? *Oikos* 103:640–650.
- Jueterbock A, Kollias S, Smolina I, et al. (2014) Thermal stress resistance of the brown alga *Fucus serratus* along the North-Atlantic coast: acclimatization potential to climate change. *Mar Genomics* 13:27–36.
- Koivikko R, Eränen JK, Loponen J, V. J (2008) Variation of phlorotannins among three populations of *Fucus vesiculosus* as revealed by HPLC and colorimetric quantification. *J Chem Ecol* 34:57–64.

Partie 2 : Implication des phlorotannins dans la réponse aux stress biotiques et abiotiques chez *F.vesiculosus*

- Koivikko R, Loponen J, Honkanen T, Jormalainen V (2005) Contents of soluble, cell-wall-bound and exuded phlorotannins in the brown alga *Fucus vesiculosus*, with implications on their ecological functions. *J Chem Ecol* 31:195–212.
- Lesser MP (1996) Acclimation of phytoplankton to UV-B radiation : oxidative stress and photoinhibition of photosynthesis are not prevented by UV-absorbing compounds in the dinoflagellate *Prorocentrum micans*. *Mar Ecol Prog Ser* 132:287–297.
- Lopes G, Sousa C, Silva LR, et al. (2012) Can phlorotannins purified extracts constitute a novel pharmacological alternative for microbial infections with associated inflammatory conditions? *PLoS One* 7:e31145.
- Maxime Hervé (2014) RVAideMemoire: Diverse basic statistical and graphical functions.
- Meslet-Cladiere L, Delage L, J.-J. Leroux C, et al. (2013) Structure/Function Analysis of a Type III Polyketide Synthase in the Brown Alga *Ectocarpus siliculosus* Reveals a Biochemical Pathway in Phlorotannin Monomer Biosynthesis. *Plant Cell* 25:3089–3103.
- Michel G, Tonon T, Scornet D, et al. (2010) The cell wall polysaccharide metabolism of the brown alga *Ectocarpus siliculosus*. Insights into the evolution of extracellular matrix polysaccharides in Eukaryotes. *New Phytol* 188:82–97.
- Nielsen HD, Brownlee C, Coelho SM, Brown MT (2003) Inter-population differences in inherited copper tolerance involve photosynthetic adaptation and exclusion mechanisms in *Fucus serratus*. *New Phytol* 160:157–165.
- Pavia H, Cervin G, Lindgren (1997) Effects of UV-B radiation and simulated herbivory on phlorotannins in the brown alga *Ascophyllum nodosum*. *Mar Ecol Prog Ser* 157:139–146.
- Pearson G, Hoarau G, Lago-Leston A, et al. (2010) An Expressed Sequence Tag Analysis of the Intertidal Brown Seaweeds *Fucus serratus*(L.) and *F. vesiculosus* (L.) (Heterokontophyta, Phaeophyceae) in Response to Abiotic Stressors. *Mar Biotechnol* 12:195–213.
- Pearson G, Lago-Leston A, Valente M, Serrão E (2006) Simple and rapid RNA extraction from freeze-dried tissue of brown algae and seagrasses. *Eur J Phycol* 41:97–104.
- Potin P, Bouarab K, Salaun J-P, et al. (2002) Biotic interactions of marine algae. *Curr Opin Plant Biol* 5:308–317.
- R Development Core Team (2010) R: A Language and Environment for Statistical Computing. R Found Stat Comput Vienna Austria 0:{ISBN} 3–900051–07–0.
- Ragan, Glombitza (1986) Phlorotannins, brown algal polyphenols. *Prog Phycol Res Round FE Chapman DJ (ed)* Biopress Ltd Bristol 129–241.
- Ragan MA (1976) Physodes and the Phenolic Compounds of Brown Algae. Composition and Significance of Physodes in vivo. *Bot Mar* 19:145–154.
- Renger G, Völker M, Eckert HJ, et al. (1989) On the mechanism of Photosystem II deterioration by UV-B irradiation. *Photochem Photobiol* 49:97–105.
- Roeder V, Collén J, Rousvoal S, et al. (2005) Identification of Stress Gene Transcripts in *Laminaria Digitata* (Phaeophyceae) Protoplast Cultures By Expressed Sequence Tag Analysis1. *J Phycol* 41:1227–1235.

Partie 2 : Implication des phlorotannins dans la réponse aux stress biotiques et abiotiques chez *F.vesiculosus*

Russell V. Lenth (2014) lsmeans: Least-Squares Means. R package version 2.11. <http://CRAN.R-project.org/package=lsmeans>.

S.Tugwell GMB (1992) Effects of Herbivore Gut Surfactants on Kelp Polyphenol Defenses Author (s): S . and G . M . Branch Published by : Ecological Society of America Effects of herbivore gut surfactants on kelp polyphenol defenses. Ecol Soc Am 73:205–215.

Salgado LT, Cinelli LP, Viana NB, et al. (2009) a Vanadium Bromoperoxidase Catalyzes the Formation of High-Molecular-Weight Complexes Between Brown Algal Phenolic Substances and Alginates. J Phycol 45:193–202.

Schoenwaelder MEA (2008) The Biology of Phenolic Containing Vesicles. Algae 23:163–175.

Scotto-Lavino E, Du G, Frohman M a (2006) 3' end cDNA amplification using classic RACE. Nat Protoc 1:2742–5.

Shibata T, Hama Y, Miyasaki T, et al. (2006) Extracellular secretion of phenolic substances from living brown algae. J Appl Phycol 18:787–794.

Stamp N (2003) Out Of The Quagmire Of Plant Defense Hypotheses. Q Rev Biol 78:23–55.

Steevensz AJ, Mackinnon SL, Hankinson R, et al. (2012) Profiling Phlorotannins in Brown Macroalgae by Liquid Chromatography-High Resolution Mass Spectrometry. Phytochem Anal 23:547–553.

Swanson AK, Druehl LD (2002) Induction, exudation and the UV protective role of kelp phlorotannins. Aquat Bot 73:241–253.

Tarakhovskaya ER (2013) Mechanisms of bioadhesion of macrophytic algae. Russ J Plant Physiol 61:19–25.

Targett NM, Arnold TM (1998) Minireview-predicting the effects of brown algal phlorotannins on marine herbivores in tropical and temperate oceans. J Phycol 34:195–205.

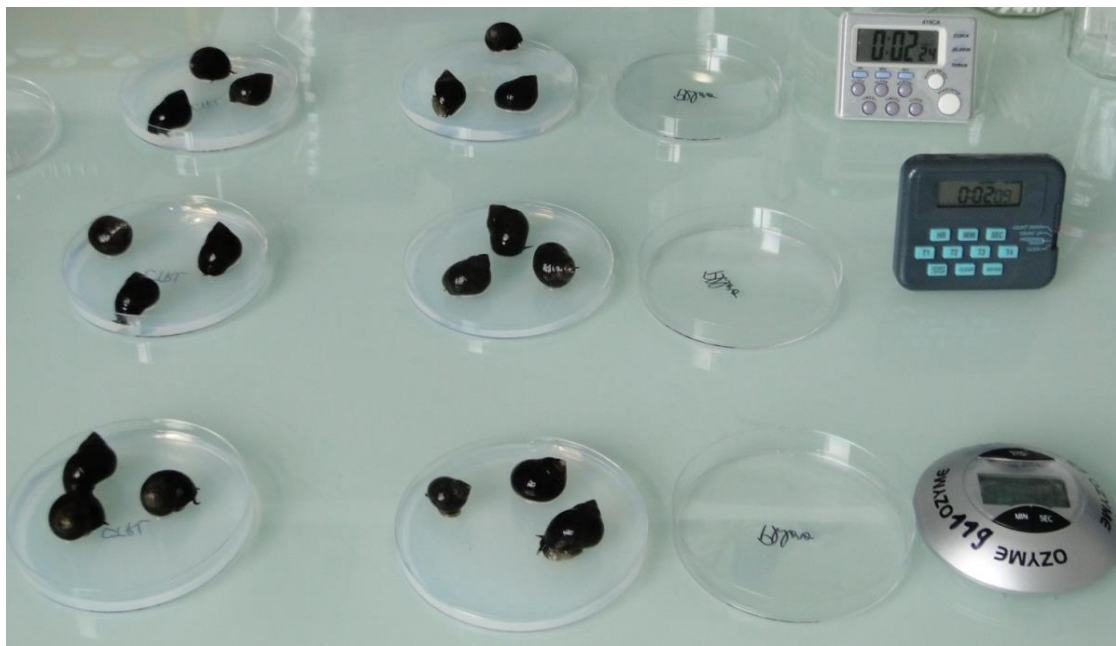
Wahl M, Jormalainen V, Eriksson BK, et al. (2011) Stress ecology in fucus: abiotic, biotic and genetic interactions. Adv Mar Biol 59:37–105.

Wang T, Jónsdóttir R, Liu H, et al. (2012) Antioxidant Capacities of Phlorotannins Extracted from the Brown Algae *Fucus vesiculosus*. J Agric Food Chem.

Yates JC, Peckol P (1993) Effects of nutrient availability and herbivory on polyphenols in the seaweed *Fucus vesiculosus*. Ecology 74:1757–1766.

Partie 2 : Implication des phlorotannins dans la réponse aux stress biotiques et abiotiques chez *F.vesiculosus*

Chapitre 6: Essai biologique : test de molécules d'intérêt sur le comportement et l'attachement au substrat des Littorines



Article en préparation

Chemical cues of algal origin determine creeping behavior, escape and retraction in the herbivorous periwinkle Littorina littorea

Florian Weinberger^{[a]*}, Melanie Schulz^[a], Emeline Creis^[b,c], Martin Zimmer^[a,d]

^aGEOMAR Helmholtz-Zentrum für Ozeanforschung, Marine Ecology Division, Düsternbrooker Weg 20, D-24105 Kiel, Germany

^bSorbonne Universités, UPMC Univ Paris 06, UMR 8227, Integrative Biology of Marine Models, Station Biologique de Roscoff, CS 90074, F-29688, Roscoff cedex, Brittany, France

^cCNRS, UMR 8227, Integrative Biology of Marine Models, Station Biologique de Roscoff, CS 90074, F-29688, Roscoff cedex, Brittany, France

*Author for correspondence: e-mail: fweinberger@geomar.de

Introduction

The activity of marine snails such as periwinkles has been studied since decades and is strongly affected by diurnal and tidal cycles ([Petpiroon & Morgan 1983](#), [Little 1989](#)). Littorinids spend most of the time attached to a substrate such as stones that provides good holding ground ([Newell 1958](#)). During periodic foraging excursions within a radius of 1.5 to 2 m ([Newell 1958](#), [Lauzon-Guay & Scheibling 2009](#)) they creep actively during 5 to 70 % of the time and browse the substrate for its suitability as food ([Norton et al. 1990](#)). The choice of potential food items is usually wide and may include microalgae and juvenile macroalgae, but also adult seaweeds. However, most species exhibit clear food preferences, which have been particularly well studied with *Littorina littorea* ([Lubchenco 1978](#), [Hunter 1981](#), [Watson & Norton 1983, 1985](#), [Barker & Chapman 1990](#)). Feeding cues that attract consumers of seaweed are often sugars that constitute the primary carbon storage compound during photosynthesis, such as glucose for consumers of green macroalgae ([Woodbridge 1978](#)) or mannitol for consumers of *F. vesiculosus* ([Weinberger et al. 2011](#)).

Together with other grazers, periwinkles often shape macroalgal communities ([Bertness et al. 2002](#), [Scheibling et al. 2009](#), [Griffin et al. 2010](#)). However, seaweeds are in most cases not undefended against this challenge and besides of structural and associational defense chemical defense against consumers is particularly prominent. Various compounds have been identified in the past that significantly reduce the palatability of seaweeds to consumers and in several cases an increased production of such compounds after enemy attack has been demonstrated, which strongly suggests that dynamic algal responses to increased feeding pressure are often possible ([Toth & Pavia 2007](#)).

Phlorotannins are the longest known example of algal chemical defenses against herbivores. They are polymers of phloroglucinol (1,3,5-trihydroxybenzene) that are particularly prominent in rockweeds, but also present in other brown seaweeds, such as kelps. Several reviews summarizing the chemistry of phlorotannins and their possible functions in seaweed-herbivore interactions and at the cellular level (for example, as UV shielding compounds) are available ([Arnold & Targett 2002](#), [Schoenwaelder 2002](#), [Arnold & Targett 2003](#), [Amsler & Fairhead 2005](#)).

([Geiselman & McConnell 1981](#)) reported for the first time that a herbivore, the periwinkle *Littorina littorea*, rejected artificial food that was made up from agar and contained phlorotannins which had been extracted from the rockweeds *Fucus vesiculosus* and *Ascophyllum nodosum*. Since then, numerous studies have explored the possible role of phlorotannins for the defenses of brown seaweeds. Phlorotannins deterred consumers in many studies and it was also demonstrated that herbivore attack or simulated herbivory may result in an increased presence of phlorotannins in brown seaweeds ([Pavia et al. 1997](#), [Pavia & Toth 2000](#), [Borell et al. 2004](#), [Jormalainen et al. 2007](#)). In particular molluscs and fish were often reported to be deterred by this group of compounds ([Targett & Arnold 1998](#)).

Phlorotannins are a chemically heterogeneous group of compounds that includes small as well as relatively large components with different degrees of polymerisation, hydroxylation and substitution. Further, different assays for the quantification of phenols often detect different aromatic and phenolic compounds. For example, the widely used Folin-Ciocalteu- (hereafter FC-) assay – based upon a color reaction of phosphotungsten-polymolybdic acid with hydroxylated aromatic compounds in the presence of lithium sulfate and at alkaline conditions ([Folin & Ciocalteu 1927](#)) – is relatively unspecific and detects not only phlorotannins and phloroglucinol, but also proteins (precisely aromatic / phenolic amino acids) and some other reactive compounds ([Van Alstyne 1995](#)). In contrast, the radial diffusion assay (hereafter RDA) – widely used in terrestrial ecology and generally based upon complex formation between a standard protein such as BSA and tannins or tannic acid ([Hagerman & Butler 1978](#)) – has been reported to be more selective among brown algal phenols: Complex formation between BSA and phlorotannins can be due to hydrogen bonding, covalent bonding after spontaneous oxidation or hydrophobic interactions and is highly affected by the specific conditions employed during the assay ([Tugwell & Branch 1992](#), [Stern et al. 1996](#)). Phloroglucinol is not detected by the RDA-method (own unpublished observations), suggesting that this assay selects to some extend for phlorotannins with high molecular weight.

Given that the molecular structure of a compound usually determines its biological effects different impacts of the various phlorotannins upon algal palatability may be expected. Nonetheless, the overwhelming part of all studies addressing the ecological role of

phlorotannins so far treated these compounds as a group, which is perhaps mainly due to two reasons: (i) although phlorotannins are easy to extract their preparative separation for use in bioassays is still far from the routine and (ii) many of the consumers that are deterred by phlorotannins are truly herbivorous and they largely reject artificial food. The second point is also true for periwinkles: consumption of agar-based artificial food as described by [Geiselman & McConnell, 1981](#) was extremely rarely observed in our own studies with *L. littorea*. In this light direct tests of the palatability of isolated phlorotannins or any other potential deterrents of these consumers appear as a challenge and new alternative bioassays are required.

Ecological theory predicts that induced or activated defenses against consumers should primarily evolve if the target organism is motile and can be deterred ([Tiffin et al. 2006](#)). Corresponding with this model feeding attacks on *Ascophyllum nodosum* by *Littorina obtusata* induced not only increased phlorotannin production in the alga and reduced consumption by the herbivore ([Pavia & Toth 2000, Borell et al. 2004](#)), but also an increased tendency for escape and dispersal in the consumer: *L. obtusata* moved significantly faster on herbivore-induced than on uninduced *A. nodosum* tissue ([Borell et al. 2004](#)). Further, *L. littorea* and other periwinkles have been reported to be deterred or attracted by the olfactory or gustatory characteristics of seaweeds and their exudates ([Woodbridge 1978, Watson & Norton 1983, Imrie et al. 1989, Shumway et al. 1993](#)). Those reports incited us to investigate whether creeping and escaping behaviour may be used as an indicator of the deterrence of marine herbivorous snails by seaweed and seaweed-derived compounds, using the *Littorina littorea*-*Fucus vesiculosus* interaction as a model. We hypothesized that *L. littorea* would not only consume less of relatively strongly defended *F. vesiculosus* specimens, but would also try to escape from them, primarily through directed creeping or - in extreme cases – through retraction into the shell and thereby detachment. In the intertidal and upper subtidal behaviour of the second type may be expected to result in a successful separation of snail and alga in most of the cases, given that both are frequently moved by currents and waves. To test those hypotheses *F. vesiculosus* was in a first step experimentally manipulated, in order to obtain specimens that were differently palatable to *L. littorea*. Two different approaches were used: (1) exposure to *L. littorea* grazing was expected to induce chemical defenses in *F. vesiculosus* ([Rohde et al. 2004](#)) and (2) exposure

to UV-B radiation was expected to induce phlorotannin production and thereby possibly reduced palatability ([Deal & Hay 1996](#), [Pavia et al. 1997](#)). It was then tested whether *L. littorea* exhibited different escaping behaviour toward those algal specimens. In a second step the escaping behaviour of *L. littorea* from substrates containing extracts of *F. vesiculosus* as well as phloroglucin (#and mannitol – still to be realized) was analyzed, using a novel bioassay.

Material and methods

Fucus vesiculosus L. was collected at Hubertsberg (N54°23.073' E10°30.864') and at Bülk (N54°27.274' E10°11.869') at several occasions between 2005 and 2010, brought to the laboratory within 1 h and immediately used as described below. *Littorina littorea* L. was collected at the same site in Bülk and at Mönkeberg (N54°21.141' E10°10.660) at several occasions between 2009 and 2014. A hole gauge was used to select animals of 10 to 16 mm of diameter, which were maintained in aerated aquaria containing seawater from the Kiel Fjord (at least one exchange of medium per d).

Experimental manipulation of phenols in *F. vesiculosus* tissue.

In spring 2009, two subsequent experiments were conducted that aimed at manipulating the phlorotannin contents of *F. vesiculosus* through herbivory and treatment with UV-B, respectively. In the herbivory experiment, 14 individual thalli of 30 g fresh weight were placed separately into aquaria (3 L) with permanent seawater and air supply. They were incubated in a climate room at 15 °C and exposed to artificial cool white light (75 µmol m⁻² s⁻¹; day:night cycle of 14:10 h). Between 10 and 20 individuals of *L. littorea* were added into half of these aquaria, so that each aquarium contained approximately 1 g of periwinkle body DW, which could be estimated from the shell diameter, using a previously determined regression formula between both measures ([Hammann et al. 2013](#)). To prevent *L. littorea* from escaping, all aquaria (also those containing no periwinkles) were covered with mesh wire. After 7 d of incubation, all algae were weighed again to verify that consumption by *L. littorea* had happened. Immediately afterwards the creeping activity of *L. littorea* on all specimens was investigated (see below). The algae were then conserved at -20°C and concentrations of phenols were quantified (see below).

In the UV-B experiment, 20 specimens of *F. vesiculosus* were incubated for two weeks under the same conditions as described above, but without periwinkles. Instead, half of the aquaria were – in addition to the common treatment with cool white light – exposed to broad band UV-B radiation (intensity?) for 12 h d⁻¹. For this purpose a TL 40W/12RS SLV tubular fluorescent lamp (Philips Deutschland GmbH, Hamburg) – emitting light in the wave length range between 280 nm and 400 nm – was placed in a distance of 10 cm above the aquaria. As after the feeding experiment the creeping activity of *L. littorea* on all algal specimens was immediately investigated (see below), while phenols were quantified after conservation at -20°C (see below).

Quantification of phenols and mannitol.

Phenolic compounds and mannitol were extracted from freeze-dried and ground *F. vesiculosus* with 70 % acetone for 1 h. FC-phenols were quantified spectrophotometrically according to (Zhang et al. 2006), using reagents from Sigma-Aldrich (#City) and phloroglucinol as standard. RDA-phenols were quantified following [Bärlocher & Graça \(2005\)](#), using tannic acid (#Hersteller, Stadt) as standard. Of each sample 72 µl were pipetted into wells that had been punched out (3 mm diameter) of bovine serum albumin (#Hersteller, Stadt) (BSA)-containig (0.1 %) agarose gel plates and incubated for 4 days at 20 °C. Afterwards, the surface area of the whitish phenolic-protein complexes resulting from protein-precipitation around the wells was measured and compared to tannic acid-treated standard wells. Mannitol was quantified according to ([Vas'kovskii & Isai 1972](#)), with the difference that periodate oxidation was stopped after 10 s. In order to allow for direct comparisons of concentrations of phenols and mannitol among algal samples and artificial substrates all concentrations were related to biomass volumes. Depending on air exposure the water tissue content of living *F. vesiculosus* varies by a factor of 5 ([Pearson et al. 2000](#)) and the DW content of Fucoids can go up to 30 % ([Kremer 1975](#)). In the atidal Baltic Sea, *F. vesiculosus* is most of the time fully hydrated and a dry weight content of 10 % was therefore used for the conversion of dry weight concentrations into biomass volume concentrations.

Creeping assays with living algae.

Creeping assays with living *F. vesiculosus* were conducted at 15°C with periwinkles and algae that were acclimatized to the same temperature. Single algal specimens were cut into sections of 9 cm and diametrically spread in different angles into a Petri dish (diameter: 9 cm) so that the bottom of the dish was fully covered with algal tissue. A single periwinkle exhibiting creeping activity was then centrally placed onto the tissue and the Petri dish was covered with a specially made lid that was marked with a grid of square centimetres. The position of the periwinkle on the algal tissue was recorded every ten minutes during the course of 30 min. On the basis of these data, the distance covered by the periwinkles and their crawling velocity was calculated. In order to prevent damage from desiccation each algal specimen was tested immediately after it had been removed from its aquarium.

Creeping and attachment assays with algal extracts and pure compounds.

To test the effect of algal metabolites upon the behaviour of *L. littorea* without the possibly confounding effect of other factors such as texture 50 individuals of *F. vesiculosus* from Hubertsberg were freeze-dried and ground. Of the resulting powder 20 g were extracted over night in 200 mL of 70 % acetone. After filtration and evaporation of the solvent 2285 mg of crude extract - containing 578 (SE: ± 29; n = 6) mg FC-phenols, 22 mg RDA-phenols and 74.4 (SE: ± 1.9, n = 6) mg mannitol - remained and were diluted in 5 ml dimethylsulfoxide (DMSO). To prepare agar substrates 750 mg of agar (Carl Roth, Karlsruhe, Germany) were mixed with 25 ml of Baltic Sea water in a beaker and boiled in a microwave stove for 3 min at 800 W. This procedure resulted not only in a complete dilution of the agar, but also in evaporation of approximately 5.5 ml of water. After cooling to 40 °C 500 µl DMSO containing various aliquots of the *F. vesiculosus* extract stock solution were added and suspended with a spatula. Thus, all agar substrates contained 5 % DMSO, but extract stock solution aliquots ranging from 0 to 500 µl. The highest tested concentration of extract (228.5 mg, representing 2 g of algal DW) approximately represented the natural concentration in *F. vesiculosus* if one assumes the DW content of fully hydrated specimens to be 10 % of the fresh weight. After gelification a single periwinkle that exhibited creeping activity was centrally placed on the agar substrate and its velocity was recorded as described above. Periwinkles that occasionally escaped from the algal tissue by creeping onto the inside of the lid were placed back into the center of the Petri dish.

To investigate the readiness of *L. littorea* to attach to substrate containing *F. vesiculosus* extract at various concentrations Petri dishes containing agar gel were prepared as described above and ten periwinkles were placed upon the agar. Most snails immediately started to explore the substrate. After 3 min the Petri dishes were turned by 180° (see video online supplement) and the number of attached and unattached snails was recorded. This procedure was repeated two times with each Petri dish, using each time naïve periwinkles.

In addition to crude extracts from *F. vesiculosus* phloroglucin (# Hersteller) was also tested at various concentrations in creeping and attachment assays. The methodology was basically as described above, but instead of algal extract phloroglucin was mixed into the agar substrate. The compound was diluted in Methanol (300 mg ml-1) and added in different amounts into the agar prior to gelification. The added aliquot of stock solution was complemented with pure solvent so that the final amount of methanol added into the mixture was always 3.3 % - a concentration that did not affect *L. littorea* when phloroglucin was absent (see online video supplement).

Statistics.

Data were plotted and analyzed using Prism 4 (GraphPad Software Inc, Golden, Co., and U.S.A.) and Statistica 8.0 (#). The t-test for heteroscedastic independent samples was employed to compare data obtained with grazed and ungrazed and with UV-B-treated and untreated *F. vesiculosus*. The same test was also used to compare creeping velocities and escape frequencies among agar substrates containing and not containing algal extract or phloroglucin. The Mantel-Haenzel method as described in ([Fisher & Van Belle 1993](#)) was used to calculate the odds for preferential attachment of periwinkles to substrates containing extract or phloroglucin relative to substrates containing no such supplements: Ratios of attached and unattached periwinkles were calculated for treatments and the corresponding control treatments and divided. Odds ratios that are larger or smaller than 1 indicate a tendency of periwinkles for preferential attachment to treatment substrates or control substrates, respectively. Odd ratios may be considered as significantly different from 1 if 1 is not included into their 95 % confidence interval ([Fisher & Van Belle 1993](#)).

Statistical modelling by stepwise regression – using the "step"-procedure in R (#) that identifies best fitting models based upon the Akaike information criterion - was conducted to analyze the interactive effect of deterrents and feeding cues upon the retraction behaviour of *L. littorea*.

Results

Littorina littorea visibly consumed *F. vesiculosus* during 7 d of incubation. Due to this activity, the initial algal fresh weight was on average reduced by 5 % (SE: $\pm 3\%$). Ungrazed specimens of *F. vesiculosus*, in contrast, increased their weight in the same period by 30 % (SE: $\pm 3\%$). Major differences were observed in the crawling velocity of *L. littorea* on different specimens of *F. vesiculosus* (Figure 6.1 A). However, these differences were not significant when previously grazed and ungrazed algal individuals were compared as substrates (t-test, $p = 0.522$). Similarly, *L. littorina* crawled at no significantly different speed on UV-B treated *versus* untreated specimens of *F. vesiculosus* (t-test, $p = 0.239$). By contrast, the speed on untreated controls was significantly reduced in the UV-B experiment as compared to the feeding experiment (t-test, $p = 0.021$). Also the content of *F. vesiculosus* in FC-phenols (Figure 6.1 B) did not vary significantly among grazed and ungrazed specimens (t-test, $p = 0.12$) or among individuals that were or were not treated with UV-B (t-test, $p = 0.547$), while control specimens used in the feeding experiment had a significantly higher content in phlorotannins than control specimens used in the UV-B experiment (t-test, $p = 0.017$). Likewise, the content of *F. vesiculosus* in RDA-phenols (Figure 6.1 C) differed in no case significantly among controls and treatments (t-tests, $p = 0.811$ and $p = 0.841$), while a major difference was detected among control specimens of *F. vesiculosus* used in the feeding experiment and in the UV-B experiment (t-test, $p < 0.0001$).

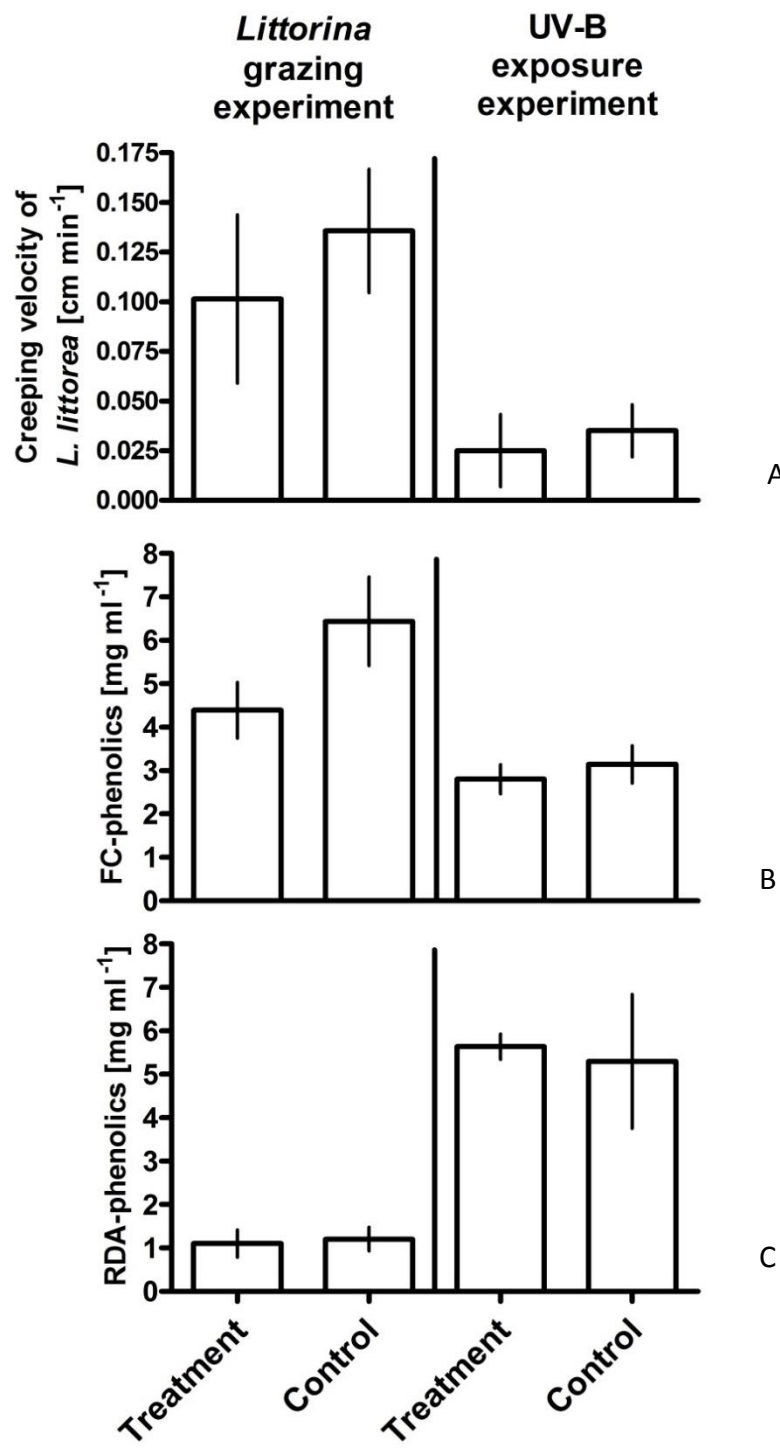


Figure 6.1: Crawling velocity of *L. littorea* on specimens of *F. vesiculosus* that were previously exposed and unexposed to grazing by *L. littorea* or to UV-B (A), as well as Folin-Ciocalteu phenols (B) and RDA-phenols (C) in the same algal individuals. Average +/- SE, n = 7 (Littorina experiment) and n = 10 (UV-B experiment).

Regression analysis detected a significant non-linear relationship between creeping velocity and FC-phenols (Tab. 6.1).

*Table. 6.1: Analysis of non-linear regression between FC phenols and creeping velocity of *L. littorea* on living specimens of *F. vesiculosus*. $r^2 = 0.3998$, $p < 0.0001$.*

	SS	df	MS	F	p
Intercept	0.023690	1	0.023690	6.11235	0.020016
FC-phenols	0.065012	1	0.065012	16.77404	0.000344
FC-phenols ^2	0.049268	1	0.049268	12.71189	0.001380
Error			0.104645	27	0.003876

In the concentration range below 7.5 mg.ml⁻¹ the creeping velocity increased with increasing content of FC-phenols (Figure 6.2A), and it was exclusively due to a single sample that was much higher in FC phenols and incited a relatively low creeping velocity in *L. littorea* that a polynomial function of second order better fitted the complete data set than a linear function (linear regression: $r^2 = 0.1401$, $p = 0.029$). A significant negative correlation between RDA-phenols and FC-phenols was detected when data originating from both experiments were merged ($r^2 = 0.3386$, $p = 0.0036$). However, separate analysis of the two experiments detected no significant correlations (Figure 6.2 B). The creeping velocity of *L. littorea* on *F. vesiculosus* specimens used in the two experiments was not significantly correlated with their content in RDA-phenols, neither when data from both experiments were analyzed separately nor when they were regarded together (data not shown).

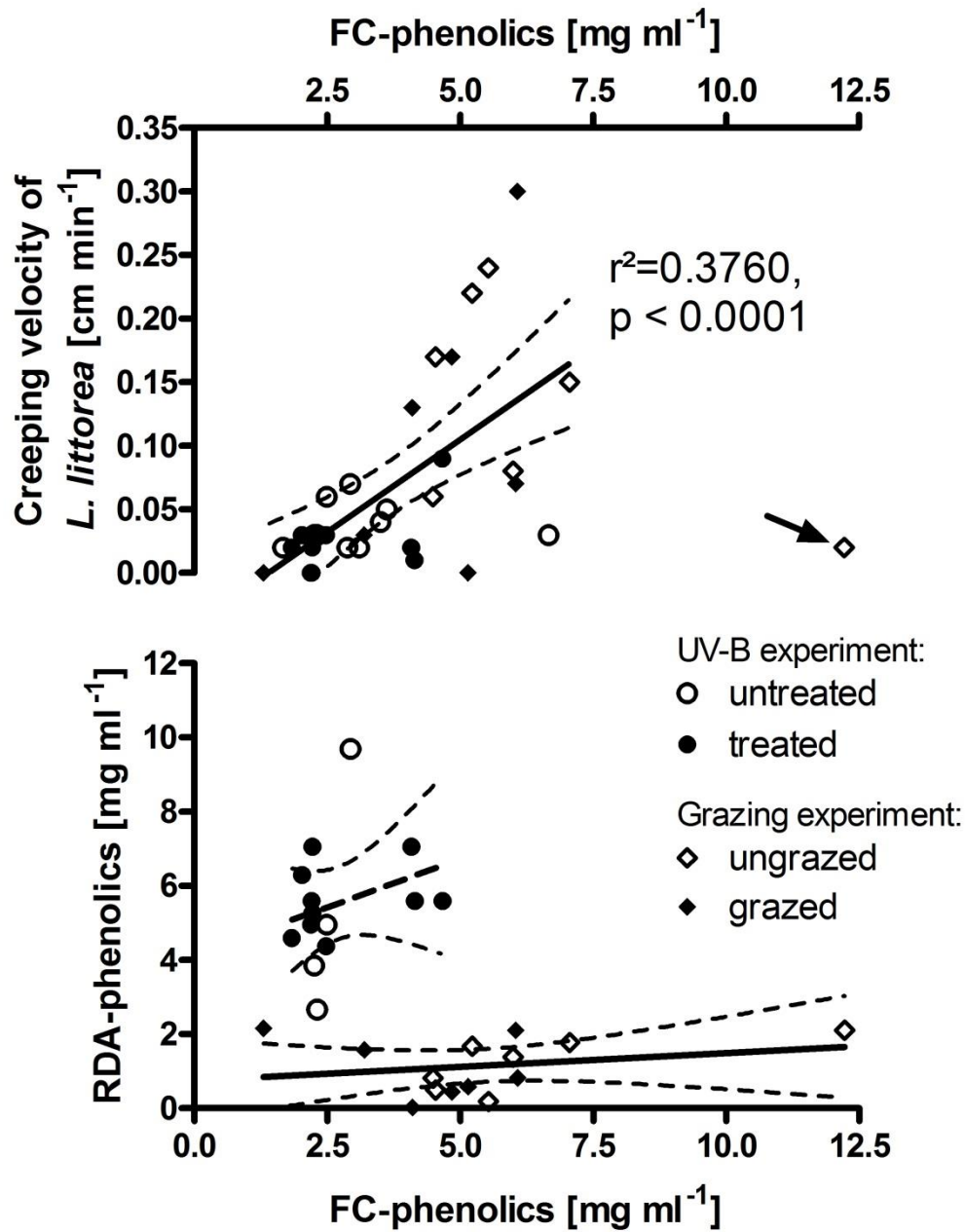


Figure 6.2: Relationships between FC phenols in *F. vesiculosus* individuals and (A) creeping velocity of *L. littorea* and (B) RDA phenols in the same specimens. Prior to analysis the algae were exposed to *L. littorea* grazing or to UV-B radiation, while control algae were unexposed. Lines represent best fitting linear functions with 95 % confidence intervals: (best fit with the full data set except of one outlying data point (arrow) in (A) and best fits with separate data from the UV-B and grazing experiments in (B)). See text for more details.

Similar as with living *F. vesiculosus*, the creeping behaviour of *L. littorea* on agar substrate was also affected in a non-linear dose-dependent manner by acetone extracts of *F. vesiculosus* that were rich in phenols (Figure 6.3 A). Compared to controls without extract, a significantly increased crawling velocity was observed when the substrate contained extract at concentrations that represented 1 % and 3 % of the natural concentration, corresponding with 29 to 87 µg FC-phenols per ml, respectively. With higher contents of extract *L. littorea* increasingly responded with shorter periods of crawling and longer periods of inactivity, which resulted in lower mean creeping velocities. Escapes of *L. littorea* from the agar substrate happened generally rarely and their frequencies were not significantly different among treatments (Figure 6.3 B). Agar containing extract from *F. vesiculosus* at natural concentration (corresponding with 2.89 mg FC-phenols per ml) deterred *L. littorea* to such a degree that a significantly increased number of periwinkles retained from attachment to the substrate (Figure 6.3 C). In contrast, agar containing lower than natural concentrations of this extract had no significant effect upon snail attachment.

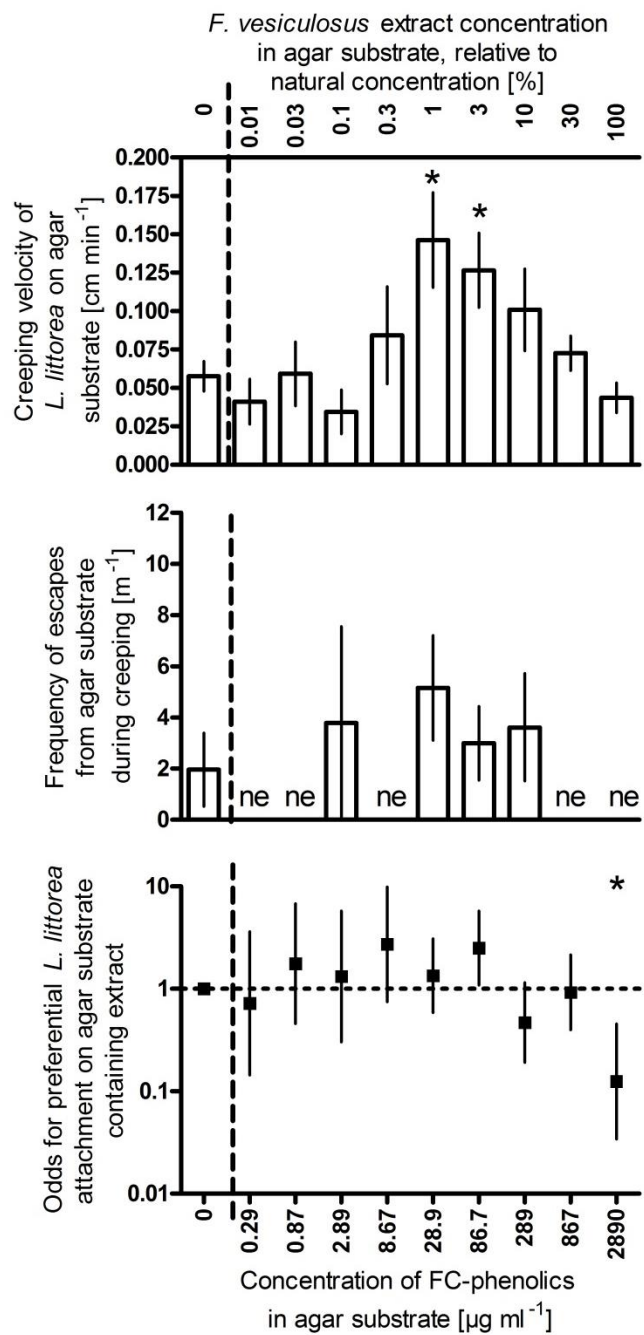


Figure 6.3: Crawling velocity (A), frequency of escapes (B) and odds variation for attachment (C) of *Littorina littorea* on agar substrate containing crude acetone extract from *F. vesiculosus* at natural and various subnatural concentrations. Error bars indicate standard errors ($n = 10$ to 30) in (A) and (B) and 95% confidence intervals in (C). Asterisks mark treatments that resulted in significantly different effects compared to the control without extract ($p < 0.05$; t-test in (A) and, Mantel-Haenzel-test in (C)). ne = no escape observed.

The concentration of *L. littorea*-deterring compounds in *F. vesiculosus* may potentially vary with factors such as season or consumer density. For this reason, more extracts were tested. They were prepared from 35 algal individuals that had been collected at Hubertsberg between March 2005 and March 2007 in monthly intervals, lyophilized and stored at -20°C. The extracts were examined with respect to their content in FC-phenols, RDA-phenols and mannitol, as well as their retraction-inducing effect upon *L. littorea* at natural and 30 % natural concentration. At natural concentration, all extracts consistently reduced the probability of *L. littorea* attachment to the substrate (Figure 6.4). In contrast, this was only observed with some of the extracts when they were present at 30 % natural concentration, suggesting that the necessary concentrations of bioactive compounds were not always reached under this condition. Significant correlations between the probability of attachment and the concentrations of FC-phenols and RDA-phenols in substrates containing extract at 30 % natural concentration were detected, which was not the case with mannitol (Figure 6.4). However, stepwise regression analysis identified a model as the best predictor of attachment probability that assigned significant effects not only to concentrations of FC-phenols and RDA-phenols and to the interaction of FC- and RDA-phenols, but also to mannitol (Tab. 6.2A). Mannitol was also required as a (non-significant) factor in the second best fitting model which assigned significant linear and non-linear effects to FC-phenols and did not include RDA-phenols (Tab. 6.2B).

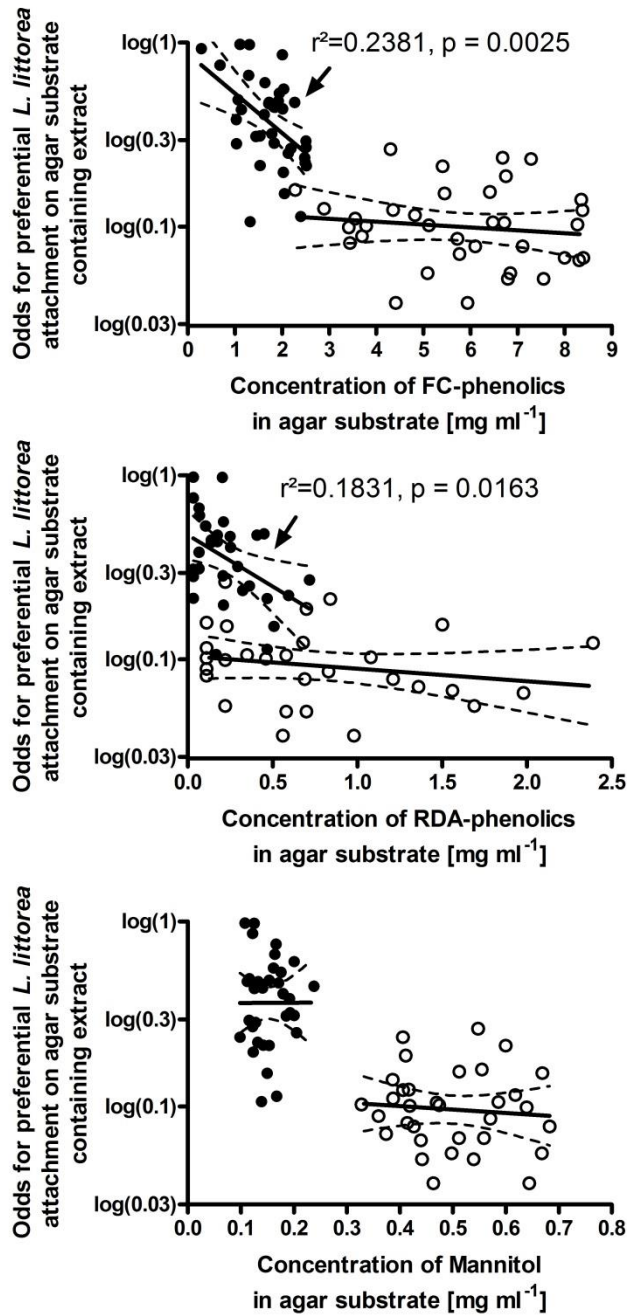


Figure 6.4: Odds for attachment of *Littorina littorea* on agar substrate containing crude acetone-MeOH-extracts from *F. vesiculosus* with different contents in FC phenols, RDA phenols and mannitol, relative to agar substrate containing no extract. All extracts were tested at natural (○) and 30 % natural (●) concentration. Lines represent best fitting linear functions with 95 % confidence intervals; r^2 is indicated for significant fits. See text for further details.

*Table. 6.2: Stepwise regression of FC phenols, RDA phenols and mannitol in extracts of *F. vesiculosus* at natural and 30 % natural concentration and odds for attachment of *L. littorea* to agar substrates containing those extracts. Shown are the two best fitting models.*

(A) Adjusted $r^2 = 0.6383$, $p < 0.0001$.

	SS	df	MS	F	p
Intercept	0.130612	1	0.130612	2.662163	0.108373
FC-phenols (1)	0.458329	1	0.458329	9.341784	0.003429
RDA-phenols (2)	0.198781	1	0.198781	4.051617	0.048946
Mannitol	0.240525	1	0.240525	4.902455	0.030907
(1)*(2)	0.240054	1	0.240054	4.892848	0.031065
Error	2.747484	56	0.049062		

(B) Adjusted $r^2 = 0.6338$; $p < 0.0001$

	SS	df	MS	F	p
Intercept	0.000234	1	0.000234	0.004743	0.945314
FC-phenols	0.478205	1	0.478205	9.708752	0.002761
FC-phenols ²	0.278456	1	0.278456	5.653357	0.020469
Mannitol	0.129571	1	0.129571	2.630613	0.109816
Error	3.103069	63	0.049255		

To test the validity of those models, effects of phloroglucinol (#and mannitol – still missing) upon the behaviour of *L. littorea* were investigated. Similar effects as after application of acetone extract were also observed when phloroglucinol was embedded into the agar substrate. The periwinkles responded with significantly increased creeping velocities when the substrate contained 0.3 or 1 mg of phloroglucinol per ml (Figure 6.5 A). At a concentration of 3 mg ml⁻¹ phloroglucinol, the creeping velocity was at a similar level as in controls that only contained agar. However, at the same concentration the frequency of escapes from the substrate per m creeping distance was significantly increased – *L. littorea* obviously tried to escape in a more directed way (Figure 6.5 B). No creeping activity was observed on substrates containing phloroglucinol at 10 mg ml⁻¹. After short examination, the periwinkles obviously avoided all contact with the substrate (see video in online supplement 1). They were therefore unable to escape by creeping (Figure 6.5 B) and none of the tested periwinkles attached to the substrate. Thus, the probability of attachment to the substrate was strongly reduced (Figure 6.5 C). Significantly, but

less severely reduced attachment to the substrate was also observed at phloroglucinol concentrations of 1 and 3 mg ml⁻¹ (Figure 6.5C).

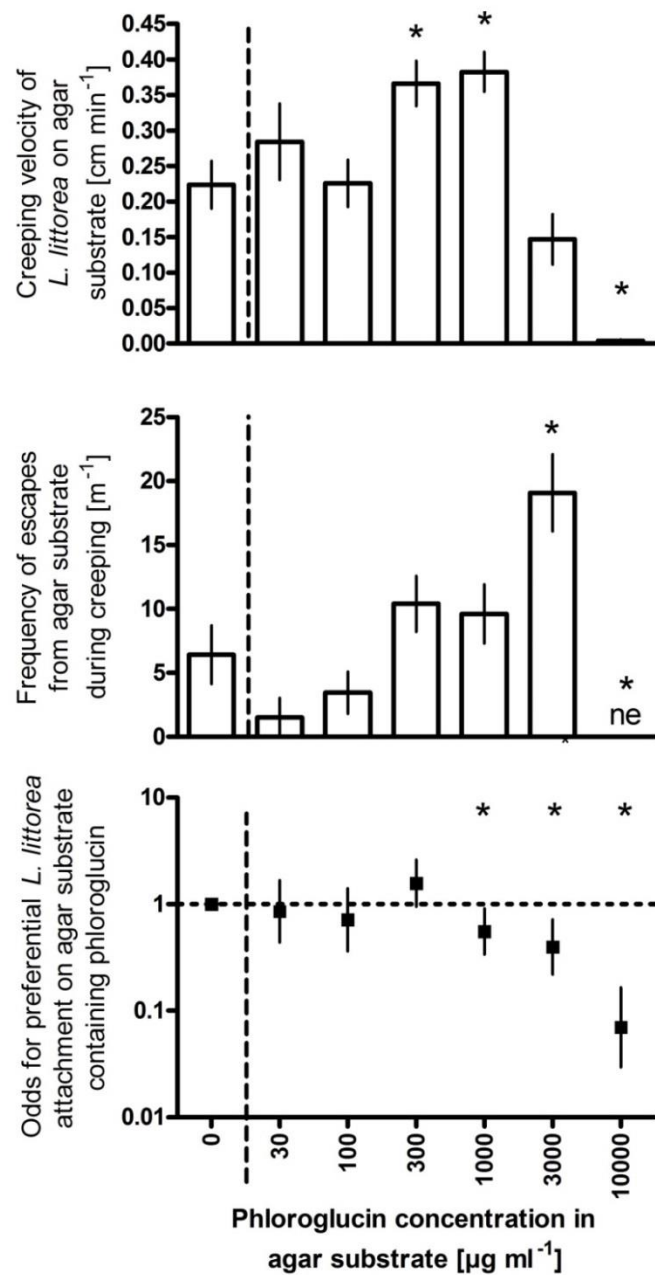


Figure 6.5: Crawling velocity (A), frequency of escapes (B) and odds for attachment (C) of *Littorina littorea* on agar substrate containing phloroglucinol at various concentrations. Error bars indicate standard errors ($n = 10$ to 30) in (A) and (B) and 95% confidence intervals in (C). Asterisks mark treatments that resulted in significantly different effects compared to the control without extract ($p < 0.05$; t-test in (A) and (B), Mantel-Haenzel-test in (C)). ne = no escape observed.

Include here results for mannitol...

Discussion

Obviously the natural concentrations of FC-phenols, RDA-phenols and mannitol in *F. vesiculosus* vary both individually and over time. Variations by factors of 4, 22, and 2, respectively, were detected among specimens that were collected at the same site at different times of the year (Figure 6.4). Even on the same day, considerable variation was observed (Figure 6.1). However, neither herbivory nor UV-B affected the concentration of those compounds. Corresponding with ([Scott & Marsham 2006](#)) - but not ([Rohde et al. 2004](#)) - grazing by *L. littorea* resulted in no significant modification of the palatability of *F. vesiculosus* for this snail. Likewise, both RDA-phenols and FC-phenols were unaffected by grazing, as well as by treatment with UV-B, suggesting that the production of polyphenols in *F. vesiculosus* may be overall less dynamic than in kelps or in *A. nodosum*. Nonetheless, the natural variability of phenols and mannitol in *F. vesiculosus* allowed us to investigate the interactive effect of these compounds upon the behaviour of *L. littorea*.

The content of *F. vesiculosus* in FC-phenols and RDA-phenols did not necessarily correspond, probably due to the different selectivity of both assays ([Van Alstyne 1995, Stern et al. 1996](#)). RDA-phenols were in most cases less concentrated than FC-phenols, but the inverse was also occasionally observed. Thus, RDA-phenols were not simply a fraction of FC-phenols, although considerable overlap between both detection methods must be assumed. We expected that concentrations determined with both assays might potentially not correlate to the same degree with the biological effects exhibited by *F. vesiculosus* extracts, as different molecular structures of phlorotannins should render different biological effects ([Geiselman & McConnell 1981](#)). This turned out to be true: FC-phenols were the most significant factor both in the best- and in the second best-fitting statistical model for prediction of *L. littorea* attachment. In contrast, RDA-phenols were less significant in the best fitting model and not required in the second best fitting model.

The deterrent effect of phenols upon *L. littorea* was confirmed in experiments with phloroglucinol. The compound clearly affected the behaviour of *L. littorea* in our experiments in a dose-dependent manner. This generally corresponds with (Geiselman & McConnell 1981), who reported that *L. littorea* increasingly refused to eat artificial agar-based food when its phloroglucinol content increased from 10 µg.g⁻¹ (no effect) to 5000 µg.g⁻¹ (75 % reduction). In our experiments, the behaviour of *L. littorea* was significantly affected at 300 µg.ml⁻¹ - a concentration which reduces palatability by approximately 40 % (Geiselman & McConnell 1981)- or more. At 300 µg.ml⁻¹ the snails increased their creeping velocity and at a tenfold higher concentration they exhibited a clearly increased tendency to detach from the substrate, which resulted in reduced creeping velocity. At the same concentration, the probability of escapes was approximately doubled. A further concentration increase to 10000 µg.ml⁻¹ deterred the snails to such a degree that they avoided any contact with the substrate.

A similar pattern as with substrates containing phloroglucin was also observed with substrates containing algal extract. However, *L. littorea* exhibited a ten times higher sensitivity toward phlorotannins than toward phloroglucinol, as its creeping velocity increased already significantly when the concentration of FC-phenols was 30 µg.ml⁻¹. Given that the FC assay tends to overestimate phlorotannins due to a limited specificity (Van Alstyne 1995), this discrepancy may probably not result from underestimation. Much rather, the phenols present in *F. vesiculosus* extract appear as more efficient signals than phloroglucinol. The palatability of fractionated polyphenols from *F. vesiculosus* to *L. littorea* was studied by (Geiselman & McConnell 1981) and the most active fractions – soluble in acetone, which was used as solvent in our study - were also 10 times more efficient than phloroglucinol. Thus, the creeping assay conducted by us features a similar sensitivity as direct feeding assays, while it is considerably faster (some hours versus 1 week) and overall probably easier to conduct.

Similar as in the interaction between *A. nodosum* and *L. obtusata* (Borell et al. 2004)- and corresponding with our observations with artificial substrates - *L. littorea* also responded with an increasing velocity when it crept on living specimens of *F. vesiculosus* with increasing content of phenols. This tendency was significant in the concentration range up to 7.5 mg.ml⁻¹. Thus, it occurred at considerably (approximately 100 times) higher concentrations than in artificial

substrates, which is probably due to the lower apparentness of phlorotannins in living seaweed. Approximately 90 % of all phlorotannins in *F. vesiculosus* are located within cells (Koivikko et al. 2005) and much of the apoplastic fraction of phlorotannins is probably also to some extent shielded and thereby less apparent to *L. littorea* than phlorotannins in freshly prepared agar gels. Interestingly, a particularly low creeping velocity was observed on one specimen of *F. vesiculosus* that contained a much higher concentration of FC-phenols than all other individuals that were examined. This could be due to coincidence, but it may also reflect the reduction in creeping velocity at relatively high concentrations of phenols due to retraction that was generally observed with artificial substrates. The algal specimen in question had a dry matter content of FC-phenols of 12.2 %, which is close to the maximum of approximately 15 % that has been reported for *F. vesiculosus* (Ragan & Glombitza 1986). Assays with more specimens that are as rich in FC-phenols would be necessary to verify the effect upon *L. littorea* attachment. The relative rarity of such specimens suggests that effects observed with extracts in the high concentration range (10 % natural concentration or more) will rarely happen in nature. Nonetheless, the readiness of a periwinkle to attach to a substrate containing a given compound at a given concentration provides relevant information about the capacity of this compound to repel or attract.

At 10 % natural concentration or more the repelling effect of *F. vesiculosus* phlorotannins upon *L. littorina* was less severe than the effect of pure phloroglucinol. An increased tendency for escapes was not observed, and snail attachment was in many cases only significantly reduced at the highest tested (1-fold natural) concentration. This probably resulted from counteracting effects of deterrents and feeding cues. The available information about compounds that act as feeding cues for marine snails is much more limited than the information about repellents. Glucose has been identified as an attractant to *L. littorea* (Woodbridge 1978), but the concentration of free glucose in *F. vesiculosus* is relatively low, given that the primary carbon storage compound in this alga is mannitol. In our study mannitol concentration was identified as a significant predictor of periwinkle attachment to artificial substrates containing *F. vesiculosus* extract. #(Discuss here the result of experiment with mannitol - to be conducted).

Conclusion...

Literature

- Amsler C, Fairhead V (2005) Defensive and Sensory Chemical Ecology of Brown Algae. *Advances in Botanical Research* 43:1-91
- Arnold TM, Targett NM (2002) Marine tannins: The importance of a mechanistic framework for predicting ecological roles. *Journal of chemical ecology* 28:1919-1934
- Arnold TM, Targett NM (2003) To grow or defend: lack of tradeoffs for brown algal phlorotannins. *Oikos* 100:406-408
- Barker KM, Chapman ARO (1990) Feeding preferences of periwinkles among four species of *Fucus*. *Mar Biol* 106:113-118
- Bertness MD, Trussell GC, Ewanchuk PJ, Silliman BR (2002) Do alternate stable community states exist in the Gulf of Maine rocky intertidal zone? *Ecology* 83:3434-3448
- Borell EM, Foggo A, Coleman RA (2004) Induced resistance in intertidal macroalgae modifies feeding behaviour of herbivorous snails. *Oecologia* 140:328-334
- Deal MS, Hay ME (1996) Variation in palatability of the seaweed *Fucusvesiculosus* across an intertidal gradient: Induction or physical effects?, Vol
- Fisher LD, Van Belle G (1993) Biostatistics: A Methodology for the Health Sciences, Vol. John Wiley & Sons
- Folin O, Ciocalteu V (1927) On tyrosine and tryptophane determinations in proteins. *J BiolChem* 73:627-650
- Geiselman JA, McConnell OJ (1981) Polyphenols in brown algae *Fucusvesiculosus* and *Ascophyllumnodosum* - Chemical defenses against the marine herbivorous snail, *Littorinalittorea*. *Journal of chemical ecology* 7:1115-1133
- Griffin JN, Noel LMLJ, Crowe TP, Burrows MT, Hawkins SJ, Thompson RC, Jenkins SR (2010) Consumer effects on ecosystem functioning in rock pools: roles of species richness and composition. *Marine Ecology Progress Series* 420:45-56
- Hagerman AE, Butler LG (1978) Protein precipitation method for the quantitative determination of tannins. *J Agric Food Chem* 28:944-947
- Hunter J (1981) Feeding preferences and competitive herbivory studies on two species of periwinkles, *Littorinaobtusata* and *Littorinalittorea*. *Biological Bulletin, Marine Biological Laboratory, Woods Hole* 161:328
- Imrie DW, Hawkins SJ, McCrohan CR (1989) The olfactory-gustatory basis of food preference in the herbivorous prosobranch, *Littorinalittorea* (Linnaeus). *J Mollusc Stud* 55:217-225

Partie 2 : Implication des phlorotannins dans la réponse aux stress biotiques et abiotiques chez *F.vesiculosus*

- Jormalainen V, Honkanen T, Vesakoski O (2007) Geographical divergence in host use ability of a marine herbivore in alga-grazer interaction. *EvolEcol* 22:545-559
- Koivikko R, Loponen J, Honkanen T, Jormalainen V (2005) Contents of soluble, cell-wall-bound and exuded phlorotannins in the brown alga *Fucusvesiculosus*, with implications on their ecological functions. *Journal of chemical ecology* 31:195-212
- Kremer BP (1975) Physiological and chemical characteristics of different thallus regions of *Fucusserratus*. *HelgolWissMeeresunters* 27:115-127
- Lauzon-Guay J-S, Scheibling RE (2009) Food Dependent Movement of Periwinkles (*Littorinalittorea*) Associated with Feeding Fronts. *Journal of Shellfish Research* 28:581-587
- Little C (1989) Factors governing patterns of foraging activity in littoral marine herbivorous molluscs. *Journal of Molluscan Studies* 55:273-284
- Lubchenco J (1978) Plant Species Diversity in a Marine Intertidal Community: Importance of Herbivore Food Preference and Algal Competitive Abilities. *The American Naturalist* 112:23-39
- Newell GE (1958) The behaviour of *LittorinaLittorea* (L.) under natural conditions and its relation to position on the shore. *Journal of the Marine Biological Association of the United Kingdom* 37:229-239
- Norton TA, Hawkins SJ, Manley NL, Williams GA, Watson DC (1990) Scraping a living: a review of littorinid grazing. *Hydrobiologia* 193:117-138
- Pavia H, Cervin G, Lindgren A, Aberg P (1997) Effects of UV-B radiation and simulated herbivory on phlorotannins in the brown alga *Ascophyllumnodosum*. *Marine Ecology Progress Series* 157:139-146
- Pavia H, Toth GB (2000) Inducible chemical resistance to herbivory in the brown seaweed *Ascophyllumnodosum*. *Ecology* 81:3212-3225
- Pearson G, Kautsky L, Serrao E (2000) Recent evolution in Baltic *Fucusvesiculosus*: reduced tolerance to emersion stresses compared to intertidal (North Sea) populations. *Marine Ecology Progress Series* 202:67-79
- Petpiroon S, Morgan E (1983) Observations on the tidal activity rhythm of the periwinkle *Littorinanigrolineata* (Gray). *Marine Behaviour and Physiology* 9:171-192
- Ragan CM, Glombitza KW (1986) Phlorotannins, brown algal polyphenols. *Progress in Phycological Research* 4:129-241
- Rohde S, Molis M, Wahl M (2004) Regulation of anti-herbivore defence by *Fucus vesiculosus* in response to various cues. *Journal of Ecology* 92:1011-1018
- Scheibling RE, Kelly NE, Raymond BG (2009) Herbivory and community organization on a subtidal cobble bed. *Marine Ecology Progress Series* 382:113-128
- Schoenwaelder MEA (2002) The occurrence and cellular significance of physodes in brown algae. *Phycologia* 41:125-139
- Scott GW, Marsham S (2006) Can juvenile Fucus (Phaeophyta) really deter grazing by *Littorinalittorea* (Mollusca)? *Phycologia* 45:158-160

Partie 2 : Implication des phlorotannins dans la réponse aux stress biotiques et abiotiques chez *F.vesiculosus*

- Shumway SE, Lesser MP, Crisp DJ (1993) Specific dynamic action demonstrated in the herbivorous marine periwinkles, *Littorinalittorea* L. and *Littorinaobtusata* L. (Mollusca, Gastropoda). Comparative Biochemistry and Physiology A Comparative Physiology 106:391-395
- Stern JL, Hagerman AE, Steinberg PD, Mason PK (1996) Phlorotannin-protein interactions. Journal of chemical ecology 22:1877-1899
- Targett NM, Arnold TM (1998) Predicting the effects of brown algal phlorotannins on marine herbivores in tropical and temperate oceans. Journal of Phycology 34:195-205
- Tiffin P, Innouye BD, Underwood N (2006) Induction and herbivore mobility affect the evolutionary escalation of plant defence. EvolEcol Res 8:265-277
- Toth GB, Pavia H (2007) Induced herbivore resistance in seaweeds: a meta-analysis. Journal of Ecology 95:425-434
- Tugwell S, Branch GM (1992) Effects of Herbivore Gut Surfactants on Kelp Polyphenol Defenses. Ecology 73:205-215
- Van Alstyne KL (1995) Comparison of three methods for quantifying brown algal polyphenolic compounds. Journal of chemical ecology 21:45-58
- Vas'kovskii VE, Isai SV (1972) Determination of the amount of mannitol in brown seaweeds. KhimPrirSoed 8:596-600
- Watson DC, Norton TA (1983) Algal palatability and selective grazing by littorinid snails. Br Phycol J 18:212
- Watson DC, Norton TA (1985) Dietary preferences of the common periwinkle, *Littorinalittorea* (L.). Journal of Experimental Marine Biology and Ecology 88:193-211
- Weinberger F, Rohde S, Oschmann Y, Shahnaz L, Dobretsov S, Wahl M (2011) Effects of limitation stress and of disruptive stress on induced antigrazing defense in the bladder wrack *Fucusvesiculosus*. Marine Ecology Progress Series 427:83-94
- Woodbridge RG (1978) The common periwinkle, *Littorina littorea*,Linne, attracted by sugars. Experientia 34:1445
- Zhang Q, Zhang J, Shen J, Silva A, Dennis DA, Barrow CJ (2006) A simple 96-well microplate method for estimation of total polyphenol content in seaweeds. Journal of Applied Phycology 18:445-450

Synthèse de la Partie II

L'étude de l'implication des phlorotannins dans la réponse aux stress biotiques et abiotiques chez *Fucus vesiculosus* a révélé des réponses différentielles en fonction du stress appliqué.

En effet, la surexpression de gènes impliqués dans les stress globaux, tel que le gène codant l'HSP70, ainsi que le suivi des paramètres photosynthétiques, nous ont permis de montrer que l'UV-B avait un effet de stress global sur la physiologie de l'algue (**Chapitre 4**). En revanche, les gènes que nous avions ciblés comme susceptibles d'intervenir dans le métabolisme des phlorotannins, soit les gènes codant pour la polyketide synthase III (PKSIII), la vanadium bromoperoxidase (vBPO) et l'arylsulfotransférase (AST), n'ont révélé aucune expression différentielle face au stress UV-B.

La quantification totale et la quantification après semi-purification de la fraction soluble en phlorotannins n'a également mis en évidence aucun changement significatif des teneurs en phénols durant les quatre semaines de cinétique. Ces résultats suggèrent l'hypothèse d'une corrélation entre, d'une part, l'absence d'induction de l'expression du gène codant pour la pksIII, et donc l'absence d'induction de la production de phloroglucinol (précurseur de la voie de biosynthèse des phlorotannins), et, d'autre part, l'absence d'augmentation des teneurs en composés phénoliques solubles dans les tissus de *F. vesiculosus*.

En corollaire, nous émettons l'hypothèse que cette espèce utilise le pool de phénols sous la forme d'une défense constitutive face à une irradiation chronique aux UV-B. En effet, les teneurs élevées en phlorotannins présentes dès les premiers stades de développement de l'algue suggèrent un double rôle de ces composés, primaire au niveau de la constitution de la paroi cellulaire et secondaire dans les mécanismes de photoprotection, pouvant être selon l'occurrence inductibles ou non.

En ce qui concerne le broutage par *Littorina littorea* (**Chapitre 5**), nous avons observé des réponses significatives de l'expression de gènes à 24 heures pour les gènes *pksIII* et *X22181*. Ce dernier gène a une fonction pour l'instant inconnue, mais une étude précédente sur les interactions entre *Littorina* et *Fucus* a montré qu'une expression différentielle importante avait lieu après 2 jours d'incubation avec les Littorines ([Flöthe et al. 2014](#)), ce qui corrobore nos résultats. En revanche, l'expression du gène *hsp70* n'a pas varié significativement dans notre

étude, ce qui implique une réponse plus spécifique de ce gène pour des stress abiotiques comme le stress UV ou des chocs thermiques. L'augmentation faible mais significative des teneurs en phlorotannins solubles dès les premières 12 heures nous a amené à nous interroger quant au décalage observé dans la surexpression du gène *pks III* survenant à 24 heures. Nous émettons l'hypothèse que le pool d'ARN messagers présents dans la cellule avant application du stress pourrait induire la production de PKSIII dès les premières heures du stress, permettant ainsi d'intensifier la synthèse précoce d'oligophénols puis de polyphénols. La surexpression du gène *pksIII* à 24 heures pourrait ensuite permettre une mobilisation plus importante du métabolisme. Néanmoins, nous savons qu'il existe trois gènes codants pour les PKS de type III dans le génome d'*Ectocarpus*, le gène codant la PKS1 étant le plus exprimé, sans pouvoir affirmer qu'il en est de même chez *F.vesiculosus*.

Des études plus approfondies sur la biosynthèse des phlorotannins seront donc à prévoir afin d'identifier les gènes et les protéines impliquées dans cette voie. Toutefois, nous avons d'ores et déjà montré que l'acquisition de connaissances sur la voie de biosynthèse des phlorotannins était cruciale pour le développement d'outils biomoléculaires permettant d'aborder sous un angle nouveau l'étude des réponses écophysiologiques des Fcales (et au-delà des Phéophycées) aux pressions environnementales.

Le **Chapitre 6** présente une autre manière d'appréhender l'implication des phlorotannins dans la réponse à l'herbivorie. Il s'agit de ne plus se limiter aux réponses des algues, mais aussi d'étudier les réactions comportementales des herbivores, notamment dans le cadre de leur perception des phlorotannins. Le développement de cet essai biologique simple et rapide devrait permettre à l'avenir de tester rapidement l'effet d'un grand nombre de molécules potentiellement impliquées dans la défense des macroalgues contre le broutage, en parallèle avec la caractérisation chimique des extraits.

Conclusions et Perspectives

- Des progrès majeurs dans la caractérisation biochimique d'enzymes-clés 166
- De nouveaux outils au service de la caractérisation fonctionnelle des gènes d'*Ectocarpus*..... 167
- Poursuivre la caractérisation biochimique des sulfotransférases et étudier leurs fonctions chez *Ectocarpus* et dans le développement de *Fucus*..... 168
- Vers une compréhension plus fine de l'implication des phlorotannins dans les mécanismes de défense et de photoprotection 169
- Un essai biologique adapté aux études des interactions algues/ herbivores..... 171
- La biosynthèse des phlorotannins et sa localisation au niveau cellulaire 172
- Les phlorotannins : questions en suspens et nouvelles pistes..... 174



Des progrès majeurs dans la caractérisation biochimique d'enzymes-clés

Durant ce projet de thèse, nous nous étions fixés plusieurs objectifs : le premier consistait à utiliser des outils de clonage et de surexpression d'enzymes recombinantes, afin de caractériser des enzymes pouvant intervenir dans la voie de biosynthèse des phlorotannins. La caractérisation fonctionnelle et structurale de la première *polyketide synthase de type III* ([Meslet-Cladiere et al. 2013](#)), réalisée en amont de cette thèse, a révélé l'implication de cette enzyme dans l'initiation de la voie de biosynthèse des phlorotannins, par la synthèse du phloroglucinol (**Chapitre 1**). Par ailleurs, cette étude a montré une corrélation entre l'expression du gène codant la PKSIII et la synthèse du phloroglucinol lors de l'acclimatation à l'eau de mer d'une souche d'eau douce d'*Ectocarpus*, révélant ainsi la fonction biologique de cette enzyme *in vivo*. Cette étude a également pu révéler l'origine de cette fonction qui pourrait être issue d'un transfert latéral de gènes depuis les actinobactéries vers l'ancêtre de la lignée des Straménopiles à l'origine des algues brunes, il y a plus de 200 millions d'années.

Nous avons ensuite poursuivi cette investigation par l'étude des deux protéines *chalcones isomérase-like* (EsiCHIL1 - EsiCHIL2) d'*Ectocarpus* (**Chapitre 2**). La fonction de ces protéines étant encore inconnue chez les plantes terrestres au début du projet, nous avons donc émis l'hypothèse qu'elles seraient des enzymes intervenant tout comme les chalcone isomérasées de plantes, dans la formation de flavanone à partir de chalcone par une réaction de Michael. Aucun test de substrat ne révèlera cette fonction, car en effet l'étude des chalcones isomérasées de type III chez les plantes terrestres a démontré une toute autre spécificité de ces protéines dans la liaison aux acides gras ([Ngaki et al., 2012](#)). Les CHIL seraient issues de l'évolution des *fatty acid binding proteins* (FAP) d'origine procaryotique ne possédant pas les acides aminés catalytiques des chalcone isomérasées de type I impliquées dans la synthèse des flavanones ([Ralston et al., 2005; Morita et al., 2014](#)). Au vu de des études phylogénétiques et de modélisation structurale présentées dans le chapitre 2 (Figure 2.4), EsiCHIL1 et 2 sont plus proches des FAP3 que des FAP1 et 2. L'étude de [Ngaki et al. \(2012\)](#) a montré une conformation du site actif des FAP3 en forme de « fer à cheval » (Figure 22) ainsi qu'une spécificité de cette classe pour des acides gras de type C16:0 comme le palmitate ou de type C18. Alors que les

FAP1 retiennent préférentiellement des acides gras en C12:0. D'après nos résultats, la protéine recombinante EsiCHIL1 peut également fixer des chaines d'acides gras en C16 et C18. Les tests préliminaires effectués en thermophorèse révèlent une spécificité plus importante pour des ligands en C16 et surtout pour du C16 CoA ($K_d=31.2\mu M \pm 3.7\mu M$). L'utilisation d'autres substrats nous permettra de confirmer ces résultats et également de mesurer la compétition qu'il peut y avoir entre les substrats pour chacune des deux protéines recombinantes dans de nouvelles expériences de thermophorèse.

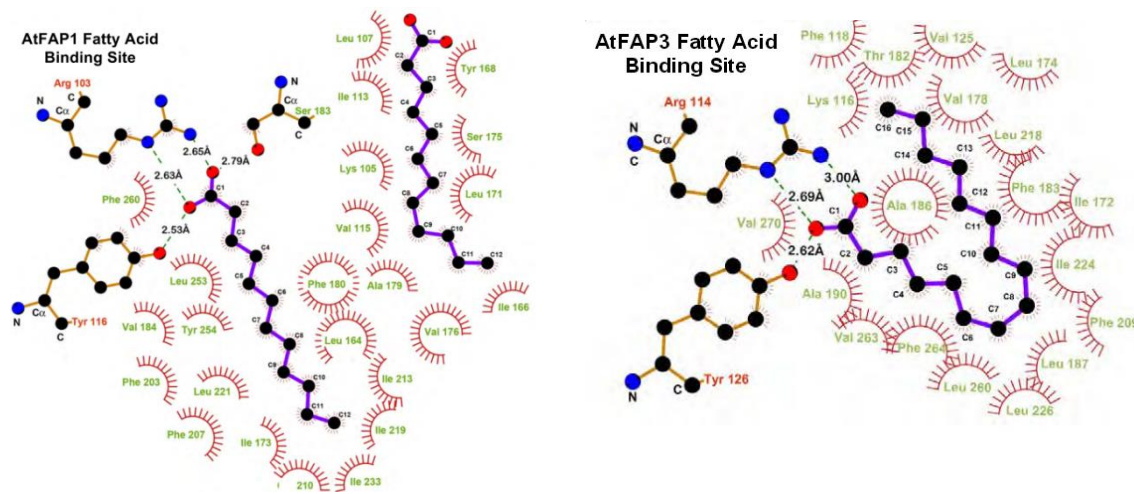


Figure 22: Modélisation schématique de la cavité de liaison des acides gras comparée entre AtFAP1 et AtFAP3. (Ngaki et al., 2012)

De nouveaux outils au service de la caractérisation fonctionnelle des gènes d'Ectocarpus

A cette étude de caractérisation biochimique s'ajoute pour la première fois dans l'étude de protéines d'algues brunes, la caractérisation fonctionnelle utilisant le modèle plante *Arabidopsis thaliana*. Les outils biomoléculaires tel que le tilling, permettant de cribler une collection de mutants pour un gène spécifique afin de déterminer un phénotype indiquant leur fonction, étant en cours de développement chez *Ectocarpus*, l'utilisation du modèle *Arabidopsis* est une réelle opportunité pour l'étude fonctionnelle des gènes d'*Ectocarpus*. L'utilisation de la technologie de clonage Gateway (Liang, et al, 2013) pour exprimer les ADNc d'*Ectocarpus* dans

le tabac, nous a tout d'abord permis d'étudier la localisation subcellulaire des deux protéines EsiCHIL1/2. Ici le tabac est utilisé pour sa facilité de transformation par l'infection d'*Agrobacterium* directement dans les feuilles (Sparkes, et al. 2006). Ainsi nous avons pu montrer une localisation des protéines dans le chloroplaste tout comme pour les FAP d'*Arabidopsis*. La complémentation de mutants d'*Arabidopsis* est actuellement en cours, ainsi le phénotypage, l'analyse de l'expression des gènes et la quantification des acides gras chez les plants contrôle seront comparées aux plants complémentés. Certaines perspectives de valorisation pourront selon les résultats être envisagées au vu des brevets déjà déposés sur les FAPs (US20110223667 A1). Les recherches agronomiques portants sur le métabolisme des acides gras chez les plantes représentent des enjeux importants notamment dans la nutrition humaine mais aussi dans l'industrie des biofouls ou encore des cosmétiques.

 **Poursuivre la caractérisation biochimique des sulfotransférases et étudier leurs fonctions chez *Ectocarpus* et dans le développement de *Fucus*.**

En ce qui concerne l'étude des sulfotransférases d'*Ectocarpus* (**Chapitre 3**) la caractérisation biochimique est encore trop partielle pour conclure sur l'activité enzymatique et la spécificité de ces protéines. Les travaux de caractérisation chimique de certains oligomères de phlorotannins effectués dans le cadre de cette thèse par U-HPLC-MS (Partie 2 Chapitre 4) seront testés afin de caractériser les produits sulfatés de ces activités. Des tests préliminaires avec du PAPS non marqué radioactivement ont été planifiés, mais il pourra s'avérer également important de développer une méthode de dosage en radioactivité pour disposer d'une plus grande sensibilité dans le cas où l'activité spécifique des enzymes recombinantes ne soit pas optimale.

D'autre part, l'étude de la régulation de ces STs dans un contexte écophysiologique, comme sur le modèle *Ectocarpus*, pourra apporter des réponses sur la fonction biologique de ces enzymes notamment dans un contexte d'acclimatation et d'adaptation à la salinité (Dittami et al. 2011). Le développement polarisé du zygote de *Fucus* pourra aussi être un très bon modèle d'étude de la régulation de ces STs, ainsi que des PKS de type III, car des résultats non publiés du laboratoire indiquent qu'une partie des composés sulfatés secrétés au pôle rhizoïdien par le

zygote de *Fucus* seraient des phlorotannins sulfatés (Bouget, Berger, Potin et al., communication personnelle). L'utilisation de la cytologie avec des inhibiteurs de sulfatation ainsi que des colorants spécifiques comme le Fast Red B ([Schoenwalder & Clayton, 1999](#)), pourra être couplée à la microscopie électronique pour visualiser les physodes. Ces approches seront susceptibles de révéler les fonctions primaires des phlorotannins au cours du développement et de la modification de l'architecture pariétale.

 **Vers une compréhension plus fine de l'implication des phlorotannins dans les mécanismes de défense et de photoprotection**

Dans la deuxième partie de cette thèse nous nous sommes intéressés à l'étude de deux paramètres écophysiologiques, l'UV-B et le broutage, qui sont tous deux des paramètres pouvant agir sur la production des phlorotannins chez *Fucus vesiculosus*. La quantification du contenu soluble par des méthodes de dosage colorimétrique tel que le Folin Denis ou Ciocalteu sont des méthodes limitées pour étudier les phlorotannins. Ces réactifs agissent en effet sur tous les composés aromatiques y compris les protéines ce qui peut surestimer la concentration réelle en phlorotannins contenus dans les extraits. Les outils génomiques s'étant développés ces dernières années sur les Phéophycées et notamment sur *Fucus vesiculosus*, ils offrent aujourd'hui de nouvelles perspectives dans l'étude de la régulation des mécanismes de réponse aux stress. Ainsi nous avons recherché et sélectionné dans les banques de données EST, des gènes intervenant dans les mécanismes de stress globaux tel que l'HSP70 mais aussi et surtout des gènes pouvant être impliqués dans le métabolisme des phlorotannins.

Nous avons ainsi montré dans le **Chapitre 4** que les radiations UV-B avaient un effet de stress marqué sur la physiologie de l'algue au vu de l'expression différentielle du gène codant l'HSP70 à 12 et 24 heures sur les individus soumis à l'UV-B, ainsi que par la diminution significative de leur capacité photosynthétique liée au photosystème II à 1 et 4 semaines. En revanche, les gènes que nous avions ciblés comme intervenant dans le métabolisme des phlorotannins : les gènes codant pour la polyketide synthase III (PKSIII), la vanadium bromoperoxidase (vBPO), et l'arylsulfotransférase (AST) n'ont révélés aucune expression différentielle face au stress UV-B.

La quantification totale de la fraction soluble en phlorotannins n'a également révélé aucune variation durant les quatre semaines de cinétique. En revanche la fraction semi purifiée a pu montrer une diminution significative des contenus en phlorotannins à 24 heures sous forte irradiation UV-B ce qui pourrait être corrélé à une forte condensation des phlorotannins ou à un pontage des composés à la paroi qui limiterait la fraction de plus petits oligomères sélectionnées par la méthode de purification. Néanmoins au vu de la variabilité interindividuelle trop importante dans l'expression du gène vBPO aucune corrélation ne peut être effectuée dans cette étude. L'utilisation d'un plus grand nombre de réplicats biologiques ou d'autres conditions expérimentales, sera nécessaire pour valider cette hypothèse. La semi-purification des extraits nous a également permis d'analyser différents degrés de polymérisation allant dans le sens d'une étude plus approfondie de la composition qualitative des extraits. Il reste néanmoins un certain nombre d'optimisations à réaliser, afin d'obtenir un seuil de détection suffisant pour l'analyse et l'identification structurale de ces composés. Mais au-delà de ces limitations expérimentales, l'irradiation chronique aux UV-B chez *Fucus vesiculosus* révèle l'importance d'une protection constitutive des phlorotannins car ni l'expression du gène codant la PKSIII ni la quantification des phlorotannins solubles n'ont révélé d'induction de ce métabolisme.

En suivant les mêmes approches, l'étude réalisée sur le broutage de *Fucus vesiculosus* par *Littorina littorea* a cette fois montré une induction du métabolisme des phlorotannins (**Chapitre 5**). Dès les premières 24 heures de mise en contact des deux espèces, le gène codant la PKSIII ainsi que le gène X22181 sont surexprimés en condition de broutage. L'induction du gène X22181 de fonction encore inconnue avait également été mise en évidence lors d'une étude précédente en condition de broutage (Flöthe, et al., 2014), ce qui appuie l'hypothèse de l'implication de ce gène dans la réponse à l'herbivorie. Dans notre étude, seule la quantification totale de la fraction soluble des phlorotannins a été réalisée. Les résultats obtenus montrent une augmentation des teneurs dès 12 heures de broutage et aucune autre variation significative sur le reste de la cinétique. Cette réponse précoce n'avait encore jamais été montrée auparavant, ce qui souligne une réactivité importante des algues et une perception des signaux de stress très efficace.

 **Un essai biologique adapté aux études des interactions algues/herbivores**

L'étude de l'attachement des littorines au substrat contenant notamment du phloroglucinol, a pu montrer un comportement dose dépendant chez les littorines (**Chapitre 6**). A de faibles concentrations en phloroglucinol ($30\text{-}100 \mu\text{g.mL}^{-1}$) aucun effet n'est observé, puis lorsque l'on augmente la concentration ($300 \mu\text{g.mL}^{-1}$) les déplacements augmentent, et enfin les littorines se décrochent à partir de $1000 \mu\text{g.mL}^{-1}$.

Cette étude comportementale est très intéressante afin de comprendre l'effet des molécules produites par les algues en réponse aux herbivores. Des études plus globales seraient donc à réfléchir afin d'intégrer les résultats obtenus sur la réponse des algues, mais aussi sur la réponse des herbivores, ce qui permettra d'aller plus loin dans la compréhension des mécanismes de communication et de défense sur ce type de modèles. Le milieu marin étant un milieu très diffusif, l'utilisation de ce type d'essai biologique permet de s'affranchir de cette contrainte, néanmoins nous testons ici l'effet comportemental et non le rôle anti-appétant des molécules car l'herbivore ne consomme pas le substrat. Cet essai biologique permet ainsi de tester des molécules pouvant avoir un rôle répulsif sur les herbivores.

La compréhension de ces interactions reste néanmoins encore complexe au vu des multiples facteurs mis en jeux et nécessitera l'utilisation de compétences pluridisciplinaires pour répondre à ces questionnements.

 **La biosynthèse des phlorotannins et sa localisation au niveau cellulaire**

Afin d'approfondir ces recherches et d'élargir le champ des connaissances, il serait intéressant d'utiliser des outils d'imagerie tels que l'imagerie chimique couplée à la localisation par immunologie des enzymes-clés de la voie de biosynthèse des phlorotannins. Les premiers résultats de localisation de la protéine PKS1 chez *Ectocarpus* (Figure 23) montrent une localisation majoritairement pariétale de cette enzyme, mais une détection au niveau des chloroplastes et leur périphérie est également visible. Ceci peut donc suggérer qu'une synthèse de phloroglucinol est possible au niveau du chloroplaste et que ce phloroglucinol et des phlorotannins seraient ensuite encapsulés dans les physodes en réserve. Les physodes sont ensuite secrétés vers la paroi pour y jouer des fonctions primaires comme il a pu être décrit dans des études antérieures ([Schoenwaelder and Clayton 1999](#)), mais également aussi dans le contexte des réponses au stress. Néanmoins, la localisation majoritaire des protéines détectées par les anticorps spécifiques anti-PKS1 couplés aux grains d'or se trouve dans la paroi ce qui peut poser des questions quant à la localisation de la biosynthèse du phloroglucinol. La première hypothèse est que la protéine PKS1 est relativement stable et qu'elle pourrait être secrétée vers la paroi cellulaire avec les phlorotannins. La deuxième hypothèse serait que l'enzyme PKS1 pourrait être aussi active dans la paroi à partir de substrats acyl-CoA présents dans les physodes et utiliseraient des dérivés d'acides gras des membranes des vésicules pour former des composés comme des acylphloroglucinols. Si les limites de la résolution des techniques le permettent, le suivi de la localisation du phloroglucinol ou d'oligomères de phlorotannins par imagerie de spectrométrie de masse en DESI-MS ou en MALDI-MS ou encore des expériences de marquage au ¹³C pourraient permettre une meilleure compréhension de la compartimentation de ce métabolisme.

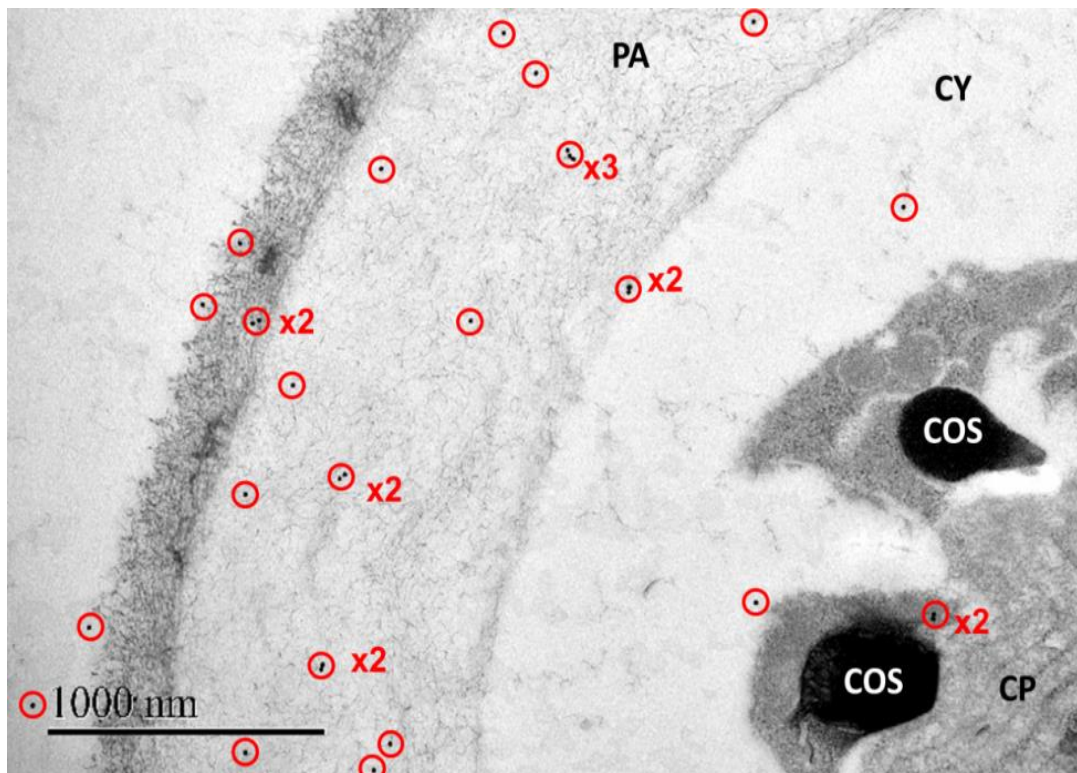


Figure 23: Coupe d'*Ectocarpus* observée en microscopie électronique à transmission, montrant la localisation subcellulaire de la polyketide synthase de type III *EsiPKS1* par marquage aux grains d'or avec des anticorps spécifiques anti-PKS1. **PA**: Paroi, **CY**: Cytoplasme, **COS**, Corps osmophiles = physodes, **CP**: Chloroplaste. (Issu des travaux de Ludovic Delage & Sophie Le Panse, Plateforme Imagerie MERImage Roscoff)

 **Les phlorotannins : questions en suspens et nouvelles pistes**

A l'issue de ces travaux de thèse, beaucoup de questions restent ouvertes concernant la biosynthèse des phlorotannins chez les algues brunes.

Comment sont formés les oligomères de phloroglucinol ? La condensation fait-elle appel à des étapes intermédiaires de bromination et à des pontages oxydatifs catalysés par des vanadium bromoperoxydases ? L'expression de la vBPO recombinante d'*Ectocarpus* demeure une priorité, néanmoins les progrès récents dans le clonage et l'expression de vBPO chez *Ascophyllum nodosum* (Wischang et al. 2012) devraient permettre de tester cette enzyme sur différents substrats comme le phloroglucinol et / ou des oligomères purifiés de phlorotannins, comme du difucol ou du diphlorétol.

Dans quelle mesure la sulfatation et / ou la glycosylation des phlorotannins interviennent-elles pour faciliter leur compartimentation dans la cellule ou leur transport de l'appareil de Golgi vers le pourtour de la cellule puis leur excrétion au niveau de la paroi cellulaire ?

Les données acquises lors de l'annotation du génome d'*Ectocarpus* pourront être comparées avec les nouveaux génomes et transcriptomes d'algues brunes qui sont déjà disponibles ou le seront très prochainement (*Saccharina japonica*, *Undaria pinnatifida*, *Fucus vesiculosus*). Cette comparaison devrait faciliter l'identification de nouveaux gènes candidats de la voie de biosynthèse des phlorotannins.

Ainsi, les résultats obtenus et les nouveaux outils développés dans le cadre de ces travaux de thèse illustrent l'intérêt d'acquérir des connaissances sur les gènes codant pour les enzymes de la voie de biosynthèse des phlorotannins, afin de poursuivre l'élucidation de cette voie de biosynthèse certes, mais aussi pour disposer de plus d'outils pour mieux cerner les diverses fonctions biologiques et écologiques de ces composés chez les algues brunes.

Références bibliographiques

- Abe I, Morita H (2010) Structure and function of the chalcone synthase superfamily of plant type III polyketide synthases. *Nat Prod Rep* 27:809–38. doi: 10.1039/b909988n
- Allen DJ, McKee IF, Farage PK, Baker NR (1997) Analysis of limitations to CO₂ assimilation on exposure of leaves of two *Brassica napus* cultivars to UV-B. *Plant, Cell Environ* 20:633–640. doi: 10.1111/j.1365-3040.1997.00093.x
- Van Alstyne K (1995) Comparison of three methods for quantifying brown algal polyphenolic compounds. *J Chem Ecol* 21:45–58.
- Van Alstyne K (1988) Herbivore Grazing Increases Polyphenolic Defenses in the Intertidal Brown Alga *Fucus Distichus*. *Ecology* 69:655–663.
- Amsler CD, Fairhead VA (2006) Defensive and Sensory Chemical Ecology of Brown Algae. In: Callow JA (ed) *Adv. Plant Pathol.* Academic Press, pp 1–91
- Appel HM (1993) Phenolics in ecological interactions : The importance of oxidation. *J Chem Ecol* 19:1521–1552.
- Apt KE, Clendennen SK, Powers DA, Grossman AR (1995) The gene family encoding the fucoxanthin chlorophyll proteins from the brown alga *Macrocystis pyrifera*. *Mol Gen Genet* 246:455–464.
- Apt KE, Grossman AR (1993) Characterization and transcript analysis of the major phycobiliprotein subunit genes from *Aglaothamnion neglectum* (Rhodophyta). *Plant Mol Biol* 21:27–38. doi: 10.1007/BF00039615
- Arnold, T.M. and N.M. Targett. 1998. Quantifying in situ rates of phlorotannin synthesis and polymerization in marine brown algae. *Journal of Chemical Ecology* 24:577-595.
- Arnold TM, Targett NM (2000) Evidence for metabolic turnover of polyphenolics in tropical brown algae. *J Chem Ecol* 26:1393–1410. doi: 10.1023/A:1005588023887
- Arnold TM, Targett NM (2002) Marine Tannins: The Importance of a Mechanistic Framework for Predicting Ecological Roles. *J Chem Ecol* 28:1919–1934.
- Arnold TM, Targett NM (2003) To grow and defend: lack of tradeoffs for brown algal phlorotannins. *Oikos* 100:406–408.
- Arnold TM, Targett NM (1998) Quantifying in Situ Rates of Phlorotannin Synthesis and Polymerization in Marine Brown Algae. *J Chem Ecol* 24:577–595. doi: 10.1023/A:1022373121596
- Archibald JM, Keeling PJ (2002) Recycled plastids: a “green movement” in eukaryotic evolution. *Trends Genet* 18:577–584. doi: 10.1016/S0168-9525(02)02777-4
- Arzel, P. (1987) Les goémoniers Douarnenez : Le Chasse-Marée
- Baldauf SL (2008) An overview of the phylogeny and diversity of eukaryotes. *J Syst Evol* 46:263–273. doi: 10.3724/SP.J.1002.2008.08060
- Baldauf SL (2003) The deep roots of eukaryotes. *Science* 300:1703–6. doi: 10.1126/science.1085544

- Berglin M, Delage L, Potin P, et al. (2004) Enzymatic cross-linking of a phenolic polymer extracted from the marine alga *Fucus serratus*. *Biomacromolecules* 5:2376–83. doi: 10.1021/bm0496864
- Bieza K, Lois R (2001) An *Arabidopsis* mutant tolerant to lethal ultraviolet-B levels shows constitutively elevated accumulation of flavonoids and other phenolics. *Plant Physiol* 126:1105–15.
- Bischof K, Gómez I, Molis M, et al. (2006) Ultraviolet radiation shapes seaweed communities. *Rev Environ Sci Bio/Technology* 5:141–166. doi: 10.1007/s11157-006-0002-3
- Bitton R, Ben-Yehuda M, Davidovich M, et al. (2006) Structure of algal-born phenolic polymeric adhesives. *Macromol Biosci* 6:737–46. doi: 10.1002/mabi.200600073
- Bonaventure G, Salas J (2003) Disruption of the FATB gene in *Arabidopsis* demonstrates an essential role of saturated fatty acids in plant growth. *Plant Cell* ... 15:1020–1033. doi: 10.1105/tpc.008946.2
- Breton F, Cérantola S, Ar Gall E (2011) Distribution and radical scavenging activity of phenols in *Ascophyllum nodosum* (Phaeophyceae). *J Exp Mar Bio Ecol* 399:167–172. doi: 10.1016/j.jembe.2011.01.002
- La Barre S, Potin P, Leblanc C, Delage L (2010) The Halogenated Metabolism of Brown Algae (Phaeophyta), Its Biological Importance and Its Environmental Significance. *Mar Drugs* 8:988–1010. doi: 10.3390/md8040988
- Bowles D, Isayenkova J, Lim E-K, Poppenberger B (2005) Glycosyltransferases: managers of small molecules. *Curr Opin Plant Biol* 8:254–63. doi: 10.1016/j.pbi.2005.03.007
- Butler A, Walker J (1993) Marine haloperoxidases. *Chem Rev* 1937–1944.
- Cabioc'h J., Floc'h J.-Y., Le Toquin A., Boudouresque C.F., Meinesz A., Verlaque M., (2014) Algues des mers d'Europe, Delachaux et Niestlé.
- Cock JM, Sterck L, Rouzé P, et al. (2010) The Ectocarpus genome and the independent evolution of multicellularity in brown algae. *Nature* 465:617–21. doi: 10.1038/nature09016
- Cock, JM. Peters, AF. Coelho S (2011) Brown algae. *Curr. Biol.* pp R573–5
- Cock JM, Godfroy O, Macaisne N, Peters AF and Coelho SM (2013). Evolution and regulation of complex life cycles: a brown algal perspective. *Curr. Opin Plant Biol* 17C:1-6.
- Cock, J.M., Peters, A.F. and Coelho, S.M. (2011). Brown Algae. *Current Biology*, 21, R573-R575.
- Coleman R a., Ramchunder SJ, Moody a. J, Foggo a. (2007) An enzyme in snail saliva induces herbivore-resistance in a marine alga. *Funct Ecol* 21:101–106. doi: 10.1111/j.1365-2435.2006.01210.x
- Connan S, Goulard F, Stiger V, et al. (2004) Interspecific and temporal variation in phlorotannin levels in an assemblage of brown algae. *Bot Mar* 47:410–416.

- Caldwell MM, Björn LO, Bornman JF, et al. (1998) Effects of increased solar ultraviolet radiation on terrestrial ecosystems. *J Photochem Photobiol B Biol* 46:40–52. doi: 10.1016/S1011-1344(98)00184-5
- Carlson DJ, Carlson ML (1984) Reassessment of exudation by fucoid macroalgae. *Limnol Oceanogr* 29:1077–1087.
- Chapman E, Best MD, Hanson SR, Wong C-H (2004) Sulfotransferases: structure, mechanism, biological activity, inhibition, and synthetic utility. *Angew Chem Int Ed Engl* 43:3526–48. doi: 10.1002/anie.200300631
- Cheynier V, Comte G, Davies KM, et al. (2013) Plant phenolics: recent advances on their biosynthesis, genetics, and ecophysiology. *Plant Physiol Biochem* 72:1–20. doi: 10.1016/j.plaphy.2013.05.009
- Clough SJ, Bent AF (1999) Floral dip : a simplified method for Agrobacterium-mediated transformation of *Arabidopsis thaliana*. *Plant J* 16:735–743.
- Cockell CS KJ (1999) Ultraviolet radiation screening compounds. *Biol Rev* 74:311–345.
- Cooper JE (2007) Early interactions between legumes and rhizobia: disclosing complexity in a molecular dialogue. *J Appl Microbiol* 103:1355–65. doi: 10.1111/j.1365-2672.2007.03366.x
- Crato E (1892) Die physode, ein organ des zellenleibes. *Deut. Bot Ges Ber* 10:295–302.
- Crato E (1893a) a. Morphologische und microchemische untersuchungen über die physoden. *Bote Zeit X/XI*:157–195.
- Crato E (1893b) Über die Hansteen'chen fucosan körner. *Bot Ges Ber* 11:235–241.
- Davison I, Reed R (1985) The physiological significance of mannitol accumulation in brown algae: the role of mannitol as a compatible cytoplasmic solute. *Phycologia* 24:449–457.
- Davison IR, Pearson GA (1996) Stress tolerance in intertidal seaweeds. *J Phycol* 32:197–211. doi: 10.1111/j.0022-3646.1996.00197.x
- Deal MS, Hay ME, Wilson D, Fenical W (2003) Galactolipids rather than phlorotannins as herbivore deterrents in the brown seaweed *Fucus vesiculosus*. *Oecologia* 136:107–14. doi: 10.1007/s00442-003-1242-3
- De Reviers B (2003a) Biologie et Phylogenie des algues, tome 1. Edition Belin, Paris, pp 255
- De Reviers B (2003b) Biologie et Phylogenie des algues, tome 2. Edition Belin, Paris, pp 255
- Dombrovski L, Dong A, Bochkarev A, Plotnikov AN (2006) Crystal structures of human sulfotransferases SULT1B1 and SULT1C1 complexed with the cofactor product adenosine-3'- 5'-diphosphate (PAP). *Proteins* 64:1091–4. doi: 10.1002/prot.21048
- Dittami SM, Proux C, Rousvoal S, et al. (2011) Microarray estimation of genomic inter-strain variability in the genus *Ectocarpus* (Phaeophyceae). *BMC Mol Biol* 12:2. doi: 10.1186/1471-2199-12-2

- Emiliani G, Fondi M, Fani R, Gribaldo S (2009) A horizontal gene transfer at the origin of phenylpropanoid metabolism: a key adaptation of plants to land. *Biol Direct* 4:7. doi: 10.1186/1745-6150-4-7
- Fang G, Hammar S GR (1992) A quick and inexpensive method for removing polysaccharides from plant genomic DNA. *Biotechniques* 13:52–56.
- Flöthe CR, John U, Molis M (2014a) Comparing the Relative Importance of Water-Borne Cues and Direct Grazing for the Induction of Defenses in the Brown Seaweed *Fucus vesiculosus*. *PLoS One* 9:e109247. doi: 10.1371/journal.pone.0109247
- Flöthe CR, Molis M, John U (2014b) Induced resistance to periwinkle grazing in the brown seaweed *Fucus vesiculosus* (Phaeophyceae): molecular insights and seaweed-mediated effects on herbivore interactions. *J Phycol* 50:564–576. doi: 10.1111/jpy.12186
- Flöthe CR, Molis M, Kruse I, et al. (2014c) Herbivore-induced defence response in the brown seaweed *Fucus vesiculosus* (Phaeophyceae): temporal pattern and gene expression. *Eur J Phycol* 49:356–369. doi: 10.1080/09670262.2014.946452
- Franklin LA, Forster RM (1997) Review The changing irradiance environment : consequences for marine macrophyte physiology , productivity and ecology. *Eur J Phycol* 207–232.
- Gidda SK, Varin L (2006) Biochemical and molecular characterization of flavonoid 7-sulfotransferase from *Arabidopsis thaliana*. *Plant Physiol Biochem* 44:628–36. doi: 10.1016/j.plaphy.2006.10.004
- Glombitza K-W, Knoss W (1992) Sulphated phlorotannins from the brown alga *Pleurophycus gardneri*. *Phytochemistry* 31:279–281.
- Gomez I, Huovinen P (2010) Induction of Phlorotannins During UV Exposure Mitigates Inhibition of Photosynthesis and DNA Damage in the Kelp *Lomentaria nigrescens*. *Photochem Photobiol* 86:1056–1063. doi: 10.1111/j.1751-1097.2010.00786.x
- Gross GG (2008) From lignins to tannins: forty years of enzyme studies on the biosynthesis of phenolic compounds. *Phytochemistry* 69:3018–31. doi: 10.1016/j.phytochem.2007.04.031
- Häder D, Figueroa FL (1997) Photoecophysiology of Marine Macroalgae. *Photochem Photobiol* 66:1–14.
- Häder, D.P., Kumar, H.D., Smith, R.C., Worrest, R.C., (2007). Effects of solar UV radiation on aquatic ecosystems and interactions with climate change. *Photochem. Photobiol. Sci.* 6, 267–285.
- Harborne JB (1975) Flavonoid sulphates: A new class of sulphur compounds in higher plants. *Phytochemistry* 14:1147–1155. doi: 10.1016/S0031-9422(00)98585-6
- Hashiguchi T, Sakakibara Y, Hara Y, et al. (2013) Identification and characterization of a novel kaempferol sulfotransferase from *Arabidopsis thaliana*. *Biochem Biophys Res Commun* 434:829–35. doi: 10.1016/j.bbrc.2013.04.022

- Hashiguchi T, Sakakibara Y, Shimohira T, et al. (2014) Identification of a novel flavonoid glycoside sulfotransferase in *Arabidopsis thaliana*. *J Biochem* 155:91–7. doi: 10.1093/jb/mvt102
- Henry BE, Van Alstyne KL (2004) Effects of uv radiation on growth and phlorotannins in *Fucus gardneri* (Phaeophyceae) juveniles and embryos. *J Phycol* 40:527–533. doi: 10.1111/j.1529-8817.2004.03103.x
- Hupel M, Lecointre C, Meudec A, et al. (2011a) Comparison of photoprotective responses to UV radiation in the brown seaweed *Pelvetia canaliculata* and the marine angiosperm *Salicornia ramosissima*. *J Exp Mar Bio Ecol* 401:36–47. doi: 10.1016/j.jembe.2011.03.004
- Hupel M, Poupart N, Gall EA (2011b) Development of a new in vitro method to evaluate the photoprotective sunscreen activity of plant extracts against high UV-B radiation. *Talanta* 86:362–71. doi: 10.1016/j.talanta.2011.09.029
- Hirschmann F, Krause F, Papenbrock J (2014) The multi-protein family of sulfotransferases in plants: composition, occurrence, substrate specificity, and functions. *Front Plant Sci* 5:556. doi: 10.3389/fpls.2014.00556
- Hollósy F (2002) Effects of ultraviolet radiation on plant cells. *Micron* 33:179–197. doi: 10.1016/S0968-4328(01)00011-7
- Holzinger A, Lutz C (2006) Algae and UV irradiation: Effects on ultrastructure and related metabolic functions. *Micron* 37:190–207. doi: DOI: 10.1016/j.micron.2005.10.015
- Jakoby W, Ziegler D (1990) The enzymes of detoxication. *J Biol Chem* 265:20715–20718.
- Jansen M a K, Martret B Le, Koornneef M (2010) Variations in constitutive and inducible UV-B tolerance; dissecting photosystem II protection in *Arabidopsis thaliana* accessions. *Physiol Plant* 138:22–34. doi: 10.1111/j.1399-3054.2009.01293.x
- Jennings JG, Steinberg PD (1994) In situ exudation of phlorotannins by the sublittoral kelp *Ecklonia radiata*. *Mar Biol* 121:349–354. doi: 10.1007/BF00346744
- Jormalainen V, Honkanen T, Koivikko R, Eränen J (2003) Induction of phlorotannin production in a brown alga: defense or resource dynamics? *Oikos* 103:640–650. doi: 10.1034/j.1600-0706.2003.12635.x
- Jormalainen V, Honkanen T (2004) Variation in natural selection for growth and phlorotannins in the brown alga *Fucus vesiculosus*. *J Evol Biol* 17:807–820.
- Jones P, Vogt T (2014) Glycosyltransferases in secondary plant metabolism: tranquilizers and stimulant controllers. *Planta* 213:164–174. doi: 10.1007/s004250000492
- Jueterbock A, Kollias S, Smolina I, et al. (2014) Thermal stress resistance of the brown alga *Fucus serratus* along the North-Atlantic coast: acclimatization potential to climate change. *Mar Genomics* 13:27–36. doi: 10.1016/j.margen.2013.12.008
- Koivikko R, Loponen J, Honkanen T, Jormalainen V (2005) Contents of soluble, cell-wall-bound and exuded phlorotannins in the brown alga *Fucus vesiculosus*, with implications on their ecological functions. *J Chem Ecol* 31:195–212. doi: 10.1007/s10886-005-0984-2

- Koivikko R, Eränen JK, Loponen J, V. J (2008) Variation of phlorotannins among three populations of *Fucus vesiculosus* as revealed by HPLC and colorimetric quantification. *J Chem Ecol* 34:57–64.
- Koivikko R (2008) Brown algal phlorotannins improving and applying Chemical methods.
- Knoss W, Glombitza K-W (1993) A phenolsulphatase from the marine brown alga *Cystoseira tamariscifolia*. *Phytochemistry* 32:1119–1123.
- Kylin H (1912) Über die Inhaltskörper der Fucoideen. *Ark Bot* 11:1–26.
- Kylin H (1918) Über die fucosanblasen der Phaeophyceen. *Bot Ges Ber* 36:10–19.
- Lesser MP (1996) Acclimation of phytoplankton to UV-B radiation : oxidative stress and photoinhibition of photosynthesis are not prevented by UV- absorbing compounds in the dinoflagellate *Prorocentrum micans*. *Mar Ecol Prog Ser* 132:287–297.
- Liang X, Peng L, Baek C-H, Katzen F (2013) Single step BP/LR combined Gateway reactions. *Biotechniques* 55:265–8. doi: 10.2144/000114101
- Lopes G, Sousa C, Silva LR, et al. (2012) Can phlorotannins purified extracts constitute a novel pharmacological alternative for microbial infections with associated inflammatory conditions? *PLoS One* 7:e31145. doi: 10.1371/journal.pone.0031145
- Mabeau S, Kloareg B (1987) Isolation and Analysis of the Cell Walls of Brown Algae: *Fucus spiralis*, *F. ceranoides*, *F. vesiculosus*, *F. serratus*, *Bifurcaria bifurcata* and *Laminaria digitata*. *J Exp Bot* 38:1573–1580.
- Maxime Hervé (2014) RVAideMemoire: Diverse basic statistical and graphical functions.
- Markham JE, Li J, Cahoon EB, Jaworski JG (2006) Separation and identification of major plant sphingolipid classes from leaves. *J Biol Chem* 281:22684–94. doi: 10.1074/jbc.M604050200
- Martiny VY, Carbonell P, Lagorce D, et al. (2013) In silico mechanistic profiling to probe small molecule binding to sulfotransferases. *PLoS One* 8:e73587. doi: 10.1371/journal.pone.0073587
- Meslet-Cladiere L, Delage L, J.-J. Leroux C, et al. (2013) Structure/Function Analysis of a Type III Polyketide Synthase in the Brown Alga *Ectocarpus siliculosus* Reveals a Biochemical Pathway in Phlorotannin Monomer Biosynthesis. *Plant Cell* 25:3089–3103. doi: 10.1105/tpc.113.111336
- Michel G, Tonon T, Scornet D, et al. (2010a) Central and storage carbon metabolism of the brown alga *Ectocarpus siliculosus*: insights into the origin and evolution of storage carbohydrates in Eukaryotes. *New Phytol* 188:67–81. doi: 10.1111/j.1469-8137.2010.03345.x
- Michel G, Tonon T, Scornet D, et al. (2010b) The cell wall polysaccharide metabolism of the brown alga *Ectocarpus siliculosus*. Insights into the evolution of extracellular matrix polysaccharides in Eukaryotes. *New Phytol* 188:82–97. doi: 10.1111/j.1469-8137.2010.03374.x

- Moon, S. & Nikolau BJ (2009) Plantmetabolomics Platform2: fatty acids. In: <http://www.plantmetabolomics.org>.
- Morita Y, Takagi K, Fukuchi-Mizutani M, et al. (2014) A chalcone isomerase-like protein enhances flavonoid production and flower pigmentation. *Plant J* 78:294–304. doi: 10.1111/tpj.12469
- Mueller-Harvey I (2001) Analysis of hydrolysable tannins. *Anim. Feed Sci. Technol.* 91:
- Negishi M, Pedersen LG, Petrotchenko E, et al. (2001) Structure and function of sulfotransferases. *Arch Biochem Biophys* 390:149–57. doi: 10.1006/abbi.2001.2368
- Nelson BK, Cai X, Nebenführ A (2007) A multicolored set of in vivo organelle markers for co-localization studies in *Arabidopsis* and other plants. *Plant J* 51:1126–36. doi: 10.1111/j.1365-313X.2007.03212.x
- Ngaki MN, Louie G V, Philippe RN, et al. (2012) Evolution of the chalcone-isomerase fold from fatty-acid binding to stereospecific catalysis. *Nature* 485:530–3. doi: 10.1038/nature11009
- Niehrs, C., Beisswanger, R., and Huttner,W. B. (1994). Protein tyrosine sulfation, 1993 – an update. *Chem. Biol. Interact.* 92, 257–271. doi: 10.1016/0009-2797(94)90068-X
- Nielsen HD, Brownlee C, Coelho SM, Brown MT (2003) Inter-population differences in inherited copper tolerance involve photosynthetic adaptation and exclusion mechanisms in *Fucus serratus*. *New Phytol* 160:157–165. doi: 10.1046/j.1469-8137.2003.00864.x
- Nishino T, Nishioka C, Ura H, Nagumo T (1994) Isolation and partial characterization of a novel amino sugar-containing fucan sulfate from commercial *Fucus vesiculosus* fucoidan t. 255:
- Ossipov V, Salminen J, Ossipova S, et al. (2003) Gallic acid and hydrolysable tannins are formed in birch leaves from an intermediate compound of the shikimate pathway. *Biochem Syst Ecol* 31:3–16. doi: 10.1016/S0305-1978(02)00081-9
- Pavia H, Cervin G, Lindgren (1997) Effects of UV-B radiation and simulated herbivory on phlorotannins in the brown alga *Ascophyllum nodosum*. *Mar Ecol Prog Ser* 157:139–146. doi: 10.3354/meps157139
- Pavia H, Toth GB (2000) Influence of light and nitrogen on the phlorotannin content of the brown seaweeds *Ascophyllum nodosum* and *Fucus vesiculosus*. *Hydrobiologia* 440:299–305.
- Parys S, Rosenbaum A, Kehraus S, et al. (2007) Evaluation of quantitative methods for the determination of polyphenols in algal extracts. *J Nat Prod* 70:1865–70. doi: 10.1021/np070302f
- Paul P, Suwan J, Liu J, et al. (2012) Recent advances in sulfotransferase enzyme activity assays. *Anal Bioanal Chem* 1491–1500. doi: 10.1007/s00216-012-5944-4
- Pearson G, Hoarau G, Lago-Leston A, et al. (2010) An Expressed Sequence Tag Analysis of the Intertidal Brown Seaweeds *Fucus serratus*(L.) and *F. vesiculosus* (L.) (Heterokontophyta, Phaeophyceae) in Response to Abiotic Stressors. *Mar Biotechnol* 12:195–213.

- Pearson G, Lago-Leston A, Valente M, Serrão E (2006) Simple and rapid RNA extraction from freeze-dried tissue of brown algae and seagrasses. *Eur J Phycol* 41:97–104. doi: 10.1080/09670260500505011
- Pelletreau KN, Targett NM, Patterns I (2008) New Perspectives for Addressing Patterns of Secondary Metabolites in Marine Macroalgae. 121–146.
- Potin P, Bouarab K, Salaun J-P, et al. (2002) Biotic interactions of marine algae. *Curr Opin Plant Biol* 5:308–317. doi: DOI: 10.1016/S1369-5266(02)00273-X
- Potin, P and Leblanc, C. (2006) Phenolic-based adhesives of marine brown algae, In Biological Adhesives. Chapter 6. Ed By AM Smith and JA Callow, Springer, Berlin, Germany, pp. 105-119.
- R Development Core Team (2010) R: A Language and Environment for Statistical Computing. R Found Stat Comput Vienna Austria 0:{ISBN} 3–900051–07–0.
- Raffogianis B (1997) Sulfotransferase molecular biology : cDNAs and genes. *The FASEB* 11:3–14.
- Ragan, Glombitza (1986) Phlorotannins, brown algal polyphenols. *Prog Phycol Res Round FE Chapman DJ (ed) Biopress Ltd Bristol* 129–241.
- Ragan MA (1976) Physodes and the Phenolic Compounds of Brown Algae. Composition and Significance of Physodes in vivo. *Bot Mar* 19:145–154.
- Ralston L, Subramanian S, Matsuno M, Yu O (2005) Partial Reconstruction of Flavonoid and Isoflavonoid Biosynthesis in Yeast Using Soybean Type I and Type II Chalcone Isomerase. *Plant Physiol* 137:1375–1388. doi: 10.1104/pp.104.054502
- Renger G, Völker M, Eckert HJ, et al. (1989) On the mechanism of Photosystem II deterioration by UV-B irradiation. *Photochem Photobiol* 49:97–105. doi: 10.1111/j.1751-1097.1989.tb04083.x
- Reed R, Davison I, Chudek J, Foster R (1985) The osmotic role of mannitol in the Phaeophyta: an appraisal. *Phycologia* 24:35–47.
- Reyes-Prieto A, Weber APM, Bhattacharya D (2007) The origin and establishment of the plastid in algae and plants. *Annu Rev Genet* 41:147–68. doi: 10.1146/annurev.genet.41.110306.130134
- Roeder V, Collén J, Rousvoal S, et al. (2005) Identification of Stress Gene Transcripts in *Laminaria Digitata* (Phaeophyceae) Protoplast Cultures By Expressed Sequence Tag Analysis1. *J Phycol* 41:1227–1235. doi: 10.1111/j.1529-8817.2005.00150.x
- Rohde S, Molis M, Wahl M (2004) Regulation of anti-herbivore defence by *Fucus vesiculosus* in response to various cues. *J Ecol* 92:1011–1018.
- Rozema J. BLO (2002) The role of UV-B radiation in aquatic and terrestrial ecosystems - an experimental and functional analysis of the evolution of UV-absorbing compounds. *J Photochem Photobiol B Biol* 66:2–12.
- Russell V. Lenth (2014) lsmeans: Least-Squares Means. R package version 2.11. <http://CRAN.R-project.org/package=lsmeans>.

- Salgado LT, Cinelli LP, Viana NB, et al. (2009) a Vanadium Bromoperoxidase Catalyzes the Formation of High-Molecular-Weight Complexes Between Brown Algal Phenolic Substances and Alginates. *J Phycol* 45:193–202. doi: 10.1111/j.1529-8817.2008.00642.x
- Salminen J-P, Karonen M (2011) Chemical ecology of tannins and other phenolics: we need a change in approach. *Funct Ecol* 25:325–338. doi: 10.1111/j.1365-2435.2010.01826.x
- Schoenwaelder MEA, Clayton MN (1998) Secretion of phenolic substances into the zygote wall and cell plate in embryos of *Hormosira* and *Acrocarpia* (Fucales, Phaeophyceae). *J Phycol* 34:969–980. doi: 10.1046/j.1529-8817.1998.340969.x
- Schoenwaelder M, Clayton M (1999) The role of the cytoskeleton in brown algal physode movement. *Eur J Phycol* 34:223–229.
- Schoenwaelder MEA, Clayton MN (1999) The presence of phenolic compounds in isolated cell walls of brown algae. *Phycologia* 38:161–166. doi: 10.2216/i0031-8884-38-3-161.1
- Schoenwaelder MEA, Clayton MN (2000) Physode formation in embryos of *Phyllospora comosa* and *Hormosira banksii* (Phaeophyceae). *Phycologia* 39:1–9. doi: 10.2216/i0031-8884-39-1-1.1
- Schoenwaelder MEA (2002) The occurrence and cellular significance of physodes in brown algae. *Phycologia* 41:125–139. doi: 10.2216/i0031-8884-41-2-125.1
- Schoenwaelder MEA (2008) The Biology of Phenolic Containing Vesicles. *Algae* 23:163–175.
- Scotto-Lavino E, Du G, Frohman M a (2006) 3' end cDNA amplification using classic RACE. *Nat Protoc* 1:2742–5. doi: 10.1038/nprot.2006.481
- Seidel SAI, Dijkman PM, Lea WA, et al. (2013) Microscale thermophoresis quantifies biomolecular interactions under previously challenging conditions. *Methods* 59:301–15. doi: 10.1016/j.ymeth.2012.12.005
- Senthilkumar K, Kim S-K (2014) Anticancer effects of fucoidan. *Adv Food Nutr Res* 72:195–213. doi: 10.1016/B978-0-12-800269-8.00011-7
- Shibata T, Hama Y, Miyasaki T, et al. (2006) Extracellular secretion of phenolic substances from living brown algae. *J Appl Phycol* 18:787–794. doi: 10.1007/s10811-006-9094-y
- Shibata T, Miyasaki T, Miyake H, et al. (2014) The Influence of Phlorotannins and Bromophenols on the Feeding Behavior of Marine Herbivorous Gastropod *Turbo cornutus*. *Am J Plant Sci* 05:387–392. doi: 10.4236/ajps.2014.53051
- Sieburth JM, Conover JT (1965) Sargassum Tannin, an Antibiotic which Retards Fouling. *Nature* 208:52–53. doi: 10.1038/208052a0
- Solovchenko AE, Merzlyak MN (2008) Screening of Visible and UV Radiation as a Photoprotective Mechanism in Plants. *Russ J Plant Physiol* 55:719–737.
- Sparkes I a, Runions J, Kearns A, Hawes C (2006) Rapid, transient expression of fluorescent fusion proteins in tobacco plants and generation of stably transformed plants. *Nat Protoc* 1:2019–25. doi: 10.1038/nprot.2006.286

- Stamp N (2003) Out Of The Quagmire Of Plant Defense Hypotheses. *Q Rev Biol* 78:23–55. doi: 10.1086/367580
- Steevensz AJ, Mackinnon SL, Hankinson R, et al. (2012) Profiling Phlorotannins in Brown Macroalgae by Liquid Chromatography-High Resolution Mass Spectrometry. *Phytochem Anal* 23:547–553. doi: 10.1002/pca.2354
- Stewart, WN, & Rothwell G (1993) Paleobotany and the evolution of plants. Cambridge Univ. Press.
- Swanson AK, Druehl LD (2002) Induction, exudation and the UV protective role of kelp phlorotannins. *Aquat Bot* 73:241–253. doi: DOI: 10.1016/S0304-3770(02)00035-9
- Tarakhovskaya ER (2013) Mechanisms of bioadhesion of macrophytic algae. *Russ J Plant Physiol* 61:19–25. doi: 10.1134/S1021443714010154
- Targett NM, Arnold TM (1998) Minireview-predicting the effects of brown algal phlorotannins on marine herbivores in tropical and temperate oceans. *J Phycol* 34:195–205. doi: 10.1046/j.1529-8817.1998.340195.x
- Toth GB, Pavia H (2000) Water-borne cues induce chemical defense in a marine alga (*Ascophyllum nodosum*). *Proc Natl Acad Sci U S A* 97:14418–20. doi: 10.1073/pnas.250226997
- Tugwell, S., Branch GM (1992) Effects of Herbivore Gut Surfactants on Kelp Polyphenol Defenses. *Ecol Soc Am* 73:205–215.
- Varin L (2008) Chapter 6 Sulfotransferases from Plants , Algae and Phototrophic. 111–130.
- Varin L, Chamberland H, Lafontaine JG, Richard M (1997) The enzyme involved in sulfation of the turgorin, gallic acid 4-O-(-D-glucopyranosyl-6'-sulfate) is pulvini-localized in *Mimosa pudica*. *Plant J* 12:831–837.
- Varin L, DeLuca V, Ibrahim RK, Brisson N (1992) Molecular characterization of two plant flavonol sulfotransferases. *Proc Natl Acad Sci* 89:1286–1290. doi: 10.1073/pnas.89.4.1286
- Vinebrooke RD, Cottingham KL, Norberg J, et al. (2004) Impacts of multiple stressors on biodiversity and ecosystem functioning : the role of species co-tolerance. *Oikos* 3:451–457. doi: 0.1111/j.0030-1299.2004.13255.x
- Vreeland V, Waite JH, Epstein L (1998) Minireview-polyphenols and oxidases in substratum adhesion by marine algae and mussels. *J Phycol* 34:1–8. doi: 10.1046/j.1529-8817.1998.340001.x
- Wahl M, Jormalainen V, Eriksson BK, et al. (2011) Stress ecology in fucus: abiotic, biotic and genetic interactions. *Adv Mar Biol* 59:37–105. doi: 10.1016/B978-0-12-385536-7.00002-9
- Wang T, Jónsdóttir R, Liu H, et al. (2012) Antioxidant Capacities of Phlorotannins Extracted from the Brown Algae *Fucus vesiculosus*. *J Agric Food Chem*. doi: 10.1021/jf3003653
- Waterman Peter G. MS (1994) Analysis of phenolic plant metabolites. 238p.

- Welling M, Ross C, Pohnert G (2011) A desulfatation-oxidation cascade activates coumarin-based cross-linkers in the wound reaction of the giant unicellular alga *Dasycladus vermicularis*. *Angew Chem Int Ed Engl* 50:7691–4. doi: 10.1002/anie.201100908
- Welling MA (2010) The Role of Sulfated Metabolites in the Wound Response of Siphonous Green Algae.
- Wikström S a, Pavia H (2004) Chemical settlement inhibition versus post-settlement mortality as an explanation for differential fouling of two congeneric seaweeds. *Oecologia* 138:223–30. doi: 10.1007/s00442-003-1427-9
- Wischang D, Radlow M, Schulz H, et al. (2012) Molecular cloning, structure, and reactivity of the second bromoperoxidase from *Ascophyllum nodosum*. *Bioorg Chem* 44:25–34. doi: 10.1016/j.bioorg.2012.05.003
- Yates JC, Peckol P (1993) Effects of nutrient availability and herbivory on polyphenolics in the seaweed *Fucus vesiculosus*. *Ecology* 74:1757–1766.
- Yun HY, Engelen AH, Santos RO, Molis M (2012) Water-borne cues of a non-indigenous seaweed mediate grazer-deterrant responses in native seaweeds, but not vice versa. *PLoS One* 7:e38804. doi: 10.1371/journal.pone.0038804

Résumé

Les phlorotannins, polymères du phloroglucinol, sont des composés phénoliques (CP) uniquement retrouvés chez les algues brunes (Phéophycées). Ces métabolites présentant des activités anti-oxydantes, interviendraient dans la formation de la paroi, mais à ce jour leur voie de biosynthèse reste non élucidée. L'annotation du génome de l'algue brune *Ectocarpus*, a permis d'identifier des gènes homologues codant pour des enzymes de la biosynthèse des CP chez les plantes terrestres. Une polyketide synthase de type III (PKSIII), a été caractérisée: elle synthétise le phloroglucinol. La recherche d'autres cibles a été poursuivie sur des gènes codant pour des chalcone-isomérases-like (CHIL), ainsi que pour des phénol-sulfotransférases homologues d'enzymes de sulfatation des flavonoïdes. Les CHIL se sont révélées être des fatty acid binding protein (FAP) impliquées dans le métabolisme des acides gras. L'intérêt pour cette nouvelle famille a justifié leur caractérisation biochimique puis fonctionnelle par complémentation de mutants FAP d'*Arabidopsis thaliana*. L'élucidation progressive des voies de biosynthèse des phlorotannins a servi de base pour étudier les mécanismes de régulation de ce métabolisme chez les Phaeophycées. En combinant des approches intégrées d'expression de gènes cibles, de dosages et de profilages de phlorotannins solubles, nous avons pu montrer que ces composés assurent une protection constitutive chez *Fucus vesiculosus* en réponse aux UV-B, et que leur métabolisme serait induit très précocement au cours de l'herbivorie. Le développement d'outils moléculaires spécifiques de ces voies métaboliques, ouvre de nouvelles perspectives en écophysiologie et en écologie.

Abstract

Phlorotannins are polymers of phloroglucinol that are specific phenolic compounds of brown algae (Phaeophyceae). These metabolites present antioxidant activities and are potentially involved in the formation of cell-walls but their biosynthetic pathway is currently uncharacterized. The genome annotation of the brown algae *Ectocarpus* provided some information about conserved genes which are implicated in the synthesis of phenolics in terrestrial plants. One polyketide synthase of type III (PKSIII) has been successfully characterized: it produces phloroglucinol. The search for other targets has been pursued in brown algae focusing mainly on chalcone isomerase-like (CHI-like) genes, as well as on phenol-sulfotransferases, which are implicated in the sulfation of flavonoids. The characterization of CHIL has revealed their implication in fatty acid binding (FAP). However, the level of interest for this new family has led to their biochemical characterization and to functional studies by complementation of gene in the *Arabidopsis thaliana* FAP mutant. The progressive elucidation of the phlorotannin biosynthesis pathway has been used in order to discover mechanisms which regulate this metabolism in brown algae. By combining integrated approaches of gene expression profiling with the quantification and profiling of soluble phlorotannins, we have shown that these metabolites ensure the constitutive protection in *Fucus vesiculosus* against UV-B radiation and could also be induced as a very early response to grazing. The development of specific molecular tools for this metabolic pathway opens some news perspectives in ecophysiological and ecological studies.